Coordination and Organometallic diamido-donor Iron and Cobalt Complexes

by

Zohreh Moatazedi

M.Sc. Iran Polymer and Petrochemical Institute, 2004
B.Sc., Sharif University of Technology, 2001

A Thesis Submitted In Partial Fulfillment
of the Requirements for the Degree of
Doctor of Philosophy

in the
Chemistry Department

SIMON FRASER UNIVERSITY

Spring 2013

Approval

Name: **Zohreh Moatazedi**

Degree: **Doctor of Philosophy**

Title of Thesis: ***Coordination and Organometallic diamido donor Iron and Cobalt Complexes***

Examining Committee: **Chair:** Firstname Surname
Position

Dr. Daniel. B. Leznoff
Senior Supervisor
Professor

Dr. Andrew. J. Bennet
Supervisor
Professor

Dr. Vance. E. Williams
Supervisor
Associate Professor

Dr. Tim.Storr
Internal Examiner
Assistant Professor
SFU/Department or Chemistry

Dr. Kevin. M. Smith
External Examiner
Associate Professor
UBC Okanagan/Department or Chemistry

Date Defended/Approved: April 2nd, 2013

Partial Copyright Licence

Abstract

The structures, reactivity and magnetic properties of high-spin iron and cobalt complexes of diamido donor ligands were investigated. Unusual multinuclear, halide-bridged Fe(II) and Co(II) complexes with the basic dinuclear unit $M_2X_2[^{tBu}NON]$ (X= Br, M= Fe (**1**), Co (**2**); X= Cl, M= Fe (**3**), Co (**4**)), ($[^{tBu}NON]^{2-}$= $[Me_3CN(SiMe_2)]_2O^{2-}$) were synthesized, structurally and magnetically characterized. The reduction reaction of **3** with KC_8 and addition of CO and dmpe ($Me_2P(CH_2)_2PMe_2$) generated $\{Fe_2[^{tBu}NON]\}_2$ and, with dmpe also $FeCl_2(dmpe)_2$. However, the addition of 1,3-bis-(2,4,6-trimethylphenyl)imidazol-2-ylidene (NHC) carbene to **3** resulted in the new $\{[NHC]FeCl_2\}_2$.

Alkyl for halide metathesis via the reaction of $LiCH_2SiMe_3$ in **1**-**4** generated rare high-spin mixed alkyl/halide $\{[^{tBu}NON]M_2X(CH_2SiMe_3)_2\}_2$ (**8**-**11**) complexes and unusual high-spin dialkyl dinuclear iron and cobalt complexes of the form $\{M_2(CH_2SiMe_3)_2[^{tBu}NON]\}$ (M = Fe (**6**) and Co (**7**)); reaction with MeLi to form the dimethyl analogue was not successful, while addition of one equivalent of methyl reagent per dinuclear unit in **3** and **4** resulted in $\{Fe_2Br(Me)[^{tBu}NON]\}_2$ and $\{Co_2Cl(Me)[^{tBu}NON]\}_2$. Neither **6** nor **7** act as polymerization catalysts for ethylene; addition of $B(C_6F_5)_3$ as a cocatalyst was found to further *hinder* any activity of **6** and **7** by the formation of $\{Co_2(C_6F_5)_2[^{tBu}NON]\}$ and $\{Fe_2Cl(C_6F_5)[^{tBu}NON]\}_2$. Upon exposing **6** to *excess* CO, a rare dicarbamoyl trinuclear iron complex was obtained, which results from CO binding, isocarbonyl binding and Fe-C and Fe-N CO insertions.

Attempts towards obtaining high oxidation state iron and cobalt complexes with strong oxidizing agents showed that the [NON] ligand did not support such systems. Addition of benzyl bromide to $\{Fe[^{Me_3Ph}NON]\}_2$ resulted in $\{FeBr[^{Me_3Ph}NON]\}_2$ and reaction

of $\{FeCl[^{tBu}NON]\}_2$ with dmpe led to a rare tetrahedral iron(III) complex $\{FeCl[^{tBu}NON]\}_2(\mu\text{-}Me_2PCH_2CH_2PMe_2)$.

To overcome potential difficulties with limited Si-N bond stabilities, carbon-backbone diamido $\{M[^{iPr}NN'N]\}_2$ and $\{M[^{iPr}NO'N]\}_2$ (M= Fe, Co) $[MeN((CH_2)_2N^-iPr)_2]$ ($[^{iPr}NO'N]^{2-}$) and $[O((CH_2)_2N^-iPr)_2]$ ($[^{iPr}NN'N]^{2-}$) were synthesized, structurally characterized and compared with similar diamido Fe(II) and Co(II) complexes. Monomeric diamine complexes $\{MCl_2[H_2{}^{iPr}NN'N]\}$ (M= Fe; Co) and $\{FeCl_2[H_2{}^{iPr}NO'N]\}$ were obtained from oxidations of the diamido precursors.

All complexes described were characterized by elemental analysis, ^1H NMR spectroscopy and single crystal X-ray diffraction and, in some cases by SQUID magnetometry.

Keywords: diamido iron, diamido cobalt, organometallic iron and cobalt, bimetallic iron and cobalt, high-spin organometallic, carbamoyl iron

Dedication

To my love Reza and my beloved son Ilya.

Acknowledgements

I would like to express my deep gratitude to my advisor, Prof. Daniel Leznoff who has had a profound influence on my research. Beside being a knowledgeable teacher, he has also been an understanding, supportive, patient, and helpful advisor with a strong personality.

I would like to thank the members of my thesis committee: Prof. Williams Vance and Andrew Bennet for their time and help during my graduate studies. It has been a great honor to have Dr. Tim Storr and Prof. Kevin Smith as the internal and external examiners of my thesis defense.

I greatly benefited from research experiences of the past and current members of Leznoff lab, including: Farzad Hafrbaradarn who trained me the airsensitive work for the first time, Michael Katz who thought me to run and solve my own X-ray structures, Edwin Wong and Cassandra Hayes who shared the airsensitive work and lab space together, Jasmin korcok, Julie Lefebvre, Jeffrey Ovens, Andrew Geisheimer, Garry Mund, and Madhvi Ramnial.

At the end, my special thanks goes to my family for their endless support, care, and love throughout my PhD journey.

Table of Contents

List of Tables

List of Figures

List of Schemes

Glossary

Å	Angstrom (10^{-10} m)
Ad	adamantyl
Anal	analysis
Ar_F	2,5-C_6H_3FM
$B(Ar_f)_4$	{B[3,5-$(CF_3)_2$Ph]$_4$}
μ_B	Bohr magneton
br	broad
^nBu	n-butyl (-$CH_2CH_2CH_2CH_3$)
^tBu	t-butyl [-$C(CH_3)_3$]
^oC	degrees Celsius
Calcd	calculated
cm^{-1}	wave number
Cp	cyclopentadienyl
D	donor(s)
D	doublet
Deg	degree(s)
Dmpe	1,2-bis(dimethy1phosphino)ethane
EI	electron impact
Et	ethyl (-CH_2CH_3)
Et_2O	diethylether
G	gram(s)
^1H	proton
H	external applied magnetic field
K	Kelvin
M	central metal atom (or "molar" when referring to concentration)
M	multiplet
Me	methyl (-CH_3)
Mes	mesityl
MHz	megahertz
mL	millilitre
Mm	millimetre

Mmole	millimole(s)
MS	mass spectrometry
m_s	spin quantum number
m/z	mass to charge ratio
NHC	“N-heterocyclic” carbene
Nm	nanometre
NMR	nuclear magnetic resonance
$[NON]^{2-}$	$[(RCN^{-}(SiMe_2))_2O]$
$[NN'N]^{2-}$	$[MeN((CH_2)_2N^{-}iPr))_2]$
$[NO'N]^{2-}$	$[O((CH_2)_2N^{-}iPr))_2]$
ORTEP	Oak Ridge Themal Ellipsoid Plot
Ph	phenyl
Ppm	parts per million
iPr	isopropyl [$-CH(CH_3)_2$]
S	total electron spin
S	singlet or seconds
SQUID	superconducting quantum interference device
T	temperature
T	triplet
THF	tetrahydrofuran
TMS	Me_3SiCH_2-
UV-vis	ultraviolet-visible
Br	very broad
vs.	versus
ZFS	zero field splitting
γ	gamma ray
χ_g	gram magnetic susceptibility
χ_m	molar magnetic susceptibility
δ	isomer or chemical shift
μ_{eff}	effective magnetic moment
$\mu_{s.o.}$	spin-only magnetic moment
E	extinction coefficient
^{o}	degrees

1. Introduction

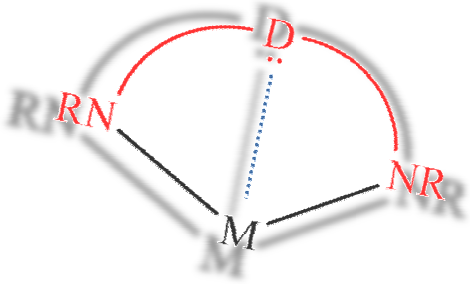

1.1. Transition metal organometallic chemistry

Organometallic chemistry is broadly defined as the study of metal-carbon or metal-hydrogen bonds.[1] It could be said that organometallic chemistry is an important subfield of coordination chemistry, i.e. the coordination chemistry of carbon-based ligands.[2-4] One big difference in organometallic coordination complexes compared to classical coordination compounds is that organometallic compounds are more covalent as a result of covalent nature of the M−C bond. Due to this, the bond can be activated by the metal centre and can result in interesting reactivity.

The history of organometallic chemistry started with main-group element alkyl compounds such as Li, Na and Mg alkyls. The importance of alkyllithium and Grignard reagents in organic synthesis is obvious.[5] Transition-metal organometallic chemistry only started to be explored in the late 19th century[6-7] and was challenging because most of the targeted transition-metal alkyl complexes were unstable due to their easy decomposition pathway.[8] As a result it took time for transition-metal organometallic chemistry to flourish and it was transformed by the synthesis of ferrocene by Pauson in 1951.[9] For about half a century Cp-type ligands and ferrocene chemistry were dominant in transition metal-organometallic chemistry.[10-11]

1.1.1. Applications of transition-metal organometallic chemistry

The organometallic chemistry of transition metals started to expand dramatically, especially after they were found to have key roles in many catalytic applications. For example, organometallic compounds are excellent olefin polymerization catalysts[11-12] and have catalytic applications in organic synthesis in, e.g. C−C or C−heteroatom bond coupling reactions on an industrial scale, and they are known to act as intermediates in many catalytic process. [2, 8, 13-16] The importance of organometallic transition metal chemistry was highlighted more after the discovery and investigation into enzyme structures and their inclusion of transition metals like Fe, Co, Ni, Zn, etc. It all started to investigated more with the discovery of coenzyme B12[17]. Many studies in biosystems show that nature uses organometallic chemistry in important aspects of life so much so that the subfield of bioorganometallic chemistry have grown very fast.[18-22] These important applications could not be achieved without the synthesis, investigation and study of new and interesting coordination chemistry at the interface of organometallic chemistry.

1.1.2. Role of ligands in organometallic coordination chemistry

As mentioned before, many organometallic transition-metal complexes are dominated by Cp-type ancillary ligands (examples of Cp-type complexes in Figure 1.1).[23] The advantage and the popularity of the Cp-type ligand can partly be attributed to its innocent nature as an “ancillary” ligand, meaning that it is not participating in reactions at the metal centre in contrast with “active” ligands that undergo some chemical interaction during a reaction at the metal centre.[2] Even though ancillary ligands are supposed to remain unchanged during metal reactivity, the ancillary ligand’s role in this chemistry is important. The ligand is the key to control the solubility of the metal complex in organic solvents. Furthermore, the geometric, steric and electronic properties of the ancillary ligand has a huge effect on the metal centre’s geometry and electron density. Choosing a suitable ligand can direct the metal centre towards a specific coordination sphere and hence reactivity.[24-25]

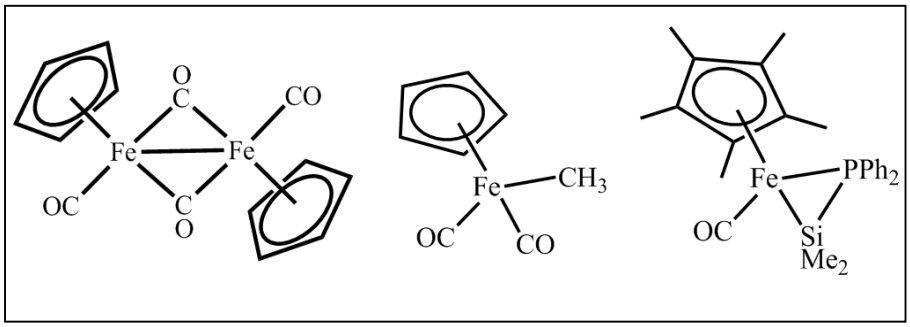

Figure 1.1. Examples of Cp-type organometallic iron complex[26]

The nature of the ligand first depends on its donor atoms, for example the “P” atom in phosphines or the “N” atom in amido or amine ligands. The donor atom substituents are another important part of the ligand, since this sterically and electronically impacts metal centre activity. For example, an electronically rich group such as a t-butyl substituent can render the metal centre electron rich compared to a strongly electron-withdrawing group such as C_6F_5. The steric property of the ligand can be tuned to control access to the metal, thereby impacting the coordination number and geometry and hence the reactivity of the metal centre dramatically.[27-30] The Tolman plot of electronic parameters and cone angles for phosphine ligands is a good example of varying the steric and electronic nature of the ligand environment of a complex.[31] Thus, research on new classes of ancillary ligands is critical for organometallic chemistry.

From the 1980s, ligands other than Cp started to gain attention as ancillary ligands, resulting in interesting metal centre reactivity. Two important categories of non-Cp ancillary ligands are phosphines[32-34] and amido ligands,[7-8, 35-36] and with interesting and promising reported results, they have been developing rapidly.[37-43] Phosphine donors usually stabilize metal centres in lower oxidation states, while amido donors are more suitable to stabilize metals in higher oxidation states.[44-45]

1.1.3. Paramagnetic organometallic chemistry

It should be mentioned that due to the relative ease of studying diamagnetic systems compared to paramagnetic ones, which is the result of the complication in characterization and chemistry of the paramagnetic metal centre from the presence of

unpaired electrons, diamagnetic organometallic chemistry has been developed and investigated to a much larger extent[46-47] compared to paramagnetic ones, even though the latter have a lot of potential and are much less understood.

Avoiding ancillary ligands completely by using very bulky alkyl groups did lead to the isolation of paramagnetic, homoleptic metal alkyls[48-50] such as MR_3 in which R= $CH(SiMe_3)_2$ (M= Ti, V, Cr),[51-52] MR_2 (M= Mn, Fe; R= $C(SiMe_3)_3$) and $(SiMe_3)_2CH)Zn(C(SiMe_3)_3$. The bulky aryl group 2,4,6-trimethylphenyl has been used to stabilize low-coordinate homoleptic aryl complexes with transition metals such as V, Cr, Mn, Fe and Co.[2] However, the use of ancillary chelating phosphine and amido-ligands in conjunction with metal-alkyl groups has flourished since they are much better at supporting controlled reactivity at the transition metal compared to the homoleptic alkyl complexes.[2] The synthesis of paramagnetic metal alkyl complexes also opened the door to investigate interesting magnetic properties[53-56] and metal-carbon bond reactivity[23, 57-59] linked to the existence of unpaired electrons at the metal centre. In many cases studies led to the catalytic application of paramagnetic systems, such as highly active well-developed Cr-based alkene polymerization and oligomerization catalysts[14-15, 60-64] and the activation of small molecules such as CO_2[65] and N_2.[66]

1.1.4. High-spin iron and cobalt organometallic chemistry

The organometallic chemistry of high-spin iron(II) and cobalt(II) has been limited compared to their diamagnetic counterparts as a result of their paramagnetic nature.[67] In particular, iron has unique properties among transition metals that makes it very special. It is among the most abundant metal on earth; as a result it is very cheap and easily accessible compared to other transition metals.[68] Thus, it also can be readily used on a large scale in catalytic processes and still costs less compared to other expensive metals such as Pt. As a result, iron chemistry has been a centre of attention of many research groups recently. [40, 69-73] Iron(II) complexes became one of the most recently investigated systems for highly active non-metallocene polymerization catalysts.[74] Due to iron's environmentally friendly and green chemistry nature and its abundance in the human body, which contains between 4 and 5 g of iron, it gains even more attention.[75]

The early organometallic chemistry of cobalt and especially iron has been dominated by carbonyl and Cp-type ligands due to their vast application in organic synthesis. [27-30, 76-78] These systems have generally been shown to be low-spin [39, 79] due to the strong field nature of the alkyl group and the drive for an 18 electron configuration for CO-containing species, however some non-Cp high-spin organometallic complexes also have been reported. To date most of the high-spin iron and cobalt alkyl complexes have either imine or amido ligands as part of their coordination sphere.[40, 80-82] At present, paramagnetic iron and cobalt coordination complexes are being more extensively investigated; in some cases they show unusual and interesting magnetic properties[54, 83] and in other cases they support activation of CO molecules,[84] N_2 functionalization,[71, 85] CO_2 activation,[86] dinitrogen activation,[66] C−C coupling ,[87-89] C−H bond activation,[90] polymerization catalysis,[91] hydroformylation of alkenes,[92] coupling of alkyl halides with aryl Grignard reagents[93] and also can act as reactive intermediates.[94] However, due to the limited number of high-spin organometallic iron and cobalt complexes, their reactivity and chemical differences compared to more common low-spin systems is relatively unexplored.

1.2. Transition metal-amido coordination chemistry

Although the transition-metal amido unit was historically relatively neglected compared to other ligands, studies showed that the M−N amido bonds are strong and inert, hence amido donor ligands could be used as ancillary ligands to stabilize metal centres for further reactivity.[35] More generally, nitrogen-based ligands present a very vast and important field of chemistry, including amines, pyridines, nitric oxide, nitrite, nitride, azide, cyanate, thiocyanate and important ligands in biochemistry such as amino acids, peptides and proteins. Transition metals with N-donor ligands have shown unusual coordination geometries as well, which further results in unusual and interesting reactivity of the metal centre.[7-8, 45]

Metal tetrakis(diphenylamide) complexes, $M(NPh_2)_4$ (M= Mn, Fe, Co) were reported as the first open-shell transition-metal diamido complexes in 1935 by Dermer and Ferlenius and $U(NEt_2)_4$ was synthesized in 1956 by Gilman.[95] Bradley and Thomas greatly expanded transition-metal amido coordination chemistry starting in 1959,

reporting the formation and isolation of a series of air-sensitive, room temperature stable transition-metal dialkylamido complexes, including with Ti, Zr, Hf, V, Nb, Nb, Ta, Cr, Mo and W[96-97] using $^{-}N(SiMe_3)_2$ and $^{-}NPh_2$ as amido ligands in particular. Since then the huge interest and growth in transition-metal amido chemistry and the accompanying variety of reported amido ligands has been summarized in several reviews and book chapters, which cover modified amido ligands and their coordination with different transition-metals.[98-103] The fast growth has probably been assisted by the fairly simple synthetic route to prepare amido salts, via the reaction of an amine with ^{n}BuLi. As well, interest accelerated after studies on group(IV) amido complexes showed them to be excellent olefin polymerization catalysts.[98, 100-101, 103-105]

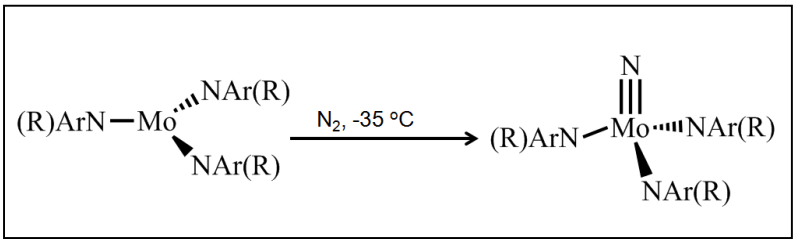

Figure 1.2. The first reported dinitrogen cleavage- accomplished by a three-coordinate metal amido complex (R= t-Butyl, Ar= 3,5-Me_2Ph).[106]

Current advances in metal amido coordination chemistry in particular target a broad range of coordination and bonding configurations, which can result in different kinds of reactivity of TM−C and other bonds. One breakthrough in this field was the discovery that metal amido complexes were able to activate and split dinitrogen (Figure 1.2),[106] in addition to the activation of other small molecules such as CO, CO_2 and C−H bonds as well. [107-108]

1.2.1. Low-coordinate Transition Metal Amides

The stabilization of a transition metal centre in a complex is highly dependent on the coordination sphere of the metal centre; on the other hand, the nature of the ligand is a big factor in determining the coordination sphere.[2, 47] Although the metal electron count usually needs to be satisfied, stable, electronically unsaturated metal centres with coordination numbers of four, three and even two have been reported. These complexes

are categorized as “low-coordinate compounds”.[95, 109-111] The importance of developing low-coordinate metal complexes was highlighted after it was reported that low-coordinate metal sites can play key roles in biological systems. One very well-known example in nature is the MoFe cofactor,[75, 112] which is responsible for nitrogen fixation (reduction of N_2 to NH_3) in bacteria in roots of green legume plants. Based on its structure, high-spin iron centres are coordinated by three sulfur atoms in a trigonal geometry.

The coordination number and geometry of transition metals depends in part on the steric effect of the ligands. Since less bulky ligands naturally result in higher coordination numbers, the formation and stabilization of low-coordinate complexes highly depends on using bulky ligands.[52, 113-114] The aforementioned complexes of Bradley represent very first well-known example of low-coordinate transition metal amido species, including $M\{N(SiMe_3)_2\}_2$ (M= Mn, Fe, Co)[115-118] and $M(NPh_2)_2$ (M= Mn, Fe, Co) complexes, Power also reported two-coordinate $[M\{N(SiPh_2Me)_2\}]$ (M= Fe, Co).[69] Some examples are shown in Figure 1.3.

Since then, other bulky amido ligands have been synthesized, modified and applied in order to target lower coordination transition-metal centres (some examples are shown in Figure 1.6 and Figure 1.8).

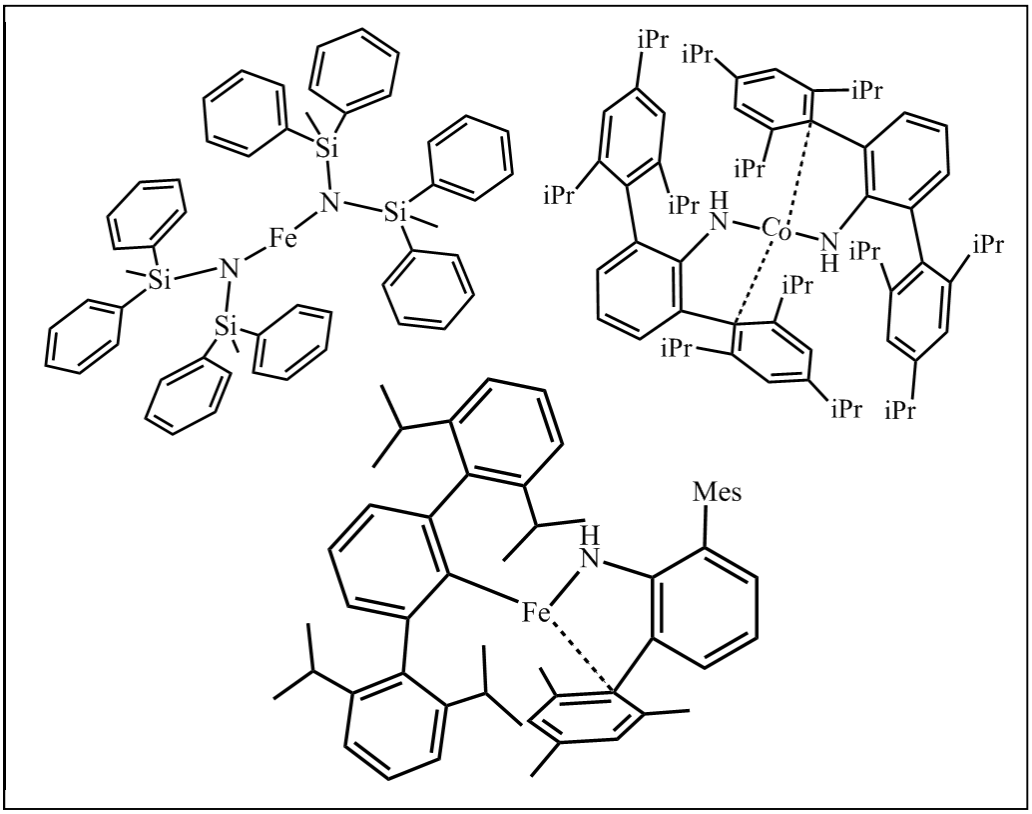

Figure 1.3. Examples of low-coordinate homoleptic (top) and heteroleptic (bottom) transition metal amido complexes.[53, 69, 114]

During the past decade this new category of low coordinate transition-metal complexes has attracted lots of attention since such unsaturated metal centres provide open sites and Lewis acidity for unusual reactivity.[70] The most important reactivates of such complexes include small molecule activation chemistry with substrates such as N_2 (Figure 1.2), CO and CO_2.[45, 119-122] Recently, the number of low-valent transition-metal complexes have been growing fast,[69, 113, 123] however heteroleptic transition metal amides are still limited in number.

1.2.2. Amido ligand synthesis and bonding

The synthetic routes and reaction conditions to form metal amido complexes are quite simple. Generally, in the first step an inorganic amido ligand can be formed by the

deprotonation of the corresponding amine, for example with commercially available ^{n}BuLi in solution and has the general formula –NRR′ (Scheme 1.1).[8]

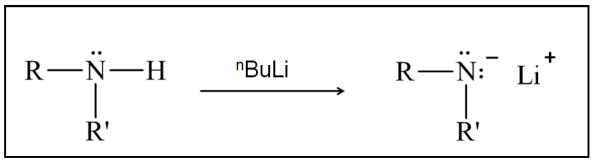

Scheme 1.1. Formation of an amido salt.

Lithium amides are among the most important amido ligand transfer reagents. The advantage of lithium amides (Scheme 1.2) is that they are more soluble in hydrocarbon solvents compared to heavier element salts such as Na, K, Mg and Ca. This is a result of the smaller size of lithium and the more covalent properties of the lithium-amide pair.[8]

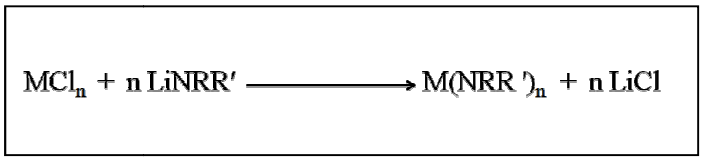

Scheme 1.2. Transmetallation.

In the second step, a transition-metal halide is reacted with an amide salt (such as lithium amide); this reaction is called transmetallation, which leads to the formation of a metal amido complex and the halide salt precipitation (depending on the solvent employed). This method is the most common route to synthesize metal amido complexes, even though there are other different important synthetic approaches of making them such as transamination, alkane or hydrogen elimination and disproportionation and redistribution routes which are more common for early transition metals.[8]

The growth in the synthesis of early transition-metal amido complexes, especially group 4 to 6, was very fast compared to late transition-metal analogues. The main reason is the fact that amido ligands can act as both a 2- or 4-electron donor (Scheme 1.3), which matches well with early transition-metals due to their empty d-orbitals;

electron-rich late transition-metals do not usually benefit from this bonding. Empty d-orbitals of the transition-metal can facilitate π-electron donation from the amido group in addition to the σ-bonding and as a result a stronger M−N bond is formed.[8]

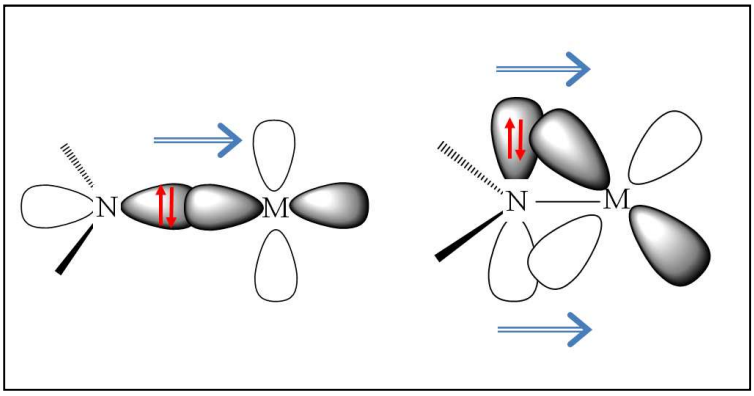

Scheme 1.3. σ-bonding (left) with additional ***π***-donor bonding (right) in amido systems.

This π-donating ability is readily observed with terminal amido groups with a trigonal geometry. However, amido ligands can also bridge between two metal centres using both σ-bond and a π-bond (Figure 1.4). Measured M−N bond strengths[8] and short M−N bond distances compared to the sum of the covalent radii of M and N support the concept of π-donation from the amido group and moreover a planar coordination geometry around nitrogen in amido ligands supports the concept of p-orbital participation in M−N (transition metal-amido) bonds as well.[8]

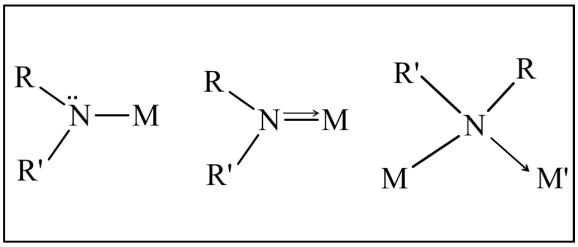

Figure 1.4. A 2-e⁻ amido donor (left), a 4-e⁻ amido donor to one metal (middle), and a 4-e⁻ amido ligand bonding two metal centres (right).

1.2.3. Amido ligand development and design

The first amido ligands were basic monodentate units such as $^{-}NR_2$ (R= $SiMe_3$, Ph or $SiMePh_2$), however amido ligand modification and development has led to many chelating bidentate and multidentate amido ligands; such chelating multidentate ligands provide more stability to the metal complex.

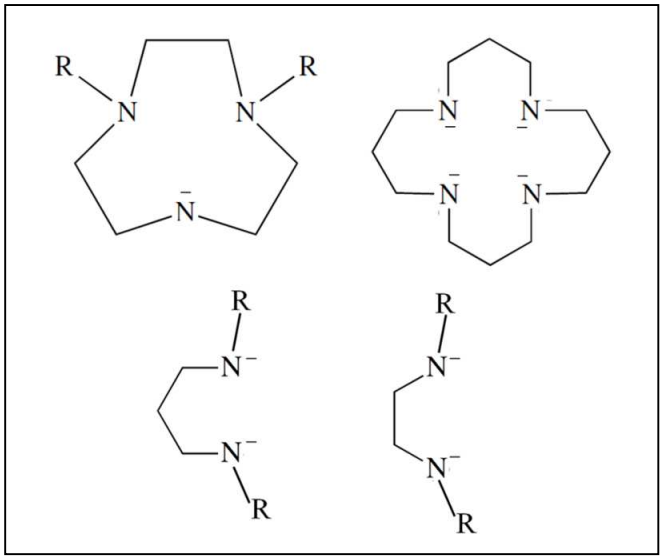

Figure 1.5. Cyclic (top) and acyclic (bottom) amido ligands.

Multidentate amido ligands (which can include more than one amido group) can be divided into cyclic and acyclic categories (Figure 1.5). Acyclic multidentate amido ligands have much more flexibility compared to their cyclic counterparts in terms of their coordination motif. Diamido ligands are the most well-known subgroup of multidentate amido ligands,[7, 38, 124] and include substantial modifications on the amido R-group to tune their steric and electronic properties. In particular, the steric properties of amido ligands can considerably change the coordination geometry and hence the chemistry of the metal centres.[8, 96, 125-126]

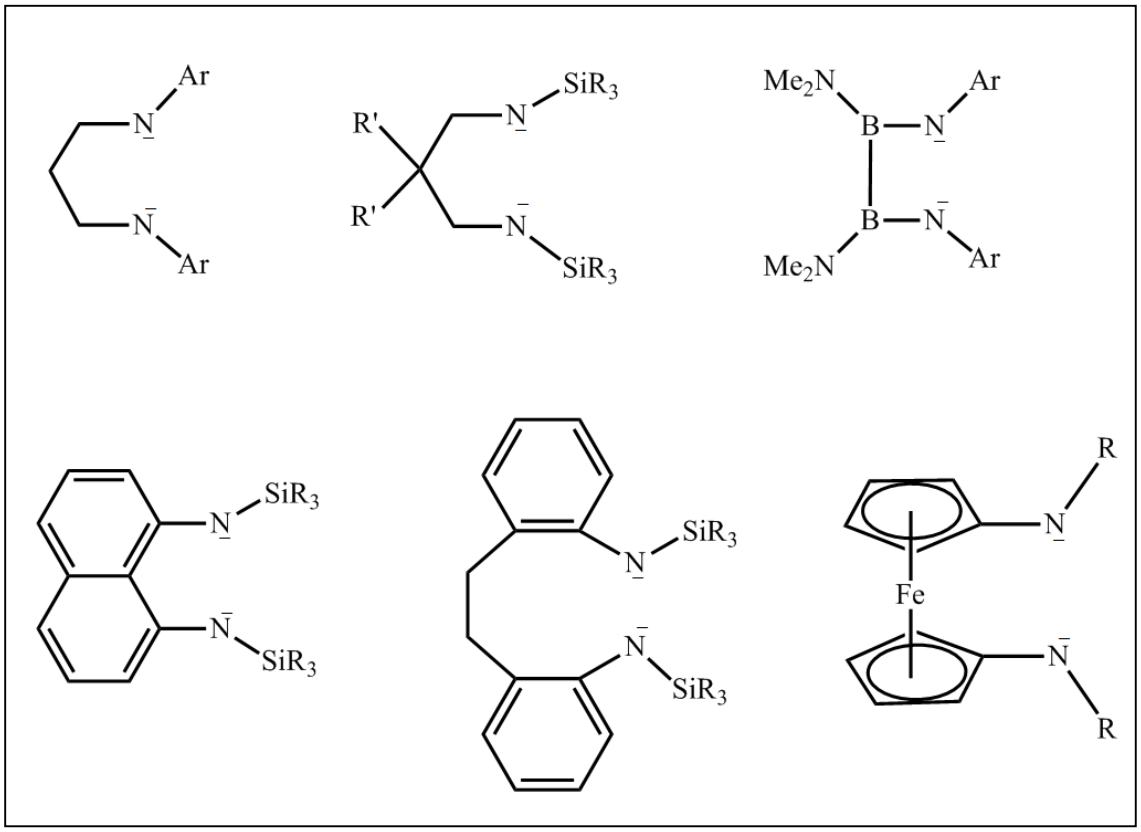

Figure 1.6. Examples of ligand backbone modification in chelating diamido ligands

Many modifications also have been done on the diamido ligand backbone, including varying the backbone chain length from two to six carbon atoms (or other atoms), and adding aromatic rings or ferrocene units as shown in Figure 1.6. Diamido ligands are usually designed to chelate to the metal centre, however in some case they can bridge between two metal centres,[127] as shown in Figure 1.7.

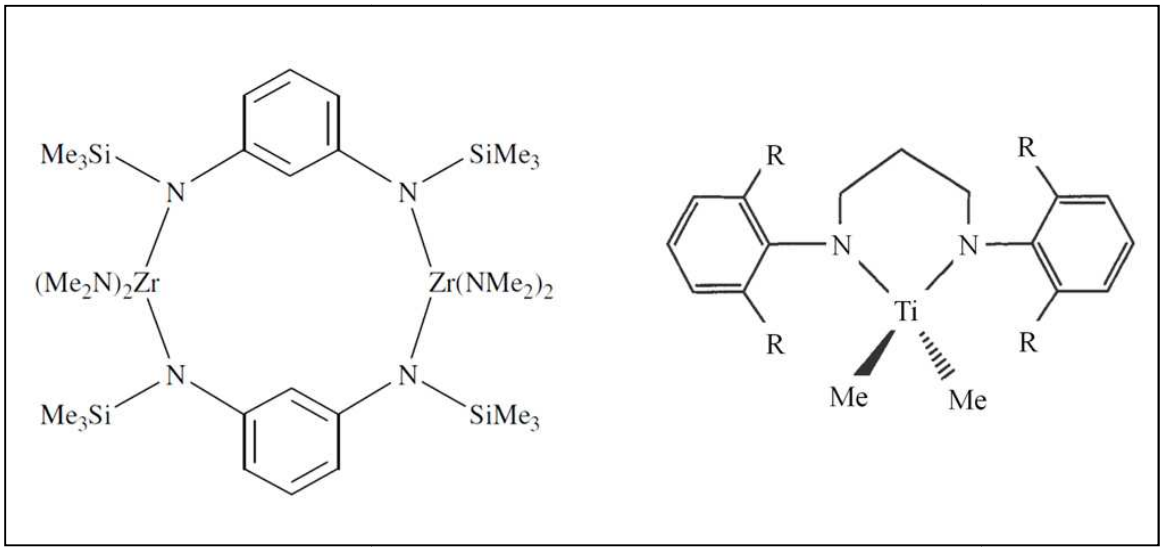

Figure 1.7. Chelating and bridging diamido ligands to metal centres.[128] [129]

Another important development of amido ligand systems was the incorporation of one or more neutral donor atoms such as O, NR, PR or S in the ligand backbone (Scheme 1.4); this potentially adds stability at the metal centre.

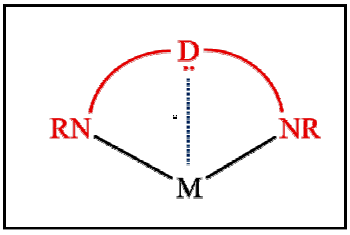

Scheme 1.4. Drawing of diamido-donor ligand chelated to a metal (M = metal; D = neutral donor atom).

This donor atom often interacts with the metal centre (sometimes in a hemi-labile fashion[130]) and hence can affect the reactivity of the metal centre considerably depending on its nature and substitution pattern.[39, 55, 100, 125, 131-138]

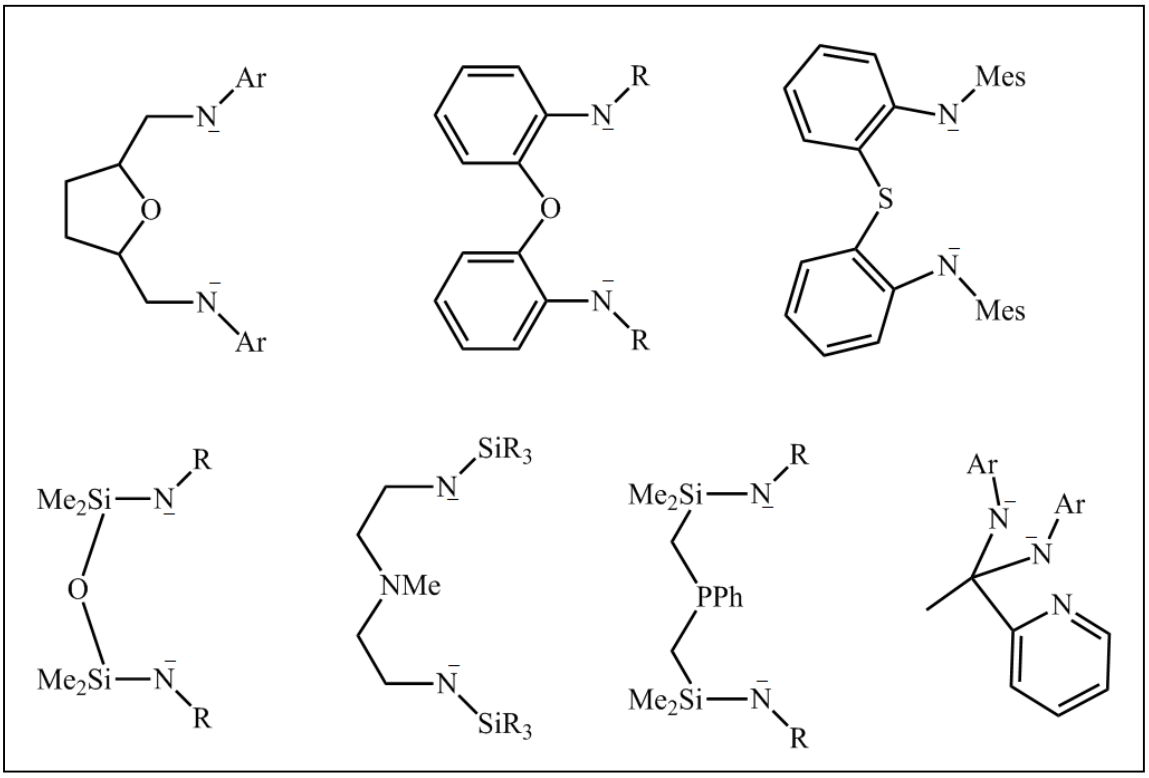

Figure 1.8. Examples of diamido-donor ligands.

Such diamido donor-based complexes (Figure 1.8) have showed catalytic applications and small molecule activation,[8, 44-45, 98-99, 139] including dinitrogen activation as shown in Figure 1.9.

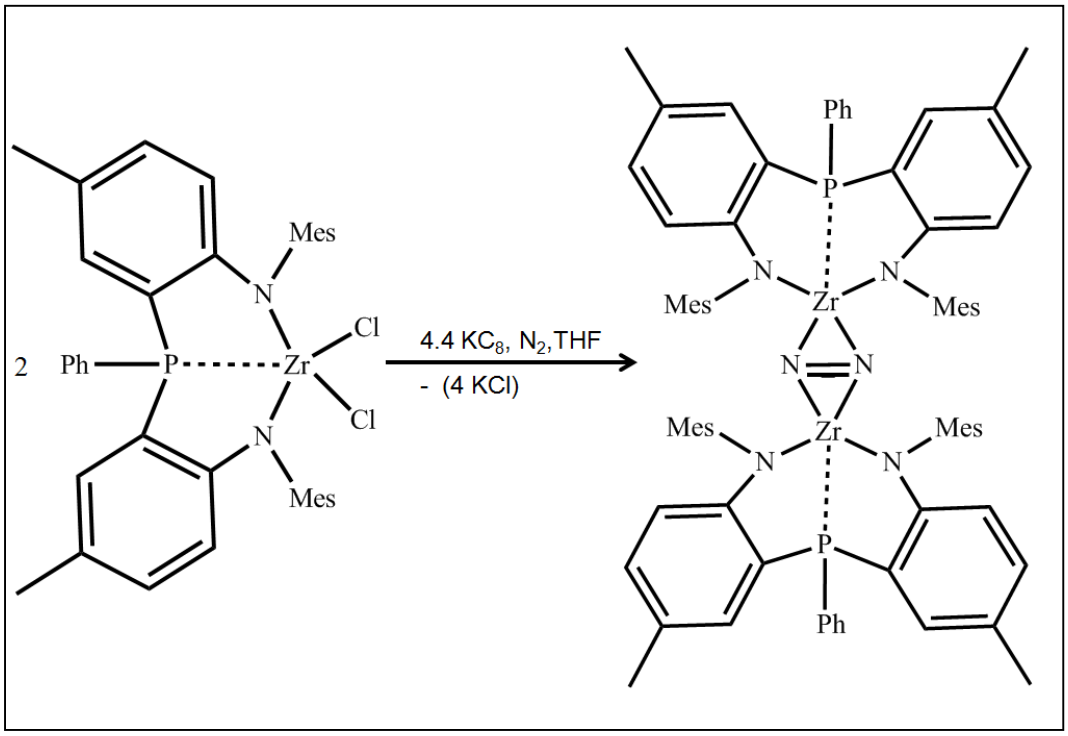

Figure 1.9. Example of dinitrogen activation with a diamido-donor complex[139]

To date, diamido-donor complexes with many transition-metals have been structurally, characterized and their reactivity reported, especially with group 4 to 6 metals (Figure 1.10),[98-103, 131, 139] however the number of paramagnetic complexes are much more limited, leaving a great potential for investigation. Elias and his coworkers synthesized and characterized paramagnetic transition metal complexes containing diamido-ether ligands in 1992.[140] Particularly using MX_2 to form $\{M[^{tBu}NON]\}_2$ dimers, which are of direct relevance to this thesis research.

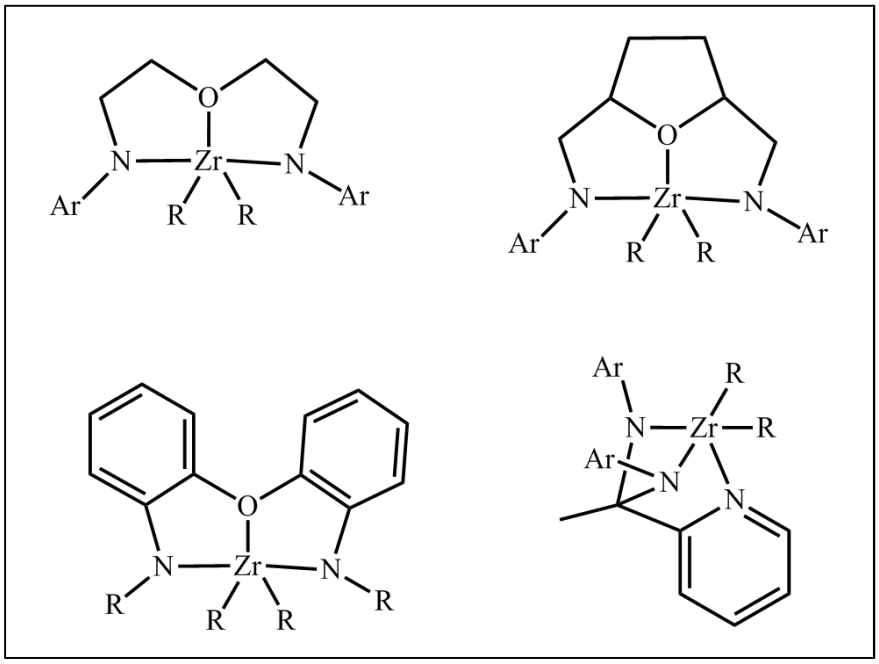

Figure 1.10. Examples of organometallic chelating diamido-donor zirconium(IV) complexes that act as olefin polymerization catalysts. [98, 105, 141-144]

1.3. Iron and cobalt-diamidoether complexes

The Leznoff group has worked extensively with diamido-ether donor $[(RN^{-}(SiMe_2))_2O]$ (NON^{2-}) ligands and first-row transition metals, in particular paramagnetic Co, Cr and Fe systems. These are typically formed by addition of $[^{R}NON]Li_2$ (R= ^{t}Bu, 2,4,6-Me_3Ph, 2,6-iPr_2Ph, 3,5-$(CF_3)_2$Ph) to a transition metal dihalide MX_2 (Figure 1.11).[55, 135-138, 145]

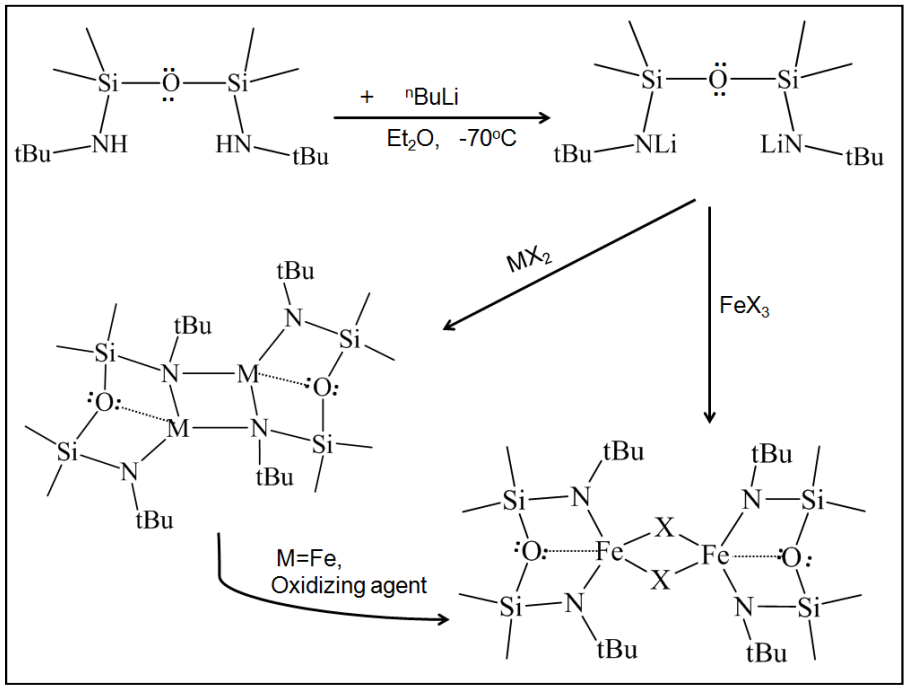

Figure 1.11. The formation of Fe(II) and Fe(III) diamidoether complexes.

The single crystal X-ray structures for {[$^{t\text{Bu}}$NON]M}$_2$ (M = Cr, Mn, Fe, Co) show a dimeric structure in which each metal centre is coordinated by one terminal amido and one bridging amido ligand (Figure 1.11). The Leznoff group has targeted the reactivity of these systems, especially with respect to accessing more reactive higher oxidation-state metal complexes and also new organometallic complexes of the diamidoether donor systems. Higher oxidation-state iron(III) systems were obtained by the addition of [$^{t\text{Bu}}$NON]Li$_2$ to FeX_3 (X = Cl, Br), yielding a rare spin-admixed, five coordinate, trigonal bipyramidal {[$^{t\text{Bu}}$NON]FeX}$_2$[55] dimer structure, while addition of [^{Me_3Ph}NON]Li$_2$ to FeX_3 (X = Cl, Br) instead yielded ate-complexes which retained LiX of the form {FeX_2[$^{t\text{Bu}}$NON]Li·(THF)}$_2$ (Figure 1.12).[137] However, the lithium-free {FeX[^{Me_3Ph}NON]}$_2$ could be prepared by addition of oxidizing agents such as I_2 to the dimer {Fe[^{Me_3Ph}NON]}$_2$, resulting in the {FeX[^{Me_3Ph}NON] }$_2$ systems (Figure 1.12).

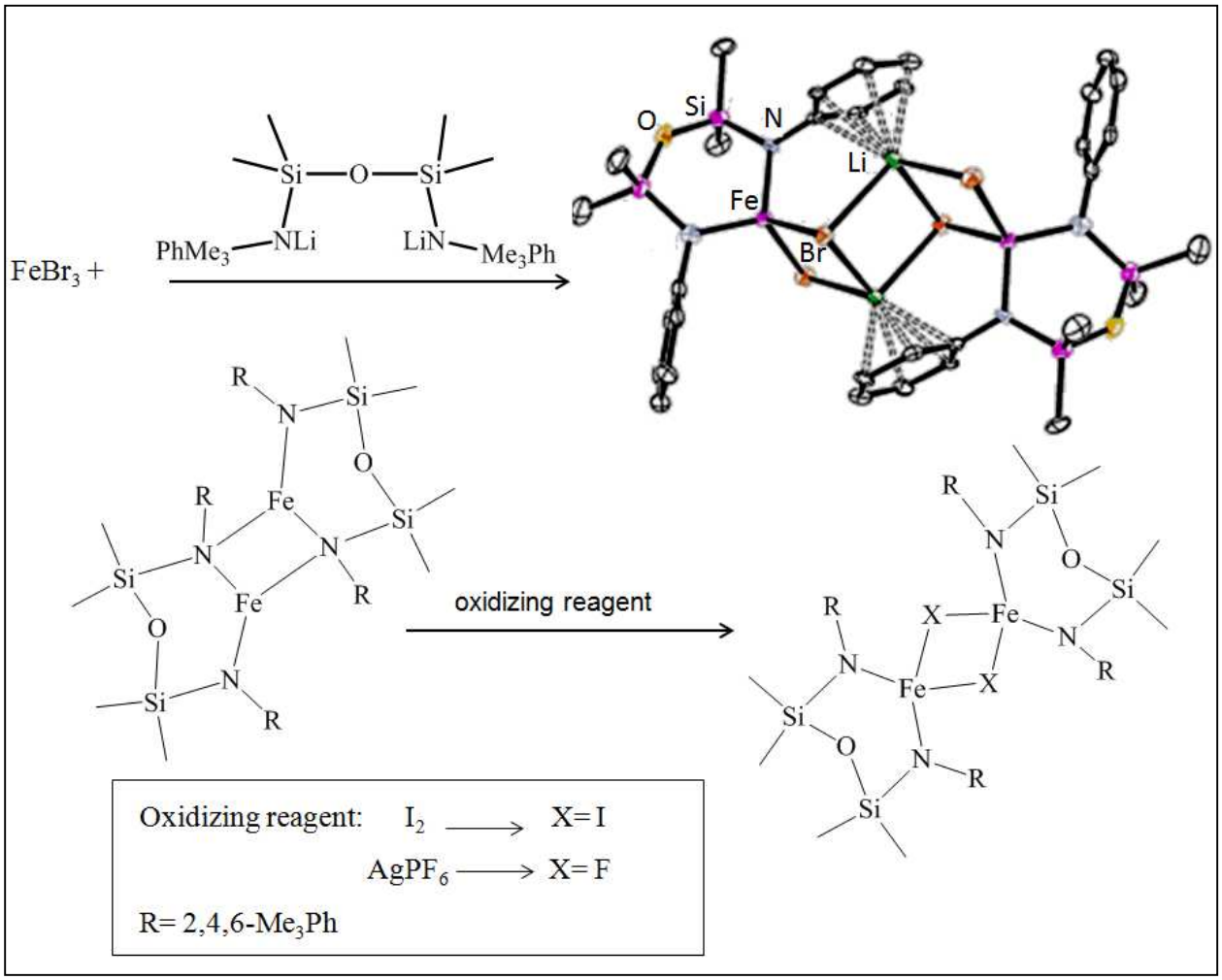

Figure 1.12. Formation of iron(III) “ate” complex and iron(III)-lithium free complex.

The analogous diamidoether cobalt(III) systems could not be prepared. In addition, attempts to alkylate the iron(III) complexes did not result in stable iron(III)-diamidoether organometallic complexes; most substitution reactions of the iron(III) halide complexes resulted in the formation of reduced iron(II) species. Due to the lack of halide substituent in the reported iron(II) and cobalt(II) systems of $\{M[^{R}NON\}_2$, these compounds do not readily act as precursors to new organometallic complexes. This is a substantial disadvantage of these systems.

1.4. Research scope of the thesis

The goal of the research in this thesis is to synthesize new chelating diamido-donor ligands of the form $[NDN]^{2-}$ (D = O, NR) and to use these new and existing ligands to target the synthesis of low-coordinate iron and cobalt complexes and investigate their properties. In particular, the structural and magnetic properties and the reactivity of these systems are of interest. A majority of this thesis incorporates the diamidoether ligand $[^{tBu}NON]^{2-}$. As mentioned above, with the combination of ligands and first-row transition metals, Leznoff and others prepared complexes that showed unusual bonding motifs, low coordination numbers, and interesting magnetic properties and reactivities. However, with the iron and cobalt complexes, attempts to prepare alkylated systems to date were unsuccessful. In Chapter 2 the development of new diamido iron and cobalt complexes by changing the stoichiometric addition of ligand to metal will be examined, targeting new coordination numbers and geometries, and hence potentially new reactivity at the metal centres. Chapter 3 focuses on the alkylation of these compounds to generate rare high-spin cobalt and iron alkyl complexes and survey their reactivity. Due to the π-donating ability of the diamidoether ligand, their potential for stabilizing metal centres in higher oxidation-states (Fe(IV), Co(III)) is examined in Chapter 4. More flexible carbon backbone-based diamido donor ligands of the type $[^{iPr}NO'N]^{2-}$ ($[O((CH_2)_2N^-iPr))_2]$) and $[^{iPr}NN'N]^{2-}$ ($[MeN((CH_2)_2N^-(iPr))_2]$) and their iron and cobalt complexes will be prepared and their coordination geometries and reactivity compared with the previous diamidoether complexes.

There are some fundamental questions that will be examined throughout this research. Specifically, an investigation into new low-coordinate iron(II) and cobalt(II) systems, their organometallic derivatives and investigation into their magnetic properties and reactivity is of great interest. Are diamido donor ligands capable of stabilizing higher oxidation state metal centres? What is the effect of the ligand backbone on the structure and properties of the metal centre; for example how would the spin state and hence the reactivity of the metal centres change or how coordination number and geometry at the metal centre impact the stability and reactivity of the complexes.

1.5. Characterization methods for paramagnetic coordination and organometallic compounds

In addition to the typical characterization methods commonly utilized for diamagnetic organometallic compounds, some methods and techniques are helpful in overcoming the challenges associated with studying paramagnetic compounds.

1.5.1. Magnetic measurements

Examining the magnetic properties of paramagnetic transition metal complexes is an important part of their characterization, since the paramagnetic properties of such materials reflects the coordination sphere of the paramagnetic ion and can address useful information such as oxidation state, spin state and the presence of a metal-metal interaction.[15] Using a Superconducting Quantum Interference Device (SQUID), the magnetic moment of the complex in the solid state can be measured and potentially correlated to the number of unpaired electrons. The basis of this technique is on the behaviour of an unpaired electron in a magnetic field. This section will very briefly describe some magnetism terms and definitions since the solid state magnetic behaviour of some of the synthesized iron and cobalt complexes will be discussed in this thesis. Paramagnetism results from the spin (spin angular momentum) and orbital motion (orbital angular momentum) of unpaired electrons in the sample, which align themselves with an applied magnetic field.[15] With both spin and orbital motion of the electrons the equation for μ_{eff} (the effective magnetic moment) is quite complicated. However, for paramagnetic first-row transition metal compounds, the spin only formula is often applicable to determine the number of unpaired electrons to a good approximation.

The volume magnetic susceptibility χ_v, is defined as:

$$\chi_v = M / H \text{ (M: magnetization and H: external magnetic field)}$$

χ_v, which is measured in the SQUID magnetometer as an emu value and can be converted to gram magnetic susceptibility (χ_g) or molar magnetic susceptibility (χ_M), as follows:.

$$\chi_M = \text{emu} * MW / H * m(mg) \qquad (MW = \text{molecular wieght})$$

Based on the following equation, the effective magnetic moment (μ_{eff}) can be calculated.

$$\mu_{eff} = 2.282\ (\chi_m\ T)^{1/2}\quad (\mu_B)$$

The effective magnetic moment corresponds to the number of unpaired electrons assuming the 'spin only' formula is applicable:

$$\mu_{eff} = 2\{S(S+1)\}^{1/2}\ (S : \text{total spin quantum number})$$

$$\mu_{S.O} = g[S\ (S+1)]\ \text{B.M.}$$

Assuming that there is no orbital contribution to the magnetic moment, values for the 'spin-only' magnetic moments in units of Bohr magnetons (B.M.) are summarized in Table 1.1.

Table 1.1. Spin-only values corresponding to the number of unpaired electrons.

Number of unpaired electrons	**S**	**$\mu_{S.O}$ (μ_B)**
1	1/2	1.73
2	1	2.83
3	3/2	3.87
4	2	4.90
5	5/2	5.92

The unpaired electron(s) in multinuclear metal centres can also interact with each other through ligands (termed superexchange) or a direct metal-metal orbital overlap in either a ferromagnetic or antiferromagnetic fashion. In ferromagnetic coupling the unpaired electrons will align in the same direction with each other so that μ_{eff} will be higher than the spin-only value. In antiferromagnetic coupling unpaired electrons in neighbouring metal centres are coupled and align in opposite directions so that the μ_{eff} will be lower than the spin-only value.

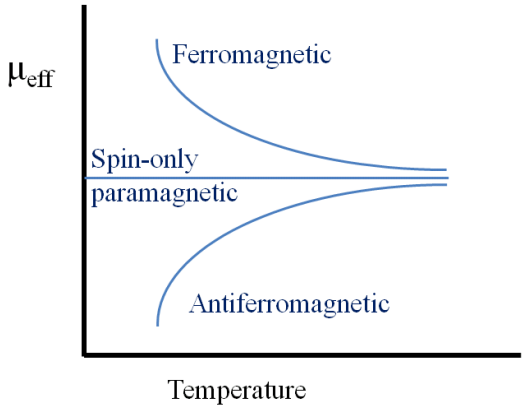

Figure 1.13. A typical plot for the μ_{eff} vs T for paramagnetic, ferromagnetic, and antiferromagnetic systems.

The magnetic moment (μ_{eff}) does not vary with temperature in case of ideal paramagnetic compounds (spin-only with no coupling). However, at lower temperatures, the coupling constant of the electrons becomes more significant relative to KT, thus ferromagnetic materials show higher μ_{eff} values compared to isolated paramagnetic metal centres, as T decreases. On the other hand, antiferromagnetic interactions manifest as lower μ_{eff} values with decreasing temperature. The magnetic moment for the sample can eventually go to zero. The high-T values of μ_{eff} and the speed and extent to which the curves change with decreasing T gives an indication as to the strength of the magnetic interaction between the metals.

1.5.2. Nuclear magnetic resonance spectroscopy

The study of paramagnetic organometallic compounds did not develop as quickly as diamagnetic organometallic chemistry and one reason appears to be the characterization challenges imposed by the relatively limited utility of nuclear magnetic resonance spectroscopy (especially multinuclear NMR), since NMR was and remains a critical characterization tool for the diamagnetic systems, especially historically, in the absence of routine X-ray crystallography infrastructure. Unlike for diamagnetic compounds, the NMR spectra of paramagnetic complexes are highly shifted and very

broad to the point that sometimes they are not even observable.[146-147] The broadening of the signals is caused by the fast relaxation of the protons in the sample by interactions with the unpaired electrons on the paramagnetic metal(s) due to the uncertainty in the energy of transition.[148] The degree of broadening depends on how fast the electrons relax the nuclei and to a certain extent, the number of unpaired electrons. Nuclear-nuclear coupling is unobservable most of the time due to the large peak half-widths as well. Peak shifts are due to the magnetic field of the unpaired electron that affects the local field around the NMR-nucleus and is both a through-space and a through-bond process. In general, resonances that correspond to protons closer to the metal centre through bonds or space will be shifted more compared to those that are more remote.[147] However the amount of the shifts and broadening of the peaks in the NMR spectrum are useful and can provide extra information such as the unpaired electron density at the metal centre, the interaction between metal centres in multinuclear compounds and how different parts of the molecule interact with the metal centre's spin. All of these need precise calculations in order to access quantitative information and since it is beyond the scope of this thesis, it is not explained in any further detail.[149]

A typical ^{1}H NMR spectrum of a paramagnetic transition metal complex usually has resonances in the range of +200 to -200 ppm. Fortunately, even for paramagnetic compounds the integration of peaks is still reflective of the relative number of protons associated with each resonance, hence the integration ratio can be useful to assign peaks, as long as they are not so broad as to render inaccurate integration. With the help of an X-ray structure peaks can be assigned more accurately based on the relative distance of each set of protons to the paramagnetic metal centre. Although it is much more difficult to assign NMR spectra of paramagnetic compounds, even without the full assignment the spectrum can still act as a fingerprint for the new compound, as long as the peaks are observable.

Evans NMR

One additional use of NMR spectroscopy in the characterization of paramagnetic complexes is the use of the Evans method.[150] This method determines μ_{eff} (and potentially the number of unpaired electrons) of complexes in solution and has been extensively used in this thesis as well. The Evans method is based on the difference in

the NMR chemical shift of a diamagnetic solvent or reference standard caused by the unpaired electrons in a paramagnetic sample. The reference material that was used in this thesis was ferrocene, which produces a single sharp peak at a chemical shift of 4 ppm. It is the shift in this peak which is measured, and also corresponds to the shift in the solvent peak as well. The experimental set-up is described in Scheme 1.5.

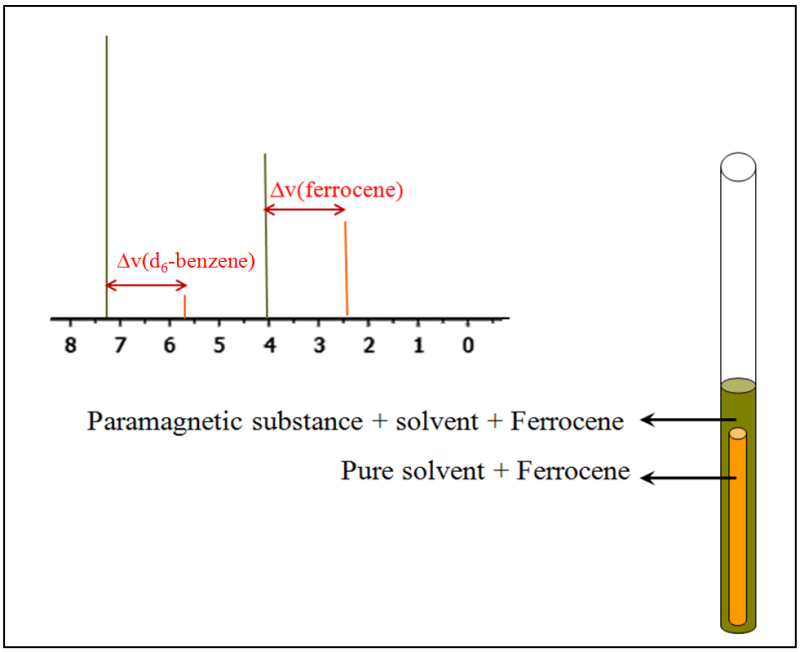

Scheme 1.5. Evans NMR tube and its typical NMR spectrum.

In this method, two NMR tubes are used: a small flame-sealed inner tube (Evans tube) filled with solvent and ferrocene, and an ordinary NMR tube with the paramagnetic sample, solvent and ferrocene. The inner tube can be prepared from a simple melting point tube of about 1/2 the standard NMR tube height. The inner tube is then placed in the outer one (Scheme 1.5). The ferrocene in the inner tube gives a single, sharp peak, while the ferrocene plus the paramagnetic ion in the outer tube gives a single, shifted peak (two other similar peaks will be observed, corresponding to the two NMR solvent peaks as well). Then, the Hz difference in the shifted ferrocene or solvent peak (both should be the same value) can be measured and corresponds to the magnetic susceptibility of the paramagnetic sample. The advantage of this method is its equipment simplicity in addition to the small quantities of paramagnetic sample required, and generates information about the magnetic moment in solution.To calculate the

magnetic moment of the paramagnetic sample, the shift in reference or solvent peak in Hz is given theoretically by following equation:

$$\Delta\nu = \nu_0 4\pi(\chi_v - \chi_{v'})/3$$

($\Delta\nu$: frequency shift, ν_o: proton resonance frequency, χ_v: solution plus the paramagnetic ion volume susceptibility and χ_v': solvent volume susceptibility). The mass susceptibility, χ_g (χ_o: the mass susceptibility of the solvent), of the dissolved ion is given by equation below.

$$\chi_g = (3\Delta\nu/4\pi\nu_o m) + \chi_0 + (\chi_0 (d_0-d_s)/m)$$

Since for highly paramagnetic ions, the last term is negligible, and even the χ_0 (mass susceptibility of the solvent can be ignored), it can be simplified as:

$$\chi = (3\Delta\nu/4\pi\nu_o m)$$

(Δ_ν: frequency shift (Hz); m: the mass of substance contained in 1 cm^3 of solution, , d_o: solvent density and d_s: solution density). It has been shown above that χ_g can be correlated to the molar susceptibility and the number of unpaired electrons via the calculation of μ_{eff}.

1.5.3. Single crystal X-ray crystallography

As mentioned above, the power of NMR spectroscopy is limited for paramagnetic complexes compared to diamagnetic compounds. Since obtaining single crystals of products allows for a generally unambiguous determination of the sample's three-dimensional structure, it is critically important for the characterization of paramagnetic compounds. An X-ray crystal structure reveals the connectivity, bond distances and angles and can provide information about chemical bonds, disorder and various other information. X-ray structural determination (especially with modern CCD detectors) revolutionized the field of coordination chemistry and plays a particularly large role in studying paramagnetic complexes. As a result, in this thesis a substantial number of crystal structures are reported. It should be mentioned that crystals needed for this step are required to be single and within a specific dimension range to remain within the X-

ray beam. Details of the theoretical background of X-ray diffractions can be found in a variety of textbooks on the subject.[147]

2. Halide-bridged iron(II) and cobalt(II) diamido complexes and their reactivity[1]

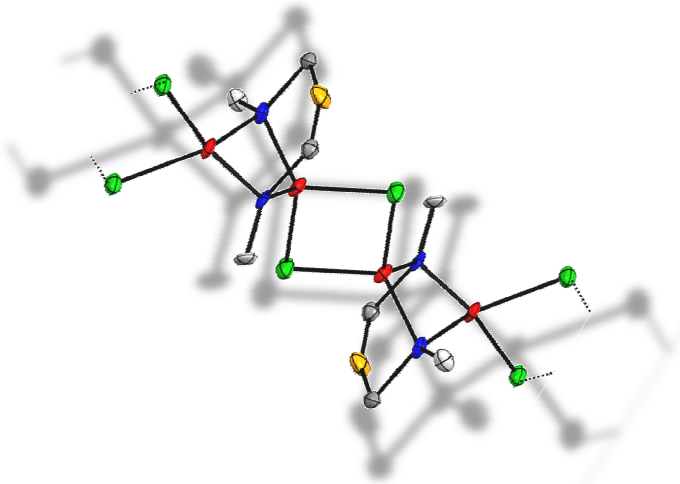

2.1. Introduction

As described in Chapter 1, amido complexes of transition metals are platforms for unusual reactivity and play key roles in the stabilization of intermediates in many catalytic process.[7-8, 151-152] In particular, there has been considerable interest in metal complexes with chelating diamido ancillary ligands because of the ability of the amido ligand to combine steric and electronic flexibility via the straightforward synthetic modification of the R-groups, coupled with the added stability of the chelate effect.[38, 55, 99, 101, 125, 131-134, 136, 143, 153-154] Chelating diamido ligands have been matched with paramagnetic first-row transition metals to a far lesser extent than for diamagnetic metals, especially group 4 to 6 metals such as Zr and Ti; such systems have been investigated vastly and optimized for catalysis applications such as alkene polymerization, and for the activation of small molecules.[135, 140, 155-156]

[1]* Parts of this chapter are adapted with permission from Z. Moatazedi, M. J. Katz and D. B. Leznoff,"Synthesis and characterizaion of a series of halide-bridged, multinuclear iron(II) and cobalt(II) diamido complexes and a dinuclear, high-spin cobalt(II) alkyl derivative" Dalton Trans., 2010, Vol 39, 9889-9896. Copyright Royal Society of Chemistry.

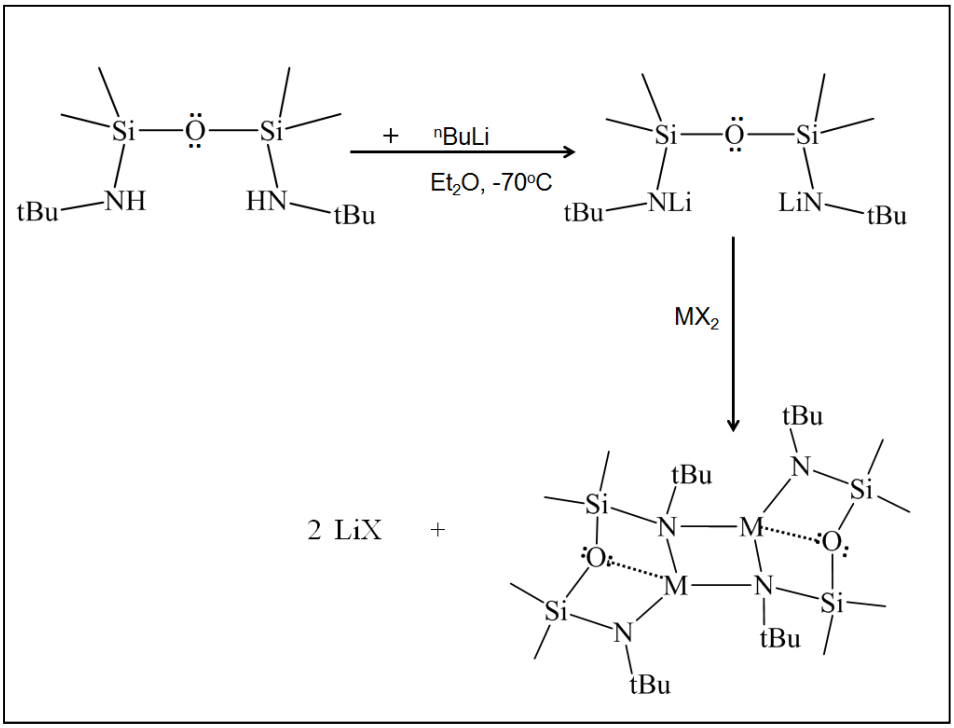

Scheme 2.1 The formation of M(II) diamido-ether complexes (M= Cr, Mn, Fe, Co, Ni and Cu)

The Leznoff group and others have previously described the synthesis of a series of first-row transition metal diamidosilylether- bridged dimer complexes of the form $\{M[^{R}NON]\}_2$ ($[^{R}NON]^{2-}$= $[(RCN^{-}(SiMe_2))_2O]$; R = ^{t}Bu, 2,4,6-$Me_3C_6H_2$, etc), by a 1:1 reaction of M : ligand (Scheme 2.1);[37, 55, 135-137, 140, 145, 155, 157] the silylether donor is hemilabile, binding only in some cases.[137] From the reactivity point of view, the metathesis chemistry of these $\{M[^{R}NON]\}_2$ systems is limited by their lack of a substitutable halide ligand in most cases. Such mixed halide/amido complexes of first-row M(II) centres are very rare and could provide an opportunity for further functionalization at the metal centre via standard metathesis protocols. (see Chapter 3 for the synthesis of metal(II) amido/alkyls).

Thus, the focus of the beginning part of this chapter will be the synthesis and structural characterization of four multinuclear, halide-bridged iron(II) and cobalt(II) diamidosilylether complexes which contain the basic unit $M_2X_2[^{tBu}NON]$ (M=Fe and Co;

X= Cl, Br). Incorporation of both metal-bromo and metal-chloro units were examined in order to evaluate the impact of halide type on structure and reactivity. As mentioned before, there are very few reported examples of mixed amido/halide or amido/alkyl M(II) systems: for example, the $[N_2P_2]MX$ [41, 158-159] (M = Co, Fe; X = Cl, alkyl; $[N_2P_2]$ = $^{t}BuN^{(-)}SiMe_2N(CH_2CH_2P^{i}Pr_2)_2$) and Ar′MN(H)Ar″[53] (M = Mn, Fe, Co; Ar' = C_6H_3-2,6-(C_6H_3-2,6-$^{i}Pr_2$)$_2$, Ar″ = C_6H_3-2,6-(C_6H_2-2,4,6-Me_3)$_2$) systems were recently described.

Moreover, in the new synthesized compounds described here the metal centres are three-, four- or five-coordinate; the three-coordinate site in particular is considered to be a low-coordinate metal centre, in which the metal centre is very sterically and electronically (according to the 18 electron rule) unsaturated. Recent studies have shown that such low-coordinate metal centres can be very reactive and exhibit unusual reactivity, for example toward activation of small molecules.[45, 119, 121] Hence, later in this chapter some reactivity studies of $M_2X_2[^{tBu}NON]$ will also be described.

2.2. Results and Discussion

The reaction of two equivalents of MX_2 with one equivalent of $Li_2[Me_3CN(SiMe_2)]_2O$ ($Li_2[^{tBu}NON]$) generated clusters of the general empirical formula $M_2X_2[^{tBu}NON]$, where X = Br, M = Fe (**1**) and Co (**2**) (Scheme 2.2), and X = Cl, M= Fe (**3**). For M = Co, X = Cl, the LiCl bi-product was retained in the product and $\{Co_2Cl_2[^{tBu}NON](LiCl)\cdot 2THF\}_2$ (**4**) was isolated.

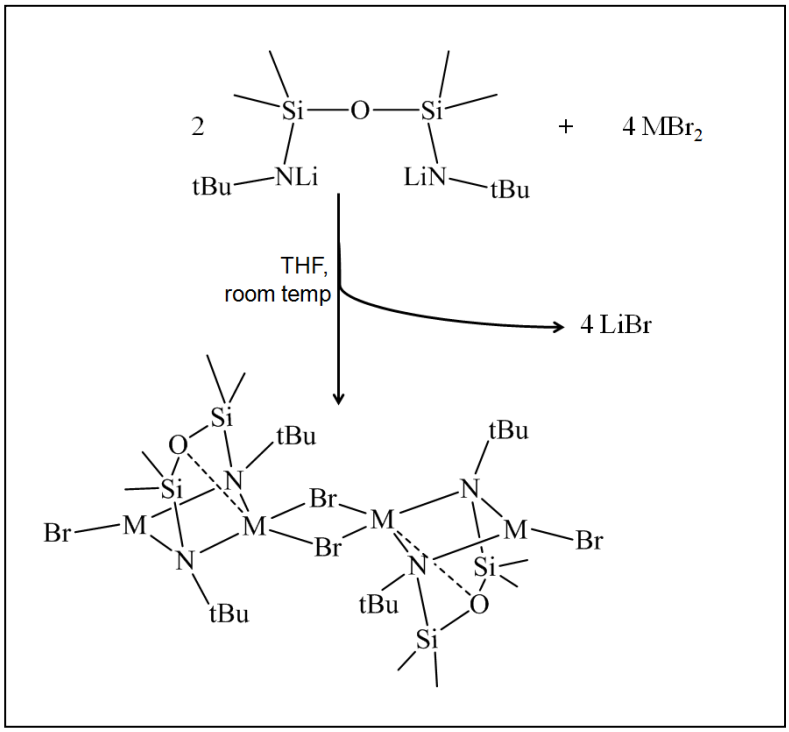

Scheme 2.2. Synthesis of $\{M_2Br_2[^{tBu}NON]\}_2$, (M = Fe(**1**) and Co(**2**)).

Note that the stoichiometry and slow addition of ligand to metal are critical. The 1:1 reaction of $Li_2[^{tBu}NON]$ with MX_2 generates $\{M[^{tBu}NON]\}_2$ (Scheme 2.1),[136, 155] and rapid mixing in a 0.5:1 ligand : metal ratio generates a mixture of $\{M[^{tBu}NON]\}_2$ and $M_2X_2[^{tBu}NON]$. Single crystals suitable for X-ray diffraction were obtained by slow evaporation of a diethylether solution of **1**–**3** and a THF solution of **4**. Attempts to prepare the LiCl-free form of **4** by mixing $CoCl_2$ and $Li_2[^{tBu}NON]$ in diethylether were unsuccessful due to the metal salt's relative insolubility in diethylether; salt extraction in other solvents was also unsuccessful.

2.2.1. Synthesis and characterization of amido/bromide-containing clusters

The X-ray crystal structures of $\{Fe_2Br_2[^{tBu}NON]\}_2$ (**1**) and $\{Co_2Br_2[^{tBu}NON]\}_2$ (**2**) reveal that they have a similar structure, consisting of a binuclear unit with a single $[^{tBu}NON]^{2-}$ ligand bridging between two metal centres in such a way that each amido

ligand is bound to both metal centres. This unit dimerizes via bromide bridges to form a tetranuclear cluster (Figure 2.1). This unusual binding motif has only been previously observed with this type of diamido ligands in $\{Fe_2(NPh_2)_2[^{tBu}NON]\}$.[137]

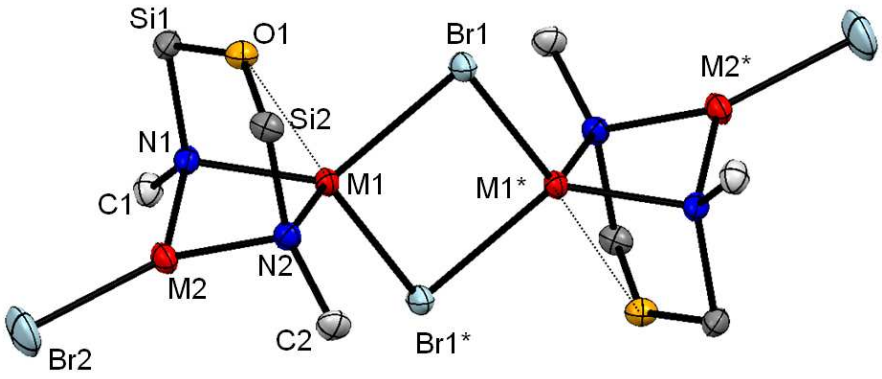

Figure 2.1. Tetranuclear molecular structure of **1** (M= Fe) and **2** (M=Co) (^{t}Bu and $SiMe_2$ groups simplified for clarity).

Table 2.1. Selected interatomic distances (Å) and angles (^{o}) for **1** and **2** $\{M_2Br_2[^{tBu}NON]\}_2$ (M= Fe and Co)

M	Fe(**1**)	Co(**2**)
M1–M2	2.6453(6)	2.5899(3)
M1–M1*	3.6670(8)	3.5815(4)
M1–O1	2.5696(17)	2.5248(10)
M2–O1	3.0809(17)	3.0382(10)
M1–Br1	2.5129(5)	2.4516(2)
M1–Br1*	2.5715(5)	2.5392(3)
M2–Br2	2.3231(6)	2.3112(3)
Si1–N1	1.763(2)	1.7636(13)
Si2–N2	1.765(2)	1.7579(13)
M1–N1	2.068(2)	2.0379(12)

M1–N2	2.0702(19)	2.0281(12)
M2–N1	2.024(2)	1.9799(13)
M2–N2	2.027(2)	1.9840(12)
Br1–M1–Br1*	87.695(17)	88.302(8)
Br1–M1–N1	120.83(6)	126.31(4)
Br1–M1–N2	127.22(6)	121.68(3)
Br1*–M1–N1	115.89(6)	112.92(3)
Br1*–M1–N2	113.39(6)	115.04(4)
O1–M1–Br1	89.15(4)	87.87(2)
O1–M1–Br1*	176.38(4)	175.88(3)
O1–M1–N1	67.34(7)	68.38(4)
Br1*–M1–N2	113.39(6)	115.04(4)
O1–M1–N2	67.31(7)	68.40(4)
N1–M1–N2	93.61(8)	94.08(5)
N1–M2–N2	96.29(8)	97.30(5)

Symmetry operation: -x+1,-y+1,-z+1 for Fe; *: -x+1, -y+2, -z+1 for Co.

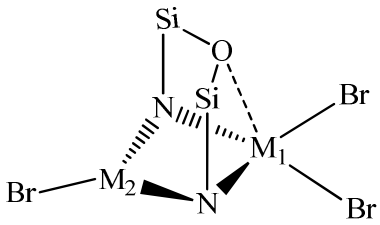

Figure 2.2. The structure of the dinuclear unit and scheme of geometry around each metal centre.

The coordination geometries about the M1 and M2 centres are different (Figure 2.2). The M1 centre is coordinated to both amido donors, two bridging bromides and also interacts with the silylether oxygen donor in the ligand backbone, yielding a

distorted trigonal-bipyramidal geometry with the silylether and one bridging bromide occupying the axial site (Figure 2.2). On the other hand, M2 exists in a roughly trigonal geometry in which it is coordinated only to one terminal bromide and the two amido groups, as shown in Figure 2. 2. The Fe1–O1 and Co1–O1 distances of 2.5696(17) and 2.5248(10) Å respectively (Table 2.1) indicate that a M–O interaction is present; these values compare well with those in $\{[^{tBu}NON]Co\}_2$[136] (Co–O: 2.448(4) Å) and $\{[^{tBu}NON]Fe\}_2$[155] (Fe–O: 2.512(2) Å). Conversely, there is no interaction between the M2 centres and the silylether donor, with Fe2–O1 and Co2–O1 distances of 3.0809(17) and 3.0382(10) Å respectively. The Fe amido distances range from 2.024(2) to 2.0702(19) Å and the analogous Co-amido distances span 1.9799(13) to 2.0379(12) Å; these are comparable with the M–N bond lengths (M = Fe, Co) in the $\{[^{tBu}NON]M\}_2$ systems, despite the fact that both amido groups are bridging metal centres in **1** and **2** vs. a combination of terminal and bonding amides in $\{[^{tBu}NON]M\}_2$. The terminal Fe2–Br2 bond length of 2.3231(6) Å is considerably shorter and the Fe1–Br1 bond length of 2.5715(5) Å is considerably larger compared to the bridging Fe–Br bond length of 2.4601(11) Å in $\{FeBr_2Li[Me_3PhNSiMe_2]_2O\}_2$.[43] A similar spread exists in **2**, with Co1–Br1 and Co2–Br2 bond lengths of 2.5392(3) and 2.3112(3) Å respectively. The long M1–Br1 lengths in the central core are consistent with their bridging nature, and also reflect the fact that M1 is more electron rich by virtue of its higher coordination number. The Fe1–Fe1* distance of 3.6670(8) Å and Co1–Co1* distance of 3.5815(4) Å preclude any bonding interaction between these metal centres (i.e., between dimers), but the Fe1–Fe2 distance of 2.6453(6) Å and Co1–Co2 distance of 2.5899(3) Å are much shorter and can be compared with those in other related complexes in which direct metal-metal interactions could be present, including Fe–Fe: 2.5795(6) Å in $\{Fe_2[NPh_2]_2[^{tBu}NON]\}$,[28] Co–Co: 2.468(3) Å in $\{[^{tBu}NON]Co\}$,[136] Co–Co: 2.566(3) Å in $[Co_2(NPh_2)_4]$,[158] and Fe–Fe: 2.503(2) in $Fe_2(CO)_6S_2$.[160-161]

The ^{1}H NMR spectra of **1** and **2** have similar features (Figure 2.3): as expected for paramagnetic iron and cobalt complexes, they both show broad, shifted peaks. However as described in Chapter 1, the integration can still be valid. All of the silyl-methyl groups are equivalent, as are the t-butyl groups. The equivalency of the silyl-methyl groups suggests that the silylether donor is likely oscillating rapidly between the two metal centres in a fluxional process at room temperature, yielding an average signal.

In addition, in THF solution the halide bridges likely break up, yielding simple dinuclear clusters (see magnetism below); this can also contribute to the observation of equivalent signals for the silyl-methyl groups .

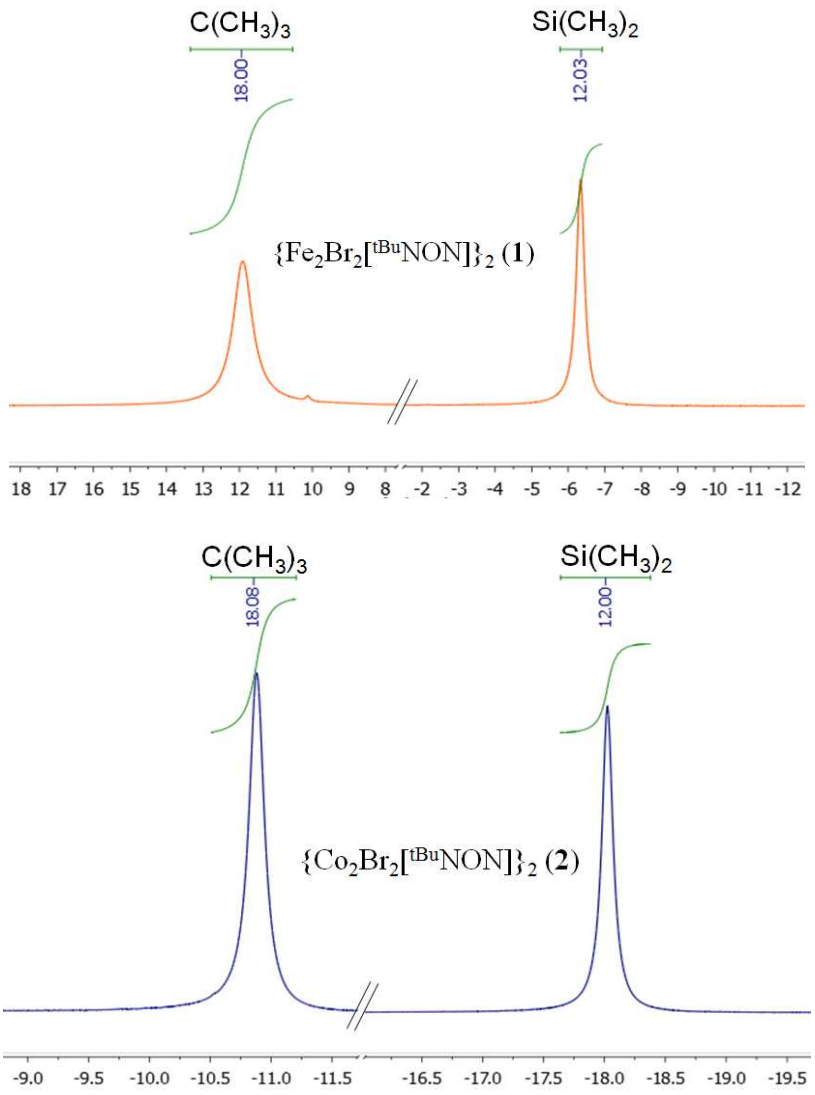

Figure 2.3. ^{1}H NMR spectra of **1** and **2** in THF-d_8.

This behaviour in the ^{1}H NMR spectra is unlike what was observed for the {[^{tBu}NON]M}$_2$ (M = Co, Fe) systems, for which their ^{1}H NMR spectra showed two peaks

assignable to each t-butyl and $SiMe_2$ group, consistent with their inequivalence in the solid state. The peaks are broader for the two Fe(II) complexes than for the Co(II) analogue. For example the half-height width of the t-butyl peak is 0.75 ppm for $\{Fe_2Br_2[^{tBu}NON]\}_2$ (**1**), compared to 0.25 ppm for $\{Co_2Br_2[^{tBu}NON]\}_2$ (**2**). As mentioned in Chapter 1, the unpaired electron density around nuclei results in peaks broadening. Since the metal centres in both **1** and **2** have a similar geometry and coordination sphere, their total spin difference is small (only one unpaired electron different), hence the difference in the broadening for iron and cobalt complexes is not huge.

2.2.2. Synthesis and characterization of amido/chloride containing systems

Upon switching the bromide for chloride (via reaction of $Li_2[^{tBu}NON]$ with MCl_2 in place of MBr_2; M = Fe, Co), different structures are obtained, although the basic $M_2Cl_2[^{tBu}NON]$ unit remains intact. The X-ray crystal structure of $\{Fe_2Cl_2[^{tBu}NON]\}_n$ (**3**) reveals that, unlike the discrete tetranuclear clusters found in **1** and **2**, it consists of an infinite 1-D chain of chloride-bridged $Fe_2Cl_2[^{tBu}NON]$ units (Figure 2.4).

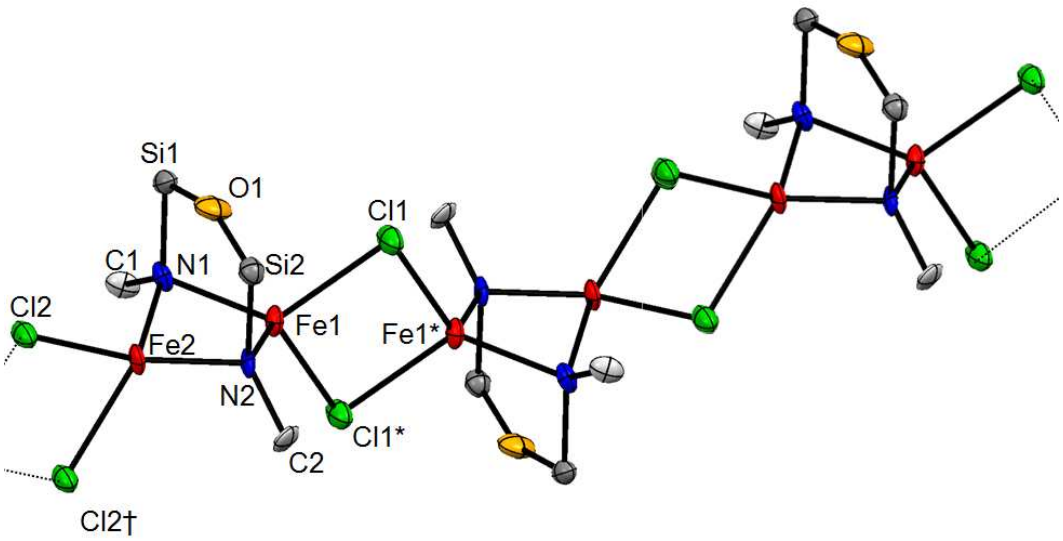

Figure 2.4. Extended 1-D chain structure of **3** (^{t}Bu and $SiMe_2$ groups simplified for clarity).

Table 2.2. Selected interatomic distances (Å) and angles (°) for $\{Fe_2Cl_2[^{tBu}NON]\}_n$ (**3**)

Fe1–Fe2	2.656(2)	Cl2–Fe2–N1	116.7(2)
Fe1–Fe1*	3.539(4)	Cl1–Fe1–Cl1*	85.06(13)
Fe1–O1	2.782(8)	Cl2–Fe2–Cl2†	83.44(11)
Fe2–O1	2.922(7)	Cl1–Fe1–N1	122.2(3)
Fe1–Cl1	2.398(3)	Cl1–Fe1–N2	117.7(3)
Fe2–Cl2	2.409(3)	Cl2–Fe2–N1	116.7(2)
Fe2–N1	2.085(9)	Cl2–Fe2–N2	123.9(2)
Fe2–N2	2.061(8)	Cl1* –Fe1–N1	122.1(2)
Si1–O1	1.648(7)	Cl1*–Fe1–N2	115.9(2)
Si2–O1	1.637(7)	Cl2–Fe2–N1	118.3(3)
Si1–N1	1.778(8)	Cl2–Fe2–N2	120.5(3)
Fe1–Cl1*	2.405(3)	Si1–O–Si2	154.8(5)
Fe2–Cl2†	2.400(3)	N1–Fe1–N2	96.0(3)
Fe1–N1	2.061(9)	N1–Fe2–N2	96.29(8)
Fe1–N2	2.089(9)		
Si2–N2	1.785(8)		

Symmetry operation: *: -x,-y+1,-z and †:-x,-y+1,-z+1.

Although there are two crystallographically different iron sites in the cluster, the coordination geometries about both iron centres are similar: a distorted tetrahedral centre with coordination to both amido donors and two chloride bridges. Unlike in **1** and **2**, where the silylether donor was preferentially bonded to one M site, in **3** the Fe1–O1 and Fe2–O2 distances of 2.782(8) and 2.922(7) Å respectively indicate that this bonding is more equally shared, and is very weakly bound, if at all, to both iron centres (Table 2.2). The Fe–amido distances are comparable with those in $\{[^{tBu}NON]Fe\}_2$,[25] **1** and **2**, while the Fe1–Cl1 distances of 2.398(3) to 2.400(3) Å are unremarkable and comparable to the Fe–Cl distances of 2.318(1) Å in $LFeCl_2$[36] (L = tridentate

bis(imino)carbazolide ligands) as an example. The Fe1–Fe* distance of 3.539(4) Å precludes any interdimer bonding interaction between the metal centres but the intradimer Fe1–Fe2 distance of 2.656(2) Å is similar to that of **1**.

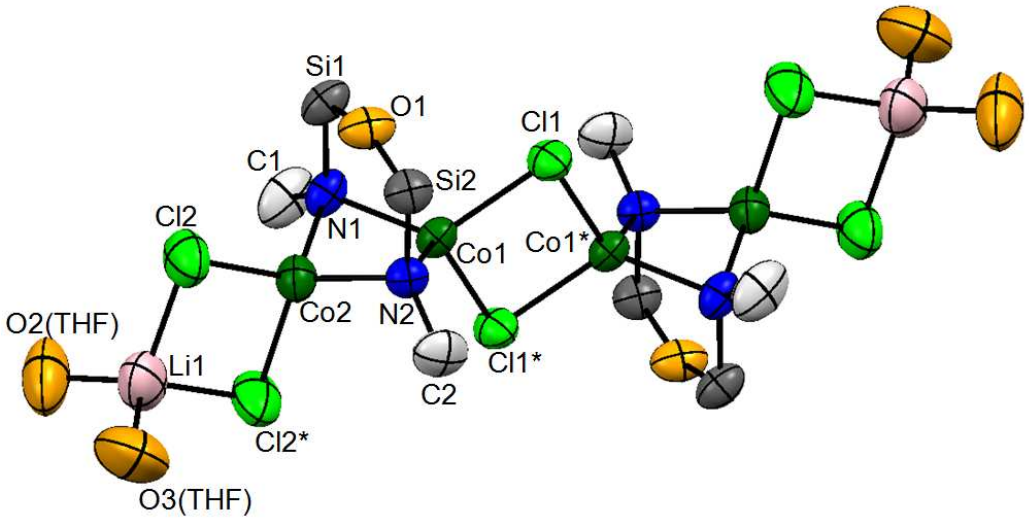

Figure 2.5. Molecular structure of **4** (^{t}Bu, $SiMe_2$ and THF groups simplified for clarity).

The structure of the chloro-cobalt analogue **4** is also different, although the dinuclear $\{Co_2Cl_2[^{tBu}NON]\}$ unit remains at the core. The X-ray structure of **4** reveals a tetranuclear "ate" complex with two dinuclear units connected via chloride bridges. Thus, unlike the Fe(II) analogue **3**, **4** does not form a 1-D chain, but is terminated by one LiCl and two THF molecules on both ends of the tetranuclear cluster (Figure 2.5).

Table 2.3. Selected interatomic distances (Å) and angles (°) for $\{Co_2Cl_2[^{tBu}NON](LiCl)\cdot 2THF\}_2$ (**4**)

Co1–Co2	2.6543(12)	Cl1–Co1–Cl1*	86.80(6)
Co1–Co1*	3.4114(16)	Cl2–Co2–Cl3	96.38(8)
Co1–O1	2.881(4)	Cl1–Co1–N1	119.22(14)
Co2–O1	2.948(4)	Cl1*–Co1–N1	120.95(15)
Co1–Cl1	2.3785(17)	Cl1–Co1–N2	118.26(13)
Co1–Cl1*	2.3164(18)	Cl1*–Co1–N1	120.95(15)
Co2–Cl2	2.296(2)	Si1–O–Si2	152.1(3)
Si2–N2	1.752(5)	Li1–Cl2–Co2	84.3(4)
Si1–O1	1.638(4)	Li1–Cl3–Co2	84.9(4)
Si2–O1	1.625(4)	Co1–N1–Co2	80.07(17)
Cl2–Li1	2.363(16)	Co1–N2–Co2	80.32(15)
Cl3–Li1	2.319(16)	N1–Co2–N2	93.46(17)
Li1–O41	1.918(14)	Si1–N1	1.750(5)
Li1–O3	1.925(13)	Co1–N2	2.046(4)
Co1–N1	2.048(5)	Co2–N1	2.078(5)
Co2–N2	2.069(4)		

Symmetry operation: *: x-1,y-1,z-1

The coordination geometry about Co1 and Co2 is approximately the same: a distorted tetrahedral geometry from binding to two chlorides and the bridging diamido ligand (not including any Co–Co interaction). The Co1–O1 and Co2–O1 distances of 2.881(4) and 2.948(4) Å respectively (Table 2.3), similar to the analogue Fe-O distances in 3, indicate that no significant interaction is present. The interdimer Co1–Co1* distance of 3.4114(16) Å is shorter and the intradimer Co1–Co2 distance of 2.6543(12) Å is longer compared to the Co1–Co1* and Co1–Co2 distances of 3.5815(4) and 2.5899(3) Å respectively in **2**. The other bond lengths are comparable to those in **1**–**3**.

Table 2.4. M1–O1 and M2–O2 distances and coordination number around M1 and M2 in **1**-**4**

	M1–O1(Å)	**M2–O1(Å)**	**Geometry of M1**	**Geometry of M2**
Fe/Br (**1**)	2.5696(17)	3.0809(17)	5, trigonal bipyramidal	3, trigonal
Co/Br (**2**)	2.5248(10)	3.0382(10)	5, trigonal bipyramidal	3, trigonal
Fe/Cl (**3**)	2.922(7)	2.782(8)	4, distorted tetrahedral	4, distorted tetrahedral
Co/Cl (**4**)	2.881(4)	2.948(4)	4, distorted tetrahedral	4, distorted tetrahedral

Examining the structures of **1**–**4** in a comparative sense, in **3** and **4**, the M–O distances in the dinuclear unit in the chloro-analogues **3** and **4** indicate an equally weak interaction with both metal centres, while the bromo- analogues **1** and **2** show asymmetry in the [^{tBu}NON] silylether metal bonding (i.e., a significant M1–O1 interaction and no M2–O1 contact) (Table 2.4). The impact of changing the halide on the structure (i.e., the formation of discrete tetranuclear clusters for bromide-based **1** and **2** vs. a 1-D cluster chain of dimers or an "ate" complex for **3** and **4**) respectively could be attributed to the larger size of bromide vs. chloride. For the bromo-based complexes **1** and **2**, the change in transition metal had no structural impact, whereas for the chloro analogues **3** and **4**, switching cobalt(II) for iron(II) resulted in different structures. This can likely be traced to solubility differences; **3** was extracted from diethylether while **4** was extracted from THF solution (attempts to obtain a salt-free version of **4** from diethylether or other solvents failed). Note that the salt-incorporation is not an impediment to further metathesis reactivity of the cobalt(II) "ate" complex (Chapter 3).[145]

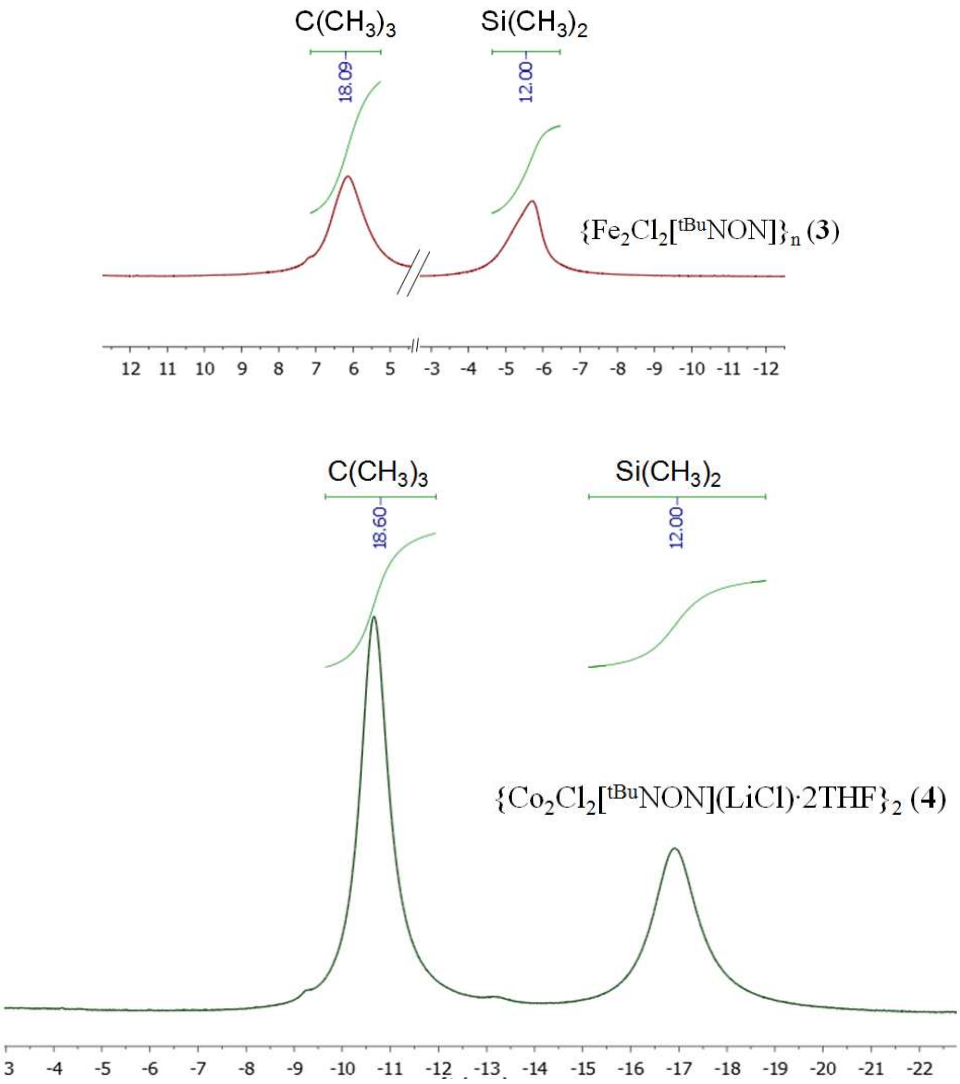

Figure 2.6. ^{1}H NMR spectra of **3** and **4** in THF-d_8.

The ^{1}H NMR spectra of **3** and **4** also have similar features as **1** and **2** (Figure 2.6): two broad, shifted peaks, assigned to the t-butyl (18 H) and silyl-methyl (12 H) groups. Comparing ^{1}H NMR spectra shows that the position of peaks in Fe-complexes **1**

and **3** are quite similar; the t-butyl group has a positive chemical shift and the $SiMe_2$ is upfield of TMS (Table 2.5).

Table 2.5. ^{1}H NMR chemical shifts of t-butyl and silyl-methyl groups for **1**-**4**.

	C(C*H*$_3$)$_3$ (ppm)	**Si(C*H*$_3$)$_2$ (ppm)**
(**1**) $\{Fe_2Br_2[^{tBu}NON]\}_2$	+12.0	-6.0
(**3**) $\{Fe_2Cl_2[^{tBu}NON]\}_n$	+6.0	-5.8
(**2**) $\{Co_2Br_2[^{tBu}NON]\}_2$	-10.9	-18.1
(**4**) $\{Co_2Cl_2[^{tBu}NON]\}_2$	-10.5	-17.0

It appears that the t-butyl (18 H) and silyl-methyl (12 H) groups are equivalent in solution and in a similar position relative to each other; in all cases the silyl-methyl peak is upfield of the t-butyl peaks. The peaks are broader for the two Fe(II) complexes than for the Co(II) analogues, due to the unpaired electron density difference as mentioned before. Looking into the position of each peak and how much it is shifted based on the ^{1}H NMR spectra can provide valuable information such as the spin-density around the metal centre, the interaction of each set of protons (and the unpaired spin density) with the metal centre through bonds or through space, but these require calculations which are beyond the scope of this thesis.

2.2.3. Magnetic properties

In order to corroborate the metal-spin state assignment and examine any potential magnetic interactions the temperature (T) dependence of the magnetic susceptibility (χ_m) of **1**–**4** was measured from 1.8–300 K.

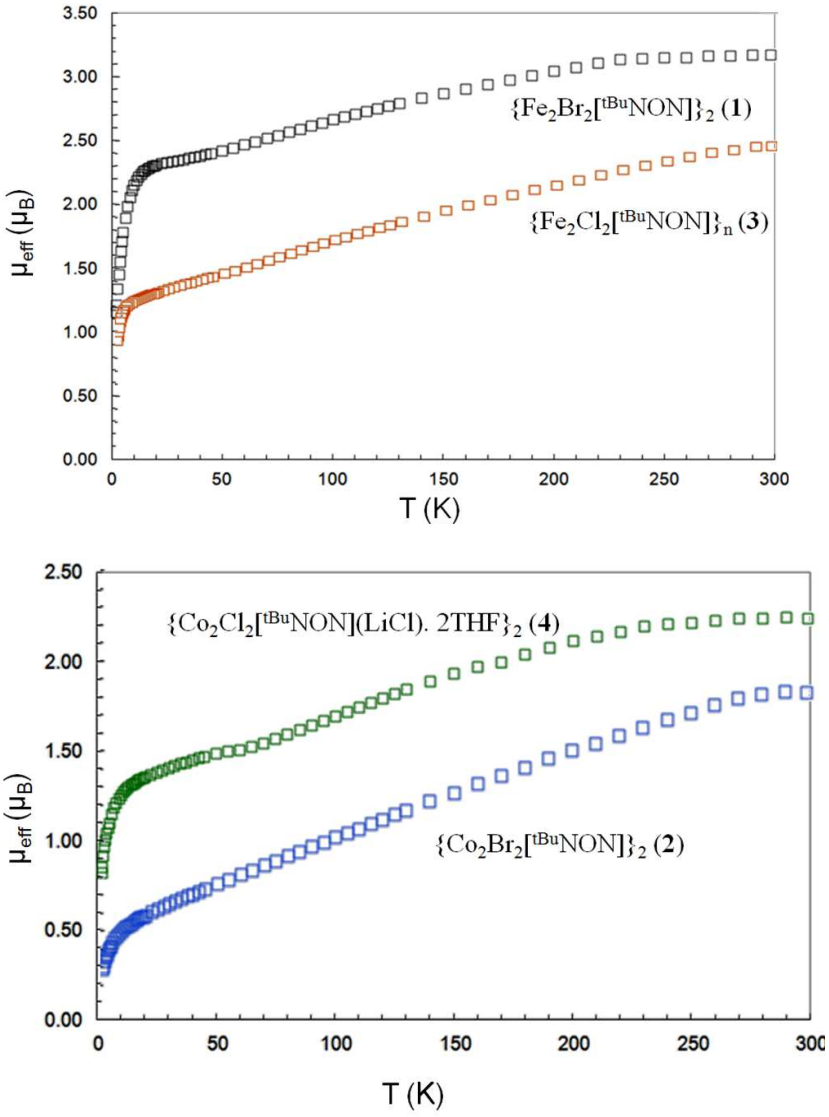

Figure 2.7. Plot of the magnetic moment (μ_{eff}) vs. temperature (T) for **1**-**4**.

Plots of μ_{eff} vs. T per metal centre for **1**–**4** are shown in Figure 2.7. The values at 300 K are smaller than what are expected for isolated high-spin mononuclear Fe(II) (S= 2, d^6) or Co(II) (S= 3/2, d^7) high spin complexes in a four-coordinate tetrahedral geometry (μ_{eff} = 4.89 and 3.87 μ_B respectively for spin-only systems). The profiles of the μ_{eff} vs. T curves are similar and drop with decreasing temperature, indicative of antiferromagnetic coupling between the metal centres; e.g., for **1** μ_{eff} = 3.15 μ_B per Fe(II)

at 300 K, dropping to 1.17 μ_B at 1.8 K. Note that for none of the reported compounds are maxima in χ_m *vs*. T present, indicating that the observed antiferromagnetic coupling is still rather weak. Complexes **1**–**4** have both short M–M distances within the $M_2X_2[^{tBu}NON]$ core and halide-bridges between cores; both structural features are capable of mediating magnetic interactions. The observed coupling in clusters **1**–**4** is qualitatively similar to that in $\{[^{tBu}NON]M\}_2$ dimers (M = Fe(II),[155] μ_{eff} = 3.37 μ_B; M = Co(II),[136] μ_{eff} = 1.84 μ_B at 300 K), however, the geometric parameters of the respective dinuclear units are quite different, as is the ligand binding motif. Below 15 K the magnetic moments of **1**–**4** drop more rapidly, likely due to zero-field splitting. The simultaneous presence of weak- to-moderate antiferromagnetic coupling and zero-field splitting renders the quantitative modeling of the magnetic properties of limited value and thus was not pursued. $Fe_2(NPh_2)_2[^{tBu}NON]$, which has the same ligand binding motif and similar bond lengths and angles in its dinuclear, $Fe_2[^{tBu}NON]$ core has a μ_{eff} of 4.5 μ_B per iron centre at 300 K in the solid-state and in solution, indicating only weak antiferromagnetic coupling between the two iron centres of the dimer at this temperature.

However, although **1** and **3** have lower μ_{eff} values at 300 K in the solid-state (3.15 and 2.47 μ_B respectively), upon dissolution in THF the μ_{eff} of **3** rises to μ_{eff} = 4.6 μ_B (Evans method),[162] [150] thereby yielding a comparable value to the strictly dinuclear $Fe_2(NPh_2)_2[^{tBu}NON]$ system and indicating that the intradimer metal-metal or amido–mediated interactions are weak despite their proximity. In solution, the chloride-bridges are likely broken, yielding discrete $Fe_2Cl_2[^{tBu}NON]$ units (see the discussion of the solution ^{1}H NMR spectra). Thus, the main antiferromagnetic contribution in **1** and **3** appears to be mediated by the halide bridges rather than Fe–Fe orbital overlap or amido-ligand-mediated superexchange. The μ_{eff} values for **3** are lower at all temperatures than for **1**, possibly due to presence of more halide bridges in 1-D **3** vs. discrete tetranuclear **1**. For the S=3/2 Co(II) clusters **2** and **4** the μ_{eff} values are smaller than for the S=2 Fe(II) analogues, as expected. The smaller value of μ_{eff} at 300 K of **2** compared to **4** (1.84 vs. 2.23 μ_B) may reflect a combination of cobalt(II) bromide *vs*. chloride orbital overlap differences and the smaller Co1–Co2 distance of 2.5899(3) Å in **2** compared to 2.6543(12) Å in **4**.

2.2.4. Metal-Metal orbital overlap in new multinuclear systems 1-4

In all of **1**-**4** there are two different metal-metal distances: M1-M1* are relatively long, however M1-M2 distances are much shorter (Figure 2.1 and Table 2.6).

Table 2.6. Room temperature magnetic moment, inter-cluster and intra-cluster M-M distances for **1**-**4**.

	M1-M2 (Å)	**M1-M1* (Å)**	**μ_{eff} (μ_B), room temperature**
(**1**) $\{Fe_2Br_2[^{tBu}NON]\}_2$	2.5899(3)	3.5815(4)	3.15
(**2**) $\{Co_2Br_2[^{tBu}NON]\}_2$	2.6453(6)	3.6670(8)	1.84
(**3**) $\{Fe_2Cl_2[^{tBu}NON]\}_n$	2.656(2)	3.539(4)	2.47, (4.6: Evans method)
(**4**) $\{Co_2Cl_2[^{tBu}NON]\}_2$	2.6543(12)	3.4114(16)	2.23

The short M-M distances could generate metal orbital overlap, but it is also possible that the coordination of the metal centre facilitates such short distances without any orbital overlap. Hence the discussion of the possibility of the presence of any M-M bonds needs more evidence than only short distances.[163-165] The Fe-Fe distances of 2.5899(3) and 2.656(2) Å in **1** and **3** respectively, are longer compared to that of the 2.371 Å in $Fe_2(HNCH)_4$,[166] which has been identified as having a viable Fe-Fe bond, and the Co-Co distances of 2.6453(6) and 2.6543(12) Å in **2** and **4** respectively are also longer compared to that of the 2.530 Å in $Co_2(CS)_2(CO)_6$, which has also a recognized Co-Co bond.[167]

However, one powerful evidence that could help is examining the magnetic properties of the metal centres because metal-metal overlap should result in strong and significant antiferromagnetic coupling due to the spin pairing.[168-169] For example, for the Co-Co distances of 2.566(3) and 2.583(1) Å in $[Co_2(NPh_2)_4]$[170] and $[Co_2(N(SiMe_3)_2)_4]$,[171] room temperature magnetic moments of 1.72 μ_B and 4.83 μ_B respectively were reported, indicating the presence of metal-orbital overlap in the first compound while metal overlap is not likely present in the second one. As similar result also was observed for $\{Co[^{tBu}NON]\}_2$[136] with a Co-Co distance of 2.5682(13) Å, higher than that of 2.468(3) Å in $\{Co[^{Me_3Ph}NON]\}_2$.[135] However the room temperature magnetic moment of 1.8 μ_B in

{Co[^{tBu}NON]}$_2$ indicates the presence of more metal orbital overlap compared to {Co[^{Me_3Ph}NON]}$_2$, with a μ_{eff} of 3.8 μ_B.

However, as mentioned in the magnetic properties discussion all of **1**-**4** show antiferromagnetic properties. Based on the Evans NMR in THF-d_8, it is clear that the main coupling comes from the halide bridges and not the metal-metal orbital overlap or amido bridge. In other words, any M-M overlap that may be present in **1**-**4** is quite weak. Molecular orbital calculations could help to have a more accurate estimation of the overlap percent and should be explored in future.

2.2.5. Attempts to prepare analogous Cr(II), Cr(III) and Fe(III) clusters:

The addition of 1 equivalent of ligand to 2 equivalents of $CrCl_2$ or $CrCl_3 \cdot 3THF$, unlike the similar reactions with Co(II) and Fe(II), resulted in the unkown products which were mainly insoluble even in THF, and attempts to isolate and characterize the products in both cases were unsuccessful.

There was also an attempt to prepare similar a Fe(III)-containing cluster, by direct reaction of 2 equivalents of $FeCl_3$ and one equivalent of Li_2[^{tBu}NON]; this resulted in a purple mixture which was identified as {FeCl[^{tBu}NON]}$_2$[55] by its ^{1}H NMR spectrum matches with the reported {FeCl[^{tBu}NON]}$_2$ ^{1}H NMR. This compound has been previously reported to be synthesized by mixing a 1:1 ratio of ligand and metal halide.

The difficulty in these cases might come from the fact that Fe(III), Cr(II) and Cr(III) have preferred different coordination geometries which do not ideally match the orbital overlap requirements of the metal centre in the M_2Cl_2[^{tBu}NON] unit, and the metal's resulting coordination geometry change would not match with the same structure any more. As well, they have less d-electrons compared to Fe(II) and Co(II), hence the low coordination number around the metal centre might be very unstable for these systems.

2.2.6. Reactivity of Multi-Nuclear Amido-halide Clusters 1-4

In this chapter we reported three- and four-coordinate iron(II) and cobalt(II) diamido complexes, which could be classified as low-coordinate species. The reactivity of low-coordinate metal centres can be very interesting, however it depends on the ligand considerably; in some cases the ligand is so bulky that it prevents the metal centre from further undergoing reactivity. Many advances in new chemistry have developed as a result of examining reactivity of metal centres in different geometries, including C−H or C−F bond activation, C−C coupling or small molecule activation.[45, 120-122] One potential reaction of **1**-**4** is the substitution of halide for alkyl groups to obtain new organometallic complexes of iron(II) and cobalt(II); this will be discussed more extensively in Chapter 3. Since **1**-**4** contain low-coordinate metal centres there is the potential to add extra neutral donor ligands to the metal coordination sphere to reach new geometries. Also, the presence of the M−halide in **1**-**4** suggests the possibility of other metathesis and also reduction reactions at the metal centres and hence, accessing unusual geometries and reactivities such as small molecule activation.

In addition the study of bimetallic complexes and metal-metal interactions, which started in the mid 1970s,[172] point out some advantages, such as the versatility in M–M bonding, the availability of multiple *d*-electrons, and additional coordination sites for substrate binding.[173] The study of such systems are also important from the theoretical point of view, looking for possible orbital interactions between the two metal centres[174-175] As shown, in **1**-**4** there is a bimetallic core, with the possibility of a weak metal-metal interaction; such an interaction might affect the reactivity of each metal centre in a cooperative manner and result in different chemistry than if the complex only contained a single metal centre.[176] In theory, such multimetallic clusters can be good models for the chemistry of metal surfaces as well.[177-179]

Reduction with KC_8

In all of the iron and cobalt **1**-**4** multinuclear compounds the presence of a metal-halide bond suggested them to be suitable candidates for reduction at the metal centre, with dinitrogen activation as a target, hence an attempt was made to reduce the metal centres in $\{Fe_2Cl_2[^{tBu}NON]\}_n$ and $\{Co_2Cl_2[^{tBu}NON](LiCl)\cdot 2THF\}_2$ with KC_8 or $KBEt_3H$ in THF.

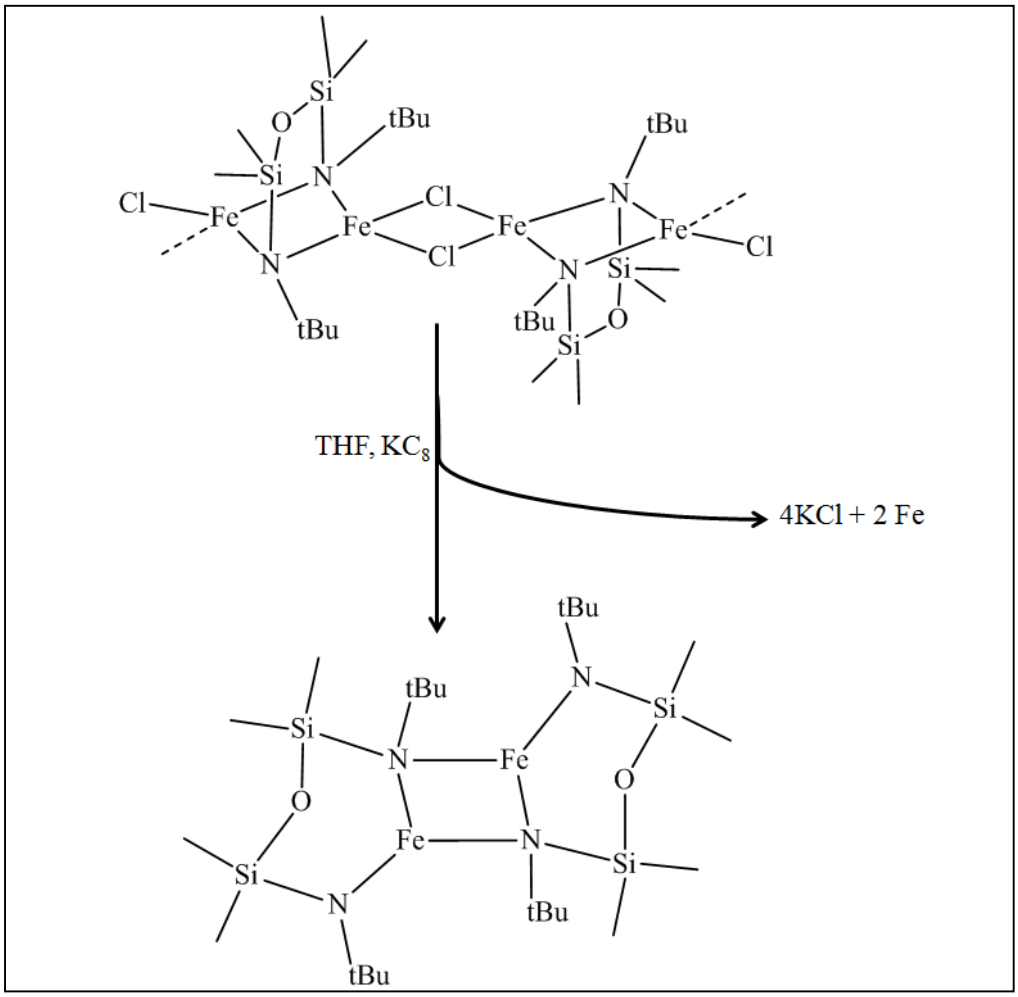

Scheme 2.3. Reduction of **3** with KC_8.

However, the two products of the reductions in both cases were the known $\{Fe[^{tBu}NON]\}_2$ and $\{Co[^{tBu}NON]\}_2$ (according to ^1H NMR data) and Fe or Co metal powder (Scheme 2.3). It is possible that instead of the reduction of each metal centre by one electron, one of the iron (or cobalt) centres was reduced to Fe(0) and the other Fe centre retained the ligand with no reduction. This could be as a result of the presence of an unstable, low-coordinate metal centre intermediate. Thus, the presence of another neutral donor ligand was thought to be potentially helpful to stabilize the low-coordinate metal centres more during the reduction, and so the reaction of **3** with a series of neutral donors was targeted, with the intent of then reducing the adducts thereby formed.

Reaction of $\{Fe_2Cl_2[^{tBu}NON]\}_n$ with neutral donor ligands

Phosphines

In order to stabilize a low-valent, low-coordinate metal centre, trialkyl phosphines ligands were targeted since they are usually weak π-acceptors and strong σ-donor ligands (depending on the R-group). In addition transition metal amide/phosphine compounds have been shown to be good candidates for further reduction and small molecule activation.[107-108] Thus, one equivalent of 1,2-bis(dimethylphosphino)ethane (dmpe) per dinuclear unit was added to $\{Fe_2Cl_2[^{tBu}NON]\}_n$ (**3**), but instead of simply adding the neutral ligand to the metal centre, it resulted in ligand redistribution to form the known $\{(dmpe)_2FeCl_2\}$[180] (identified by an X-ray crystal structure) and $\{Fe[^{tBu}NON]\}_2$ (identified by ^{1}H NMR) (Scheme 2.4).

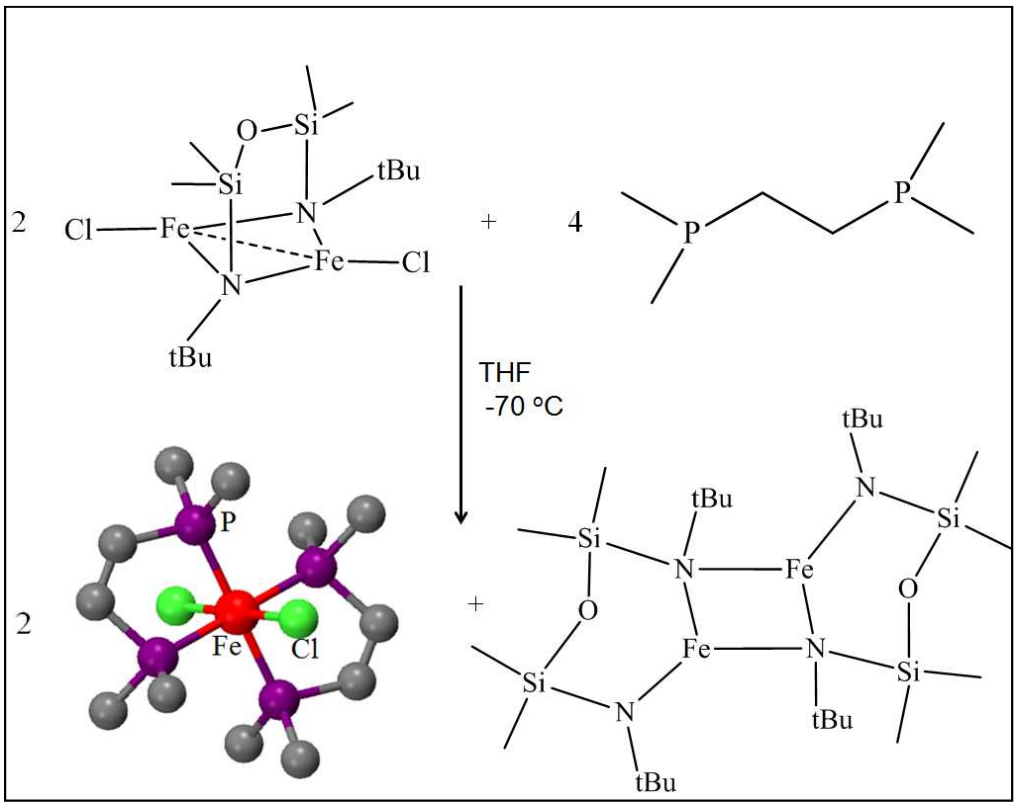

Scheme 2.4. The reaction of **3** and dmpe.

The idea of using dmpe was to bridge between two iron centres (as will be shown in Chapter 3); however, dmpe acted as a better chelating ligand in this case. Hence, with dmpe chelating to one iron centre, the coordination sphere of that metal would be too crowded to be stable, as a result leading to the formation of the two ligand-redistributed, less crowded and more stable iron(II) complexes. In future it is worth trying less bulky mono-phosphines such as PMe_3.

Carbenes

Carbene ligands are stronger σ-donors than phosphines and tend to form stronger bonds to the metal centre.[181] They have a neutral divalent carbon atom that can act as either two singly occupied nonbonding orbitals (a triplet state) or a lone pair and an accessible vacant orbital (a singlet state).[182] 1,3-bis-(2,4,6-trimethylphenyl)imidazol-2-ylidene carbene, a very common "N-heterocyclic" carbene (NHC) was chosen as the target ligand. Thus, one equivalent of 1,3-bis-(2,4,6-trimethylphenyl)imidazol-2-ylidene per iron centre was added to $\{Fe_2Cl_2[^{tBu}NON]\}_n$.

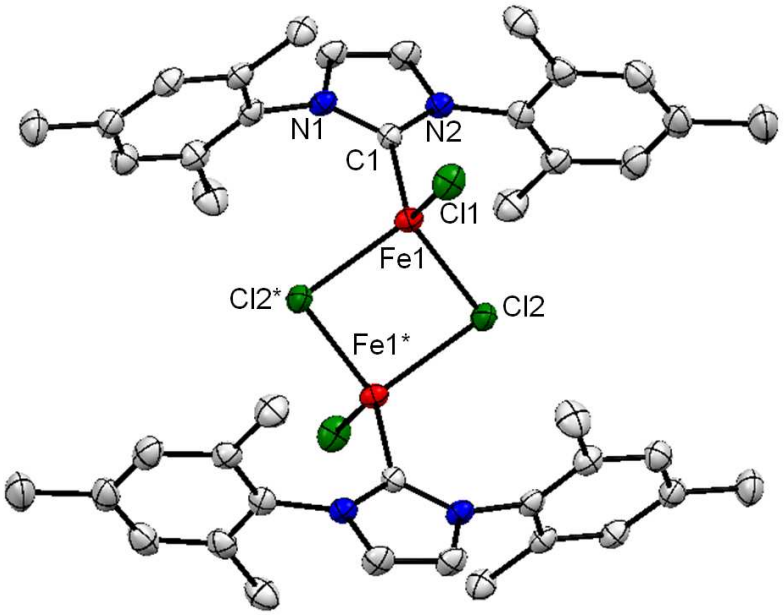

Figure 2.8. X-ray crystal structure of **5**.

However, the result was similar to the result of the reaction of dmpe and **3**: the transfer of the carbene to a $FeCl_2$ fragment and simultaneous formation of $\{Fe[^{tBu}NON]\}_2$ (Figure 2.8). The resulting $\{[NHC]FeCl_2\}_2$ (**5**) complex biproduct was previously reported by direct addition of the NHC ligand to the $FeCle_2(THF)_{1.5}$.[183]

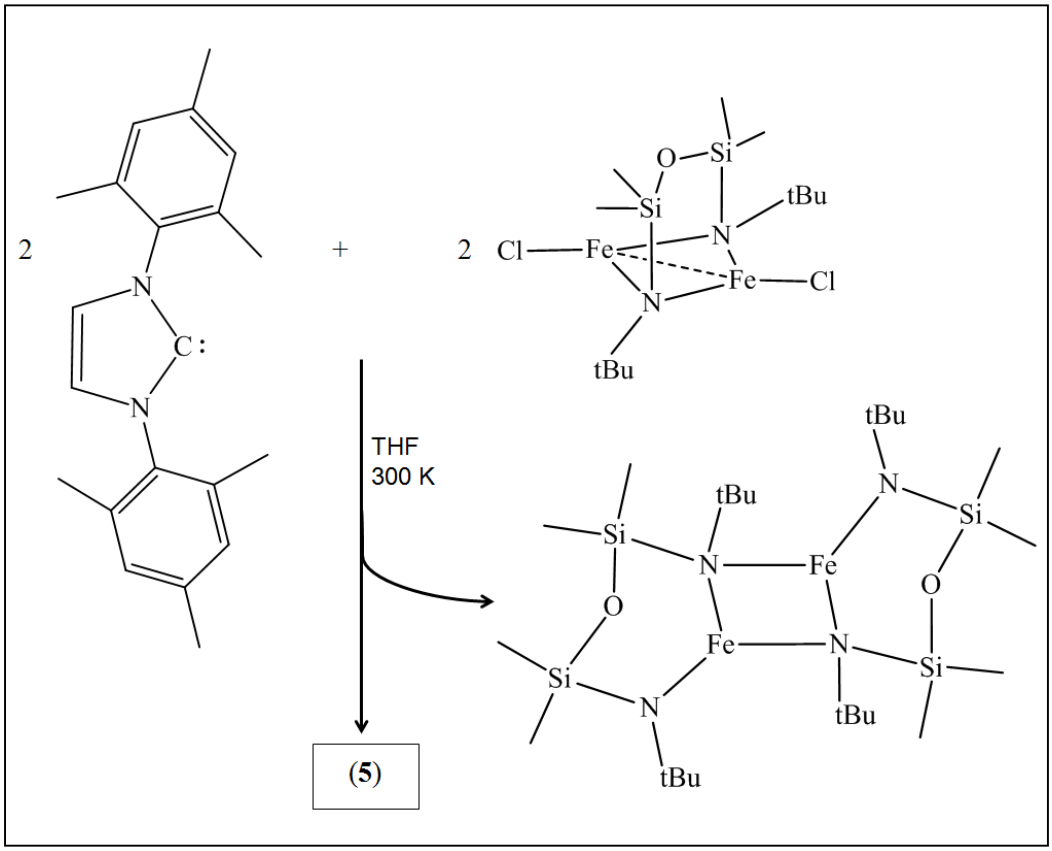

Scheme 2.5. The reaction of **3** with NHC carbene.

In order to prepare **5** rationally the direct reaction of 1,3-bis-(2,4,6-trimethylphenyl)imidazol-2-ylidene and $FeCl_2$ was conducted in THF at room and at higher temperatures- up to 70 ^oC for 72 hours. However, almost no reaction happened even at higher temperature, based on ^1H NMR spectroscopy. The reason could be that $FeCl_2$ in THF as its solvent makes THF adducts and in order to replace the THF with carbene as a ligand, there is no driving force like salt elimination for the reaction to proceed.

Table 2.7. Selected interatomic distances (Å) and bond angles (°) for $\{(NHC)FeCl_2\}_2$ (**5**)

Fe1- Fe1*	3.297(3)	C1-Fe1-Cl1	117.15(9)
Fe1-Cl1	2.236(1)	C1-Fe1-Cl2	109.27(9)
Fe1-Cl2	2.374(1)	Cl2-Fe1-Cl2*	92.48(3)
Fe1-Cl2*	2.393(8)	C1-Fe1-Fe1*	117.63(4)
Fe1- C1	2.086(3)	N1-C1-Fe1	128.4(2)
C1-N1	1.361(3)	N2-C1-Fe1	128.44(2)
C1-N2	1.362(4)	Fe1-Cl2-Fe1*	87.52(3)
C2-C3	1.336(4)	N1-C1-N2	103.0(3)
N2-C2	1.387(4)	C3-N1-C1	111.8(2)
N1-C3	1.387(4)	Fe1-Cl2-Fe1*	87.52(3)
N1-C11	1.445(4)	C2-N2-C1	111.9(2)
N2-C22	1.451(4)		

Symmetry operation: *: -x,-y,-z'

Structurally, **5** is dinuclear, with chloride bridges between two Fe(II) centres. Each iron centre in 5 has a four-coordinate geometry with the NHC carbene and two chlorides (terminal and bridging Fe−Cl distances of 2.236(1) and 2.374(1) Å respectively), one of which bridges to another iron(II) centre. The Fe-Fe distance of 3.297(3) Å is too long to consider any metal-metal overlap (Table 2.7). ^{1}H NMR spectra exhibited broad signals in the ranges of -15 to 30 ppm, consistent with the paramgnetism of the Fe(II) centre.

A similar iron carbene complex has been reported very recently, namely $(NHC)_2FeCl_2$[184] using the same carbene; this was synthesized by the reaction of $Fe\{N(SiMe_3)_2\}_2$ with 2 equivalents of NHC·HCl in toluene; its corresponding methylated compound $(NHC)_2FeMe_2$ shows high catalytic activities for hydrogen atom transfer reactions. [184] The reported $(NHC)Fe(CH_2SiMe_3)Cl$[184] complex is also very similar to **5**,

in terms of the bond distances and angles (Table 2.7). The Fe−C (carbene) distance of 2.086(3) Å is slightly shorter than 2.127(4) Å and the Fe−Cl(terminal) distance of 2.236(1) Å is very close to the 2.2372(14) Å in (NHC)Fe(CH_2SiMe_3)Cl. The only dihalide transition metal carbene similar to **5** is {(NHC)PdI_2}$_2$.[185]

Even after the rapid growth in carbene chemistry of the transition metals and the development of new generations of heterocyclic carbene (NHC) in last two decades, the chemistry of N-heterocyclic carbene complexes of iron and cobalt is getting developed and investigated compared to other transition metals.[182, 184, 186] The addition of NHC complexes towards $FeCl_2$ starting materials appears to be difficult.[187] First, it is hard to control the stoichiometry of such reactions; second, the reaction times usually are very long; and third, the reaction conditions are generally not in favour of the stability of NHC reactants. Hence, it seems that the synthesis of the iron(II) carbenes synthesized here could be used to study alkyl for halide substitution and reduction to obtain dinitrogen activation.

CO

In contrast to carbenes, CO is a more poorly electrophilic σ-donor, but a much stronger π- acceptor and usually stabilizes transition metals in low oxidation states. Both {Fe_2Cl_2[^{tBu}NON]}$_n$ (**3**) and {Co_2Cl_2[^{tBu}NON](LiCl)·2THF}$_2$ (**4**) in THF were exposed to 1 atmosphere of CO for about 24 hours at 0 ^{o}C. Again, the result was similar as for the phosphine and carbene reactions: {Fe[^{tBu}NON]}$_2$ was formed. However the other putative product, possibly an Fe-carbonyl chloride complex, could not be isolated.

2.2.7. Attempt to resynthesizse 1-4 from {M[^{tBu}NON]}$_2$

The addition of another equivalent of Li_2[^{tBu}NON] to **1** or **3** at room temperature resulted in the rapid formation of the previously reported {M[^{tBu}NON]}$_2$ complexes (Scheme 2.6), which can be prepared in high yield directly via the 1:1 metal/ligand reaction.

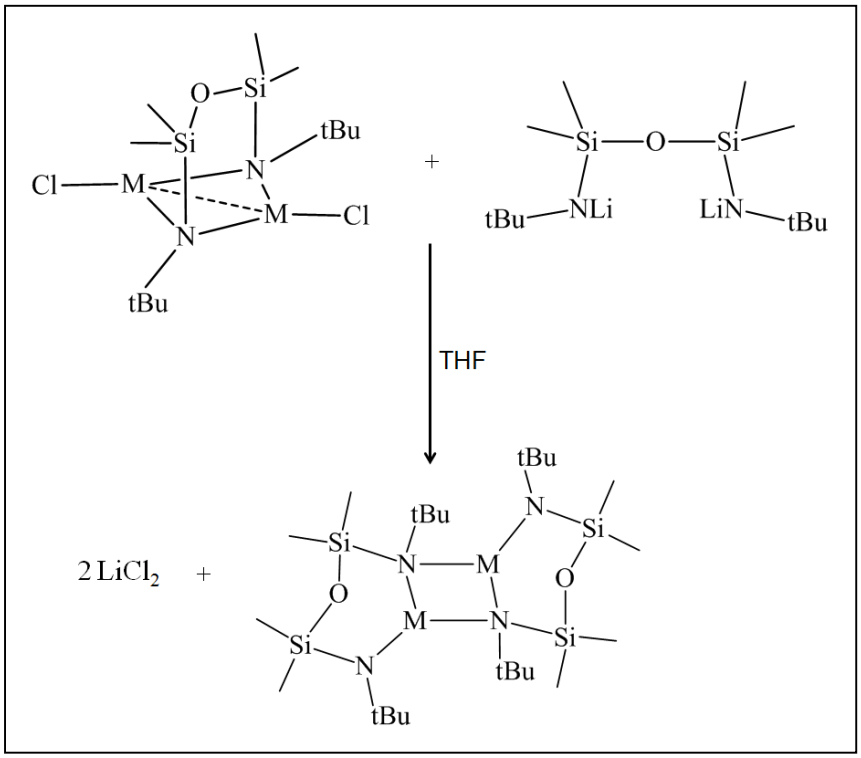

Scheme 2.6. Formation of stable dimer $\{M[^{tBu}NON]\}_2$ from **1** and **3**.

However, the reverse reaction, i.e., addition of MX_2 to the $\{M[^{tBu}NON]\}_2$ dimer to generate the $\{M_2X_2[^{tBu}NON]\}$ cluster worked at higher temperatures (40 °C) only in very low yield, less than 5% (Scheme 2.7), although this could be a useful route towards generating fluoride analogues. Although these two reactions give an indication of the relative stability of the halide-free systems vs. **1**–**4**, it also illustrates that the halide groups in **1**–**4** are readily metathesized, as will be followed up in Chapter 3.

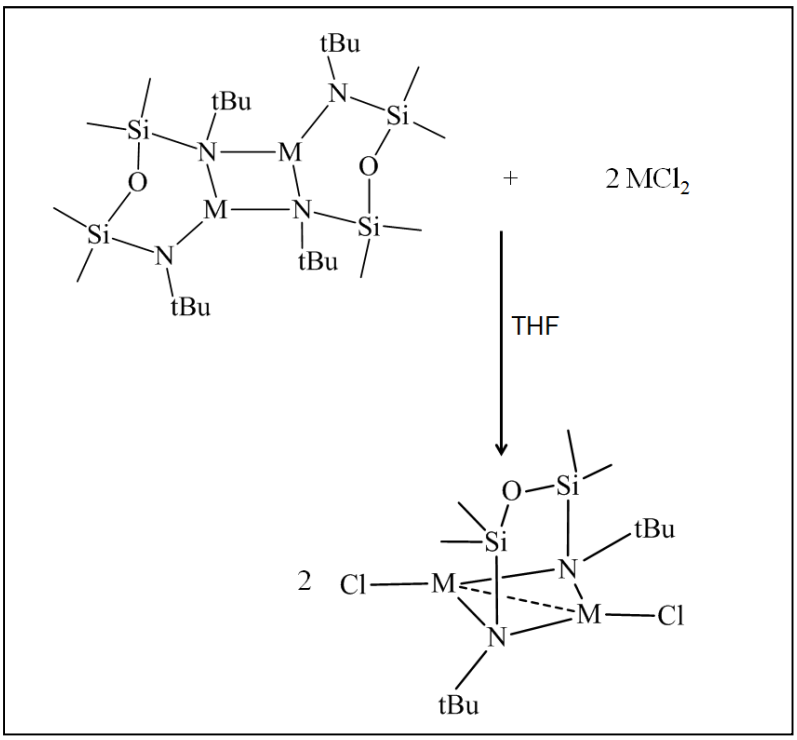

Scheme 2.7 Formation of **1** and **3** from stable dimer $\{M[^{tBu}NON]\}_2$.

2.3. Conclusion

The synthesis and characterization of a series of multinuclear clusters by the reaction of Fe(II) and Co(II) halides with a half equivalent of $Li_2[^{tBu}NON]$ was achieved. The use of sub-stoichiometric amounts of amido ligand in order to retain reactive metal-halides cleanly leads to viable metal amido-halide complexes in high yields. Complexes **1**–**4** have the same basic $M_2X_2[^{tBu}NON]$ unit: a diamido ligand bridge between two metal centres, and resulted in two different metal sites. This bonding motif is not common for normally chelating diamido ligands. The metal coordination number varies from a low three- to more standard five-coordinate. Different halides for both iron and cobalt resulted in different structures, with X =Br generating discrete tetranuclear clusters, while for X= Cl, the Fe(II) system generated a 1-D polymer; the Co(II)Cl analogue formed an “ate” complex.

The magnetic susceptibility data of all four complexes showed that the metal centres are antiferromagnetically coupled. The comparison between solid state and the

solution magnetic moments revealed that the primary coupling is through halide bridges rather than metal-metal overlap or the amido bridges.

Even though the presence of metal-halide bonds suggested the possibility of reduction reactivity towards dinitrogen activation, the first attempts were not successful, hence this needs more investigation. However, trying to stabilize metal centres with neutral ligands as a precursor to reduction, led to redistribution of ligands, which in the case of NHC lead to a new route towards new iron(II) carbenes such as $\{(NHC)FeCl_2\}_2$ (**5**).

2.4. Future work

a) It is well known that small changes in ligand can change the coordination geometry of a metal centre dramatically and result in different reactivity.[8, 24] Since different R groups are known for the $[^{R}NON]^{2-}$ type of ligand, including R= iPr, 2,4,6-Me_3Ph, $(CF_3)_2Ph$ etc, it is worth targeting $\{M_2X_2[^{R}NON]\}$-type complexes with different R groups on the ligand.

b) The search to find a suitable neutral donor ligand to stabilize iron(II) or cobalt(II) centres in order to support reduction products should continue. Even though using dmpe, an NHC and CO as neutral donors with iron(II) were not successful at first, such reactions might proceed differently under different conditions; for example, if the reduction is carried out under H_2 or a CO atmosphere or in the direct presence of neutral donors, a different result might be obtained. Analogous reactions for the Co(II) compounds should also be targeted.

c) Clearly, a change in the halide also can affect the structure and geometry of the metal centre. Lack of a suitable starting material for iron(II) and cobalt(II) fluoride restricted our efforts to access analogous fluoro-compunds. Even though the addition of MX_2 to the $\{M[^{tBu}NON]\}_2$ dimer to generate the $\{M_2X_2[^{tBu}NON]\}$ cluster is much slower at higher temperatures (40 °C) with a very low yield (less than 5%), it should be repeated with MF_2 for a longer time and at higher temperatures. Iron-fluoride bonds are known to show unusual reactivities; for example, Holland's group reported that Fe-F containing compounds can support C-F bond activation.[122] Me_2SnF_2 would be a good candidate as

a F-metathesis reagent [122] and it would be interesting to synthesize and characterize the analogous iodo-compound as well.

d) The reaction of $\{Fe_2Cl_2[^{tBu}NON]\}_n$ (**3**) with carbene led towards making iron(II) and perhaps cobalt(II) NHC complexes $FeCl_2(THF)_{1.5}$ should be used as a better starting material. (no attempts with the cobalt analogues were attempted).

e) Investigations to prepare mixed metal systems is of great interest in fundamental coordination chemistry since they might yield interesting magnetic properties; such compounds can also provide a very close comparison or synergy between the two metal centre reactivities e.g., towards halide substitution. For example it might be possible to prepare heterobimetallic $FeCoX_2[^{tBu}NON]$ (X= halide) as shown in ***Figure 2.9*** by mixing starting materials FeX_2 and CoX_2 with $Li_2[^{tBu}NON]$.

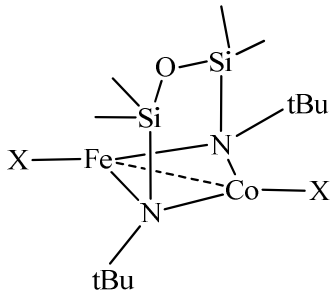

Figure 2.9 Heterobimetallic diamido metal complex target.

2.5. Experimental section

2.5.1. General Procedures and Materials.

All experiments were carried out under an atmosphere of dry, oxygen-free dinitrogen by means of standard Schlenk or glovebox techniques. The glovebox used was an Mbraun Labmaster. Diethylether (Et_2O), tetrahydrofuran (THF), hexanes and toluene were predried over sodium wire and were freshly distilled under a dinitrogen atmosphere from sodium / benzophenone. Benzene-d_6 and THF- d_8 were freeze-pump-thawed three times, dried from sodium and stored under dinitrogen. The diamidosilylether ligand $Li_2[^{tBu}NON]$ was prepared as previously described.[140] All other

reagents were bought from commercial sources and used as received. Elemental analysis (C H N) was conducted by Mr. Farzad Haftbaradaran of Simon Fraser University employing a Carlo Erba EA 1110 CHN elemental analyzer. UV-vis spectra were recorded on a CARY 300 Bio UV-Visible Spectrophotometer. NMR spectra were recorded at 294 K, unless otherwise stated, on a 500 MHz Varian Unity spectrometer or on a 600 MHz Bruker Avance spectrometer. All ^{1}H NMR shifts are reported in ppm relative to the impurity of residual internal solvent: benzene-d_6 at δ= 7.15 and THF-d_8 at δ= 1.73 and 3.58. Variable temperature magnetic susceptibility measurements over the range 1.8-300 K were made with polycrystalline samples and at a field of 10 000 G using a Quantum Design (MPMS-XL7) SQUID magnetometer equipped with an Evercool closed-cycle He compression system. Samples were prepared in low background polycarbonate gelcaps housed in straws; the data were corrected for the diamagnetism of the constituent atoms using Pascal's constants.[169] Evans method[162] also was used for the measurement of magnetic susceptibilities in solution at room temperature.

Synthesis of {$Fe_2Br_2[^{tBu}NON]$}$_2$ (1)

$Li_2[^{tBu}NON]$ (180 mg, 0.62 mmol) in 30 mL THF was added dropwise at room temperature in small portions over four hours (approximately 2 mL every 15 minutes) to a solution of anhydrous $FeBr_2$ (270 mg, 1.25 mmol) in 50 mL THF while stirring. The resulting light green mixture was stirred overnight, and then the THF was removed *in vacuo*. The product was extracted with diethylether and the resulting solution filtered through Celite. Removal of the diethylether *in vacuo* resulted in a light green product of {$Fe_2Br_2[^{tBu}NON]$}$_2$ (**1**). Crystals of **1** were obtained by slow evaporation of a diethylether solution. Yield: 152 mg (45%). Anal. Calcd. for $C_{12}H_{30}N_2Br_2Fe_2OSi_2$: C: 26.39%; H: 5.53%; N: 5.13%. Found: C: 26.53%; H: 5.48%; N: 5.20%. ^{1}H NMR (THF-d_8): -6.4 (br s, 12H, $Si(CH_3)_2$), 12.1 (br s, 18H, $C(CH_3)_3$). Solid state μ_{eff}(300 K): 3.15 μ_B.

Synthesis of {$Co_2Br_2[^{tBu}NON]$}$_2$ (2)

$Li_2[^{tBu}NON]$ (197 mg, 0.68 mmol) in 30 mL THF was added dropwise at room temperature in small portions over four hours (approximately 2 mL every 15 minutes) to a solution of anhydrous $CoBr_2$ (300 mg, 1.37 mmol) in 50 mL THF while stirring. The resulting blue mixture was stirred overnight, and then the THF was removed *in vacuo*. The product was extracted with diethylether and the resulting solution filtered through

Celite. Removal of the diethylether *in vacuo* resulted in the blue product $\{Co_2Br_2[^{tBu}NON]\}_2$ (**2**). Crystals of **2** were obtained by slow evaporation of a diethylether solution. Yield: 132 mg (35%). Anal. Calcd. for $C_{12}H_{30}N_2Br_2Co_2OSi_2$: C: 26.1%; H: 5.47%; N: 5.07%. Found: C: 26.37%; H: 5.21%; N: 5.31%. ^{1}H NMR (THF-d_8): -18.1 (br s, 12H, $Si(CH_3)_2$), -10.9 (br s, 18H, $C(CH_3)_3$). Solid state μ_{eff}(300 K): 1.84 μ_B.

Synthesis of $\{Fe_2Cl_2[^{tBu}NON]\}_n$ (3)

$Li_2[^{tBu}NON]$ (341 mg, 1.18 mmol) in 30 mL THF was added dropwise at room temperature in small portions over four hours (approximately 2 mL every 15 minutes) to a solution of anhydrous $FeCl_2$ (300 mg, 2.36 mmol) in 50 mL THF while stirring. The resulting yellow mixture was stirred overnight, and then the THF was removed *in vacuo*. The product was extracted with diethylether and the resulting solution was filtered through Celite. Removal of the diethylether *in vacuo* resulted in yellow $\{Fe_2Cl_2[^{tBu}NON]\}_n$ (**3**). Crystals were obtained by slow evaporation of a diethylether solution. Yield: 350 mg (65%). Anal. Calcd for $C_{12}H_{30}ON_2Cl_2Fe_2OSi_2$: C: 31.52%; H: 6.61%; N: 6.12%. Found: C: 31.28%; H: 6.72%; N: 6.16%. ^{1}H NMR (THF-d_8): -5.8 (br, 12H, $Si(CH_3)_2$), 6.0 (br s, 18H, $C(CH_3)_3$). Solid state μ_{eff}(300 K): 2.47 μ_B, Evans method μ_{eff}(300 K): 4.6 μ_B.

Synthesis of $\{Co_2Cl_2[^{tBu}NON](LiCl)\cdot 2THF\}_2$ (4)

$Li_2[^{tBu}NON]$ (277 mg, 0.96 mmol) in 30 mL THF was added dropwise at room temperature in small portions over four hours (approximately 2 mL every 15 minutes) to a solution of anhydrous $CoCl_2$ (250 mg, 1.92 mmol) in 50 mL THF while stirring. The resulting bluish-green mixture was stirred overnight, and then the excess THF was removed *in vacuo*. The product was extracted with THF and the resulting solution was filtered through Celite. Removal of the THF *in vacuo* resulted in a bluish-green powder of $\{Co_2Cl_2[^{tBu}NON]\ (LiCl)\cdot 2THF\}_2$ (**4**). Crystals of **4** were obtained by slow evaporation of a THF solution. Yield: 343 mg (55%). Anal. Calcd. for $C_{20}H_{46}N_2Cl_3Co_2LiO_3Si_2$: C: 36.96%; H: 7.13%; N: 4.31%. Found: C: 36.89%; H: 7.10%; N: 4.44%. ^{1}H NMR (THF-d_8): -17.0 (br s, 12H, $Si(CH_3)_2$), -10.5 (br, 18H, $C(CH_3)_3$). Solid state μ_{eff}(300 K): 2.23 μ_B.

Reaction of $CrCl_2$ and $Li_2[^{tBu}NON]$

$Li_2[^{tBu}NON]$ (298 mg, 1.04 mmol) in 20 mL THF was added dropwise at room temperature in small portions over four hours (approximately 2 mL every 15 minutes) to

the gray solution of anhydrous $CrCl_2$ (268 mg, 2.18 mmol) in 40 mL THF while stirring. The colour changed from gray to blue/green, and it was stirred overnight, then the excess THF was removed *in vacuo*. Most of the product was not even soluble in THF, hence it was hard to pursue further characterization.

Reaction of $CrCl_3 \cdot 3THF$ and $Li_2[^{tBu}NON]$

$Li_2[^{tBu}NON]$ (165 mg, 0.6 mmol) in 30 mL THF was added dropwise at room temperature in small portions over four hours (approximately 2 mL every 15 minutes) to a purple solution of $CrCl_3 \cdot 3THF$ (450 mg, 1.2 mmol) in 50 mL THF while stirring. The resulting green mixture was stirred overnight, and then the excess THF was removed *in vacuo*. The product was extracted with THF, but a pure crystalline product could not be isolated, and the ^1H NMR spectrum only contained uninformative, very broad and shifted peaks that could not be identified or integrated.

Reaction of $FeCl_3$ and $Li_2[^{tBu}NON]$

$Li_2[^{tBu}NON]$ (184 mg, 0.68 mmol) in 30 mL THF was added dropwise at room temperature in small portions over four hours to a solution of anhydrous $FeCl_3$ (227 mg,1.37 mmol) in 50 mL THF while stirring. The resulting purple mixture was stirred overnight, and then the THF was removed *in vacuo*. The product was extracted with hexanes and the resulting solution filtered through Celite. Removal of the diethylether *in vacuo* resulted in a purple product, identified by its ^1H NMR spectrum matches with reported $\{FeCl[^{tBu}NON]\}_2$.[55]16]

Reaction of $\{Fe_2Cl_2[^{tBu}NON]\}_n$ (3) and $KBEt_3H$

$KBEt_3H$ in THF (0.86 mL, 0.86 mmol, 1 M) was added dropwise at -70 ^oC to a light brown solution of $\{Fe_2Cl_2[^{tBu}NON]\}_n$ (0.42 mmol, 280 mg) in 40 mL THF while stirring. The resulting mixture changed colour from blue to dark brown immediately, and was stirred overnight. The excess THF was then removed *in vacuo*. The product was identified as $\{Fe[^{tBu}NON]\}_2$[155] based on its ^1H NMR spectrum with a 45% yield. The reaction was repeated with two equivalents of $KBEt_3H$ per $\{Fe_2Cl_2[^{tBu}NON]\}$ as well and the result was the same. There was some unisolable residue that could be iron powder.

Reaction of $\{Co_2Cl_2[^{tBu}NON](LiCl)\cdot 2THF\}_2$ (4) and $KBEt_3H$

$KBEt_3H$ in THF (0.52 mL, 0.52 mmol, 1 M) was added dropwise at -70 ^oC to a light brown solution of $\{Co_2Cl_2[^{tBu}NON](LiCl)\cdot 2THF\}_2$ (0.52 mmol, 240 mg) in 60 mL of THF while stirring. The resulting mixture changed colour from light brown to dark brown immediately and was stirred overnight. The excess THF was then removed *in vacuo*. The product was identified as a mixture of starting material and known $\{Co[^{tBu}NON]\}_2$[155] based on the ^1H NMR spectrum, with some unisolable residue that could be cobalt powder.

Reaction of $\{Fe_2Cl_2[^{tBu}NON]\}_n$ (3) and KC_8

One equivalent of KC_8 (130 mg, 1 mmol) per iron centre in **3** was added slowly at -70 ^oC to the light brown solution of $\{Fe_2Cl_2[^{tBu}NON]\}_n$ (**3**) (225 mg, 0.5 mmol) in 50 mL THF while stirring. The resulting mixture changed colour from light brown to dark brown immediately, then was stirred overnight. The excess THF was removed *in vacuo*. The product was identified as $\{Fe[^{tBu}NON]\}_2$[155] based on its ^1H NMR spectrum, with some unisolable residue that could be iron powder.

Reaction of $\{Fe_2Cl_2[^{tBu}NON]\}_n$ (3) and 1,2-Bis(dimethylphosphino)ethane (dmpe):

Dmpe (65 mg, 0.43 mmol) in 20 mL Et_2O was added dropwise at -70 ^oC to a solution of $\{Fe_2Cl_2[^{tBu}NON]\}_n$ (200 mg, 0.43 mmol) in 40 mL Et_2O while stirring. The resulting yellow mixture changed to green and was stirred overnight. The solvent was then removed *in vacuo* and the product was extracted first with hexanes to brown solution and then with THF to give a green in THF. The resulting solutions were filtered through Celite. Slow evaporation of the THF solution resulted in green crystals which were identified by X-ray crystallography as $\{FeCl_2(dmpe)_2\}$. Removal of the hexanes solvent from the first extraction *in vacuo* resulted in $\{Fe[^{tBu}NON]\}_2$,[155] identified from its ^1H NMR spectrum with a 45% yield.

Synthesis of $\{(NHC)FeCl_2\}_2$ (5)

$Li_2[^{tBu}NON]$ (202 mg, 0.7 mmol) in 30 mL THF was added dropwise at room temperature in small portions over two hours to a solution of anhydrous $FeCl_2$ (178 mg, 1.4 mmol) in 40 mL THF while stirring. The resulting yellow mixture was stirred overnight. In the next step, 1,3-bis-(2,4,6-trimethylphenyl)imidazol-2-ylidene (NHC) (213

mg, 0.7 mmol) in 20 mL THF was added to the reaction and the mixture was stirred overnight. The THF was then removed *in vacuo*. A yellow product was extracted with hexane and then a second dark green portion was extracted with a 50 : 50 mixture of hexanes / toluene (30 mL). The resulting solutions were filtered through Celite. Removal of the hexanes solvent from the first extraction *in vacuo* resulted in yellow $\{Fe[^{tBu}NON]\}_2$,[155] identified from its ^1H NMR spectrum. Removal of the solvent from the second hexanes / toluene solution *in vacuo* resulted in dark green $\{(NHC)FeCl_2\}_2$ (**5**). Crystals were obtained by slow evaporation of a hexane / toluene solution. Yield: 125 mg (45%). Anal. Calcd. for $C_{21}H_{24}N_2Cl_2Fe$: C: 58.22%; H: 6.06%; N: 6.46%. Found: C: 58.40%; H: 6.12%; N: 6.78%. THF-d_8 NMR exhibited broad, shifted signals in the ranges of -15 to 30.

Reaction of $FeCl_2$ and NHC carbene:

1,3-bis-(2,4,6-trimethylphenyl)imidazol-2-ylidene (216 mg, 0.78 mmol) in 20 mL THF was added at room temperature slowly to a solution of one equivalent of $FeCl_2$ (100 mg, 0.79 mmol) in 40 mL THF while stirring. The resulting light brown mixture was stirred overnight. The ^1H NMR spectrum in THF-d_8 of the mixture did not show that any reaction had occurred. The reaction was repeated at 70 ^oC for about 8 hours, but the ^1H NMR spectrum still showed no change.

Reaction of $\{Fe_2Cl_2[^{tBu}NON]\}_n$ and CO

Three-freeze-pump-thaw cycles were done on a solution of $\{Fe_2Cl_2[^{tBu}NON]\}$ (250 mg, 0.53 mmol) in 30 mL of THF at 0 ^oC, and then one atmosphere of CO was introduced to the bomb. The light brown solution changed to dark brown. The reaction mixture was allowed to stir at 0 ^oC for 24 hours, and then the reaction mixture was allowed to warm to room temperature and was stirred for 1 hour. Following the removal of the solvent *in vacuo*, the ^1H NMR spectrum identified the product as the $\{Fe[^{tBu}NON]\}_2$ dimer.[155]

2.5.2. X-ray crystallography

Crystals of **1** and **4** were sealed in capillaries while crystals of **2, 3** and **5** were coated in Paratone-oil and mounted onto a MiTeGen Micro Mount. Crystal descriptions for each compound are as follows: **1** is a light green block having dimensions 0.5 × 0.25

× 0.30 mm^3; **2** is a blue cube having dimensions 0.50 × 0.10 × 0.13 mm^3; **3** is a dark yellow cube having dimensions 0.40 × 0.35 × 0.25 mm^3; **4** is a bluish green needle having dimensions 0.50 × 0.15 × 0.22 mm^3 and **5** is a green block having dimensions 0.35 × 0.30 × 0.25 mm^3. All data was collected on a Bruker Smart instrument equipped with an APEX II CCD area detector at a distance of 6.0 cm from the crystal. A Mo-Kα fine-focus sealed tube operating at 1.5 kW (50 kV, 30 mA) was utilized for data collection. All frames were collected with a scan width of 0.5 in ω or ϕ with the following exposure times: 10 s for **1–3**, and 30 s for **4** and **5**. The frames were integrated with the Bruker SAINT software package. Data were corrected for absorption effects using a multi-scan correction technique. The structures were solved using direct methods (SIR 92) and refined by least-squares procedures using CRYSTALS.[188] Crystallographic data is collected in Appendix A. Hydrogen atoms were placed in idealized geometric positions. Subsequent refinement cycles linked each hydrogen atom position to its respective carbon atom using a riding model. The isotropic temperature factor of the hydrogen atoms was initially fixed at 1.2 times that of the preceding carbon atom. Subsequent refinement cycles linked the temperature factor of similar hydrogen atoms to one another. The ^{t}Bu /THF group(s) in **4** were found to be disordered. Adequate geometric restraints as well as thermal similarity restraints were used to produce an unbiased chemically consistent solution. The THF units in **4** were refined isotropically; attempts to build a reasonable, unbiased, anisotropic model were not successful due to the high level of disorder about these molecules. Although initially the refinement of the crystal structure of **3** converged, the R-value remained high with large, nonsensical, peaks remaining in the difference map. Analysis of the data in Rotax[189] revealed that an approximately 180° non-merohedral twin was obscuring the data. Subsequent refinement of the data with an appropriate twin matrix resulted in the improved R-value found. Examining the raw data with Cell_Now indicated that the data indeed contained such a twin. However, attempts to process the raw data as a twin prior to solving did not produce a further improvement in the R-value. The plots for the crystal structures were generated using CAMERON.[190]

I would like to acknowledge Dr. Mike Katz who taught me how to run and solve my own X-ray crystal structures. The X-ray structures present in this thesis were solved

by myself, however for compounds **1**-**4**, in order to make their structural refinements of publishable quality; Dr. Mike Katz did the final structural analysis.

3. Multi-nuclear Iron(II) and Cobalt(II) amido/alkyl compounds and their reactivity[2]

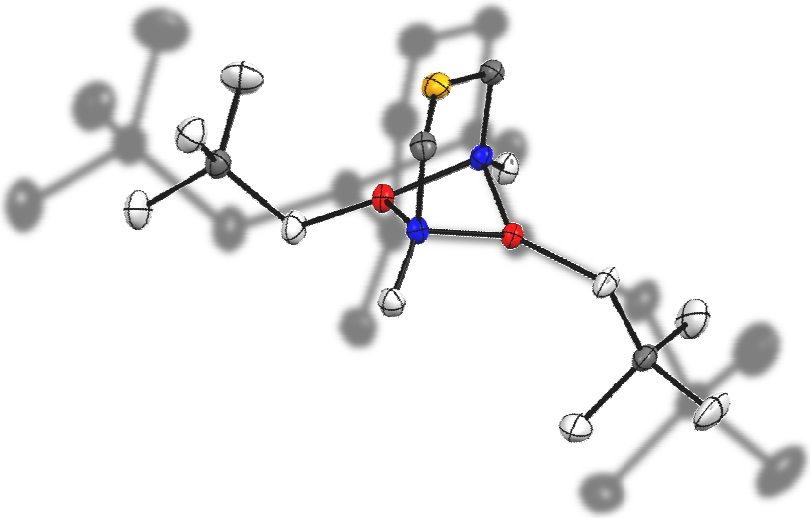

3.1. Introduction

One important goal of this thesis was to move from ordinary metal amido complexes to new organometallic systems of iron and cobalt. From the reactivity point of view, the M−C bond plays an important role in many catalytic processes, bond activation and activation of small molecules as well.[2, 8, 11-16] In particular, three-coordinate metal centres are more likely to illustrate new reactivity due to the electronic unsaturation.[45, 70, 72, 120-122] Such low coordinate metal centres can be achieved using very bulky ligands, however in some cases, this bulk prevents the metal centre from undergoing further reactivity. Three-coordinate transition metal alkyl complexes are much less investigated and studied due to the difficulty of stabilizing such systems and one challenge is to find an appropriate ligand.[53, 114]

[2]* Parts of this chapter are adapted with permission from Z. Moatazedi, M. J. Katz and D. B. Leznoff,"Synthesis and characterizaion of a series of halide-bridged, multinuclear iron(II) and cobalt(II) diamido complexes and a dinuclear, high-spin cobalt(II) alkyl derivative" Dalton Trans., 2010, Vol 39, 9889-9896. Copyright Royal Society of Chemistry.

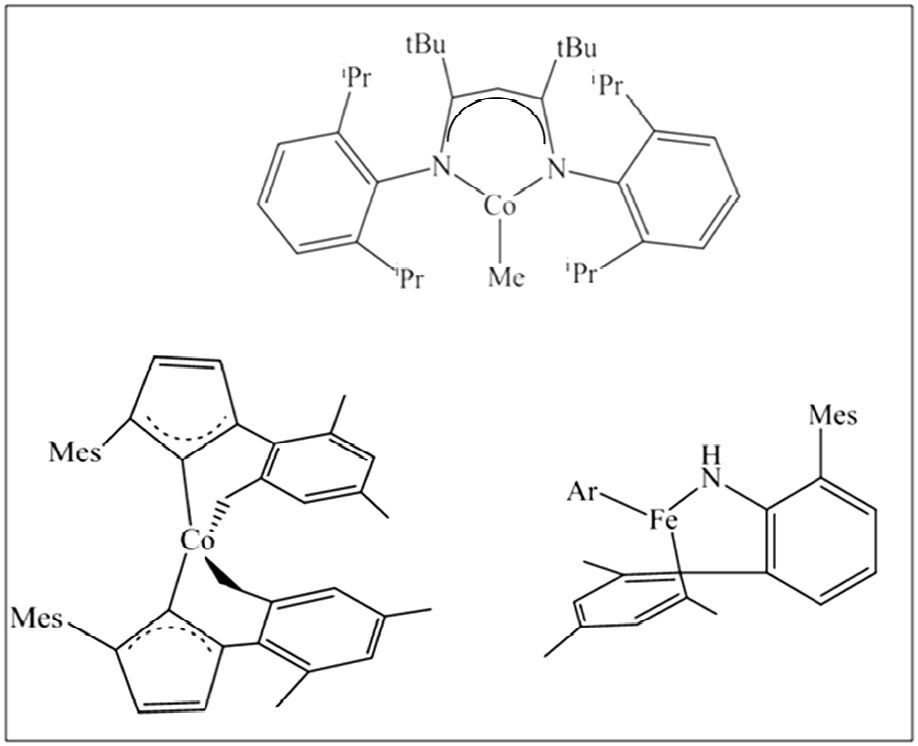

Figure 3.1. Examples of low-coordinate iron- and cobalt-alkyl complexes.[53, 88, 120]

In the case of iron and cobalt as the metal centre, in some cases low-coordinate systems have been found to show unusual magnetic properties such as spin-state crossover with structural changes in the low-coordinate organometallic cobalt(II);[53] they also were shown to be highly active in bond activations such as the intramolecular C(sp^3)–H bond activation reactions of low-valent cobalt complexes,[120] the stepwise reduction of dinitrogen by a low-coordinate iron complex,[121] and some catalytic activity as well, such as the use of low-coordinate iron(II) fluoride complexes in the catalytic hydrodefluorination of fluorocarbons,[72] low-valent iron-catalyzed C−C bond formation and C−H bond activation.[88] Examples of low-coordinate iron and cobalt alkyl complexes are shown in Figure 3.1.

As was mentioned in Chapter 2, the new metal(II) halide/diamido complexes **1**-**4**, have the potential for further substitution at the metal centre and could provide a route into metal(II) alkyl/diamido systems via salt metathesis. In **1**-**4** depending on the bonding

mode of the silylether, three-coordinate metal centres are present and thus if they can be alkylated, three-coordinate metal alkyls could result.

The first part of this chapter will describe the synthesis and structural characterization of several dinuclear dialkyl/amido iron(II) and cobalt(II) complexes of general formula [^{tBu}NON]M_2R_2 (M= Fe and Co; R= CH_2SiMe_3 and C_6F_5) and four multi-nuclear alkyl/halide amido iron(II) and cobalt(II) diamidosilylether complexes with basic unit [^{tBu}NON]M_2XR (M=Fe and Co, X= Cl, Br; R= CH_2SiMe_3, Me and C_6F_5), which dimerized further to form tetranuclear metal complexes.

3.2. Results and Discussion

The reaction of two equivalents of Me_3SiCH_2Li per dinuclear unit in {Fe_2Cl_2[^{tBu}NON]}$_n$ (**3**) and {Co_2Cl_2[^{tBu}NON](LiCl)·2THF}$_2$ (**4**) generated dinuclear organometallic complexes of iron and cobalt of the formula {$M_2(CH_2SiMe_3)_2$[^{tBu}NON]}, where M = Fe (**6**) and Co (**7**) (Scheme 3.1). Note that even though the reactions were done at room temperature, very slow addition of a diluted lithium alkyl solution to M_2Cl_2[^{tBu}NON] is important, however doing this reaction at low temperature it would not be an issue.

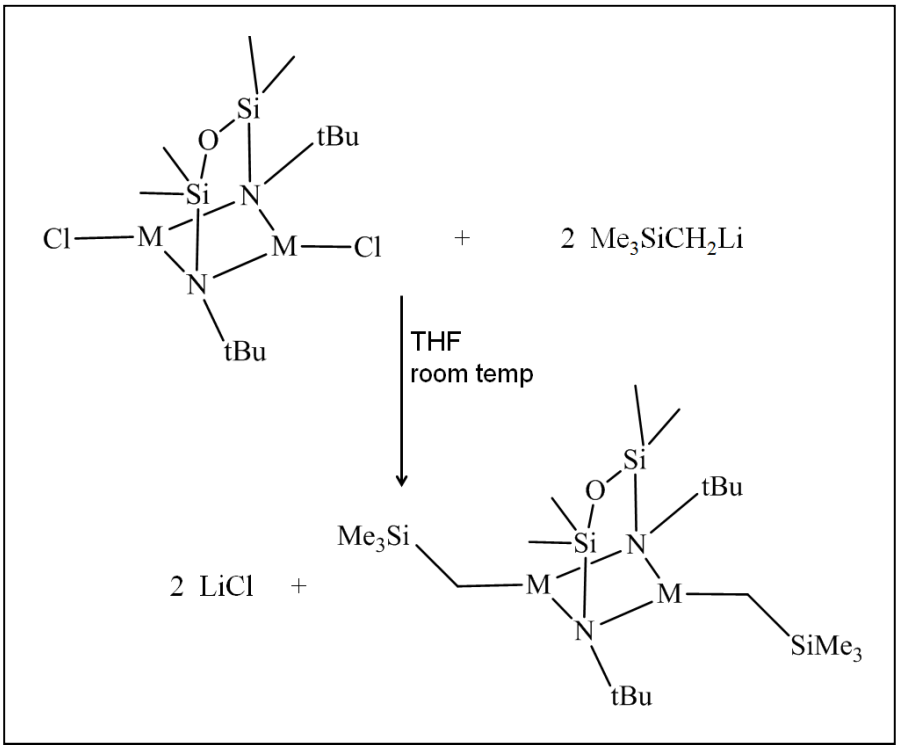

Scheme 3.1. The formation of dialkyl/amido dinuclear complexes **6** (M= Fe) and **7** (M= Co).

Switching the stoichiometry of the addition of lithium alkyl to a 1:1 reaction of $LiCH_2SiMe_3$ with $M_2X_2[^{tBu}NON]$ (X= Cl and Br) generated mixed alkyl/halide dinuclear complexes of the general formula $\{[^{tBu}NON]M_2X(CH_2SiMe_3)_2\}$, which dimerize further to form tetranuclear $\{[^{tBu}NON]M_2X(CH_2SiMe_3)_2\}_2$ (Scheme 3.2).

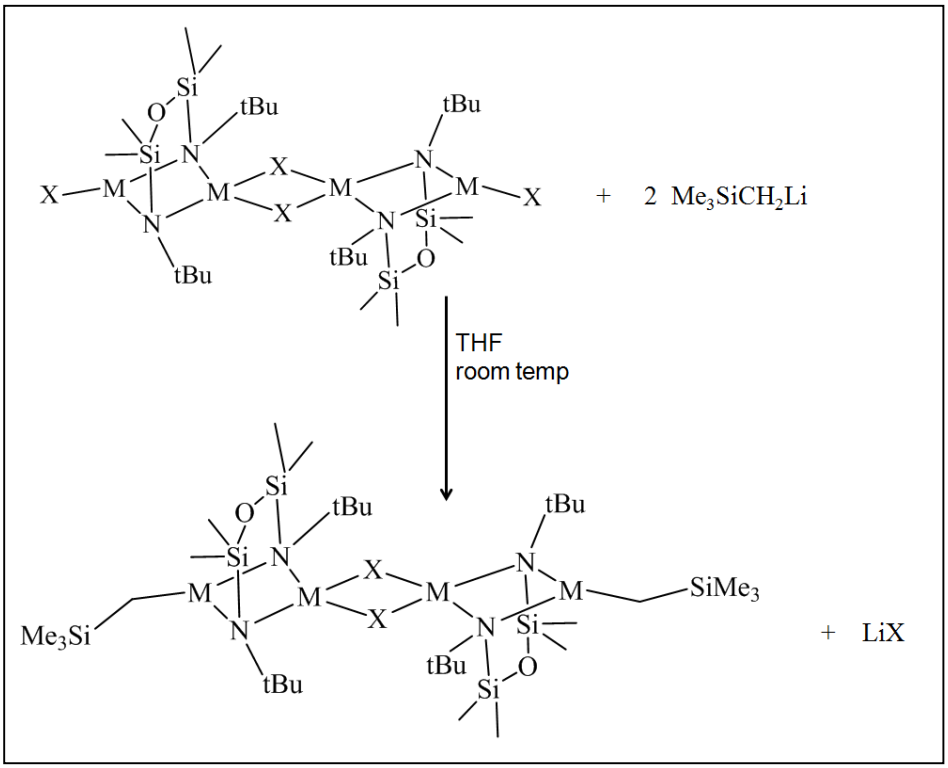

Scheme 3.2. The formation of mixed alkyl/halide diamido tetranuclear omplexes **8**-**11**, (M= Fe, Co; X= Cl, Br).

Single crystals suitable for X-ray diffraction were obtained by slow evaporation of hexane solutions of dialkyl/diamido $\{Fe_2(CH_2SiMe_3)_2[^{tBu}NON]\}$ (**6**) and $\{Co_2(CH_2SiMe_3)_2[^{tBu}NON]\}$ (**7**) and diethylether solutions of mixed alkyl/halide diamido iron and cobalt complexes $\{Fe_2Cl(CH_2SiMe_3)_2[^{tBu}NON]\}_2$ (**8**), $\{Co_2Cl(CH_2SiMe_3)_2[^{tBu}NON]\}_2$ (**9**), $\{Fe_2Br(CH_2SiMe_3)_2[^{tBu}NON]\}_2$ (**10**) and $\{Co_2Br(CH_2SiMe_3)_2[^{tBu}NON]\}_2$ (**11**). The same reactions were attempted with the bulkier $LiCH(SiMe_3)_2$ but they did not result in any clean product.

3.2.1. Synthesis and characterization of Iron(II) and Cobalt(II) dialkyl complexes.

Alkyl for halide metathesis (via reaction of one equivalent of $LiCH_2SiMe_3$ per metal centre with **3** and **4**) generated the new organometallic dinuclear

{$Fe_2(CH_2SiMe_3)_2[^{tBu}NON]$} (**6**) and {$Co_2(CH_2SiMe_3)_2[^{tBu}NON]$} (**7**) complexes (Figure 3.2). The X-ray crystal structures of 6 and **7** reveal a dinuclear $M_2[^{tBu}NON]$ core as in {$M_2Br_2[^{tBu}NON]$}$_2$ (M= Fe: **1** and M= Co: **2)**, but contains the terminal $–CH_2SiMe_3$ ligands rather than halides, and as a result no further aggregation occurs; both cobalt and iron alkyl compounds **6** and **7** are crystallographically isomorphous. The coordination geometries about the M1 and M2 centres are different: M1 is coordinated to both amido donors, one alkyl group and also interacts with the silylether oxygen donor in the ligand backbone, generating a distorted four-coordinate geometry, while M2, which does not bind the silylether donor is three-coordinate and has a roughly trigonal geometry.

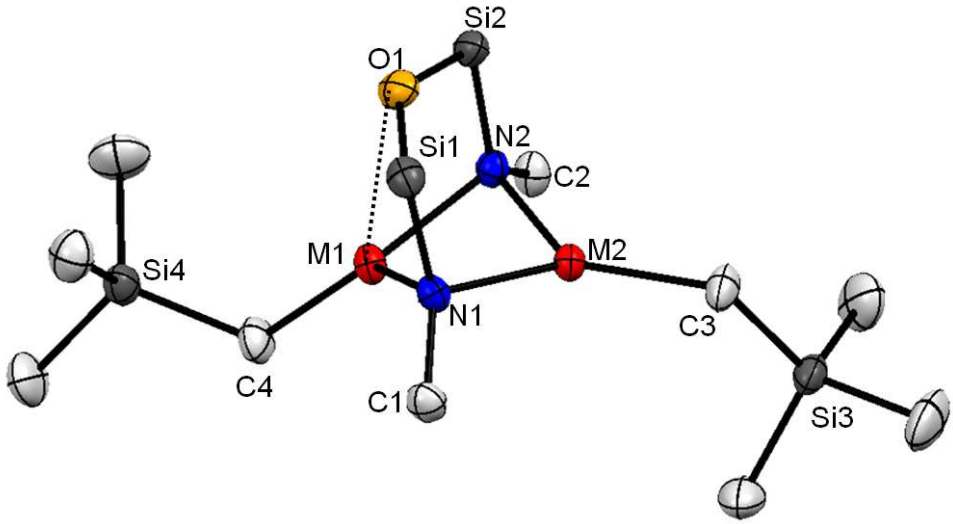

Figure 3.2. Molecular structure of **6** (M= Fe) and **7** (M=Co); (^{t}Bu and $SiMe_2$ groups simplified for clarity).

All of the core $Co_2[^{tBu}NON]$ bond lengths in **6** and **7** (Table 3.1) are similar to those of **2** ({$Fe_2Cl_2[^{tBu}NON]$}$_n$) and **4** ({$Co_2Cl_2[^{tBu}NON](LiCl)\cdot 2THF$}$_2$). The Co1–C3 and Co2–C4 bond lengths of 1.959(9) and 1.965(10) Å respectively are slightly shorter than the Co−C distances of 1.995(5) Å in $[N_2P_2]CoMe$[42] and 2.033(2) Å in $[N_2P_2]CoCH_2SiMe_3$.[42] The Fe1–C3 and Fe2–C4 bond lengths of 2.035(16) and 2.0224(16) Å respectively are similar to then 2.054(3) in $LFeCH_2SiMe_3$[191] and 2.001(6) Å in $LFeCH_3$[191] [L= 2,2,6,6-tetramethyl-3,5-bis(2,6-diisopropylphenylimido)hept-4-yl]. The Fe1–O1 and Co1–O1 distances of 2.704(2) and 2.471(12) Å in **6** and **7** compare well with those for the tetranuclear cluster **1** and **2** (Table 3.1) and indicate that a M–O

interaction is present. Conversely, there is no interaction between the M2 centres and the silylether donor, with Fe2–O1 and Co2–O1 distances of 3.165(3) and 3.012(9) Å respectively. The Fe-N (amido) distances range from 2.0486(12) to 2.0676(12) Å and the Co-N (amido) analogues span from 1.982(8) to 1.995(8) Å; these are comparable with the M–N bond lengths (M = Fe, Co) in $\{M[^{tBu}NON]\}_2$ and tetranuclear **1** and **2**. All other bond distances and angles are comparable to those in **1**-**4** halide/amido complexes. The Fe−Fe distance of 2.6406(4) Å in 6 and Co−Co distance of 2.576(8) Å in **7** respectively are very similar to that of 2.6453(6) Å in $\{Fe_2Br_2[^{tBu}NON]\}_2$ (1) and 2.5899(3) Å in $\{Co_2Br_2[^{tBu}NON]\}_2$ (**2**).

In these newly synthesized organometallic iron(II) and cobalt(II) systems, some of the metal centres are three-coordinate, which would be considered to be a low-coordinate metal centre, hence they may show interesting reactivity. Indeed, it is notable that there are very few reported examples of mixed amido/alkyl M(II) systems: the $[N_2P_2]MX$ (M = Co, Fe; X = Cl, alkyl; $[N_2P_2]$ = $^{t}BuN^{(-)}SiMe_2N(CH_2CH_2P^{i}Pr_2)_2$) and Ar'MN(H)Ar", (M = Mn, Fe, Co; Ar' = $C_6H_3^{2-}$, 6-(C_6H_3-2,6-$^{i}Pr_2)_2$,Ar" = C_6H_3-2,6-(C_6H_2-2,4,6-$Me_3)_2$) systems were recently described. As indicated before, similar mixed alkyl/halide complexes of first-row M(II) centres are very rare and could provide an opportunity for further functionalization at the metal centre via standard metathesis protocols. Later in this chapter there will be a discussion about some preliminary reactivities of these new amido alkyl clusters, such as polymerization of ethylene gas and activation of CO molecules.

Table 3.1. Selected interatomic distances (Å) and angles (°) for **6** and **7**

M	**6, Fe**	**7, Co**
M1–M2	2.6406(4)	2.576(8)
M1–O1	3.165(3)	3.012(9)
M2–O1	2.704(2)	2.471(12)
M1–C3	2.0224(16)	1.959(9)
M2–C4	2.0235(16)	1.965(10)
M1–N1	2.0676(12)	1.982(8)
M1–N2	2.0618(12)	1.993(8)
M2–N1	2.0518(12)	1.982(8)
M2–N2	2.0486(12)	1.995(8)
Si1–N1	1.7564(13)	1.720(10)
Si2–N2	1.7564(13)	1.722(10)
Si1–O1	1.6505(12)	1.634(7)
Si2–O1	1.6497(12)	1.633(8)
C3–M1–N1	130.37(7)	132.1(4)
C4–M2–N2	131.68(6)	128.6(4)
C3–M1–N2	134.61(6)	127.3(4)
N1–M1–N2	93.42(5)	95.6(3)
C4–M2–N1	131.24(6)	135.8(4)
N1–M2–N2	94.29(5)	95.6(4)
Si1–O1–Si2	138.54(8)	141.16(4)
O1–M2–C4	140.76(4)	122.24(3)
Si4–C4–M2	119.39(9)	125.84(3)
Si3–C3–M1	122.68(4)	130.11(4)

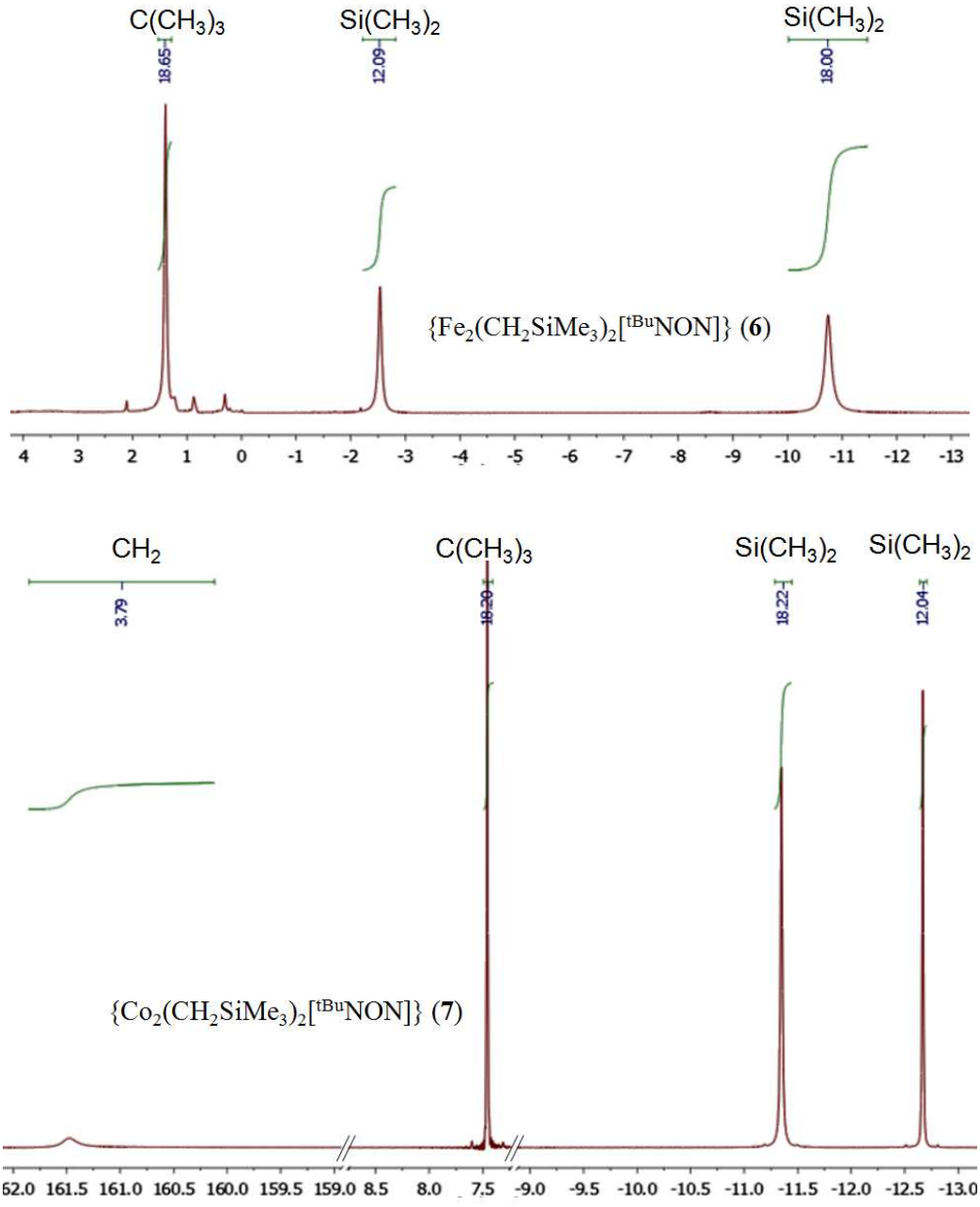

Figure 3.3. ^{1}H NMR spectra of 6 and **7** in benzene-d_6.

The ^{1}H NMR spectra for dialkyl iron and cobalt complexes **6** and **7** clearly show paramagnetically shifted peaks which integrate correctly for each group of t-butyl, $SiMe_2$ and $SiMe_3$ protons as indicated in Figure 3.3. Critically, a highly shifted peak (at δ = 161.7, integrating to 2H) assignable to the M–CH_2 group in **7** was also observed; this shift is consistent with protons in close proximity to the paramagnetic Co(II) centre, however a peak assigned to the M−CH_2 protons was not observed for the iron analogues, which may be a result of the peaks being much broader peak in the iron(II) systems compared to cobalt(II) ones, making it harder to detect. In solution, for each of **6** and **7**, like for **1**-**4,** all of the silyl-methyl groups in the ligand backbone are equivalent, as are the t-butyl groups. The equivalency of the silyl-methyl groups suggests that the silylether donor is likely oscillating rapidly between the two metal centres in a fluxional process at room temperature, yielding an average signal.

The UV-vis spectra of **4** and **7** in THF show two distinct bands in the visible region: 468 nm (ε = 360 $M^{-1}cm^{-1}$) and 673 nm (ε = 500 $M^{-1}cm^{-1}$) for **4** and 464 nm (ε = 750 $M^{-1}cm^{-1}$) and 682 nm (ε = 200 $M^{-1}cm^{-1}$) for **7**. The magnitude of the extinction coefficients implies that the transitions are assignable to d-d transitions and not to charge-transfer processes.[46] More importantly, since the two spectra are very similar, **4** and **7** likely have the same Co(II) high-spin state, so postulated since cobalt halide and amido compounds are typically high-spin.[8] Indeed, two- and three-coordinate and tetrahedral Co(II) complexes are almost invariably high-spin S= 3/2 ground state systems. [97, 135, 171, 192]

To further corroborate the spin state, the solid state magnetic moment of **7** was also examined. The μ_{eff} of $\{Co_2Br_2[^{tBu}NON]\}_2$ (**2**) and $\{Co_2Cl_2[^{tBu}NON](LiCl)\cdot 2THF\}_2$ (**4**) at 300 K are both lower than the 2.62 μ_B found for dinuclear $\{Co_2(CH_2SiMe_3)_2[^{tBu}NON]\}$ (**7**), confirming that halide-bridging is a significant pathway for antiferromagnetic exchange in **2** and **4** systems (as was discussed in Chapter 2). In terms of the spin state of **7**, the μ_{eff} of 2.62 μ_B per Co(II) at 300 K is higher than what is expected for a low-spin, non-octahedral Co(II) system. Indeed, the distorted four-coordinate and trigonal geometries of the Co(II) centres in **7** would be expected to support an S = 3/2 ground state. Furthermore, since the bond distances and angles in **7** are similar to those in the $Co_2X_2[^{tBu}NON]$ (X = Br, Cl) binuclear core of **2** and **4**, this suggests that **7** is best described as containing S = 3/2 (high-spin) Co(II) centres, partially coupled *via* a Co–Co

interaction or the bridging amido ligands; this is also consistent with the observation that the UV-vis and ^{1}H NMR spectra are similar for all three systems, as more drastic spectral changes would be expected if a spin-state change had occurred.

The Evans method for dialkyl iron **6** gives μ_{eff} = 4.6 μ_B, which is the same as observed for $\{Fe_2Cl_2[^{tBu}NON]\}_n$ (**3**). Both of them have a similar dinuclear core in the solid state with similar bond angles and distances, and the μ_{eff} values confirm the presence of a high-spin iron(II) centre in **6** as well. Based on the magnetic measurement the antiferromagnetic coupling is not sufficiently strong to consider the existence of any significant M-M orbital overlap for either **6** and **7**, as discussed for **1**-**4** in Chapter 2.

There are very few high-spin Co(II)- (S= 3/2 ground state) and Fe(II)-alkyl (S= 2 ground state) complexes reported.[91] Other examples of high-spin Fe(II) and Co(II) alkyl complexes include the two-coordinate $(2,6\text{-}Mes_2C_6H_3)_2Co$,[54] the square-pyramidal $[P_2N_2]Co\text{-}CH_2SiMe_3$[42], the trigonal $LMCH_3$[123] (M = Fe, Co; L = β-diketiminate ligand 2,2,6,6-tetramethyl-3, 5-bis(2,6-diisopropyl-phenylimido)hept-4-yl), tetrahedral Tp′M-R[76, 193] (Tp′ = hydridotris(3-R-5-R′-pyrazolyl)borate; M = Fe, Co) and $\{(Ph_2CN)_2C_2H_4\}Fe(CH_2SiMe_3)_2$[194] but most Co(II)- and Fe(II)- alkyl complexes are low-spin[39-40, 79] such as $[Co\{CPh(SiMe_3)(C_5H_4N\text{-}2)\}_2]$,[195] tetrakis(norbornyl)cobalt[196] and Cp/CO-type iron and cobalt complexes, for example $CpFe(CO)_2Me$ (see Chapter 1).[197-201] The difference between high-spin or low-spin iron(II) and cobalt(II) complexes could be result of a combination of both coordination number and geometry difference at the metal centre. In most cases, for low-spin Cp/CO iron and cobalt complexes, they show a six-coordinate metal centre with octahedral geometry,[197-201] while high-spin iron(II) and cobalt(II) are found to be low-coordinate (less than five) in most cases.[192, 194, 202-203]

The Fe−C distances of 2.0224(16) and 2.0235(16) Å in **6** are shorter than that of 2.27(4) Å in high-spin $LFeCH_2Bu$ (Bulky β-diketiminate)[202] but shorter compared with that of 2.069(2) Å in high-spin $[PNP]FeCH(SiMe_3)_2$,[40] 2.078(4) and 2.098(4) Å in $LFe(TMS)_2$,[194] and are also shorter than many Cp/CO-containing low-spin iron(II) complexes with a Fe−C distance range form 2.04 to 2.06 Å.[197-199]. The Co−C bond distances of 1.959(9) and 1.965(10) Å in **7** are shorter compared with that of 1.995(5) and 2.033(2)Å in high-spin $[N_2P_2]CoMe$ and $[N_2P_2]CoCH_2SiMe_3$[42], they are also shorter than that of the 2.009(8) Å in low-spin [PNP]CoMe[39] and 2.071(3) in low-spin

[Co{CPh(SiMe$_3$)(C$_5$H$_4$N-2)}$_2$],[195]. As a result, based on the comparisons that is shown above, there is appears to be no specific trend in high-spin M-C (M= Fe, Co) bond distances compared to low-spin [Co{CPh(SiMe$_3$)(C$_5$H$_4$N-2)}$_2$].[195]

3.2.2. Synthesis and characterization of alkyl/halide Amido Iron(II) and Cobalt(II) clusters

Upon changing the stoichiometric ratio of alkyllithium reagent: metal dimer from 2:1 to 1:1, new mixed alkyl/halide organometallic clusters were obtained. The X-ray crystal structures of {[^{tBu}NON]Fe$_2$Cl(CH$_2$SiMe$_3$)}$_2$ (**8**) and {[^{tBu}NON]Co$_2$Cl(CH$_2$SiMe$_3$)}$_2$ (**9**) show that they are structurally very similar to tetranuclear cobalt **1** and iron **2** (Figure 3.4). As before, there are two crystallographically different metal sites M1 and M2 in the cluster with different coordination geometries. The M1 centre is coordinated to both amido donors, two bridging chlorides and also interacts with the silylether oxygen donor in the ligand backbone, yielding a distorted trigonal-bipyramidal geometry with the silylether and one bridging bromide occupying the axial site. On the other hand, M2 exists in a three-coordinate, roughly trigonal geometry in which it is coordinated only to one CH$_2$SiMe$_3$ group and the two amido groups, as shown in Figure 3.4.

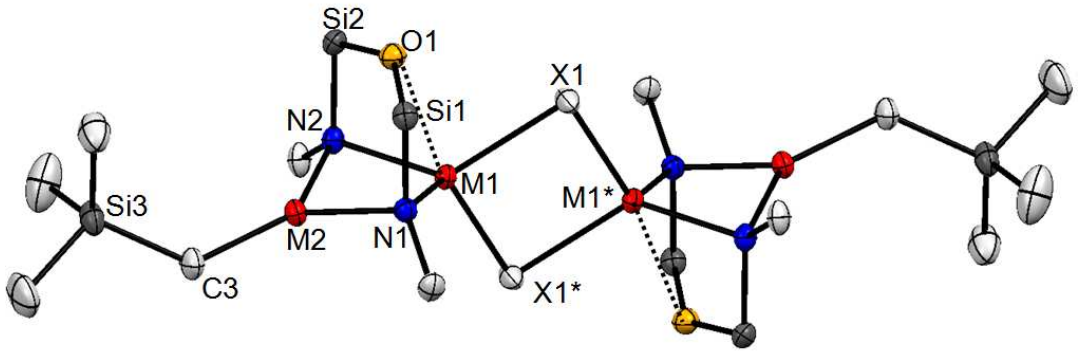

Figure 3.4. Molecular structure of **8** (M= Fe, X=Cl), **9** (M= Co, X= Cl), **10** (M= Fe, X=Br), and **11** (M= Fe, X=Br); (^{t}Bu and $SiMe_2$ groups simplified for clarity).

Switching the chloride for bromide (via using bromo/amido iron **1** and cobalt **2** instead of chloro/amido iron **3** and cobalt **4** as starting materials) resulted in the analogous bromo/alkyl complexes $\{Fe_2Br(CH_2SiMe_3)[^{tBu}NON]\}_2$ (**10**) and $\{Co_2Br(CH_2SiMe_3)[^{tBu}NON]\}_2$ (**11**). Their X-ray crystal structures show that they are isostructural to the tetranuclear cobalt and iron **8** and **9** (Figure 3.4). However, although **8** and **9** are fully characterized, **10** and **11** did not fully characterized due their low yield, given that they are side products of uncompleted alkylation reactions. The X-ray structure for both provide reliable data about their structures, however both **10** and **11** could in theory be synthesized as the main products by mono-alkylation of the $\{M_2Br_2[^{tBu}NON]\}_2$ iron **1** and cobalt **2**.

All bond distances and angles in alkyl/chloro iron **8** and cobalt **9** are very similar to those of $\{Fe_2Cl_2[^{tBu}NON]\}_n$ (**3**) and $\{Co_2Cl_2[^{tBu}NON](LiCl)\cdot 2THF\}_2$ (**4**). Fe2−C2 distances of 2.036(4) Å in **8** (Table 3.2) and Co2−C2 distances of 2.00(1) Å in **9** respectively (Table 3.4) are similar to the 2.0224(16) and 2.0235(16) Å in $\{Fe_2(CH_2SiMe_3)_2[^{tBu}NON]\}$ (**6**) and 1.959(9) and 1.965(10) Å in $\{Co_2(CH_2SiMe_3)_2[^{tBu}NON]\}$ (**7**). The bond distances and angles in alkyl/bromo iron **10** and cobalt **11** are also very similar to those in $\{Fe_2Br_2[^{tBu}NON]\}_2$ (**1**) and $\{Co_2Br_2[^{tBu}NON](LiCl)\cdot 2THF\}_2$ (**4**). The Fe2−C2 distance of 2.038(4) Å in **10** and the Co2−C2 distance of 2.009(2) Å in **11** are similar to the iron-carbon bonds of 2.0224(16) and 2.0235(16) Å in **6** and 2.036(4) Å in **8**, and the Co2−C2

distances of 1.959(9) and 1.965(10) Å in **7**. Transition metal amido/alkyl/halide complexes are not common in the literature. There is one example of a mixed alkyl halide mononuclear iron complex, $L_2Fe(CH_2SiMe_3)Cl$[204-205] (L_2: $((2,6\text{-}^iPr_2Ph)NCMe)_2$) and no example of such a mono- or dinuclear iron or cobalt complex to our knowledge. However, there are several examples of monochromium complexes reported: $[N_2P_2]Cr(Cl)CH_2SiMe_3$[206], $[N_2P_2]Cr(Cl)Me$[206] ({$H[N_2P_2]= {}^tBuN(H)SiMe_2N(CH_2CH_2P^iPr_2)_2$}), Cr(Me)Br[PNP][207] and $Cr(CH_2SiMe_3)Cl$[PNP][207]

Table 3.2. Selected interatomic distances (Å) and bond angles(°) for **8** -**11**

M/X	Fe/Cl (8)	Fe/Br (10)	Co/Cl (9)	Co/Br (11)
M1–M1*	3.515(4)	3.710(1)	3.491(2)	3.61(5)
M1–M2	2.7221(7)	2.690(2)	2.729(2)	2.649(5)
M1–O1	2.573(3)	2.611(5)	2.492(2)	2.58(2)
M2–O1	3.090(1)	3.113(3)	3.084(3)	3.12(2)
M2–C3	2.036(4)	2.038(4)	2.00(1)	2.009(2)
M1–X1	2.39549(7)	2.5293(7)	2.384(3)	2.467(5)
M1–X1*	2.400(1)	2.5668(9)	2.404(3)	2.527(7)
M1–N1	2.056(2)	2.048(3)	2.059(8)	1.96(2)
M1–N2	2.066(3)	2.064(3)	2.049(8)	2.07(2)
M2–N1	2.064(3)	2.065(3)	2.040(8)	2.05(2)
M2–N2	2.055(2)	2.060(3)	2.020(8)	1.96(2)
Si1–N1	1.757(2)	1.763(4)	1.740(9)	1.86(2)
Si2–N2	1.757(2)	1.759(4)	1.742(9)	1.70(2)
Si1–O1	1.652(2)	1.648(4)	1.654(8)	1.66(2)
Si2–O1	1.657(2)	1.658(2)	1.655(8)	1.64(3)
X1–M1–N2	124.96(7)	120.34(9)	125.0(2)	125.5(6)
X1–M1–N1	120.82(7)	126.3(1)	123.7(2)	120.6(7)

X1*–M1–N2	116.42(7)	116.19(9)	116.1(2)	115.5(6)
X1*–M1–N1	117.97(7)	115.2(1)	115.7(2)	112.9(7)
N1–M1–N2	93.56(9)	94.2(1)	92.3(3)	95.5(9)
N1–M2–N2	93.66(9)	93.83(1)	93.7(3)	95.4(8)
C3–M2–N1	127.00(1)	128.4(2)	138.6(4)	132.7(9)
C3–M2–N2	139.00(1)	132.9(2)	124.3(4)	123.7(9)
M1–N2–M2	82.68(9)	81.7(1)	83.7(3)	95.4(8)
M1–N1–M2	82.71(9)	81.4(1)	84.0(3)	81.9(8)
Si1–O1–Si2	142.24(1)	141.31(2)	140.9(5)	144.0(1)
X1–M1–X1*	85.70(3)	86.58(3)	86.4(1)	87.5(2)
M1–X1–M1*	94.30(3)	93.42(3)	93.6(1)	92.1(2)

Symmetry operation **8**, *: -x+1/2,-y+1/2,-z; **9**, **10**, **11** *: -x,-y,-z

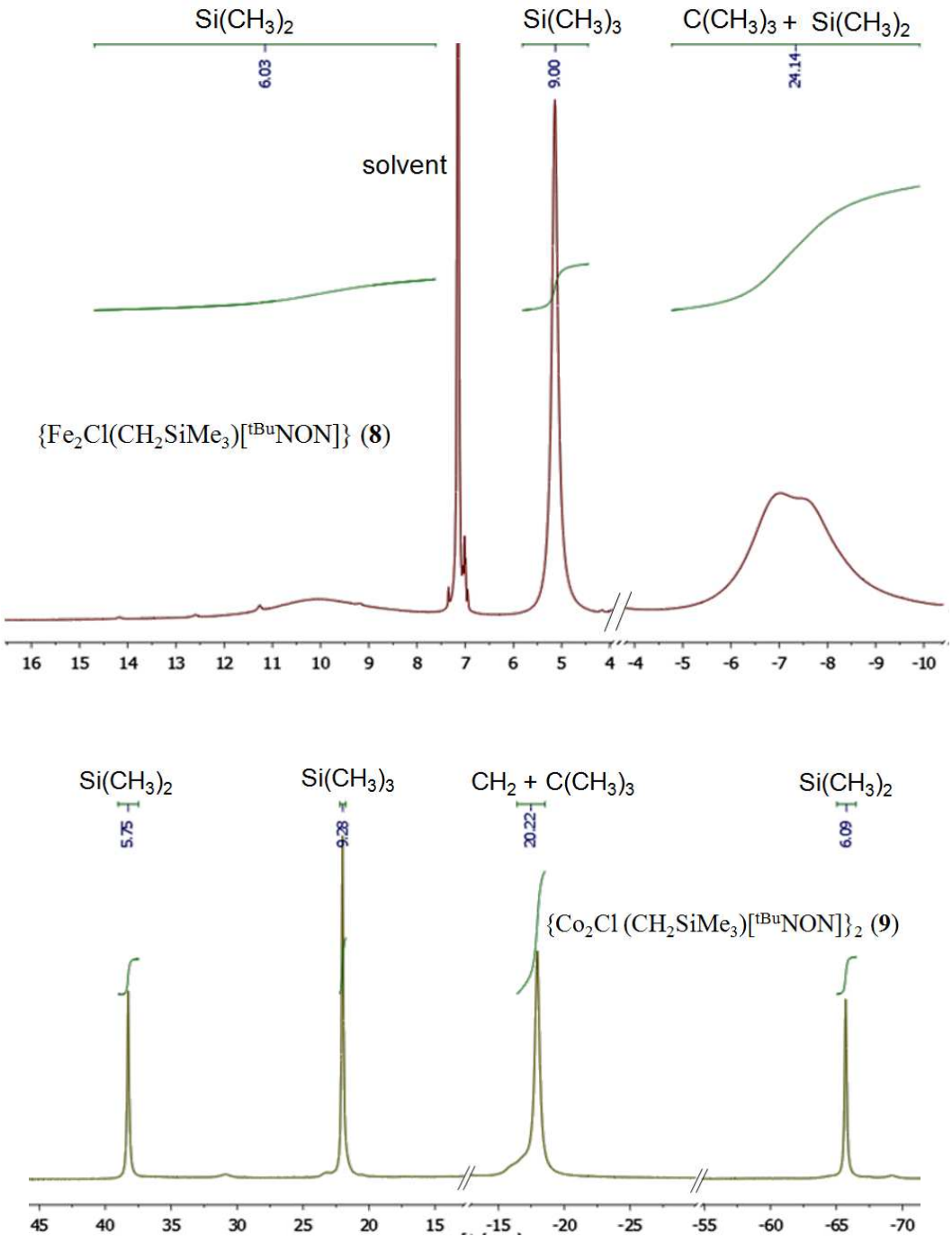

Figure 3.5. ^{1}H NMR spectra of **8** and **9** in benzene-d_6.

The ^{1}H NMR spectrum of **9** shows four peaks: two are assignable to $SiMe_2$ groups, one to the $SiMe_3$ group and one broad peak with a small shoulder is assignable to overlapping t-butyl and -*CH*$_2$-$SiMe_3$ groups (Figure 3.5). A similar spectrum, with four peaks is present for the iron analogue **8**: one peak for the $SiMe_3$ group, and two peaks for $SiMe_2$ units, one of which overlap with the t-butyl peak in the same region. However, no peak assignable to the –*CH*$_2$ group was observed; the peak is likely too small and broad to be detected (as in **7**). For both **8** and **9**, the spectra show one peak for the t-butyl groups while two different peaks could be assigned to the silyl-methyl groups, showing that the two $SiMe_2$ units on the ligand backbone are inequivalent in solution, consistent with their inequivalence in the solid state. This is unlike what was observed in the halide/amido **1**-**4** systems in which, based on their ^{1}H NMR spectra, they were solvated as simple dinuclear clusters in solution. However it is not unusual for dinuclear **8** and **9** to maintain their cluster motif in solution, similar to dinuclear $\{FeX[^{tBu}NON]\}_2$ (X= Cl and Br) systems maintaining their solid state structure in solution.[55]

The Evans method value of μ_{eff} = 3.4 μ_B per metal for $\{Fe_2Cl(CH_2SiMe_3)[^{tBu}NON]\}_2$ (**8**) is close to that of $\{Fe_2Br_2[^{tBu}NON]\}_2$ (**1**) (3.15 μ_B) but lower than the μ_{eff} of 4.6 μ_B for $\{Fe_2(CH_2SiMe_3)_2[^{tBu}NON]\}$ (**6**), which can be rationalized in that both **8** and **1** have the halide-bridged pathway for magnetic coupling and thus have significant antiferromagnetic exchange in these systems, while **7** does not**.** The Evans method value of μ_{eff} = 2.0 μ_B per metal for $\{Co_2Cl(CH_2SiMe_3)[^{tBu}NON]\}_2$ (**9**) is close to the μ_{eff} = 2.62 μ_B per metal for $\{Co_2(CH_2SiMe_3)_2[^{tBu}NON]\}$ (**7**) and the μ_{eff} of 2.23 μ_B of $\{Co_2Cl_2[^{tBu}NON](LiCl)\cdot 2THF\}_2$ (**4**), which again supports a similar spin state in these systems; they have a very similar geometry around the metal centre with similar bond angles and distances based on their X-ray structures.

3.2.3. Synthesis and characterization of iron(II) and cobalt(II) methyl/halide clusters.

In order to synthesize methylated iron and cobalt complexes, one equivalent of MeMgBr or MeLi per metal centre was added to the iron and cobalt halide/diamido **3** and **4**. Contrary to the observed dialkyl substitution from using $LiCH_2SiMe_3$ in **6** and **7**, substitution of methyl for halide on both metal centres in **3** and **4** was not successful and resulted in formation of $\{M[^{tBu}NON]\}_2$.

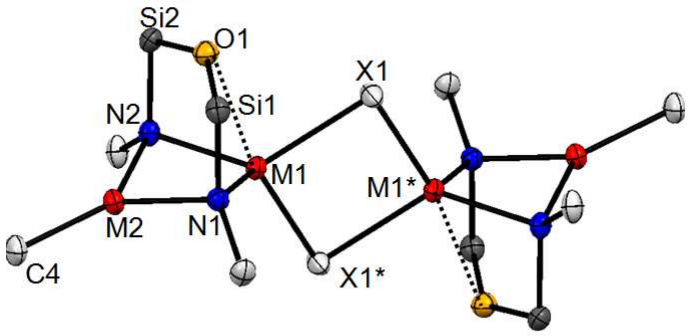

Figure 3.6. Molecular structure of **12** (M= Fe, X= Br) and **13** (M= Co, X= Cl); (^{t}Bu and $SiMe_2$ groups simplified for clarity, **12** is shown).

However reaction of one equivalent of MeLi per dinuclear $Co_2Cl_2[^{tBu}NON]$ unit (in **4**) resulted in the isolation of the greenish-brown mixed methyl/halide diamido cobalt(II) $\{Co_2Cl(Me)[^{tBu}NON]\}_2$ (**13**) cluster in low yield. Addition of one equivalent of MeMgBr per dinuclear $\{Fe_2Cl_2[^{tBu}NON]\}$ (**3**) resulted in the yellow mixed methyl/halide diamido iron(II), $\{Fe_2Br(Me)[^{tBu}NON]\}_2$ (**12**) (Figure 3.6). In this case, in addition to the alkyl metathesis, the bromide in the Grignard reagent underwent halide exchange with the chloride in the starting material as well. Similar bromide for chloride exchange has been observed and reported before, for example in zirconium cluster complexes.[208-211] Further characterization of **12** and **13** did not proceed due to their low yields and contamination with salt by-product and starting materials.

The X-ray crystal structure of $\{Fe_2Br(Me)[^{tBu}NON]\}_2$ (**12**) shows it structurally to be similar to $\{Fe_2Br_2[^{tBu}NON]\}_2$ (**1**) and mixed $\{Fe_2Br(CH_2SiMe_3)[^{tBu}NON]\}_2$ (**11**) with one trigonal and one distorted four-coordinate metal per dimer. The Fe2−C2 distance of 2.045(1) Å (Table 3.3) is slightly longer than that of 2.036(4) Å in $\{Fe_2Cl(CH_2SiMe_3)[^{tBu}NON]\}_2$ (**8**) and 2.0224(16) and 2.0235(16) Å in $\{Fe_2(CH_2SiMe_3)_2[^{tBu}NON]\}$ (**6**).

Table 3.3. Selected interatomic distances (Å) and bond angles (°) for $\{Fe_2BrMe[^{tBu}NON]\}_2$ (**12**)

Fe1–Fe1*	3.683(3)	N1–Fe1–N2	93.1(3)
Fe1–Fe2	2.738(2)	N1–Fe2–N2	93.5(3)
Fe1–Br1	2.556(2)	Fe2–N1–Fe1	82.4(2)
Fe1–Br1*	2.582(2)	Fe2–N2–Fe1	82.6(3)
Fe2–C4	2.045(1)	Br1–Fe1–Br1*	88.37(6)
Fe1 –O1	2.54(3)	O1–Fe1–Br1*	176.2(2)
Fe2–O1	3.11(3)	N2–Fe1–Br1	113.7(2)
Fe1–N1	2.075(8)	N1–Fe1–Br1	116.0(2)
Fe1–N2	2.078(8)	N2–Fe2–C4	133.4((3)
Fe2–N1	2.068(8)	N1–Fe2–C4	131.4(2)
Fe2–N2	2.075(8)	Si1–O1–Si2	140.1(4)
Si1–N1	1.741(6)		
Si2–N2	1.748(6)		
Si1–O1	1.655(7)		
Si2–O1	1.651(7)		

Symmetry operation *: -x,-y,-z

The X-ray crystal structure of $\{Co_2Cl(Me)[^{tBu}NON]\}_2$ (**13**) is also similar to $\{Co_2Br_2[^{tBu}NON]\}_2$ (**2**) and $\{Co_2Cl(CH_2SiMe_3)[^{tBu}NON]\}_2$ (**9**). The Co2−C2 distance of 1.986(6) Å (Table 3.4) is close to the Co2−C2 distances of 2.00(1) Å in $\{Co_2Cl(CH_2SiMe_3)[^{tBu}NON]\}_2$ and the 1.959(9) and 1.965(10) Å in $\{Co_2(CH_2SiMe_3)_2[^{tBu}NON]\}$ (**7**).

Table 3.4. Selected interatomic distances (Å) and bond angles (°) for $\{Co_2ClMe[^{tBu}NON]\}_2$ (**13**)

Co1–Co2	2.6572(8)	N1–Co1–N2	93.7(1)
Co1–Cl1	2.338(1)	N1–Co2–N2	94.6(1)
Co1–Cl1*	2.404(1)	Co2–N1–Co1	82.2(1)
Co2–C4	1.986(6)	Co2–N2–Co1	82.2(1)
Co2–O1	3.063(3)	Cl1*–Co1–Cl1	86.64(4)
Co1–O1	2.541(1)	O1–Co1–Cl1	174.9(4)
Co1–N1	2.033(3)	N2–Co1–Cl1	122.99(9)
Co1–N2	2.026(3)	N1–Co1–Cl1	125.55(9)
Co2–N1	2.013(3)	N2–Co2–C4	130.5(2)
Co2–N2	2.016(3)	N1–Co2–C4	131.1(2)
Si1–N1	1.748(3)	Si1–O1–Si2	141.8(2)
Si2–N2	1.748(3)		
Si1–O1	1.655(3)		
Si2–O1	1.648(3)		

Symmetry operation *: -x,-y,-z

3.2.4. Reactivity of the high-spin M-alkyl clusters 6 and 7

In the new organometallic cobalt(II) and iron(II) dinuclear dialkyl clusters $\{Fe_2(CH_2SiMe_3)_2[^{tBu}NON]\}$ (**6**) and $\{Co_2(CH_2SiMe_3)_2[^{tBu}NON]\}$ (**7**), there are two different metal centres: one is four and the other is three-coordinate. In the mono-alkylated tetranuclear iron and cobalt complexes **8**-**11** ($\{M_2XR[^{tBu}NON]\}_2$, X= Cl, Br, R= CH_2SiMe_3, Me) there are also two different metal sites; one is five- and the other is three-coordinate. High-spin iron(II) and cobalt(II) alkyl complexes, especially with M−methyl groups, are rare and as previously mentioned there are only a few reported examples. There has recently been interest in the synthetic and structural chemistry of dinuclear Fe(II) and Co(II) metal complexes showing short metal−metal distances.[212] [213] Some of

these complexes show interesting magnetic properties. [213] Since metal−metal bonds are nearly always associated with diamagnetism it is more unusual behavior for organometallic complexes.

The organometallic clusters **6**-**11** presented in this Chapter contain rare high-spin cobalt(II) and iron(II) carbon bonds of which little is known about their basic reactivity. These compounds provide the opportunity to survey high-spin M-C bond reactivity with some standard organometallic reagents and to compare them to more developed low-spin systems. With this in mind, some preliminary ethylene polymerization activity of dialkyl **6** and **7** and CO was examined. Having low-coordinate metal centres makes **6** and **7** potentially even more reactive.

Reactivity of high-spin dialkyl 6 and 7 with ethylene

In order to probe the polymerization reactivity of the high-spin M−C bond in **6** and **7**, toluene solutions of $\{Fe_2(CH_2SiMe_3)_2[^{tBu}NON]\}_2$ (**6**) and $\{Co_2(CH_2SiMe_3)_2[^{tBu}NON]\}_2$ (**7**) were placed under 1 atm of ethylene gas at room temperature, and stirred for about 24 hours. Unfortunately, the polymerization capability for both iron and cobalt was not significant; no solid polymer formed, just a small amount of oligomerization was observed by MS analysis of the solution. Ethylene polymerization was also attempted by adding one equivalent of a typical Lewis-acid, activating reagent tris(pentafluorophenyl)borane, per metal centre. Interestingly, this common cocatalyst was found to *hinder* the polymerization ability of **6** and **7**. Indeed, it was noticed that upon addition of $B(C_6F_5)_3$ to the $\{Co_2(CH_2SiMe_3)_2[^{tBu}NON]\}_2$ (**7**) solution in an ethylene atmosphere, the colour changed right away from brown to dark green. After removing the solvent, the product $\{Co_2(C_6F_5)_2[^{tBu}NON]\}_2$ (**14**) (Figure 3.7) was crystallized by slow evaporation of a hexanes solution.

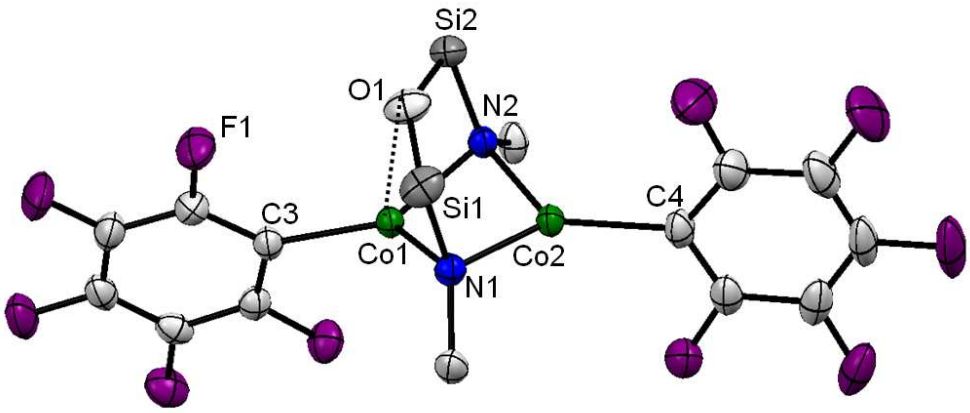

Figure 3.7. Molecular structure of **14**; (^{t}Bu and $SiMe_2$ groups simplified for clarity).

Compound **14** was also synthesized by the addition of two equivalents of tris(pentafluorophenyl)borane to one equivalent of $\{Co_2(CH_2SiMe_3)_2[^{tBu}NON]\}$ (**7**) in the absence of ethylene. Green diaryl/amido cobalt(II) **14** was obtained in good yield.

The X-ray structure reveals a diaryl cobalt(II) $\{Co_2(C_6F_5)_2[^{tBu}NON]\}$ (**14**) complex. For the iron analogue, the reaction of $B(C_6F_5)_3$ with $\{Fe_2(CH_2SiMe_3)_2[^{tBu}NON]\}$ (**6**) in the absence of ethylene was also examined but, due to residual $\{Fe_2Cl(CH_2SiMe_3)[^{tBu}NON]\}_2$ (**8**) in the sample of **6**, the product was a mixture, from which crystals of $\{Fe_2Cl(C_6F_5)[^{tBu}NON]\}$ (**15**) (Figure 3.8) were obtained through the slow evaporation of hexanes. This indicates that the iron alkyl unit in $\{Fe_2Cl(CH_2SiMe_3)[^{tBu}NON]\}_2$ (**8**) (and presumably in $\{Co_2(CH_2SiMe_3)_2[^{tBu}NON]\}$ (**7**) as well) undergoes a similar reaction with $B(C_6F_5)_3$.

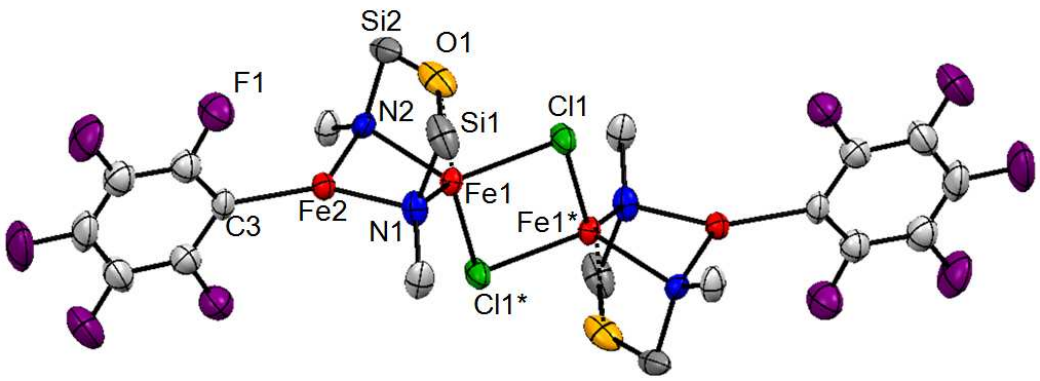

Figure 3.8. Molecular structure of **15**; (^{t}Bu and $SiMe_2$ groups simplified for clarity).

Table 3.5. Selected interatomic distances (Å) and bond angles (°) for $\{Co_2(C_6F_5)_2[^{tBu}NON]\}$(**14**)

Co1–Co2	2.5262(5)	N1–Co1–N2	98.26(9)
Co1–C3	1.995(2)	N1–Co2–N2	97.61(9)
Co2–C4	2.009(2)	Co2– N1–Co1	79.10(8)
Co2–O1	2.998(1)	Co2–N2–Co1	79.20(8)
Co1–O1	2.415(2)	O1–Co1–C3	115.72(2)
Co1–N1	1.982(2)	N2–Co1–C3	132.4(1)
Co1–N2	1.974(2)	N1–Co1–C3	129.1(1)
Co2–N1	1.985(2)	N2–Co2–C4	129.0(1)
Co2–N2	1.989(2)	N1–Co2–C4	132.6(1)
Si1–N1	1.766(2)	Si1–O1–Si2	146.8(2)
Si2–N2	1.758(2)		
Si1–O1	1.660(3)		
Si2–O1	1.663(3)		

The X-ray crystal structure of $\{Co_2(C_6F_5)_2[^{tBu}NON]\}$ (**14**) is very similar to the dialkyl $\{Co_2(CH_2SiMe_3)_2[^{tBu}NON]\}$ (**7**). They are both dinuclear cobalt(II) systems with two different cobalt centres: one is trigonal and the other one is trigonal monopyramidal (Figure 3.8). The aryl Co2−C2 distances of 1.995(2) and 2.009(2) Å (Table 3.6) are slightly longer than that of 1.931(5) Å in the similar $(\pi\text{-}C_6H_5CH_3)Co(C_6F_5)_2$ complex.[214] The Co1−O1 and Co2−O1 distances of 2.415(2) and 2.998(1) Å in **14** (Table 3.5) are very similar to the 2.471(12) and 3.012(9) Å in $\{Co_2(CH_2SiMe_3)_2[^{tBu}NON]\}$ (**7**), while the Co1−Co2 distance of 2.5262(5)Å in **14** is slightly shorter than the 2.576(8) Å in **7**. There are a few examples of Co-C_6F_5 species reported in the literature, such as $(\pi\text{-}C_6H_5CH_3)Co(C_6F_5)_2$[214] and $Co(C_6F_5)(CO)_3PPh_3$.[215]

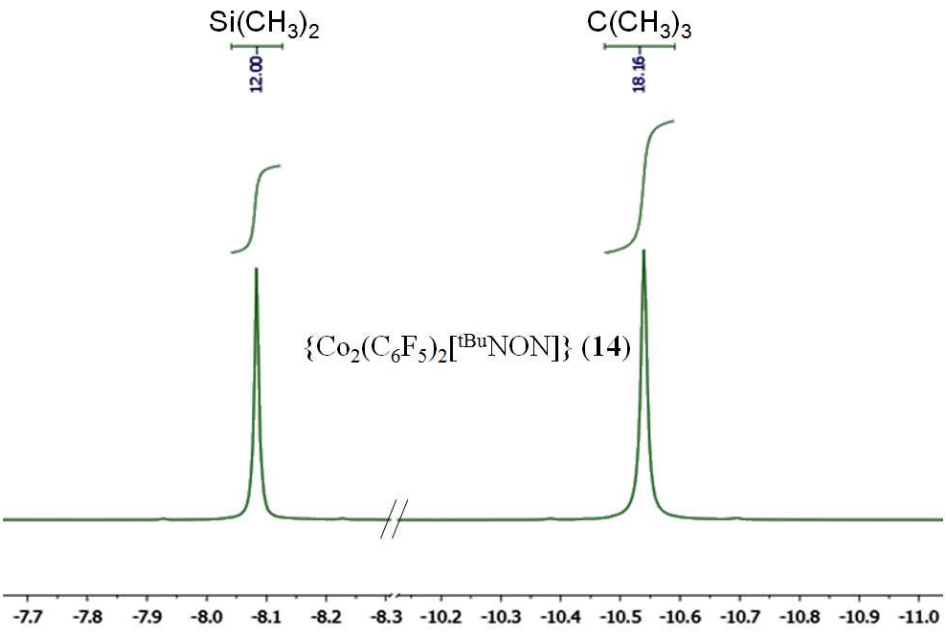

Figure 3.9. ^{1}H NMR spectrum of **14** in benzene-d_6.

The ^{1}H NMR spectrum for $\{Co_2(C_6F_5)_2[^{tBu}NON]\}_2$ (**14**) has similar features (Figure 3.9) to the halide/amido iron and cobalt **1**-**4** and dialkyl/amido iron and cobalt 6 and **7** as well, with the usual paramagnetically shifted broad peaks. All of the $SiMe_2$

groups are equivalent, as are the t-butyl groups, which again suggests that the silylether donor is likely oscillating rapidly between the two metal centres in a fluxional process at room temperature. One difference in this ^{1}H NMR spectrum is that the $SiMe_2$ peak is in a quite different position while the t-butyl peak is in a similar place as in **1**-**4**, **6** and **7**.

The solution magnetic moment of 2.6 μ_B for **14** is very close to that of high-spin $\{Co_2(CH_2SiMe_3)_2[^{tBu}NON]\}$ (**7**), suggesting that **14** is high-spin as well, consistent with its similar structure.

Table 3.6. Selected interatomic distances (Å) and bond angles (^{o}) for $\{Fe_2Cl(C_6F_5)[^{tBu}NON]\}_2$ (**15**)

Fe1–Fe1*	3.483(2)	N1–Fe1–N2	92.36(2)
Fe1–Fe2	2.680(1)	N1–Fe2–N2	95.34(2)
Fe1–Cl1	2.384(2)	Fe2–N1–Fe1	81.81(1)
Fe1–Cl1*	2.397(3)	Fe2–N2–Fe1	81.5 (9)
Fe2–C4	2.070(1)	Cl1–Fe1–Cl1*	86.4(6)
Fe 2–O1	3.105(3)	Fe1–Cl1–Fe1*	93.5(4)
Fe1–O1	2.573(4)	O1–Fe1–Cl1*	171.7 (1)
Fe1–N1	2.074(7)	N2–Fe1–Cl1	127.2(4)
Fe1–N2	2.073(3)	N1–Fe1–Cl1	117.3(4)
Fe2–N1	2.0209(8)	N2–Fe2–C4	131.1(3)
Fe2–N2	2.019(8)	N1–Fe2–C4	132.50(1)
Si1–N1	1.754(2)	Si1–O1–Si2	143.1(3)
Si2–N2	1.752(2)		
Si1–O1	1.650(1)		
Si2–O1	1.656(4)		

The X-ray crystal structure of the tetranuclear aryl chloride iron(II) $\{Fe_2Cl(C_6F_5)[^{tBu}NON]\}_2$ (**15**) complex is also very similar to its precursor $\{Fe_2Cl(CH_2SiMe_3)[^{tBu}NON]\}_2$ (**8**), with one trigonal and one five-coordinate trigonal-bipyramidal iron(II) centre. The aryl Fe2−C2 distance of 2.070(1) Å (Table 3.6) in **15** is

slightly longer than the 2.036(4) Å in $\{Fe_2Cl(CH_2SiMe_3)[^{tBu}NON]\}_2$ (**8**) and the Fe1−Fe2 distance of 2.680(1) Å in **15** is slightly shorter than the 2.7221(7) Å in **8**. The aryl Fe2−C2 distance of 2.070(1) Å in **15** is very similar to that of 2.078(7) Å in $\{[(Ph_2CN)_2C_2H_4]Fe(CH_2SiMe_3)C_6F_5\}$.[204-205] As for cobalt, there are a few examples of Fe-C_6F_5 species known, $CpFe(CO)_2$-C_6F_5,[216] however there are examples of other transition metal-C_6F_5 such as with Cr,[217] Ti,[218] Zr,[219] and Zn.[220]

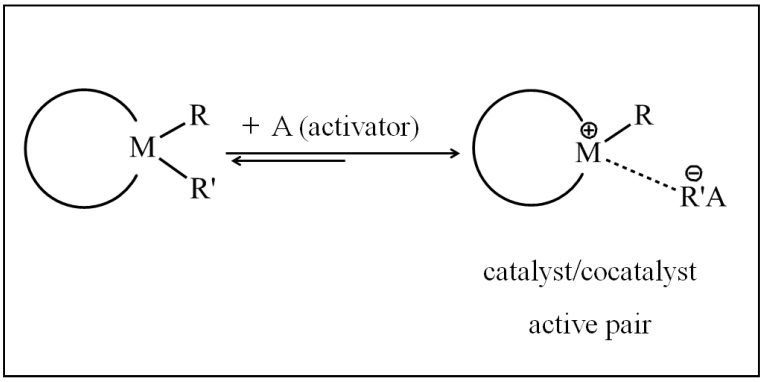

Scheme 3.3. Formation of catalyst /cocatalyst active pair (R, R′= alkyl).[221]

The major role of the activating agent in a metal-catalyzed polymerization reaction is to transform a precatalyst into an active catalyst. The reaction of the precatalyst with the Lewis-acid activating agent (or cocatalyst) usually forms cation-anion pair, in which the cation is the active catalyst site and the anionic part houses the cocatalyst, as shown in Scheme 3.3.[221]

Tris(pentafluorophenyl)borane, $B(C_6F_5)_3$[222] is a very well-known cocatalyst especially used with metallocene alkyl olefin polymerization catalysts due to its strong Lewis acidic properties.[221] For example the pyridine-diimine iron dialkyl complex $(PDI)Fe(CH_2SiMe_3)_2$ (PDI= 2,6-{2,6-*i*-$Pr_2C_6H_3NC(Me)\}_2C_5H_3N$) can form a monoalkyl iron cation by reaction with tris(pentafluorophenyl)borane and the resulting cation $[(PDI)Fe(CH_2SiMe_2CH_2SiMe_3)][MeB(C_6F_5)_3]$[223] is very active in the polymerization of ethylene.[194] Even though it is not common, $B(C_6F_5)_3$ has also been found to deactivate catalysts in some cases.[224]

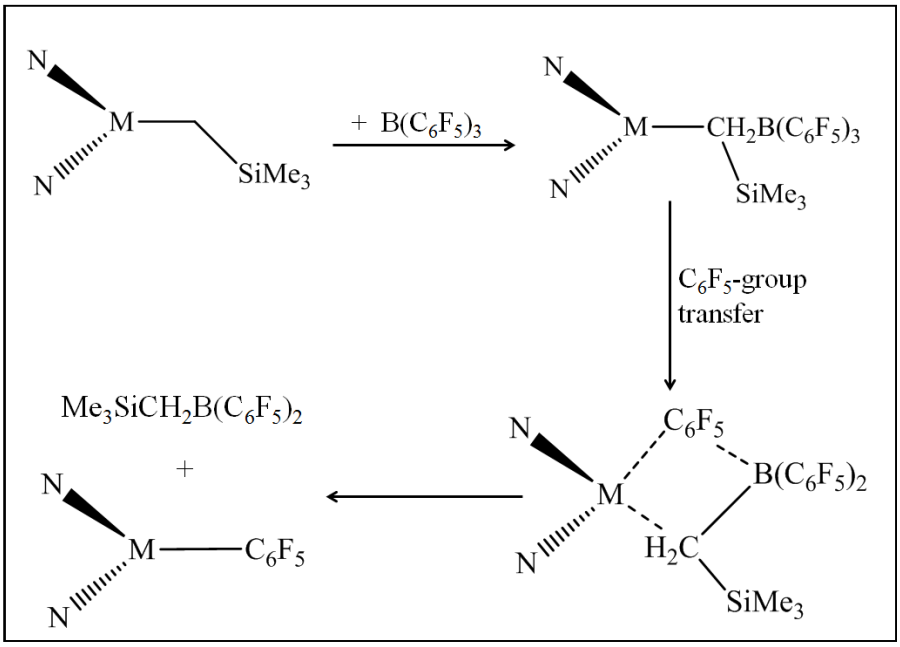

Scheme 3.4. Proposed aryl group transfer mechanism from $B(C_6F_5)_3$ to metal centre (M); (N= amido ligand).[221]

One reported deactivation mechanism is the formation of $[RB(C_6F_5)_3]^-$ and then one -C_6F_5 group transfer to the cationic metal centre, resulting in alkyl for aryl substitution at the metal centre, as shown in Scheme 3.4.[204] [225] One example is the -C_6F_5 group transfer in the reaction of $\{(Ph_2CN)_2C_2H_4\}Fe(CH_2SiMe_3)_2$ with $B(C_6F_5)_3$, which resulted in the formation of $[\{(Ph_2CN)_2C_2H_4\}Fe(CH_2SiMe_3)C_6F_5]$ in toluene; however, changing the solvent for THF generated a different result: an ethylene adduct of the iron alkyl cation.[205] On the other hand, the driving force for Co-alkyl and Fe-alkyl to form M-aryl in **14** and **15** could be the stronger M-aryl bonds compared to the M-alkyl bond due to the π–e availability in aryl ligands that can be in favour of the unsaturated transition metal centre.[226]

Reactivity of high-spin 6 and 7 with CO and CO_2

The reaction of CO with M−C bonds is a fundamental organometallic process and thus, it is important to probe the reactivity of a high-spin iron(II)-alkyl system and compare it to the common low-spin ones.

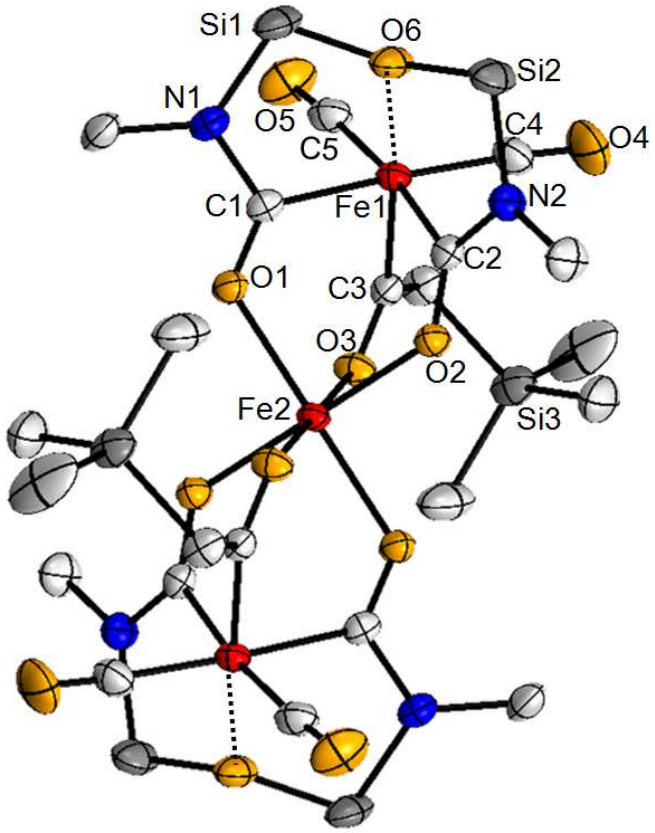

Figure 3.10. Molecular structure of **16** (^{t}Bu and $SiMe_2$ groups simplified for clarity).

Thus, upon exposing {$Fe_2(CH_2SiMe_3)_2[^{tBu}NON]$} (**6**) to an *excess* amount of CO gas (1 atm) at -70 ^{o}C, a dicarbamoyl (carboxamido) trinuclear iron derivative **16** was obtained in good yield. Brown single crystals of **16** were isolated by slow evaporation of a hexanes solution.

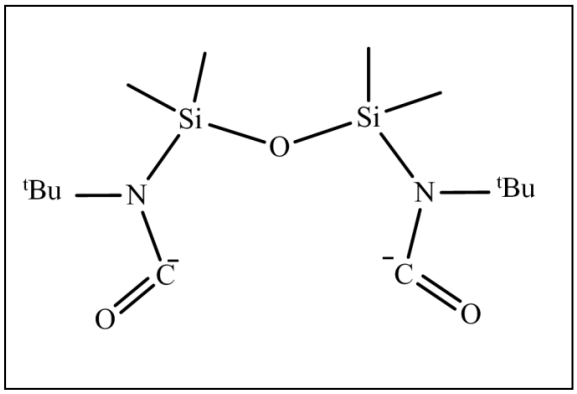

Figure 3.11. New dicarbamoyl ligand ($[C^{NON}C]^{2-}$)

The X-ray structure identified **16** as a trinuclear iron complex with two different iron sites; both are 6-coordinated in an octahedral geometry. Remarkably, the dialkyl iron(II) **6** undergoes three different modes of reactivity with CO: two CO molecules are bonded to the Fe1 centre as terminal CO ligands (C4=O4 and C5=O5 in Figure 3.9); one CO molecule has inserted into the Fe−CH_2SiMe_3 bond, as is commonly observed for CO reacting with metal alkyl complexes and remarkably two CO molecules have inserted into both Fe−N (amide) bonds of the $[NON]^{2-}$ ligand to result in the formation of a new dicarbamoyl-O donor ligand (C1=O1 and C2=O2 in Figure 3.11). Finally, all three of the inserted CO units also coordinate to the central iron site in an isocarbonyl fashion, i.e. through the O-atom (C3=O3 in Figure 3.10).

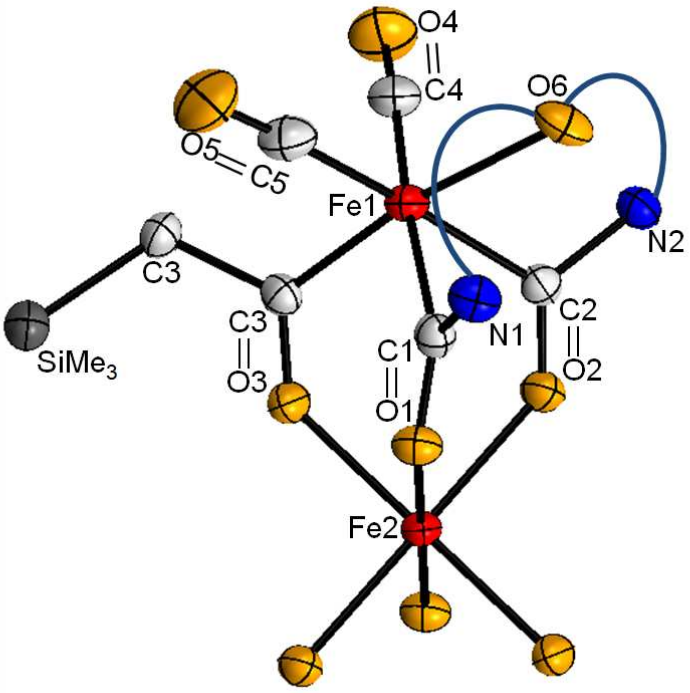

Figure 3.12. The coordination geometry around both crystallographically unique iron centres, highlighting the CO insertions in **16**.

The Fe1 centre is coordinated to two carbons of the new dicarbamoyl ligand $[CO([Me_3CN(SiMe_2)]_2O)OC]^{2-}$= $[C^{NON}C]^{2-}$, Figure 3.11), two CO, one acyl carbon of $-COCH_2SiMe_3$ and is weakly coordinated to the silylether in the ligand backbone; the central Fe2 site is coordinated by six isocarbonyl oxygens from two dicarbamoyl ligands and two $-COCH_2SiMe_3$ groups (Figure 3.12).

In order to investigate the course of the reaction and hopefully isolate some intermediate products, substoichiometric addition of CO to the iron dialkyl **6** was conducted by repeating the reaction with 1, 2 and 4 equivalents of CO per dimer. None of these reactions led to any clean product and were not pursued further. Similarly, the reaction of the analogous cobalt compound **7** with excess CO did not yield a clean product. On a different note, reaction of both $\{Fe_2(CH_2SiMe_3)_2[^{tBu}NON]\}$ and $\{Co_2(CH_2SiMe_3)_2[^{tBu}NON]\}$ with 1 atmosphere of CO_2 between -70 ^{o}C and room

temperature did not generate any change in the starting material, based on ^{1}H NMR spectral data.

Table 3.7. Selected interatomic distances (Å) and bond angles(°) for {([C^{NON}C]Fe($COCH_2SiMe_3$)$(CO)_2)_2$Fe} (**16**)

Fe1−Fe2	3.651(2)	Fe1−O6	2.187(4)
Fe1−C1	2.002(3)	Fe2−O1	2.130(2)
Fe1−C2	1.998(3)	Fe2−O2	2.068(3)
Fe1−C3	1.944(3)	Fe2−O3	2.071(2)
Fe1−C4	1.791(3)	C3−C6	1.526(4)
Fe1−C5	1.794(3)	C5=O5	1.149(4)
C1−N1	1.405(3)	C4=O4	1.148(4)
C2−N2	1.394(4)	C3=O3	1.230(3)
N2−Si2	1.752(2)	C2=O2	1.241(3)
N1−Si1	1.745(3)	C1=O1	1.241(3)
C1−Fe1−C2	84.5(1)	Si1−O−Si2	143.32
C4−Fe1−C2	91.4(1)	O1−Fe2−O2	89.91(7)
C1−Fe1−C5	88.0(1)	O2−Fe2−O3	85.26(8)
C4−Fe1−C5	96.1(1)	O1−Fe2−O3	97.00(8)
O6−Fe1−C3	172.0(1)	Fe2−O3−C3	128.9(2)
C3−Fe1−C2	93.1(1)	Fe2−O1−C1	123.2(2)
C3−Fe1−C1	92.4(1)	Fe2−O2−C2	125.2(2)
C3−Fe1−C4	87.3(1)	Fe1−C5−O5	175.4(3)
C3−Fe1−C5	85.4(1)	Fe1−C4−O4	175.5(3)

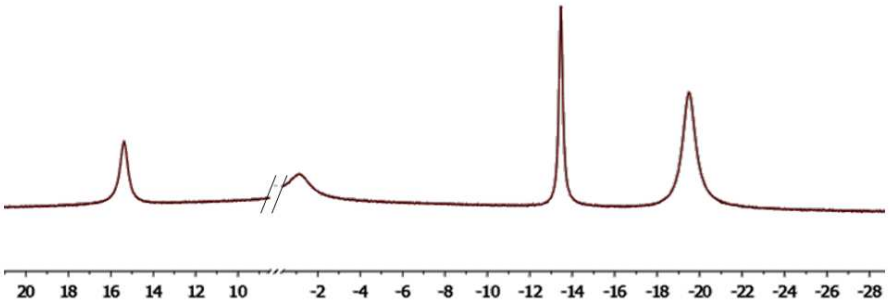

Figure 3.13. ^{1}H NMR spectrum of 16 in benzene-d_6.

The ^{1}H NMR spectrum of **16** showed paramagnetically broadend and shifted peaks between -20 and +20 ppm (Figure 3.13), indicating that at least one of the iron centres is paramagnetic. Although no magnetic measurements were made, it is expected that the iron centre with the dicarbamoyl ligand would be low-spin due to its five strong-field ligands (two carbamoyl, two carbonyl and one acyl) and the iron site in the centre, coordinated to six isocarbonyl units, to be high-spin iron(II). Having both low-spin and high-spin iron(II) sites should be observable and determinable by Mössbauer spectroscopy.

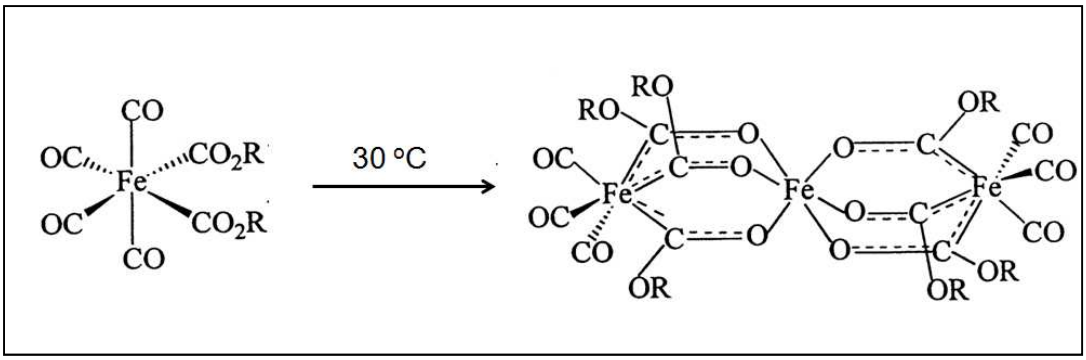

Scheme 3.5. Formation of $[(CO)_3Fe(\mu,\eta^2\text{-}CO_2R)_3]_2Fe$ (R= Me, tBu).[81]

The structure of **16** is found to be very similar to that of $[(CO)_3Fe(\mu,\eta^2\text{-}CO_2R)_3]_2Fe$[81] (R= Me, tBu) (Scheme 3.5) in which a Mössbauer study indicated, at low

temperature, the presence of a central six-coordinate high-spin iron(II) and two six-carbon-coordinate, low-spin lateral iron(II) centres. Such a mixed spin complex is rare;[227] however there are couple of similar ones reported including $(CO)_3Fe(\mu\text{-}SPh)_3Fe(\mu\text{-}SPh)_3Fe(CO)_3$,[228-229] $(CO)_3Fe(\mu\text{-}SePh)_3Fe(\mu\text{-}SePh)_3Fe(CO)_3$,[230] and $\{CpCo[P(O)(OR)_2]_3\}_2Fe$,[231] whose central irons are respectively surrounded by six sulfide, selenium, and oxygen atoms.

Table 3.7) in **16** are similar to that of 2.100(2) Å in the low-spin iron centre in $[(CO)_3Fe(\mu,\eta^2\text{-}CO_2R)_3]_2Fe$; the bridging inserted C−O bond distance of 1.230(3) and 1.241(3) in **16** are very similar to that of 1.221(4) in $[(CO)_3Fe(\mu,\eta^2\text{-}CO_2R)_3]_2Fe$ as well.

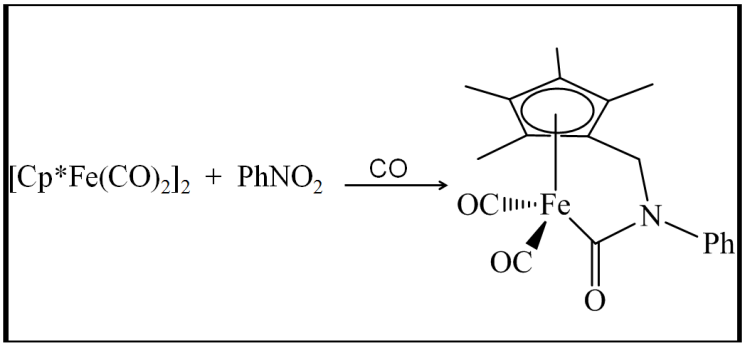

Figure 3.14. The formation of an iron carbamoyl species "**A**". [232]

A similar carbamoyl iron(II) species "**A**"[232] was obtained as shown in Figure 3.14 as a resting state in allylic aminations catalyzed by $[Cp^*Fe(CO)_2]_2$. The Fe1−C1(carbamoyl) and Fe1−C2(carbamoyl) distances of 2.002(3) and 1.998(3) Å in **16** are slightly longer than that of 1.971(2) Å in "**A**". The Fe1−C4 (terminal CO) and Fe1−C5 (terminal CO) distances of 1.791(3) Å in **16** are also longer than those of 1.762(2) and 1.757(2) Å in "**A**" while the C1−O1 and C2−O2 distance of 1.241(3) Å in **16** are also slightly longer than the 1.220(3) Å in **A**. The shorter terminal C4−O4 and C5−O5 distances of 1.148(4) and 1.149(4) Å in **16** are similar to the 1.141(3) and 1.151(3) Å (terminal CO) in "**A**".

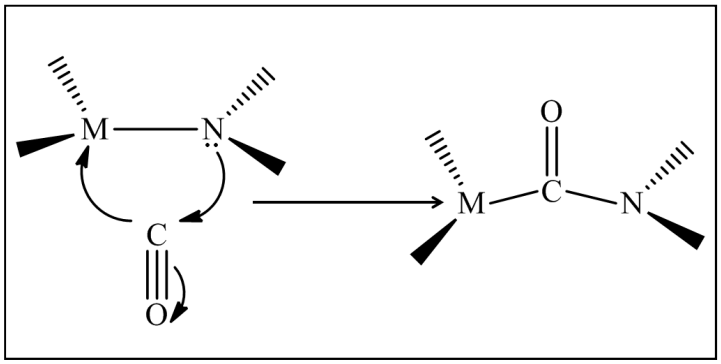

Figure 3.15. Proposed CO insertion mechanism into M−amide bond.[233]

Early studies have shown that there is strong electronic repulsion between the lone pair p orbital of the amide nitrogen atom and filled dπ atomic orbitals of late transition metals; this enhances the basicity and weakens the π-donation ability of the amido to the metal.[233-236] On the other hand, this effect increases the nucleophilicity of the amido ligands. The CO group as a σ–donor and π–acceptor ligand can be considered a suitable candidate to react with both the amido group and the unsaturated metal centre in $\{Fe_2(CH_2SiMe_3)_2[^{tBu}NON]\}$ (**6**). The main driving force for such an interesting reactivity of high-spin iron(II), **6** with CO molecules could be due to the low-coordinate, unsaturated iron(II) centre.

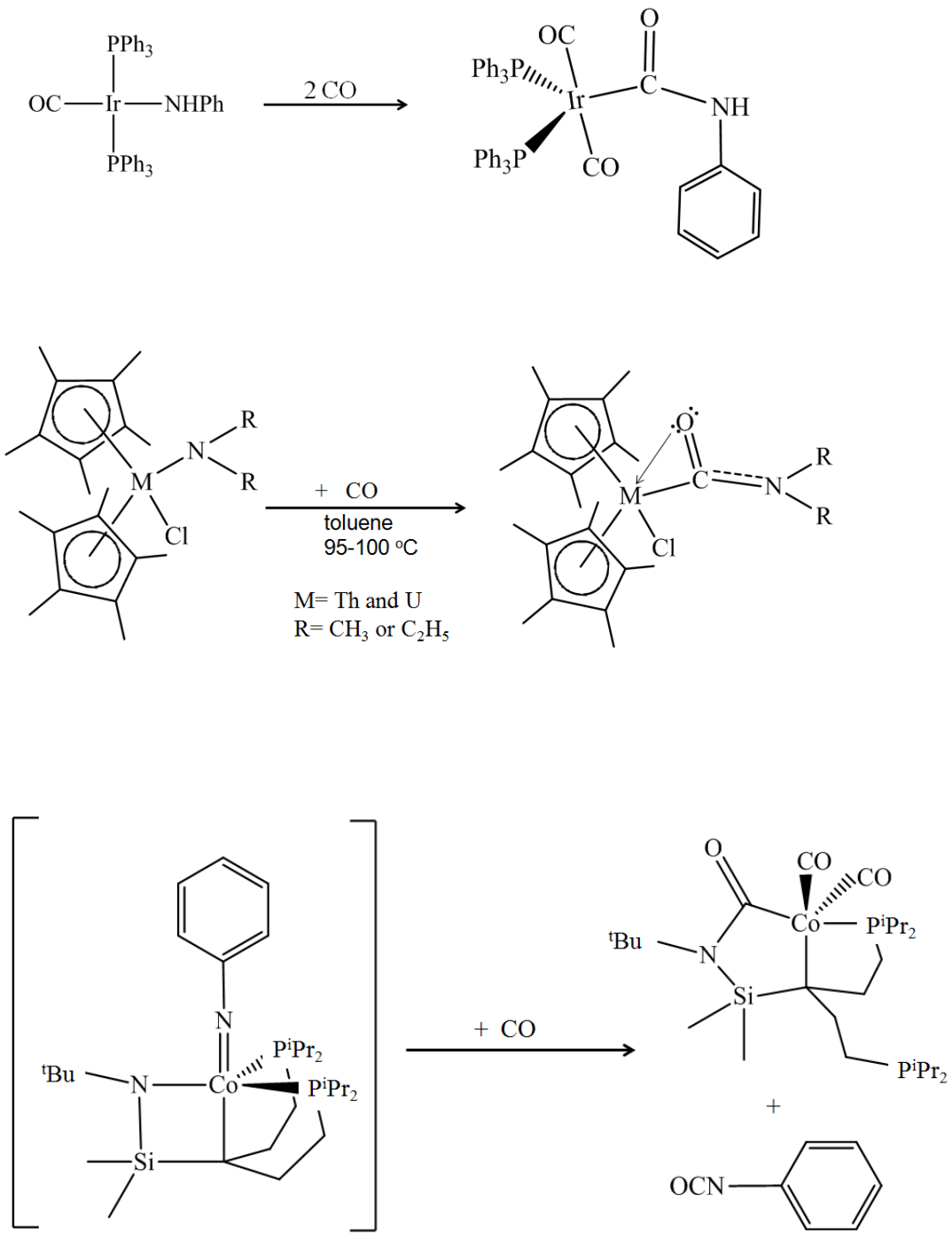

Figure 3.16. Examples of CO insertion into M−amide bond[42, 234-235]

However, the observed CO insertions in **16** are particularly noteworthy in that not only has the CO inserted into the Fe−amido bond but also bonds in an isocarbonyl fashion to another iron site. The insertion of CO into a M−amide bond and the resulting formation of a carbamoyl ligand is uncommon and has been reported a few times with different transition metals, including with Fe[237], Mo,[238] W,[238] Ni,[239] Re,[240] Ir,[234] U[235], Th[235] and Co[42]; some examples are shown in Figure 3.16.

The application of CO insertion chemistry to form carbonyl-containing molecules has been utilized regularly.[232, 241-243] Insertion of the CO into a TM−amide bond and the formation of the carbamoyl species (Figure 3.15) has been observed as an intermediate step in the synthesis of aminomethylidene,[241] is implicit in formamide C-H activation processes and as a resting state in allylic aminations.[232] On the other hand, carbamoyl chemistry has been considerably neglected compared to other ligands and this synthesis could provide a route to utilizing such ligands to support new chemistry.

3.3. Conclusion

The synthesis and characterization of a series of organometallic dinuclear dialkyl/amido and tetranuclear mixed alkyl/halide diamido high-spin iron(II) and cobalt(II) complexes by the mono and di-alkylation metathesis reaction of $M_2X_2[^{tBu}NON]$ **1**-**4** (M=Fe and Co, X=Cl and Br) with –Me and $–CH_2SiMe_3$ alkyls group was achieved. Low-coordinate organometallic complexes $M_2(CH_2SiMe_3)_2[^{tBu}NON]$ (M= Fe, **6**; Co, **7**) are similar in structure to the basic unit in $M_2X_2[^{tBu}NON]$ (**1**-**4**); the diamido ligand bridges two metal centres, generating two different metal sites, including a rare, three-coordinate iron and cobalt site. Alkyl/halide amido iron(II) and cobalt(II) clusters **8**-**11** have the basic unit of $M_2X(CH_2SiMe_3)[^{tBu}NON]$ (X= Cl and Br), which further dimerized to form tetranuclear clusters.

Even though attempts to prepare dimethyl dinuclear cobalt(II) and iron(II) clusters similar to dialkyl **6** and **7** were not successful, tetranuclear mono-methylated iron(II) and cobalt(II) with the $\{M_2XMe[^{tBu}NON]\}_2$ (M= Fe, X= Br (**12**); M=Co, X= Cl (**13**)) formula were synthesized. They both contain three-coordinate metal centres with M-CH_3 bonds.

All of these clusters contain high-spin cobalt(II) or iron(II). In addition to the magnetic data, the similarity of bond distances and angles in the dinuclear $M_2[^{tBu}NON]$ unit in iron(II) and cobalt(II) halide and alkyl complexes further support the assignment of the metal spin states being the same.

The polymerization activity of $\{Fe_2(CH_2SiMe_3)_2[^{tBu}NON]\}$ (**6**) and $\{Co_2(CH_2SiMe_3)_2[^{tBu}NON]\}$ (**7**) for ethylene was investigated and they show no polymerization activity. In order to enhance the polymerization activity, tris(pentafluorophenyl)borane was used as an activator in both cases, but this deactivated the metal centre by substitution of $-CH_2SiMe_3$ for C_6F_5 on the borane, along with concomitant C_6F_5- transfer to the metal, as illustrated by $\{Co_2(C_6F_5)_2[^{tBu}NON]\}$ (**14**) and $\{Fe_2(C_6F_5)Cl[^{tBu}NON]\}$ (**15**).

Dialkyl iron and cobalt **6** and **7** also were exposed to one atmosphere of CO gas at low temperature; in the case of dialkyl iron **6**, the result was very interesting: a trinuclear dicarbamoyl complex $\{Fe_3(CO)_3(COCH_2SiMe_3)_2[C^{NON}C]_2\}$ (**16**) was isolated. Based on the X-ray structure, two CO groups were inserted into Fe−amido bonds, generating a new dicarbamyl-O donor ligand.

3.4. Future work

3.4.1. Moving towards new alkyl iron and cobalt complexes

Changing the amido R-substitutent in the $[^{tBu}NON]^{2-}$ ligand from t-butyl to other R groups ($[^{R}NON]^{2-}$) and following the impact on the structure of the alkyl complexes of iron and cobalt could be of value. For example, the isopropyl R-group is similar to the t-butyl group but less bulky, hence it might support more reactive metal alkyl centres.

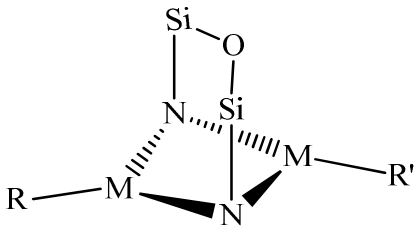

Figure 3.17. Dinuclear metal complexes with different alkyl groups (R≠R′).

The synthesis of mixed alkyl/halide systems, opens the door to preparing systems with two different alkyl groups on the dinuclear iron and cobalt, with a general formula of $M_2RR'[^{tBu}NON]$ (Figure 3.17). Such a system can provide a very good opportunity to compare the reactivity of two different alkyl (or aryl) groups very closely. Since these would be low-coordinate metal centres, it would also be interesting to examine their reactivity towards neutral donor ligands as well, such as phosphines and carbenes, which were tried with the halide systems **1**-**4**.

3.4.2. Investigation toward polymerization activity

Even though the polymerization activity of dialkyl iron and cobalt **6** and **7** with ethylene gas resulted in low oligomerization activity, it is worth looking into the polymerization activity of these compounds with different activators since different cocatalysts (such as MAO) are known to have different impacts on the catalyst systems. On the other hand there are reported catalysts which are not active toward ethylene gas but are very active toward propylene gas so the compounds could be tested as catalysts for propylene polymerization. The mixed alkyl/halides **8**-**15** can be investigated for such reactivity as well.

3.4.3. More CO and other small molecules reactivity studies

With the very interesting observed result of the CO gas reaction with dialkyliron(II) **6**, definitely it is encouraging to pursue similar reactions with the mixed alkyl/halide and aryl complexes of cobalt and iron **8**-**15** with CO gas.

Accessing transition metal hydrides are of great interest of due to their high reactivity. Trying to prepare hydride iron and cobalt complexes through halides **1**-**4** by metathesis with hydride reagents were not successful, however using the mixed alkyl/halide systems **6**-**15** might lead to the formation of mono hydride/halide cobalt(II) and iron(II) systems, very similar to the mono methyl/halide tetranuclear cluster $\{M_2XMe[^{tBu}NON]\}_2$; **12** (M= Fe, X= Br) and **13** (M= Co, X= Cl).

There was no reaction of either dialkyl iron **6** or cobalt **7** with CO_2 gas at one atmosphere. However, such a reaction could conceivably occur at higher pressure. Hence, it is worthwhile to repeat the reaction at higher gas pressure. Since the organometallic cluster dialkyl and alkyl/halide iron(II) and cobalt(II) complexes are high-spin, probing the M-C bonds with respect to activation of other small molecules like NO, NO_2, SO_2 and H_2S are of great interest. Examining possible catalytic reactivity, such as C−H and C−F bond activation with the alkylated systems with these systems are also worthwhile.

3.5. Experimental section

General procedures and materials are as described in Chapter 2 (section 2.5.1).

3.5.1. General Procedures and Materials

Synthesis of $\{Fe_2(CH_2SiMe_3)_2[^{tBu}NON]\}$ (6)

$LiCH_2SiMe_3$ (144 mg, 1.52 mmol) in 30 mL THF was added dropwise at room temperature in small portions over three hours to a solution of $\{Fe_2Cl_2[^{tBu}NON]\}_n$ (**3**) (350 mg, 0.76 mmol) in 50 mL THF while stirring (one equivalent of alkylating agent per iron(II)). The resulting brown mixture was stirred overnight, and then the THF was removed *in vacuo*. The product was extracted with hexanes and the resulting solution was filtered through Celite. Removal of the hexanes *in vacuo* resulted in a brown powder of $\{Fe_2(CH_2SiMe_3)_2[^{tBu}NON]\}$ (**6**). It was also possible to do the synthesis of **3** and subsequent alkylation step without isolation of **3**, by stirring for 24 hours prior to alkylation and **6** was still produced. Crystals of **6** were obtained by slow evaporation of a hexanes solution. Yield: 276 mg (65%). Anal. Calcd for $C_{20}H_{52}N_2Co_2OSi_4$: C: 42.84%; H:

9.34%; N: 4.99%. Found: C: 42.55%; H: 9.16%; N: 4.60%. ^{1}H NMR (benzene-d_6): -2.6 (br s, 12H, Si(CH_3)$_2$), 1.4 (br s, 18H, C(CH_3)$_3$), -10.9 (br s, 18H, Si(CH_3)$_3$). Evans method μ_{eff}: 4.6 μ_B.

Reaction of {Fe_2Cl_2[^{tBu}NON]}$_n$ (3) and MeMgBr

The reaction of one equivalent of MeLi per iron(II) in **3** was done by slow addition of MeMgBr, 1 M in THF solution (1.50 mmol, 1.5 mL) in 10 mL THF to a solution of one equivalent of {Fe_2Cl_2[^{tBu}NON]}$_n$ (**3**) (350 mg, 0.76 mmol) in 50 mL THF while stirring, at -70 ^{o}C. The resulting brown mixture was stirred overnight, and then the THF was removed *in vacuo*. The product was extracted with hexanes and the resulting solution was filtered through Celite. Removal of the hexanes *in vacuo* resulted in {Fe[^{tBu}NON]}$_2$, identified by ^{1}H NMR spectrum.

Reaction of {Fe_2Cl_2[^{tBu}NON]}$_n$ (3) and LiCH(SiMe$_3$)$_2$

LiCH(SiMe$_3$)$_2$ (124 mg, 0.76 mmol) in 30 mL THF was added dropwise at -70 ^{o}C slowly to a solution of one equivalent of {Fe_2Cl_2[^{tBu}NON]}$_n$ (**3**) (180 mg, 0.39 mmol) in 50 mL THF while stirring (one equivalent of alkylating agent per iron(II)). The resulting brown mixture was stirred overnight, and then the THF was removed *in vacuo*. The product was extracted with hexanes and the resulting solution was filtered through Celite. Removal of the hexanes *in vacuo* resulted in a gummy brown product, which could not be isolated further or crystallized.

Synthesis of {$Co_2(CH_2SiMe_3)_2$[^{tBu}NON]} (7)

Two equivalents of LiCH_2SiMe_3 (86 mg, 1 mmol) in 30 mL THF were added dropwise at room temperature in small portions over three hours to a solution of {Co_2Cl_2[^{tBu}NON](LiCl)·2THF}$_2$ (**4**) (300 mg, 0.24 mmol) in 50 mL THF while stirring (one equivalent alkyl per cobalt(II)). The resulting brown mixture was stirred overnight, and then the THF was removed *in vacuo*. The product was extracted with hexanes and the resulting solution was filtered through Celite. Removal of the hexanes *in vacuo* resulted in a brown powder of {$Co_2(CH_2SiMe_3)_2$[^{tBu}NON]} (**7**). It was also possible to do the synthesis of **4** and subsequent alkylation step without isolation of **4**, by stirring for 24 hours prior to alkylation; **7** was still produced. Crystals of **7** were obtained by slow evaporation of a hexanes solution. Yield: 162 mg (63%). Anal. Calcd for

$C_{20}H_{52}N_2Co_2OSi_4$: C: 42.37%; H: 9.24%; N: 4.94%. Found: C: 42.33%; H: 9.38%; N: 4.89%. ^{1}H NMR (benzene-d_6): -12.6 (br s, 12H, Si(CH_3)$_2$), -11.3 (br s, 18H, C(CH_3)$_3$), 7.4 (br s, 18H, Si(CH_3)$_3$) and 161.7 (br s, 4H, CH_2SiMe$_3$). Solid state μ_{eff}(300 K): 2.86 μ_B, Evans method : 2.8 μ_B.

Reaction of {Co_2Cl_2[^{tBu}NON](LiCl·2THF)}$_2$ (4) and MeMgBr

The reaction of one equivalent of MeMgBr per cobalt(II) in **4** was done by slow addition of MeLi, 1M (1 mmol, 1mL) in 10 mL THF to a solution of {Co_2Cl_2[^{tBu}NON](LiCl)·2THF}$_2$ (**4**) (300 mg, 0.24 mmol) in 50 mL THF while stirring, at -70 ^{o}C. The resulting brown mixture was stirred overnight, and then the THF was removed *in vacuo*. The product was extracted with hexanes and the resulting solution was filtered through Celite. Removal of the hexanes *in vacuo* resulted in {Co[^{tBu}NON]}$_2$, identified based on its ^{1}H NMR spectrum.

Reaction of {Co_2Cl_2[^{tBu}NON](LiCl)·2THF}$_2$ (4) and LiCH(SiMe$_3$)$_2$

LiCH(SiMe$_3$)$_2$ (167 mg, 1 mmol) in 30 mL THF was added dropwise at -70 ^{o}C in small portions over three hours to a solution of {Co_2Cl_2[^{tBu}NON](LiCl)·2THF}$_2$ (**4**) (300 mg, 0.24 mmol) in 50 mL THF while stirring (one equivalent of alkylating agent per cobalt(II)). The resulting brown mixture was stirred overnight, and then the THF was removed *in vacuo*. The product was extracted with hexanes and the resulting solution was filtered through Celite. Removal of the hexanes *in vacuo* resulted in a gummy brown product which could not be characterized further or crystallized, ^{1}H NMR spectrum.could not be any help to identical new compounds.

Synthesis of {$Fe_2Cl(CH_2SiMe_3)$[^{tBu}NON]}$_2$ (8)

$LiCH_2SiMe_3$ (52 mg, 0.55 mmol) in 30 mL THF was added dropwise at room temperature in small portions over three hours to a solution of {Fe_2Cl_2[^{tBu}NON]}$_n$ (**3**) (250 mg, 0.55 mmol) in 40 mL THF while stirring. The resulting brown mixture was stirred overnight, and then the THF was removed *in vacuo*. The product was extracted with hexanes and the resulting solution was filtered through Celite. Removal of the hexanes *in vacuo* resulted in a greenish brown powder of {$Fe_2Cl(CH_2SiMe_3)$[^{tBu}NON]}. Crystals of **8** were obtained by slow evaporation of a hexanes solution. Yield: 171 mg (61%). Anal. Calcd for $C_{16}H_{41}N_2ClFe_2OSi_3$: C: 37.76%; H: 8.12%; N: 5.50%. Found: C: 37.47%; H:

8.07%; N: 5.27%. ^{1}H NMR (benzene-d_6): -10.7, -7.4, -2.5, 10.5 (br s, 4(3H), Si(CH_3)$_2$), -7.4 (br s, 18H, C(CH_3)$_3$), 5.1 (br s, 9H, Si(CH_3)$_3$ and (br s, 4H, CH_2SiMe$_3$). Evans method μ_{eff}(300 K): 3.4 μ_B.

Synthesis of {$Co_2Cl(CH_2SiMe_3)[^{tBu}NON]\}_2$ (9)

$LiCH_2SiMe_3$ (44 mg, 0.46 mmol) in 30 mL THF was added dropwise at room temperature in small portions over four hours (approximately 2 mL every 15 minutes) to a solution of one equivalent of {$Co_2Cl_2[^{tBu}$NON]·(LiCl)·2THF$\}_2$ (**4**) (300 mg, 0.24 mmol) in 50 mL THF while stirring. The resulting brown mixture was stirred overnight, and then the THF was removed *in vacuo*. The product was extracted with hexanes and the resulting solution filtered through Celite. Removal of the hexanes *in vacuo* resulted in a brown powder of {$Co_2Cl(CH_2SiMe_3)[^{tBu}$NON]$\}_2$ (**9**). Crystals of **9** were obtained by slow evaporation of a hexanes solution. Yield: 158 mg (67%). Anal. Calcd for $C_{16}H_{41}N_2ClFe_2OSi_3$: C: 37.30%; H: 8.02%; N: 5.43%. Found: C: 37.18%; H: 7.82%; N: 5.42%. ^{1}H NMR (benzene-d_6): -65.6 and 38.4 (br s, 2(6H), Si(CH_3)$_2$), -18.8 (br s, 18H, C(CH_3)$_3$) and 22.1 (br s, 9H, Si(CH_3)$_3$). Evans method μ_{eff}: 2.0 μ_B.

Synthesis of {$Fe_2Br(CH_2SiMe_3)[^{tBu}NON]\}_2$ (10)

During the synthesis of {$Fe_2(CH_2SiMe_3)_2[^{tBu}$NON]} (**6**), using {$Fe_2Br_2[^{tBu}$NON]} (**1**) as the starting material, a few brown crystals of mono alkylated {$Fe_2Br(CH_2SiMe_3)[^{tBu}$NON]$\}_2$ (**10**) were obtained as a side product. Due to the very low yield further characterization could not proceed.

Synthesis of {$Co_2Br(CH_2SiMe_3)[^{tBu}NON]\}_2$ (11)

During the synthesis of {$Co_2(CH_2SiMe_3)_2[^{tBu}$NON]} (**7**), using {$Co_2Br_2[^{tBu}$NON]} (**3**) as the starting material, a few greenish brown crystals of mono alkylated {$Co_2Br(CH_2SiMe_3)[^{tBu}$NON]$\}_2$ (**11**) were obtained as a side product. Due to the very low yield further characterization could not proceed.

Synthesis of {$Fe_2Br(Me)[^{tBu}NON]\}_2$ (12)

One equivalent of MeMgBr per dinuclear iron(II) unit in **3**, (0.76 mL (1M), 0.76 mmol) in 10 mL THF solution was slowly added to a solution of {$Fe_2Cl_2[^{tBu}$NON]$\}_n$ (**3**) (350 mg, 0.76 mmol) in 50 mL THF while stirring, at -70 ^{o}C. The resulting light brown

mixture was stirred overnight, and then the THF was removed *in vacuo*. The product was extracted with diethylether and the resulting solution was filtered through Celite. Removal of the solvent *in vacuo* resulted in $\{Fe_2Br(Me)[^{tBu}NON]\}_2$ (**12**). A few crystals of **12** were obtained by slow evaporation of an ether solution. The product could not be purified from the salt biproduct and due to the low yield could not pursued for further characterization.

Synthesis of $\{Co_2Cl(Me)[^{tBu}NON]\}_2$ (13)

The reaction of one equivalent of MeLi per binuclear cobalt(II) in **4** was done by slow addition of MeMgCl (0.16 mL (3M), 0.48 mmol) in 10 mL THF solution to a solution of $\{Co_2Cl_2[^{tBu}NON](LiCl)\cdot 2THF\}_2$ (4) (300 mg, 0.24 mmol) in 50 mL THF while stirring, at -70 ^oC. The resulting greenish brown mixture was stirred overnight, and then the THF was removed *in vacuo*. The product was extracted with diethylether and the resulting solution was filtered through Celite. Removal of the solvent *in vacuo* resulted in $\{Co_2Cl(Me)[^{tBu}NON]\}_2$ (**13**). A few crystals of **13** were obtained by slow evaporation of an ether solution. The product could not be purified from the salt biproduct and due to the low yield could not pursued for further characterization.

Reaction of $\{Fe_2(CH_2SiMe_3)_2[^{tBu}NON]\}$ (6) with Ethylene

Three freeze-pump-thaw cycles were done on a solution of $\{Fe_2(CH_2SiMe_3)_2[^{tBu}NON]\}$ (50 mg, 0.08 mmol) in 40 mL of hexanes at 0 ^oC. One atmosphere of $CH_2{=}CH_2$ gas was introduced to the flask, the mixture was allowed to stir for 12 hours (with a continuous, slow flow of ethylene gas present), then the reaction was quenched by venting excess ethylene and addition of 20 mL of acidified methanol (10% concentrated hydrochloric acid in methanol). No solid polymer was obtained. The mass spectroscopy data indicated the presence of some oligomerization products but they were in low yield. When one equivalent of $B(C_6F_5)_3$ per iron in dinuclear unit in **6** was used as the activating agent, the $B(C_6F_5)_3$ was added to a solution of **6** in toluene; after the polymerization procedure, there was no solid polymer collected.

Reaction of $\{Co_2(CH_2SiMe_3)_2[^{tBu}NON]\}$ (7) with Ethylene

Three freeze-pump-thaw cycles were done on a solution of $\{Co_2(CH_2SiMe_3)_2[^{tBu}NON]\}$ (50 mg, 0.08 mmol) in 30 mL of hexanes at 0 ^oC. One

atmosphere of CH_2=CH_2 gas was introduced to the flask, the mixture was allowed to stir for 12 hours (with a continuous, slow flow of ethylene gas present), then the reaction was quenched by venting excess ethylene and addition of 20 mL of acidified methanol (10% concentrated hydrochloric acid in methanol). When one equivalent of $B(C_6F_5)_3$ per iron in dinuclear unit in **7** was used as the activating agent, the $B(C_6F_5)_3$ was added to a solution of **6** in toluene; upon removing the toluene solvent there was no polymer, however brown crystals of $\{Co_2(C_6F_5)_2[^{tBu}NON]\}$ (**14**) were obtained.

Synthesis of $\{Co_2(C_6F_5)_2[^{tBu}NON]\}$ (14)

To a solution of 100 mg (0.16 mmol) of $\{Co_2(CH_2SiMe_3)_2[^{tBu}NON]\}$ in 30 mL of hexanes was added $B(C_6F_5)_3$ (180 mg, 0.32 mmol) in 20 mL toluene. The reaction mixture was stirred for 12 hours. The colour immediately changed from dark brown to dark green. The solvent was removed *in vacuo*, and the resulting solid was extracted into toluene. Removal of solvent *in vacuo* resulted in a green powder of $\{Co_2(C_6F_5)_2[^{tBu}NON]\}$ (**14**). Crystals of **14** were obtained by slow evaporation of a hexanes/toluene solution. Yield: 130 mg (66%). Anal. Calcd for $C_{22}H_{30}N_2Co_2F_{10}OSi_2$: C: 39.67%; H: 4.16%; N: 3.87%. Found: C: 40.01%; H: 4.18%; N: 3.71%. ^{1}H NMR (toluene-d_8): -8.1 (br s, 12H, Si(CH_3)$_2$) and -10.5 (br s, 18H, C(CH_3)$_3$). Evans method μ_{eff} (298 K): 2.6 μ_B.

Synthesis of $\{Fe_2Cl(C_6F_5)[^{tBu}NON]\}$ (15)

To a solution of $\{Fe_2(CH_2SiMe_3)Cl[^{tBu}NON]\}$ (190mg, 0.20 mmol) in 30 mL of hexanes was added $B(C_6F_5)_3$ (230 mg, 0.40 mmol) in 20 mL toluene solution. The reaction mixture was stirred for 12 hours. The colour did not change. The solvent was removed *in vacuo*, and the resulting solid was extracted into toluene. Removal of solvent *in vacuo* resulted in a brown powder of $\{Fe_2Cl(C_6F_5)[^{tBu}NON]\}_2$ (**15**). A few crystals of **15** were obtained by slow evaporation of a hexanes/toluene mixture solution; further characterization was not possible due to the gummy nature of the bulk product.

Synthesis of $\{([CO^{NON}OC]Fe(CO)_2(COCH_2SiMe_3))_2Fe\}$ (16)

Three freeze-pump-thaw cycles were done on a solution of $\{Fe_2(CH_2SiMe_3)_2[^{tBu}NON]\}$ (350 mg, 0.63 mmol) in 30 mL of hexanes at 0 ^oC. One atmosphere of CO was introduced to the flask. The brown solution did not change, and

the reaction mixture was allowed to stir for 24 hours at 0 ^{o}C, then the reaction mixture was allowed to warm to room temperature and was stirred for 1 hour. Following the removal of solvent *in vacuum*, the crude product was extracted with hexanes. The brown solution was concentrated and cooled overnight at -40 ℃, resulting in the formation of brown crystals of {([CO^{NON}OC]Fe$(CO)_2(COCH_2SiMe_3))_2$Fe} (**16**). Yield: 250 mg (54%). Anal. Calcd for $C_{42}H_{82}N_4Fe_3O_{12}Si_6$: C: 43.07%; H: 7.05%; N: 4.78%. Found: C: 43.44%; H: 6.93%; N: 5.16%. ^{1}H NMR (benzene-d_6): -1, 15.4 (br s, 2(6H), Si(CH_3)$_2$), -19.5 (br s, 18H, C(CH_3)$_3$) and -13.5 (br s, 9H, Si(CH_3)$_3$.

Reaction of {$Co_2(CH_2SiMe_3)_2[^{tBu}$NON]} (7) with CO

Three freeze-pump-thaw cycles were done on a solution of {$Co_2(CH_2SiMe_3)_2[^{tBu}$NON]} (200 mg, 0.31 mmol) in 30 mL of hexanes at 0 ^{o}C. One atmosphere of CO was introduced to the flask. The brown solution did not change, and the reaction mixture was allowed to stir for 24 hours, then the reaction mixture was allowed to warm to room temperature and was stirred for 1 hour. The product was gummy and could not be isolated in a pure form to warrant further characterization. The ^{1}H NMR spectrum had many peaks in addition to those assigned as starting materials.

Reaction of {$Fe_2(CH_2SiMe_3)_2[^{tBu}$NON]} (6) with CO_2

Three-freeze-pump thaw cycles were done on a solution of {$Fe_2(CH_2SiMe_3)_2[^{tBu}$NON]} (350 mg, 0.67 mmol) in 30 mL of hexanes at 0 ^{o}C. One atmosphere of CO_2 was introduced to the flask. The brown solution did not change, and the reaction mixture was allowed to stir for 24 hours at 0 ^{o}C, then the reaction mixture was allowed to warm to room temperature and was stirred for 1 hour. Based on the ^{1}H NMR spectrum, there was no reaction.

Reaction of {$Co_2(CH_2SiMe_3)_2[^{tBu}$NON]} (7) with CO_2

Three-freeze-pump thaw cycles were done on a solution of {$Co_2(CH_2SiMe_3)_2[^{tBu}$NON]} (200 mg, 0.31 mmol) in 30 mL of hexanes at 0 ^{o}C. One atmosphere of CO_2 was introduced to the flask. The brown solution did not change, and the reaction mixture was allowed to stir for 24 hours, then the reaction mixture was allowed to warm to room temperature and was stirred for 1 hour. Based on the ^{1}H NMR spectrum, there was no reaction.

3.5.2. X-ray crystallography

Crystals of **6, 7, 8, 9, 12** and **15** were sealed in capillaries at room temperature while crystals of **10**, **11, 13, 14**, and **16** were coated in Paratone-oil and mounted onto a MiTeGen Micro Mount at -150 ^{o}C. Crystal descriptions for each compound are as follows: **6** is a brown block having dimensions 0.32 × 0.25 × 0.30 mm^3; **7** is a brown block having dimensions 0.40 × 0.32 × 0.25 mm^3; **8** is a greenish brown cube having dimensions 0.40 × 0.35 × 0.25 mm^3; **9** is a brown block having dimensions 0.42 × 0.17 × 0.20 mm^3, **10** is a brown block having dimensions 0.38 × 0.23 × 0.20 mm^3; **11** is a brown cube having dimensions 0.20 × 0.30 × 0.25 mm^3; **12** is a dark yellow needle having dimensions 0.15 × 0.15 × 0.40 mm^3, **13** is a dark green cube having dimensions 0.20 × 0.42 × 0.47 mm^3; **14** is a green cube having dimensions 0.46 × 0.15 × 0.37 mm^3; **15** is a brown block having dimensions 0.45 × 0.47 × 0.34 mm^3 and 16 is a green cube having dimensions 0.48 × 0.33 × 0.20 mm^3. All data was collected on a Bruker Smart instrument equipped with an APEX II CCD area detector at a distance of 6.0 cm from the crystal. A Mo-Kα fine-focus sealed tube operating at 1.5 kW (50 kV, 30 mA) was utilized for data collection. All frames were collected with a scan width of 0.5 in ω or ϕ with the following exposure times: 30 s for all **6**-**16**. The frames were integrated with the Bruker SAINT software package. Data were corrected for absorption effects using a multi-scan correction technique. The structures were solved using direct methods (SIR 92) and refined by least-squares procedures using CRYSTALS.[188] Hydrogen atoms were placed in idealized geometric positions. Subsequent refinement cycles linked each hydrogen atom position to its respective carbon atom using a riding model. The isotropic temperature factor of the hydrogen atoms was initially fixed at 1.2 times that of the preceding carbon atom. Subsequent refinement cycles linked the temperature factor of similar hydrogen atoms to one another. The plots for the crystal structures were generated using CAMERON.[190] Crystallographic data for all compounds are in Tables A.3 to A.7 in Appendix A).

4. Towards high-valent metal amides: Oxidation of Fe(II)- and Co(II)-diamido ether complexes[3]

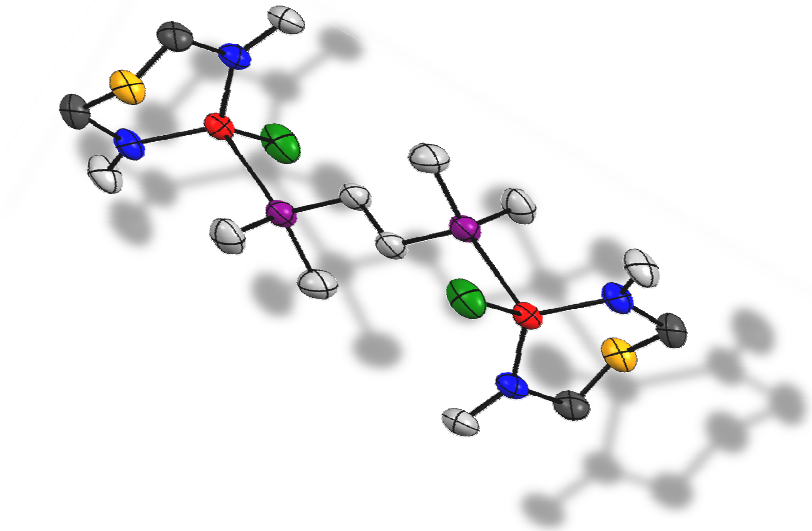

4.1. Introduction

High oxidation state iron(IV) metal centres are known to be present at the active sites of common biological systems;[244-249] for example, iron(IV)–oxo intermediates have been reported to be catalytically active oxidizing species.[250-251] In a number of cases, mononuclear non-heme iron(IV)–oxo complexes with tetradentate or pentadentate N-ligands have been synthesized.[252-264] Non-octahedral, paramagnetic Co(III) complexes are also rare[39] and are considered as high-valent metal centres as well. They have been shown to be highly reactive, such as in C−H bond activation [265-267] or in some cases also show interesting magnetic properties such as spin crossover,[267] Several Co(III)-imido complexes are known;[265-267] for example the formation of a cobalt(III) imido

[3]* Parts of this chapter are adapted with permission from, A. K. Das, Z. Moatazedi, G. Mund, A. J. Bennet, R. J. Batchelor and D. B. Leznoff. "Chelating or bridging? Halide-controlled binding mode of diamido donor ligands in Iron(III) complexes"" *Inorganic Chemistry*, **2007**, 46(2), 366-368. Copyright 2007 American chemical society.

from a cobalt(II) amido complex has been reported.[268] $PNPCo(H)_2$ (PNP= $[(^tBu_2PCH_2SiMe_2)_2N^-]$) is an example of Co(III)-dihydride species.[269]

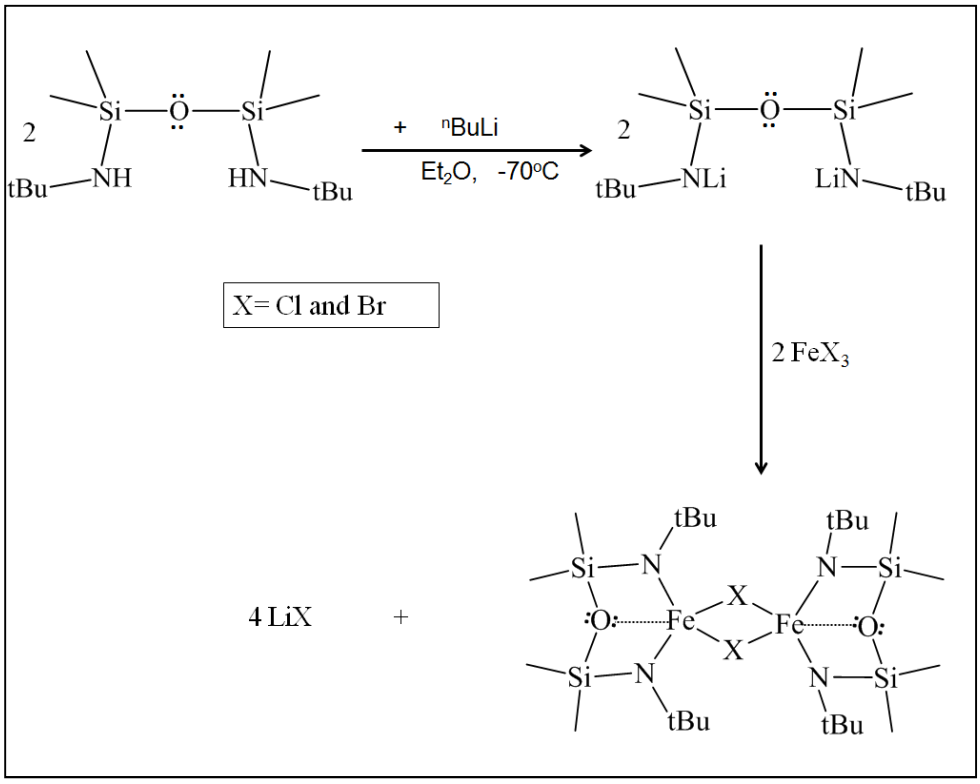

Scheme 4.1. Synthesis of $\{FeX[^{tBu}NON]\}_2$.[55]

In the Leznoff group, prior work involving the reaction of $Fe(III)X_3$ (X= Cl and Br) salts with $Li_2[^RNON]$ generated multinuclear, non-macrocyclic Fe(III) diamidoether complexes $\{FeX_2Li[^{Me_3Ph}NON]\}$[137] as the ate complexes and lithium halide-free $\{FeX[^{tBu}NON]\}_2$ (X = halide),[55] which showed the rare property of quantum mechanical spin-admixture (Scheme 4.1). The interest in such a property comes from biological iron-containing systems that also exhibit similar properties.[270]

Some preliminary reactions were previously done on the $\{Fe[^{tBu}NON]\}_2$,[140] $\{FeCl[^{tBu}NON]\}_2$ and $\{Co[^{tBu}NON]\}_2$ systems to attempt to access higher oxidation-state iron(IV) or cobalt(III) complexes. This chapter thus describes reactions of $\{Fe[^RNON]\}_2$

(R= ^{t}Bu, 2,4,6-Me_3Ph) and {Co[^{tBu}NON]}$_2$ systems with different oxidizing reagents and some reactivity of the resulting species.

4.2. Results and Discussion

The oxidation of iron(II) {Fe[^{R}NON]}$_2$ using oxidizing agents such as I_2 and $AgPF_6$ lead to the formation of iodide and fluoride-bridged dinuclear iron(III) complexes, as described by Garry Mund's Ph.D. thesis work in the Leznoff group (Scheme 4.2).

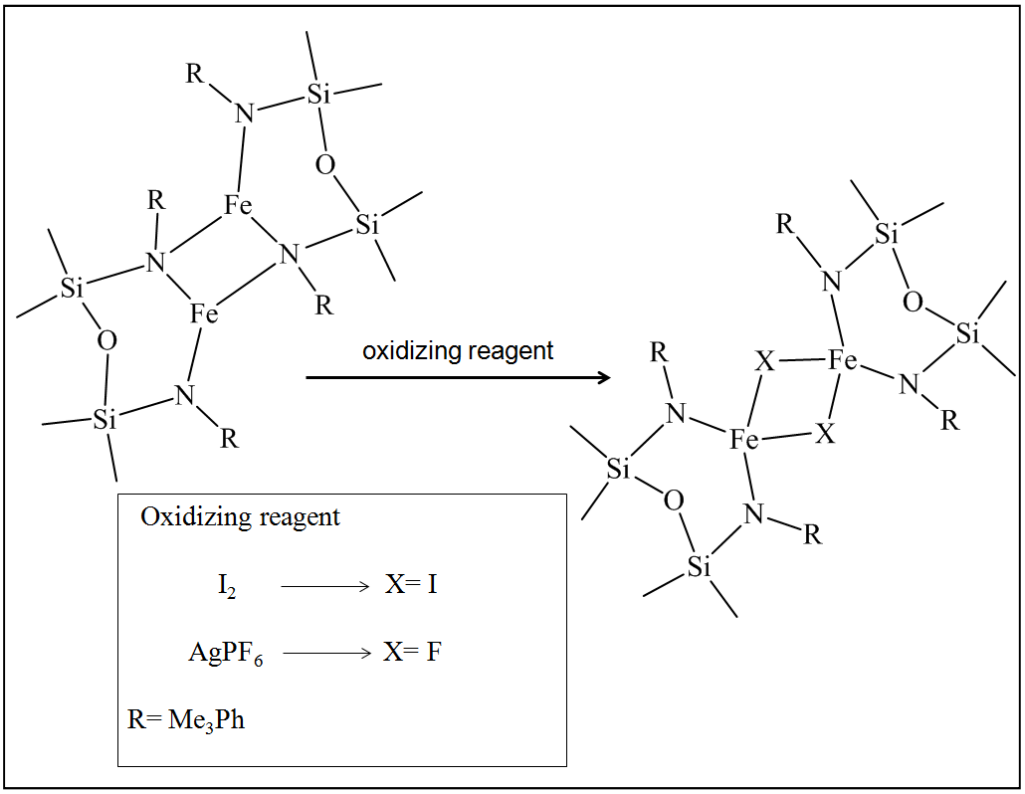

Scheme 4.2. Formation of lithium halide-free iron(III) aryl-based diamidoether systems

In a similar fashion, the cobalt(II) {Co[^{tBu}NON]}$_2$ and iron(III)-diamidoether {FeCl[^{tBu}NON]}$_2$ complexes could be viable starting materials to access cobalt(III) and iron(IV) systems, since the oxidation resistant O-donor and the π-donating ability of the

diamido ligand, as well as steric protection from bulky substituents such as t-butyl (on the amide) may be appropriate to stabilize the higher valent metal centres.

4.2.1. Oxidation using a range of oxidizing reagents

A significant effort was made towards synthesizing diamidoether iron(IV) and cobalt(III) complexes by addition of I_2, MeI, benzyl bromide, Me_3NO, AgF_2, XeF_2 and bromonium ion (Br^+) to oxidize the metal centres in $\{FeCl[^{tBu}NON]\}_2$ and $\{Co[^{tBu}NON]\}_2$ complexes. I_2 and MeI are common oxidizing reagents, used to oxidize transition metals such as Cr, Co and Fe;[271-277] benzyl bromide also can be used as an oxidizing/Br transfer agent however, surprisingly, it has been used much less than MeI.[39, 278] Me_3NO is a well-known single O-atom transfer mild oxidizing agent, although the volatile trimethylamine formed during the oxidation process could react with the products.[279] AgF_2 and XeF_2[280-281] both are strong oxidizing/F transfer agents that are convenient to use since they form insoluble AgF and gaseous Xe biproducts respectively.

In most cases, addition of the oxidizing agents to $\{Co[^{tBu}NON]\}_2$ did not generate any reaction; in the case of AgF_2 and XeF_2 no clean product could be isolated. The reactions of the oxidizing agents with $\{FeCl[^{tBu}NON]\}_2$ in most cases resulted in the formation of the reduced $\{Fe[^{tBu}NON]\}_2$ product, perhaps due to the formation of unstable Fe(IV) species undergoing intra-molecular redox chemistry (e.g. with the ligand). However, reaction with the very strongly oxidizing bromonium reagent did lead to interesting, discrete products, which are described below.

4.2.2. Oxidation with "Br^+" reagents

$[AdAdBr]^+[B(Ar_F)_4]^-$ (Ad= adamantyl; Ar_F= 3,5-$(CF_3)_2$Ph,[282] developed by Brown and Bennet,[283] is a very strong oxidizing agent since bromonium, a formally two-electron oxidant, can transfer a Br^+ ion. This reagent is formed by the reaction of adamantylideneadamantane with Br_2 in CCl_4,[284] which yields $[AdAdBr]^+Br_3^-$, which then undergoes anion replacement by $CF_3SO_3^-$[284] or B[3,5-$(CF_3)_2$Ph]$_4^-$.[282] Despite its strong oxidizing ability, so far it has not been explored much as an oxidizing reagent in inorganic chemistry. In organic chemistry bromonium ion transfer to an acceptor olefin is an important study to an easy process.[283, 285-286] The addition of $[AdAdBr]^+[B(Ar_F)_4]^-$ and

subsequent bromonium ion transfer to $Os_3(CO)_{12}$ and $Ru_3(CO)_{12}$ is a rare example of transferring a bromonium ion from an alkene to a metal complex.[282]

Garry Mund of the Leznoff group conducted some preliminary reactions of this strong oxidizing agent with $\{Fe[^{Me_3Ph}NON]\}_2$. Thus, reaction of $\{Fe[^{Me3Ph}NON]\}_2$ with one equivalent of $[AdAdBr]^+[B(Ar_F)_4]^-$ per iron(II) centre in THF resulted in the polymerization of the THF. This suggests that polymerization was catalyzed perhaps by a high-valent iron compound (note that $\{Fe^{III}X[^{R}NON]\}_2$ systems are stable in THF and do not induce any THF polymerization).[137] The iron-containing product of the reaction could not be isolated from the poly-THF. A similar reaction of $[AdAdBr]^+[B(Ar_F)_4]^-$ with $\{Fe[^{Me_3Ph}NON]\}_2$ in diethylether lead to the formation and isolation of $\{FeBr[^{Me_3Ph}NON]\}_2$.[37] The formation of $\{FeBr[^{Me_3Ph}NON]\}_2$ by $[AdAdBr]^+[B(Ar_F)_4]^-$ might proceed via an iron(IV) intermediate of the form $\{FeBr[^{Me_3Ph}NON]\}^+[B(Ar_F)_4]^-$, which then undergoes intra-molecular electron transfer to form the final iron(III) product (Scheme 4.3).

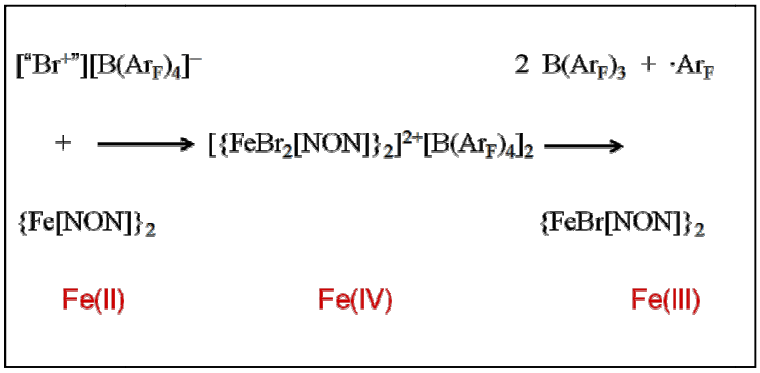

Scheme 4.3. Proposed mechanism for the formation of $\{FeBr[^{Me_3Ph}NON]\}_2$

Evidence for this mechanism includes: (1) the isolation of $B(Ar_F)_3$ and its identification by X-ray crystalography, which clearly shows that the counterion is not stable during the reaction, losing "$^{\cdot}Ar_F$"; (2) the bromonium addition reaction in THF causes solvent polymerization, but if the same $\{FeBr[^{Me_3Ph}NON]\}_2$ is prepared using benzyl bromide from the Fe(II) precursor in THF, no polymerization occurs; (3) diamidoether Fe(III) complexes are stable in THF once formed. These point to the presence of a highly reactive intermediate, which appears to be unstable due its ability to

oxidize the counterion $[(B(Ar_F)_4)]^-$.[287] Other examples of oxidizing $[(B(Ar_F)_4)]^-$ have been reported before, such as the reaction of phosphinite-dinitrogen Rh(I) complexes with $Ag[(B(Ar_F)_4)]$, which led to the cleavage of one of the B-C bonds of the $[(B(Ar_F)_4)]^-$ anion and the transfer of the cleaved aryl group to the rhodium centre.[288]

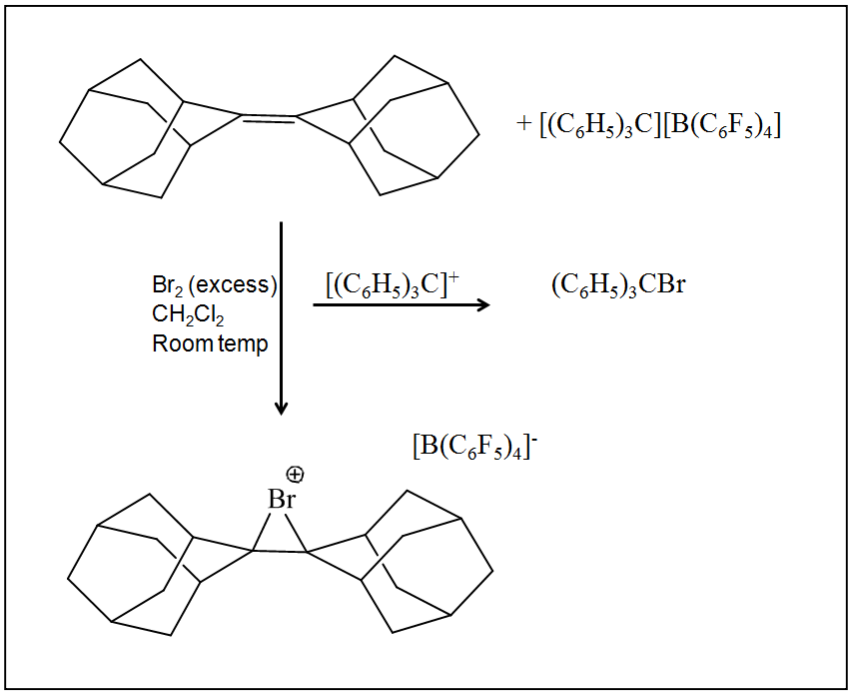

Scheme 4.4. Synthesis of $[AdAdBr]^+[B(C_6F_5)_4]^-$

Non-coordinating anions such as $B[3,5\text{-}(CF_3)_2C_6H_3]_4^-$ tend to not interact with vacant transition metal cation sites[289] and hence let the transition metal cation remain active towards, for example, bond activation or catalytic polymerization reactions.[290-292] In order to access a more oxidation-resistant non-coordinating counteranion and hence further stablize high oxidation-state iron compounds, the counteranion was substituted with $[B(C_6F_5)_4]^-$[293] since the $B(C_6F_5)_3$/ $B(C_6F_5)_3^{\cdot-}$ couple at -2.10 V *vs* $Cp_2Fe^{0/+}$[294] is known to be more stable than $B[3,5\text{-}(CF_3)_2C_6H_3]_4^-$ with respect to oxidation (the reduction potentials of $B[3,5\text{-}(CF_3)_2C_6H_3]_4^{0/-}$ and $B(C_6F_5)_4^{0/-}$ are 1.2 and 1.5 V, respectively).[289] Thus, the new $[AdAdBr]^+[B(C_6F_5)_4]^-$ salt was synthesized by the

reaction of AdAd in the presence of excess Br_2 with $[(C_6H_5)_3C]^+[B(C_6F_5)_4]^-$ in dichloromethane and at room temperature; the yellow product was washed with hexane and crystallized by slow evaporation of a dichloromethane solution (Scheme 4.4). It was characterized by ^1H NMR spectroscopy and elemental analysis.

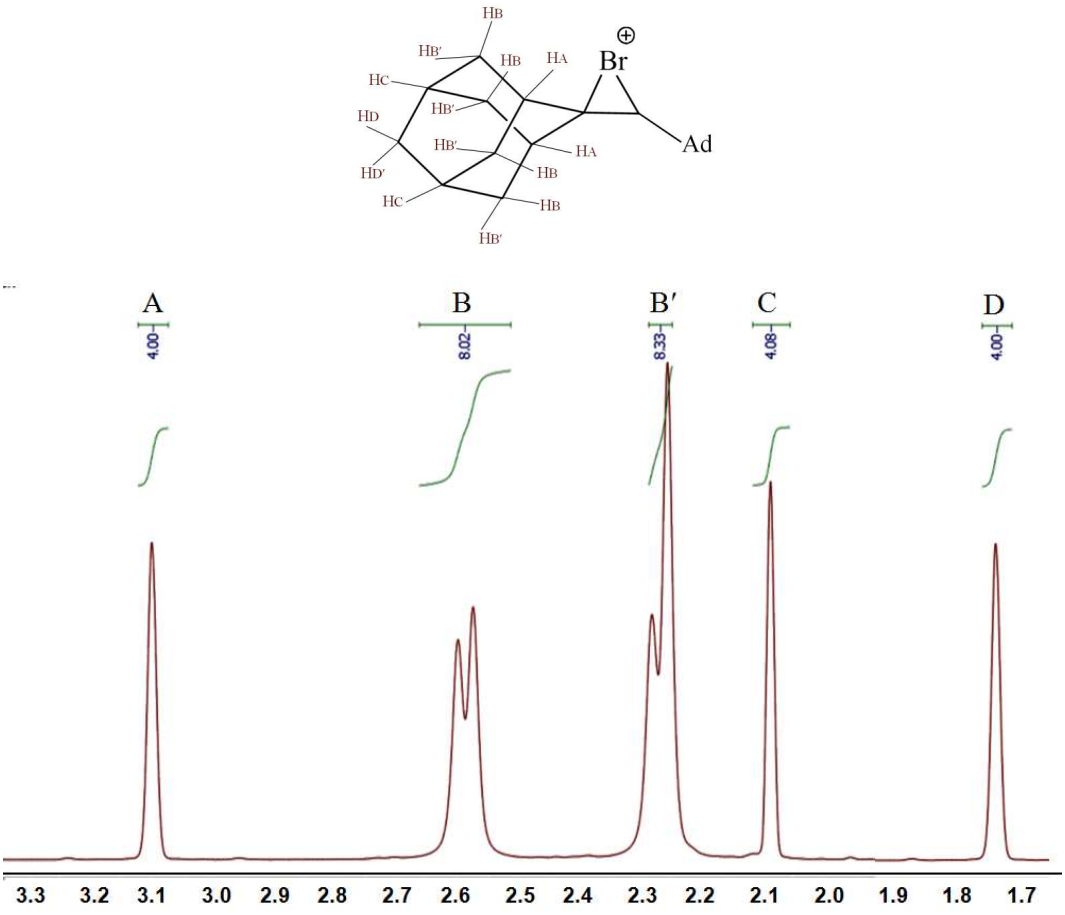

Figure 4.1. ^1H NMR spectrum of $[AdAdBr]^+[B(C_6F_5)_4]^-$ in CD_2Cl_2 and assignment of the peaks.

The ^1H NMR spectrum of the new $AdAdBr^+$ salt matches with the previous one. It shows five distinct peaks assigned to each set of the protons as shown in Figure 4.1: a single peak at 3.11 ppm (4H) corresponding to H_D, two doublet signals integrating to 8H

assigned to H_B (2.6 ppm) and $H_{B'}$ (2.27 ppm), and a single peak at 2.09 ppm (4H) corresponding to H_C and 4H assigned to H_D (1.74 ppm). As expected, the protons which are closer to the Br^+ ion are shifted more from the parent AdAd than those protons further away.

The reaction with $\{Fe[^{tBu}NON]\}_2$ was repeated with this new bromonium salt. The solution changed to deep red and remained red until warmed up to room temperature. However, the resulting product started to decompose during work up of the solvent. Even though qualitatively the red solution appears to be stable longer than with the $3,5(CF_3)_2Ph$-based analogues, it seems that this anion is still too reactive.

On a related note, $[AdAdBr]^+[B(C_6F_5)_4]^-$ was reacted with $\{Co[^{tBu}NON]\}_2$ as well and in this case, $\{Co_2Br_2[^{tBu}NON]\}_2$ (**2**) was isolated from diethyl ether as one of the products. This result suggests that in fact the Br^+ was transferred to the Co(II) centre since the $AdAdBr^+$ was the only source of "Br" in the reaction. However the Co-centre still appears to be Co(II). The proposed mechanism suggests that the Br^+ ion was transferred to the Co(II) to make Co(III) and then the Co(III) centre oxidized species such as the counteranion or the ligand to get reduced to Co(II) (Scheme 4.5), however the accurate mechanism is more compliceted and requires more investigation.

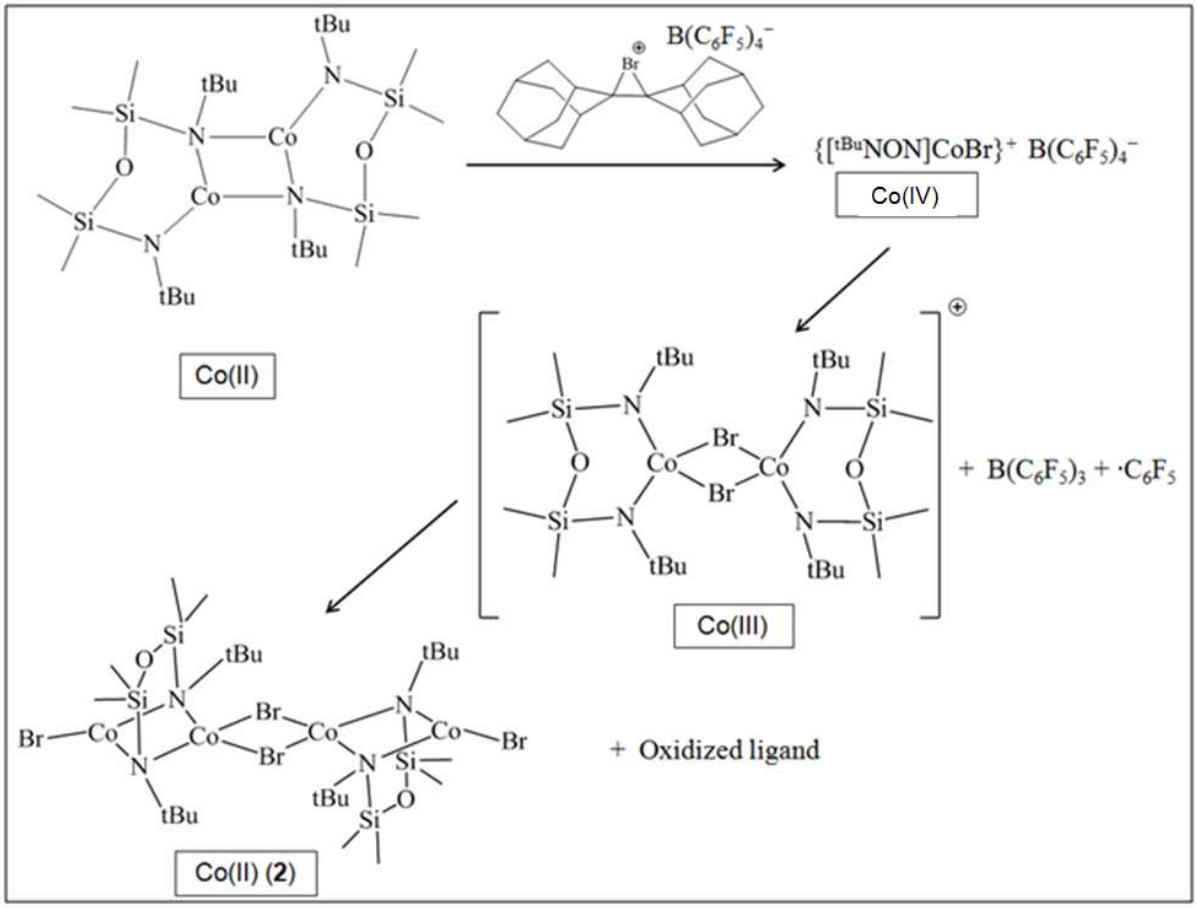

Scheme 4.5. Proposed cobalt-containing intermediates for the synthesis of $\{Co_2Br_2[^{tBu}NON]\}_2$ (**2**) with "Br^+"

These results indicate that upon oxidation, the putative iron(IV) and cobalt(III) products are susceptible to intra-molecular redox chemistry between the metal centre and the ligand or counterion which can lead to the reduction of the metal centre; therefore, this diamidoether ligand does not appear to sufficiently stabilize high oxidation states of iron(IV) and cobalt(III).

4.2.3. Synthesis and Characterization of {FeBr[^{Me_3Ph}NON]}$_2$. Oxidation with benzyl bromide.

From the previous section, it is clear that stablizing Fe(IV) diamido ether complexes from Fe(II) systems was not successful, but it has been shown that Fe(III) diamido-ether systems are stable and can be synthesized either directly from FeX_3 (X = Cl or Br), which led to the formation of ate complexes of the form {$FeX_2Li[^RNON]$}$_2$[137] in the case of using $Li_2[^RNON]$ (R= Me_3Ph). The lithium-free [^{R}NON]Fe(III) analogues could be accessed via oxidation of {Fe[^{R}NON]}$_2$; for example, the oxidation of {Fe[^{R}NON]}$_2$ with I_2 or $AgPF_6$, resulted in lithium-free {FeI[^{R}NON]}$_2$ (R= Me_3Ph) (Figure 4.2) and {FeF[^{R}NON]}$_2$ aryl-based diamidoether compounds (reported by Garry Mund).[137]

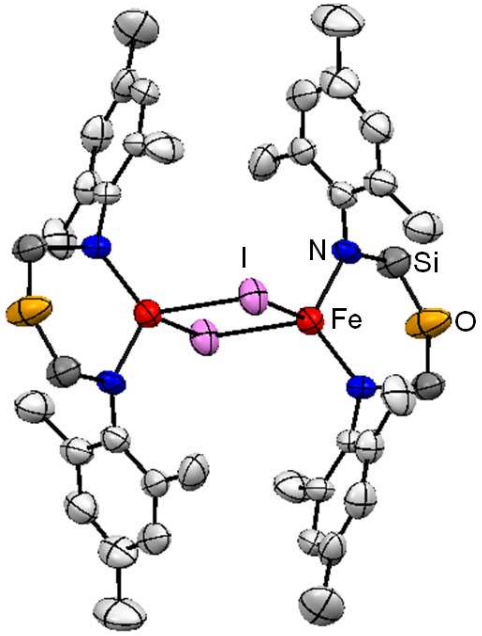

Figure 4.2. Molecular structure of {FeI[^{Me3Ph}NON]}$_2$ (chelating motif).

As was mentioned, {FeBr[^{Me_3Ph}NON]}$_2$ (**17**) could be prepared by the oxidation of {Fe[^{Me_3Ph}NON]}$_2$ with the "Br^+" reagent, however another more straightforward route is to use organic alkyl halides such as benzyl halides, which are commonly used in one–

electron redox chemistry with Cr(II)[271, 274-275] and Co(II)[39] and in some cases with Fe(II)[40] and other transition metals as well.[272-273, 276-277] In the case of iron it also has been used as a 2-electron oxidant of Fe(0) to Fe(II).[295-298]

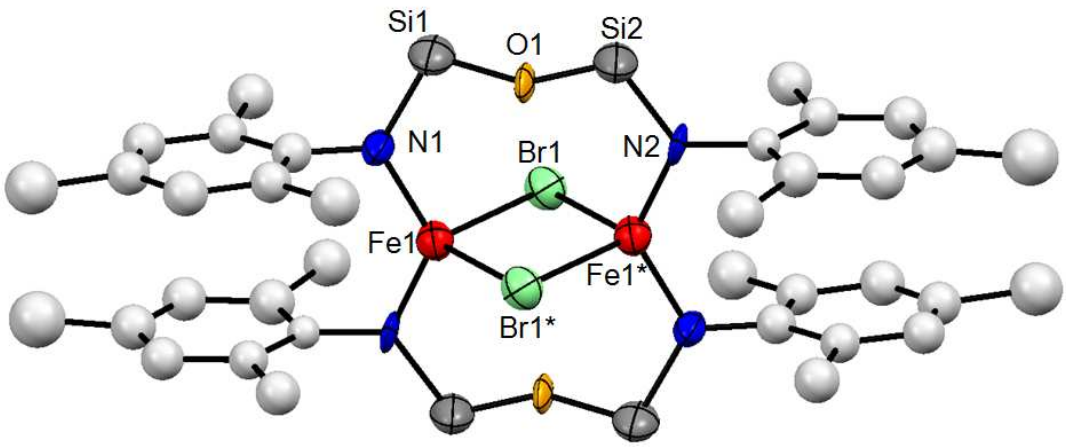

Figure 4.3. Molecular structure of {FeBr[^{Me_3Ph}NON]}$_2$ (**17**) (bridging motif).

Hence, {FeBr[^{Me_3phh}NON]}$_2$ (**17**) was synthesized by the addition of excess benzyl bromide to {Fe[^{Me_3Ph}NON]}$_2$ in hexanes solution; the colour changed from brown to deep red and the product was isolated in high yield.

The structure of **17** (Figure 4.3) shows a bromide-bridged dimer with Fe−Br distances of 2.471(2) and 2.503(2) Å and an Fe−Fe distance of 3.232(3) Å (Table 4.1). The most unusual feature is that each diamidosilylether ligand does not chelate each iron(III) centre as observed in the typical bonding motif exhibited in the iodo-based analogue (Figure 4.2), but instead bridges to both Fe atoms; the silylether donors remain unbound and remote from the metal centres. This binding mode for diamido-donor type ligands is extremely rare; related ligands such as para-N,N‘-disilylated bis(amido)benzene do bridge metal centres but, because of the para arrangement of the amido donors, cannot act as chelates.[37] An intramolecular π−π-stacked amidoaryl array of 3.770 Å is also present in **17** but is absent in the iodo-Fe(III) analogue.

Table 4.1. Selected interatomic distances (Å) and bond angles (°) for {FeBr[^{Me3Ph}NON]}$_2$ (**17**)

Fe1–Fe1*	3.230(1)	Br1–Fe1–Br1*	98.96(7)
Fe1–Br1	2.471(2)	Fe1–Br1–Fe1*	81.04(7)
Fe1–Br1*	2.503(2)	N1–Fe1–N1*	127.2(3)
Fe1–N1	1.864(8)	Br1–Fe1–N1	106.4(2)
Fe1–N1*	1.880(7)	Br1*–Fe1–N1	105.5(2)
Fe1–O1	3.154(5)	Br1–Fe1–N1*	105.8(2)
Fe1–O1*	3.219(7)	Br1*–Fe1–N1*	106.1(2)
C1–C1*	3.339(7)	Fe1–N1–Si1	121.9(5)
Si1–N1	1.755(11)	Fe1*–N2–Si2	119.0(4)
Si2–N2	1.761(10)	Si1–O–Si2	154.0(5)
Si1–O1	1.651(9)		
Si2–O1	1.626(6)		

Symmetry operation *: -x,-y,-z

Indeed, the smaller size of bromide *vs* iodide (van der Waals radii for Br/I are 1.85/1.96 Å)[299] appears to be a key factor that influences the binding mode: the larger steric strain of adjacent amido aryl groups in the chelating form (as exemplified by long Fe−Fe distance of 3.749(3) Å in the FeI-analogue) can be relieved by a switch to the bridging mode, as is observed in **17**. Consistent with this concept, the same bridging mode is also reported for the chloride analogue {FeCl[^{Me_3ph}NON]}$_2$, which can be prepared by reacting {Fe[^{Me_3ph}NON]}$_2$ with $PhICl_2$. The bridging binding motif for diamido-donor ligands reported here may have implications in the design of future diamido-supported and other chelating ligand-supported metal catalysts because it should not be assumed that a “chelating ligand” will always chelate.

The ^{1}H NMR spectra of these iron(III) complexes, consistent with their paramagnetism, have very broad, featureless peaks which are hard to assign compared

to the sharper peaks observed, integrated and assigned in amido/halide iron(II) complexes **1** and **3** presented in Chapter 2 and alkyl/amido iron(II) **6** and alkyl/halide **8** in Chapter 3. The broadening is due to a higher nuclear relaxation rate in Fe(III) compared to iron(II) or cobalt(II).[148]

The intense colours of these amido iron(III) systems are attributable to a halide-to-metal charge transfer that shifts to lower energy from Cl−Br−I (424 to 485 to 670 nm, respectively); both the very broad ^{1}H NMR spectra and the charge transfer band were previously recognized and analyzed for analogous [^{tBu}NON]-Fe^{III} complexes.[55]

4.2.4. Synthesis and characterization of {FeCl[^{tBu}NON]}$_2$(μ-Me$_2$PCH$_2$CH$_2$PMe$_2$)

Preliminary results from Garry Mund's Ph.D. research indicated that the iron(III) diamidoether halide complexes are reactive towards halide metathesis with different alkyl reagents, but although the colour changed to dark red at low temperature (indicating that a reaction had happened) it was not stable and upon warming to room temperature, in most cases the reduced {Fe^{II}[NON]}$_2$ was isolated as the main product. In other words, it seems that iron(III)-alkyl complexes possibly formed but were not stable. Hence, the strategy of incorporating another neutral donor ligand was considered in order to stabilize the iron(III) centre prior to (or during) alkylation. The weak π-acceptor, fairly strong σ-donor, non-steric and chelating dmpe was targeted as a first attempt. Addition of one equivalent of dmpe per {FeCl[^{tBu}NON]}$_2$ dimer resulted in a colour change from dark red to bright red and upon work up in hexanes and slow evaporation of the hexanes solvent, crystals of the diamido/chloride Fe(III)-dmpe bridged species {FeCl[^{tBu}NON]}$_2$(μ-Me$_2$PCH$_2$CH$_2$PMe$_2$) (**18**) were isolated. Addition of one equivalent of dmpe per iron centre also resulted in the isolation of the same product **18**.

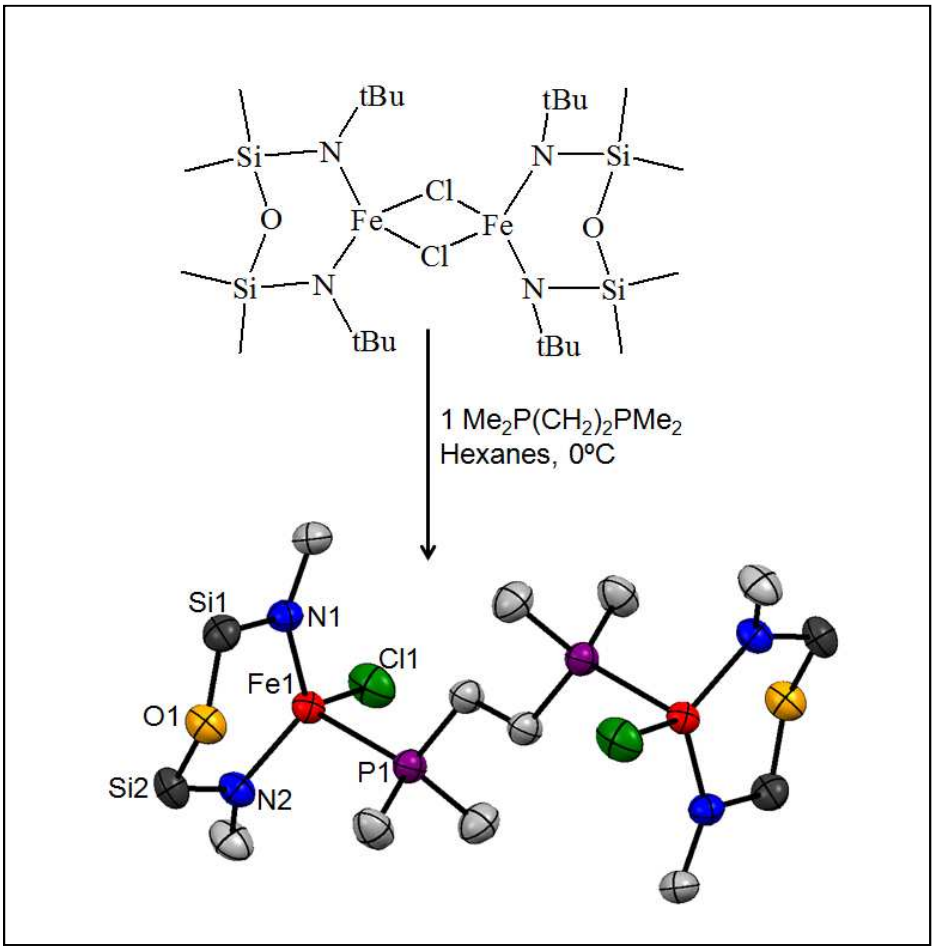

Figure 4.4. Synthesis and molecular structure of {FeCl[^{tBu}NON]}$_2$(μ-Me$_2$PCH$_2$CH$_2$PMe$_2$) (**18**). (^{t}Bu and SiMe$_2$ groups simplified for clarity).

The X-ray crystal structure of {FeCl[^{tBu}NON]}$_2$(μ-Me$_2$PCH$_2$CH$_2$PMe$_2$) (**18**) reveals a four-coordinate iron(III) centre with a distorted tetrahedral geometry. Each iron centre is bonded to a diamido ligand, one chloride and a phosphine from the dmpe bridge (Figure 4.4). The Fe1–N1 and Fe2–N2 distances of 1.932(2) and 1.934(2) Å (Table 4.2) are a little longer compared to the 1.887(5) and 1.894(4) Å in the {FeCl[^{tBu}NON]}$_2$ starting material.[55] On the other hand, the Fe–Cl distance of 2.2240(7) Å is shorter than the 2.3181(19) and 2.4652(17) Å in {FeCl[^{tBu}NON]}$_2$ since chloride in **18** is terminal, not bridging as in {FeCl[^{tBu}NON]}$_2$. The Fe–O distance of 2.807(3) Å in **18** is considerably longer than the 2.597(4) Å in {FeCl[^{tBu}NON]}$_2$, and clearly too far to be considered coordinated in **18**, hence there is an overall lowering of the coordination number. The Fe^{III}-P bond distance of 2.5254(6) Å in **18** is considerably longer compared to those of

2.350(2) and 2.330(2) Å of spin-admixed $FeBr_2[N(SiMe_2CH_2PPh_2)_2]$[40] and are slightly shorter compared to those of 2.654(4) and 2.623(4) Å in high-spin $FeCl_3(PPh_3)_2$.

Table 4.2. Selected interatomic distances (Å) and bond angles (°) for $\{FeCl[^{tBu}NON]\}_2(\mu\text{-}Me_2PCH_2CH_2PMe_2)$ (**18**)

Fe1–N1	1.934(2)	Cl1–Fe1–N1	113.14(6)
Fe1–N2	1.932(2)	Cl1–Fe1–N2	112.30(5)
Fe1–O1	2.807(3)	N1–Fe1–N2	122.24(7)
Fe1–Cl1	2.2240(7)	Cl1–Fe1–P1	100.71(2)
Fe1−P1	2.5052(6)	P1–Fe1–N2	102.52(5)
Si1–N1	1.724(2)	P1–Fe1–N1	102.10(5)
Si2–N2	1.723(2)	Si1–O–Si2	142.1(1)
Si1–O1	1.640(2)		
Si2–O1	1.639(2)		

The Evans method magnetic susceptibility of **18** was measured as 4.9 μ_B, which is less than what is expected for a high-spin d^5, S= 5/2 centre (5.92 μ_B expected for spin-only magnetic moment), however more detailed magnetic measurements, indicating variable temperature SQUID and Mőssbauer is required before any conclusion regarding spin-state can be made. The ^{1}H NMR spectrum of **18** is also consistent with its paramagnetism, showing two very broad, featureless peaks which are hard to assign (Figure 4.5).

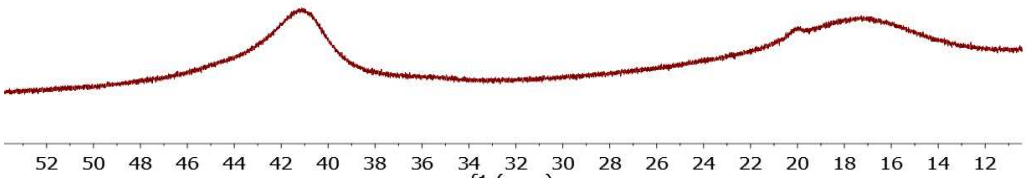

Figure 4.5. ^{1}H NMR spectrum of **18** in benzene-d_6.

The presence of both amido and phosphine ligands in one molecule is usually observed more with mixed multidentate phosphine/amido ligands.[33, 41-43] They are known to be able to stabilize metal centres in unusual oxidation states due to the different binding preferences of phosphine and amido π–donor groups. π–acceptor phosphine donors usually stabilize metal centres in lower oxidation states while π–donor amido units are more suitable to stabilize metals in higher oxidation states.[8, 34, 37-40] One rare example of a mixed amide/phosphine Fe(III) compound is $\{FeX_2[N(SiMe_2CH_2PPh_2)_2]\}$ (X= Cl and Br).[40] On the other hand tetrahedral iron(III) compounds are rare; there are only limited number of such complexes reported, such as $\{FeX_2Li[RN(SiMe_2)]_2O\}_2$ (X=Cl, Br R=2,4,6-Me_3Ph; X=Br, R=2,4,6-Me_3Ph, 2,6-iPr_2Ph)[137] $[FeI([D_5]pyridine)(NRAr_f)_2]$ (R=$C(CD_3)_2CH_3$, Ar_f=2,5-C_6H_3FMe)[300] and the thiourea iron(III) iodide complex $FeI_3[SC(NMe_2)_2]$ [301]

The important aspect of being able to synthesize **18** was to show that it is possible to incorporate neutral donor ligands in the coordination sphere of the iron(III) diamidoether complexes and it might open doors to new reactivity that could not be achieved before. Fe^{III}-C or Fe^{III}-H bonds tend to be unstable; hence, Fe(III)-organometallic compounds are very rare. One example is the 17-e radical cation iron(III)-hydride $[FeH(Cp^*)(dppe)]PF_6$.[302]

As a preliminary test, the reaction of $\{FeCl[^{tBu}NON]\}_2(\mu\text{-}Me_2PCH_2CH_2PMe_2)$ with $LiCH_2SiMe_3$ was conducted, and it gave a change in colour from dark purple to deep red at low temperature, perhaps indicative of the formation of an iron(III)-alkyl complex. Upon warming to room temperature, the colour remained red but after about 2 hours

changed to dark brown. The ^{1}H NMR spectrum of the brown residue matched that of the iron(II) dimer {Fe[^{tBu}NON]}$_2$; presumably the Fe^{III}-C bond is not stable with respect to homolysis. It seems that even though the presence of dmpe helped with the stability, it is not enough. It should be noted that, based on the X-ray structure, the choice of the alkyl group to add to **18** might be crucial as well since it should not be too bulky to conflict with other part of the structure. It is worth trying other alkyl, or fluoroaryl units known to be more thermodynamically stable, and also different phosphines like PMe_3 to form a mononuclear iron(III) complex which might be more amenable to clean halide metathesis.

4.3. Conclusion

Efforts to prepare iron(IV) and cobalt(III) diamido complexes with a range of oxidizing reagents were unsuccessful. Strong [AdAdBr]$^+$[B(Ar$_F$)$_4$]$^-$ was tried to oxidize the metal centres with diamidoether ligands to make iron(IV) and cobalt(III) systems. Even though during the reaction of Br$^+$ with {Fe[^{R}NON]}$_2$ (R= Me_3Ph), highly active intermediate Fe(IV) complexes perhaps formed, they were not stable and were reduced due to the internal oxidation of the anion, as evidenced by the isolation of B(Ar$_F$)$_3$. To overcome anion oxidation, the more oxidation-resistant [AdAdBr]$^+$[B(C_6F_5)$_4$]$^-$ was made. However, even though the high-valent intermediate appeared to show slightly greater stability, reduced products were still ultimately isolated. It seems that despite the hypothesis that the diamidoether ligand would be adept at stabilizing these higher oxidation metal centres due to its π-donating ability and silylether donor group in the ligand backbone, it is not capable of stabilizing these higher oxidation states. However benzyl bromide oxidation of the same Fe(II) systems lead to the formation of {FeBr[^{Me3Ph}NON]}$_2$ (**17**) which had an unusual bridging binding motif mode for [NON], rather than the usual diamido chelate. Any further oxidation or alkyl substitution reaction attempts at the iron centre in {FeCl[^{tBu}NON]}$_2$ resulted in the formation of reduced iron(II); the addition of dmpe to {FeCl[^{tBu}NON]}$_2$ resulted to the formation of **18**, which could not be cleanly alkylated with $LiCH_2SiMe_3$ although a different alkyl group might work.

4.4. Future work

The formation of **18** shows that a new series of iron(III) diamido-phosphine complexes should be targeted; in this chapter only dmpe was tried, however trying different phosphine ligands such as the related monodentate phosphine PMe_3 could result in a monomeric iron(III) system. The alkylation of **18** with $LiCH_2SiMe_3$ did not lead to a stable iron(III) alkyl compound, however a different choice of the phosphine and also alkyl or aryl group, especially non-bulky LiMe, might lead to the formation of stable iron(III)-alkyl complexes that are ideally also high-spin. On the other hand, it is worth trying other neutral donor ligands to replace the phosphine in **18**, such as isocyanides or carbenes as in Chapter 2.

4.5. Experimental section

4.5.1. General Procedures and Materials

General procedures and materials are as described in Chapter 2. $[AdAdBr]^+[B(Ar_F)_4]^-$ was prepared by metathesis of $[AdAdBr]^+[X]$ (X = Br_3^- or OTf^-) and $Na\{B[3,5\text{-}(CF_3)_2\text{-}C_6H_3]_4\}$ in CH_2Cl_2.[286] I would like to thank the Bennet lab at SFU for generously providing with AdAd. Trityltetra(pentafluorophenyl)borate was bought as a white powder from *Frontier Scientific* chemical company.

Reaction of $\{Fe[^{tBu}NON]\}_2$ and $[AdAdBr]^+[BArf]^-$

The beige powder $[AdAdBr]^+[BAr_F]^-$ (0.092 g, 0.076 mmol) was dissolved in 30 mL of Et_2O, whereupon a 10 mL Et_2O solution of $\{Fe[^{tBu}NON]\}_2$ (0.025 g, 0.038 mmol) was added dropwise at -78 ^oC. An immediate colour change to a deep red occurred. Upon warming to room temperature, the colour changed to dark brown; the solvent was removed *in vacuo*, the residue was extracted in a toluene/Et_2O mix (1:1) and filtered through Celite. However, removal of the solvent *in vacuo* did not result in a clean product.

Reaction of $\{Co[^{tBu}NON]\}_2$ and $[AdAdBr]^+[B(Ar_F)_4]^-$

The beige powder $[AdAdBr]^+[B(Ar_F)_4]^-$ (0.092 g, 0.076 mmol) was dissolved in 30 mL of Et_2O whereupon a 10 mL Et_2O solution of $\{Co[^{tBu}NON]\}_2$ (0.02 g, 0.038 mmol) was added dropwise at -78 ^oC. An immediate colour change to a dark green occurred. Removal of the solvent *in vacuo* gave a dark brown mixture but no clean product was isolated.

Synthesis of $[ADADBr]^+[B(C_6F_5)_4]^-$

The white powder adamantylideneadamantane (0.200 g, 0.743 mmol) was dissolved in 50 mL of distilled CH_2Cl_2 in an Erlenmeyer flask. Trityltetra(pentafluorophenyl)borate (0.700 g, 0.743 mmol) was added slowly at room temperature and stirred for one hour. Then an excess amount of reddish liquid Br_2 was added dropwise at 0 ^oC, until the colour of the solution started to get red (very dark yellow); the solution was then stirred for approximately one hour and then filtered through filter paper. The solvent was removed *in vacuo*. By adding a small amount (10 mL) of distilled CH_2Cl_2 a concentrated solution was prepared. Then excess hexane (50 mL) was added to the solution. A light yellow powder of $[AdAdBr]^+[B(C_6F_5)_4]^-$ began to precipitate and it was collected by filtration through filter paper. This crude product was crystallized through slow evaporation of a CH_2Cl_2 solution. Yield: 550 mg (55%). Anal. Calcd for $C_{44}H_{28}BBrF_{20}$: C: 55.72%; H: 2.95%. Found: C: 55.59%; H: 2.74%. ^1H NMR (CD_2Cl_2): H_A 3.11 (s, 4H), H_B 2.59 (d, 8H), $H_{B'}$ 2.27 (d, 8H), H_C 2.09 (s, 4H) and H_D 1.74 (s, 4H).

Reaction of $\{Fe[^{tBu}NON]\}_2$ and $[AdAdBr]^+[B(C_6F_5)_4]^-$

The beige powder $[AdAdBr]^+[B(C_6F_5)_4]^-$ (0.300 g, 0.29 mmol) was dissolved in 30 mL of Et_2O whereupon a 30 mL Et_2O solution of $\{Fe[^{tBu}NON]\}_2$ (0.096 g, 0.146 mmol) was added dropwise at -78 ^oC. An immediate colour change to a deep red occurred. After a few minutes of being stirred at room temperature, the solvent was removed *in vacuo*, the residue was extracted in a toluene/Et_2O mix (1:l) and filtered through Celite. After an hour, the solution had changed colour to a dark-brown red. Removal of the solvent *in vacuo* gave a dark brown red powder but no clean product could be isolated.

Reaction of $\{Co[^{tBu}NON]\}_2$ and $[AdAdBr]^+[B(C_6F_5)_4]^-$

The beige powder $[AdAdBr]^+$ $[B(C_6F_5)_4]^-$ (0.480 g, 0.466 mmol) was dissolved in 30 mL of Et_2O whereupon a 30 mL Et_2O solution of $\{Co[^{tBu}NON]\}_2$ (0.156 g, 0.233 mmol) was added dropwise at -78 ^oC. An immediate colour change to a dark green occurred. After a few minutes of being stirred at room temperature, the solvent was removed *in vacuo*, the residue was extracted with hexanes to give a brown solution and then with ether to give green solution; each was filtered through Celite. No clean product could be isolated from the hexane solution, however slow evaporation of the Et_2O solution gave green crystals of $\{Co_2Br_2[^{tBu}NON]\}_2$.(**2**), Yield: 40 mg.

Synthesis of $\{FeBr[^{Me_3Ph}NON]\}_2$ (17)

Liquid benzyl bromide (0.22 mL, 0.9 mmol) in 20 mL Et_2O was added dropwise at -70 ^oC slowly to a yellow solution of $\{Fe[^{tBu}NON]\}_2$ (375 mg, 0.82 mmol) in 40 mL Et_2O while stirring. The resulting red mixture was stirred overnight, and then the solvent was removed *in vacuo*. The product was extracted with Et_2O and the resulting solution was filtered through Celite. Removal of the Et_2O *in vacuo* resulted in red $\{FeBr[^{tBu}NON]\}_2$ (**17**). Crystals were obtained by slow evaporation of a Et_2O solution. Yield: 187 mg (45%). Anal. Calcd for $C_{22}H_{34}N_2BrFeOSi_2$: C: 49.39%; H: 6.34%; N: 5.23%. Found: C: 49.04%; H: 6.12%; N: 5.06%. ^1H NMR (benzene-d_6): two very broad featureless peaks. UV-vis(C_6H_{14}): 399 nm (ε =2005 $M^{-1}cm^{-1}$) and 485 nm (ε = 2304 $M^{-1}cm^{-1}$). Evans Method μ_{eff}: 5.8 μ_B.

Synthesis of $\{FeCl[^{tBu}NON]\}_2(\mu\text{-}Me_2PCH_2CH_2PMe_2)$ (18)

Bis(dimethylphosphino)ethane (dmpe) (0.057 g, 0.39 mmol) in 30 mL Et_2O was added dropwise at -70 ^oC slowly to a solution of $\{FeCl[^{tBu}NON]\}_2$ (0.285 g, 0.78 mmol) in 50 mL Et_2O while stirring. The resulting brown mixture was stirred overnight, and then the Et_2O was removed *in vacuo*. The product was extracted with hexanes and the resulting solution was filtered through Celite. Removal of the hexanes *in vacuo* resulted in a red powder of $\{FeCl[^{tBu}NON]\}_2(\mu\text{-}Me_2PCH_2CH_2PMe_2)$ (**18**). Crystals of **18** were obtained by slow evaporation of a Et_2O solution. Yield: 185 mg (54%). Anal. Calcd for $C_{30}H_{46}N_4Cl_2Fe_2O_2P_2Si_4$: C: 40.86%; H: 8.68%; N: 6.35.%. Found: C: 40.97%; H: 8.83%; N: 6.12%. ^1H NMR (benzene-d_6): two broad peaks at δ= 17 and 41. Evans method : 4.8 μB .

Reaction of {FeCl[^{tBu}NON]}$_2$(μ-Me$_2$PCH$_2$CH$_2$PMe$_2$) (18) with LiCH$_2$SiMe$_3$

Dark red **18** (0.158 g, 0.179 mmol) was dissolved in 30 mL of Et_2O whereupon a 10 mL solution of $LiCH_2SiMe_3$ (0.034 g, 0.358 mmol) was added dropwise at -78 ^oC. An immediate colour change to a bright red occurred. However, upon warming to room temperature a colour change to brown resulted. After 2 hours of being stirred at room temperature, the solvent was removed *in vacuo*, the residue was extracted in hexanes and filtered through Celite. The ^1H NMR spectrum of this sample gave the same NMR fingerprint as independently prepared {Fe[^{tBu}NON]}$_2$.

4.5.2. X-ray crystallography

Crystals of **17** sealed at room temperature in capillaries were mounted on an Enraf-Nonius CAD4 diffractometer while crystals of **18** were coated in Paratone-oil and mounted onto a MiTeGen Micro Mount at -150 ^oC. Crystal descriptions for each compound are as follows:**17** is a bright red block having dimensions 0.40 × 0.30 × 0.20 $mm^3$and 18 is a dark red cube having dimensions 0.45 × 0.25 × 0.30 mm^3. Data for 18 was collected on a Bruker Smart instrument equipped with an APEX II CCD area detector at a distance of 6.0 cm from the crystal. The rest of the procedure, including data collection, integration, data work up and structure solution and refinement was described in Chapter2.

5. Carbon backbone-based diamido donor complexes of iron(II) and cobalt(II)

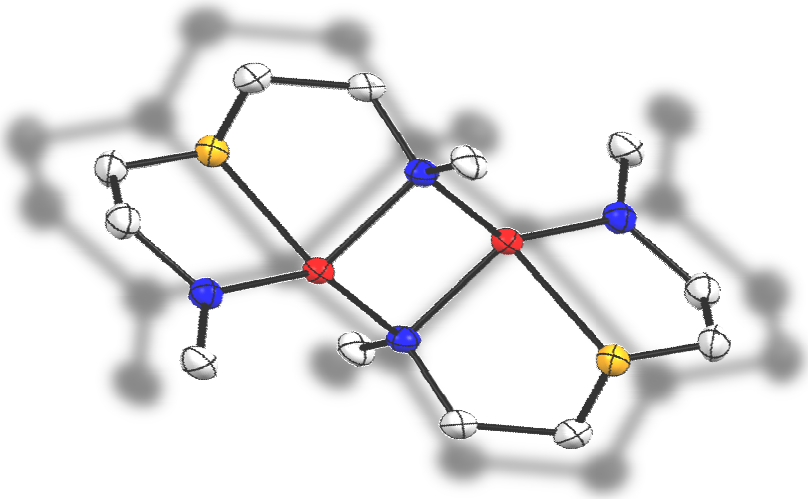

5.1. Introduction

The diamidoether $[NON]^{2-}$ ligands used in previous chapters incorporated a short silicon-based backbone which contains a neutral silylether donor of the general type $\{[RN(SiMe_2)]_2O\}^{2-}$ (R= t-butyl and Me_3Ph). As has been shown in Chapter 4, attempts to access higher oxidation state iron(IV) and cobalt(III) complexes with this $[NON]^{2-}$ ligand were not successful; a big lesson from this might be that this ligand is not suitable for the purpose of stabilizing more high-valent metal centres, perhaps since the N-Si bond is not that stable due to the presence of H_2O and H^+. Hence, using a similar ligand but with carbon-based backbone could be targeted since they are expected to be more resistant to oxidation reactions compared to the Si−N bond-containing counterparts.

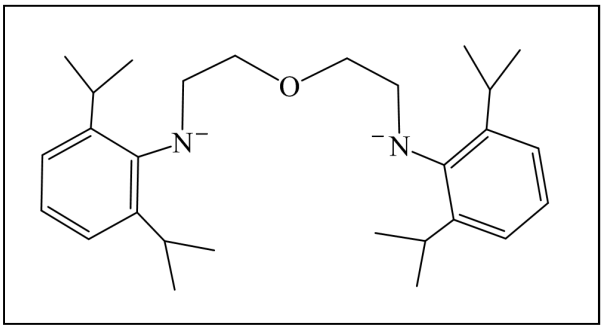

Figure 5.1. Example of a carbon backbone-based diamidoether ligand

One well-known diamidoether ligand with a carbon-based backbone is $\{[RN(CH_2CH_2)]_2O\}^{2-}$ [100, 154, 303-305] (R= 2,4,6-Me_3Ph and 2,6-$^{i}Pr_2$Ph (Figure 5.1) or bulky Me_3Si-substituent).[104, 306-307] However, for the purpose of stabilizing higher oxidation state stable metal centres, the phenyl component is not helpful and should be replaced, in order to reduce any chance of complications due to the possible oxidation of the phenyl ring through an internal oxidation reaction. Surprisingly, most reported diamido donor ligands with carbon-based backbones include phenyl rings or a Si-N bond,[308] neither of which is likely to be compatible with higher oxidation state metals. Thus, for the purpose of accessing the desired oxidation chemistry, a different kind of carbon backbone-containing ligand is required.

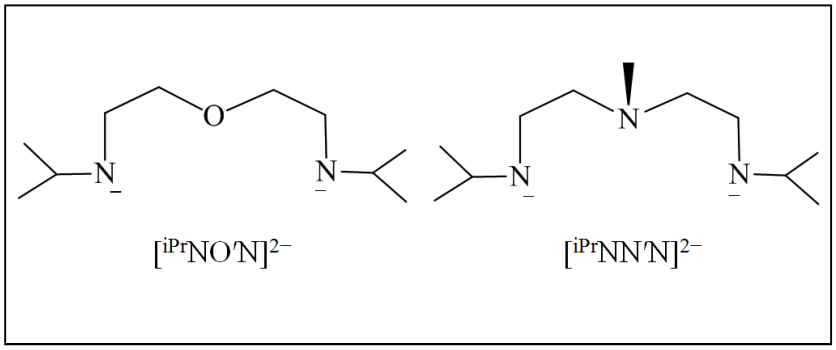

Figure 5.2. Diamidoether $[^{iPr}NO'N]^{2-}$ (left) and diamidoamine $[^{iPr}NN'N]^{2-}$ (right)

In this chapter two diamido carbon backbone-based ligands incorporating an ether donor and amine donor with formulas $[(^{i}PrNCH_2CH_2)_2NMe]^{2-}$ ($[^{iPr}NN'N]^{2-}$) and

$[(^{i}PrNCH_2CH_2)_2O]^{2-}$ ($[^{iPr}NO'N]^{2-}$) (Figure 5.2) have been chosen to target high-valent iron and cobalt complexes. These ligands are more flexible than their similar silicon-based $[NON]^{2-}$ analogues since the carbon-based ligand consists of five backbone atoms compared to only three atoms in the silicon-based ligand backbone. This flexibility could allow the complex to adapt to the coordination number and geometry around the metal centre that is most preffered upon oxidation. However, although the ligand synthesis has been reported (for the free diamine),[306] there are almost no studies of these two ligands with transition metals. The only reported compounds are $[^{iPr}NN'N]^{2-}$ with $AlCl_3$, affording the monomeric derivative $[^{iPr}NN'N]AlCl$, which then was treated with one equivalent of HCl to form $\{[^{iPr}NN'NH]AlCl{\cdot}AlCl_4\}$;[306] there is no report of the $[^{iPr}NO'N]$ ligand with any metal.

Thus, in this Chapter both the $[^{iPr}NN'N]^{2-}$ and $[^{iPr}NO'N]^{2-}$ complexes of iron and cobalt are reported and their resulting coordination chemistry will be compared to those of the analogous silicon-based complexes. As well, the oxidation of the resulting cobalt(II) and iron(II) systems were studied and showed some unexpected results.

5.2. Results and discussion

The synthesis of the carbon-backbone diamido ligands are straightforward, following a literature preparation; the parent amines are air stable as well.[306]

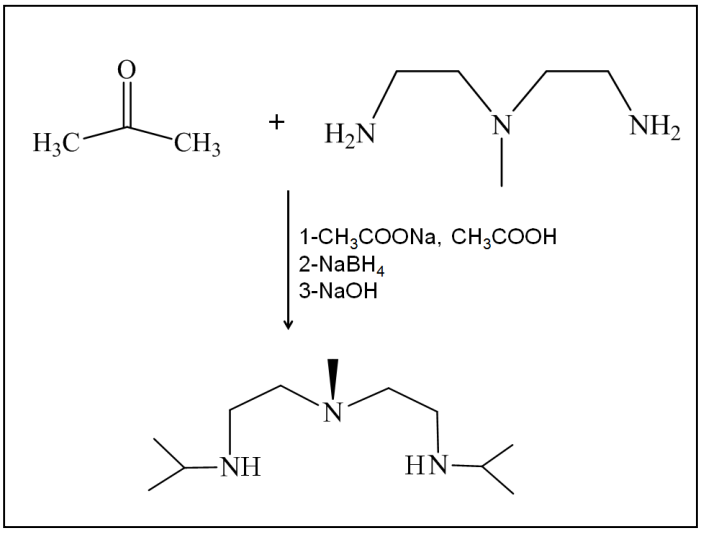

Scheme 5.1. Synthesis of $[^{iPr}NN'N]H_2$

Thus, N-methyldiethylenetriamine was added to an aqueous solution of acetic acid, $CH_3CO_2Na{\cdot}3H_2O$ and acetone. Addition of $NaBH_4$, followed by sodium hydroxide (15%) yielded $[^{iPr}NN'N]H_2$ as a colourless liquid after work up. In order to get $[^{iPr}NO'N]H_2$, diethyleneetherdiamine ($NH_2(CH_2)_2O(CH_2)_2NH_2$) was used instead of N-methyldiethylenetriamine and the rest of the procedure and reactants remained the same (Scheme 5.1).

5.2.1. Synthesis and characterization of $\{M[^{iPr}NN'N]\}_2$ (M= Fe and Co)

The reaction of one equivalent of MCl_2 (M=Fe, Co) with one equivalent of $Li_2[^{iPr}NN'N]$ at -70 ^oC generated dinuclear compounds of empirical formula $\{M[^{iPr}NN'N]\}$ (M=Fe, **19**; M= Co, **20**) (Scheme 5.2), very similar to the 1:1 reaction of $Li_2[^{tBu}NON]$ with MX_2 that generates $\{M[^{tBu}NON]\}_2$.

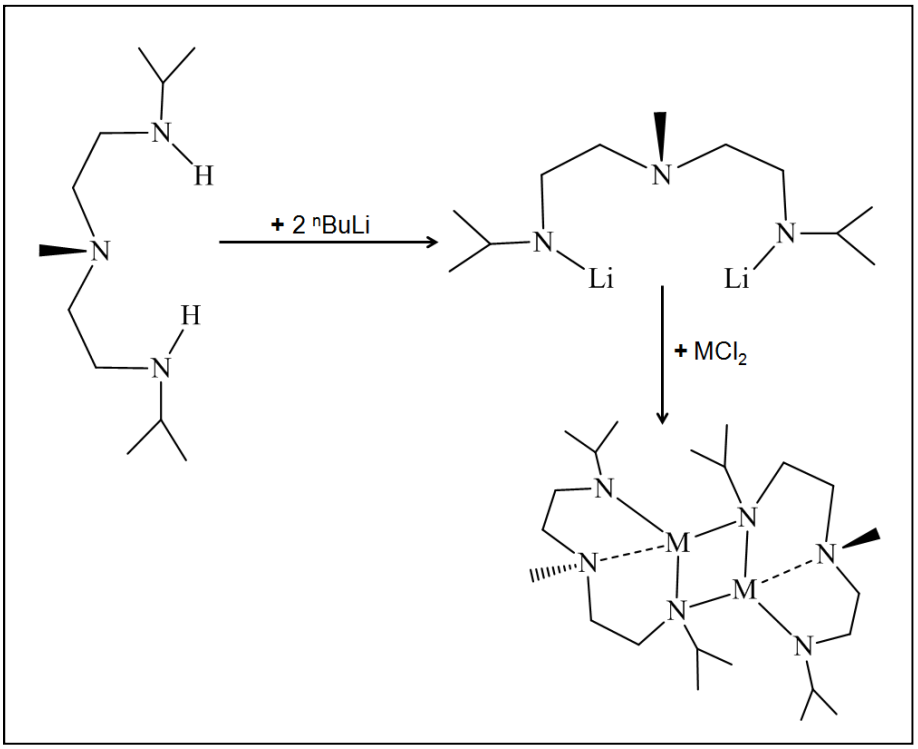

Scheme 5.2. Synthesis of **19** (M = Fe) and **20** (M = Co).

Single crystals suitable for X-ray diffraction were obtained by slow evaporation of a brown hexanes solution of **19** and a dark green solution of **20**. The X-ray structure is shown in Figure 5.3, with selected interatomic distances and bond angles detailed in Table 5.1.

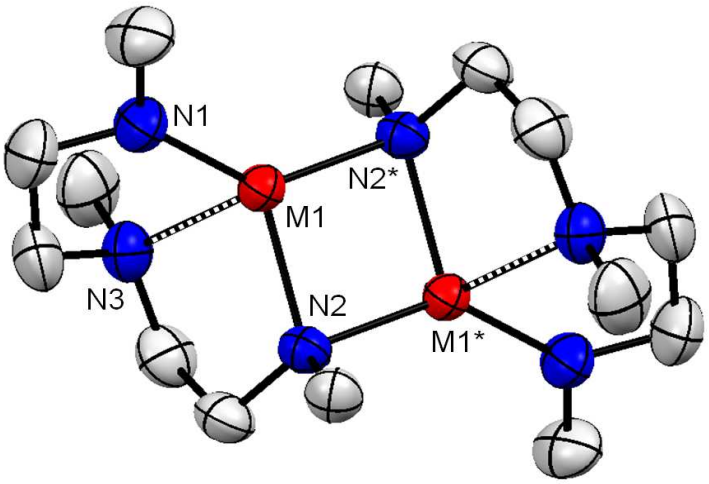

Figure 5.3. Molecular structure of **19** (M=Fe) and **20** (M= Co) (^{i}Pr group simplified for clarity).

The structure of **19** and **20** reveals a dinuclear M(II) diamidoamine complex with both bridging and terminal amido groups similar to $\{M[^{tBu}NON]\}_2$ systems.[140] The M(II) centres both have a distorted four-coordinate geometry (excluding any M−M bond) (Figure 5.4) in which the distance between the Fe atoms is 2.7428(6) and the Co atoms is 2.5644(16) Å. Each M(II) centre could be considered to have a distorted trigonal-monopyramidal geometry (Figure 5.3), with M1−N3 bonded in the apical position (Fel-N3: 2.2125(17), Col-N3: 2.196(5) Å).

Table 5.1. Selected interatomic distances (Å) and bond angles (°) for {Fe[^{iPr}NN′N]}$_2$ (**19**) and {Co[^{iPr}NN′N]}$_2$ (**20**)

M	**Fe(19)**	**Co(20)**
M1–M1*	2.7428(6)	2.5644(15)
M1–N1	1.9284(17)	1.883(5)
M1–N2	2.1014(16)	2.015(4)
M1–N2*	2.0485(16)	1.999(4)
M1–N3	2.2125(17)	2.196(5)
N1–C1	1.455(3)	1.447(7)
N1–C4	1.444(3)	1.450(8)
C4–C5	1.516(4)	1.524(10)
C6–C7	1.517(3)	1.488(10)
C2–N2	1.481(2)	1.486(7)
N2–C7	1.478(2)	1.473(7)
N3–C5	1.484(3)	1.500(9)
N3–C6	1.465(3)	1.465(9)
N2–M1–N2*	97.27(6)	100.58(16)
Fe1–N2–Fe1*	82.73(6)	79.42(16)
N1–M1–N2	124.51(7)	124.9(2)
N1–M1–N3	84.62(7)	84.6(2)
N3–M1–N2	81.59(6)	85.16(19)
N3–M1–N2*	116.48(7)	102.64(14)
N3–M1–N2	81.59(6)	84.3(2)
C5–N3–C6	113.64(19)	110.5(6)

Symmetry operation *: -x, -y, -z

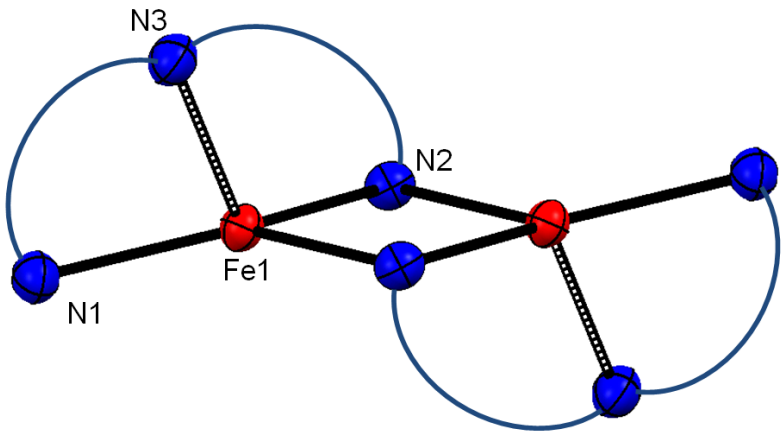

Figure 5.4. Trigonal monopyramidal geometry around M.

The Co−N and Fe−N distances for the terminal and bridging amido groups (terminal Fe−N: 1.9284(17) Å, Co−N: 1.883(5) Å, bridging Fe−N: 2.1014(16) and 2.0485(16) Å, Co−N: 1.999(4) and 2.015(4) Å) can be compared with terminal and bridging M−N bond lengths in dimeric $\{Co[^{tBu}NON]\}_2$ and $\{Fe[^{tBu}NON]\}_2$ (terminal Fe−N: 1.934(3) Å, Co−N: 1.906(3) Å, bridging Fe−N: 2.157(3) and 2.058(3) Å, Co−N: 2.051(4) and 2.029(3) Å).[155]

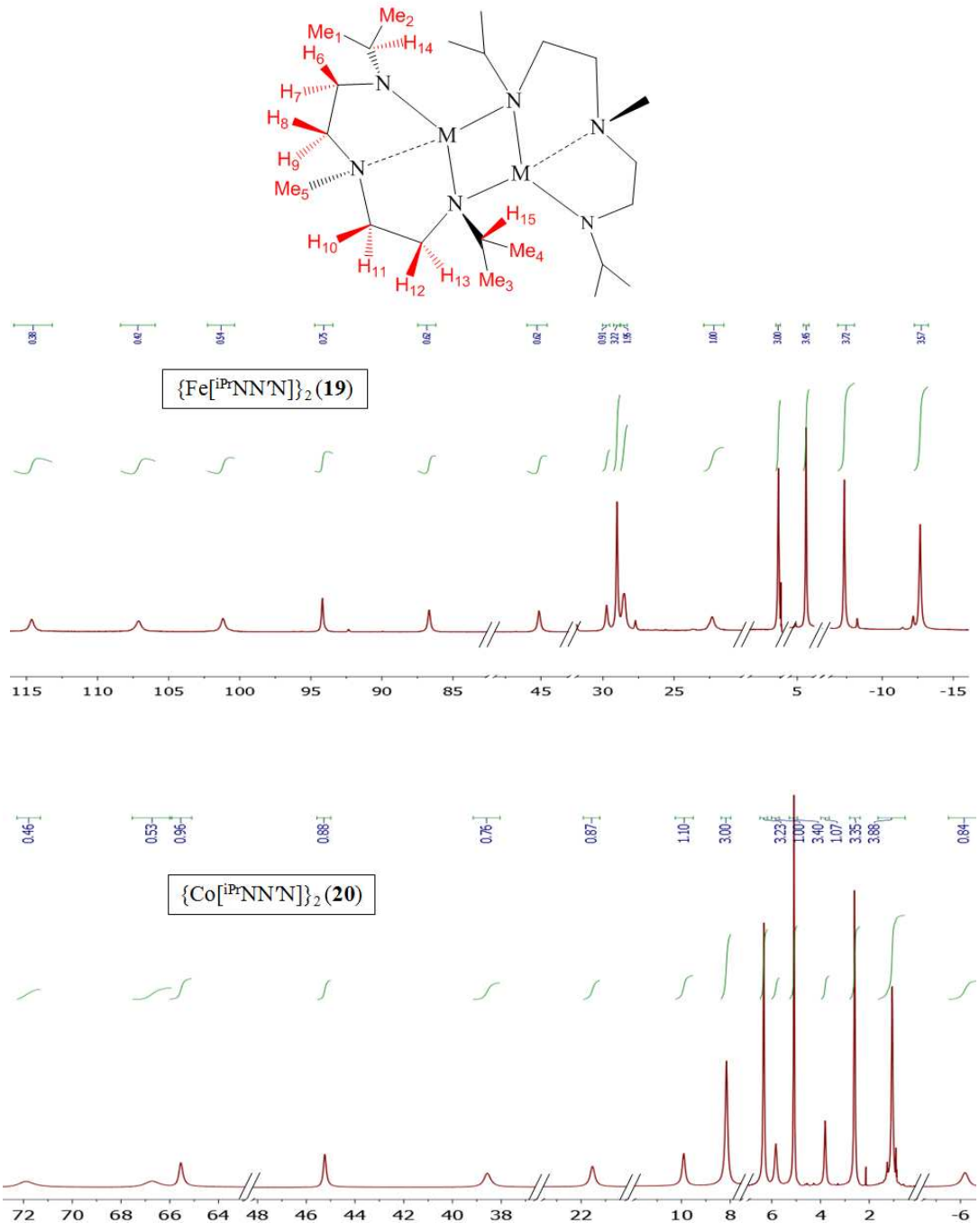

Figure 5.5. ^{1}H NMR spectra of **19** and **20** in benzene-d_6

The ^{1}H NMR spectra of **19** showed paramagnetically shifted peaks in the range of -25 to +115 ppm. Based on the solid state structure of both **19** and **20** (Figure 5.5), if it remains the same in solution, the ^{1}H NMR spectrum should contain five CH_3 protons (one amine-*CH*$_3$, Me_5, and four isopropyl-CH_3, Me_1, Me_2, Me_3, Me_4), eight peaks for the eight protons in the ligand backbone ($H_{6\text{-}13}$; they are all different due to the non-planarity of the amine-*CH*$_3$ group) and two peaks corresponding to the isopropyl-*CH* groups (H_{14} and H_{15}). In total, 14 peaks were observed in ^{1}H NMR spectrum of **19**, and although the integration values are crude (due to the broadness of some of the peaks) five peaks at -12.8, -7.5, +4.2, + 7.4, +28.8 clearly correspond to five methyl groups and nine peaks of similar intensity correspond to the remaining ten H in the ligand backbone plus isopropyl-*CH* protons (the peak at +28.3 ppm, which has approximately integration of 2, may contain two overlapping peaks). The ^{1}H NMR spectrum of **20** also showed a similar pattern: paramagnetically shifted peaks in the range of -7 to +75 ppm; in total 15 peaks were observed, corresponding to the five CH_3 groups, eight peaks for the eight protons in the ligand backbone ($H_{6\text{-}13}$) and two peaks for the isopropyl-*CH* groups (H_{14} and H_{15}).Thus, based on the number of peaks for both **19** and **20** the solid state structure remains intact in solution, similar to what was observed for $\{M[NON]\}_2$ (M= Fe and Co).[140]

5.2.2. Synthesis and characterization of $\{M[^{iPr}NO'N]\}_2$ (M= Fe, Co)

The reaction of one equivalent of MX_2 with one equivalent of $Li_2[^{iPr}NO'N]$ at -70 ^{o}C also generated dinuclear complexes similar to **19** and **20** with the empirical formula $\{M[^{iPr}NON]\}$ (M= Fe, **21**; M= Co, **22**).

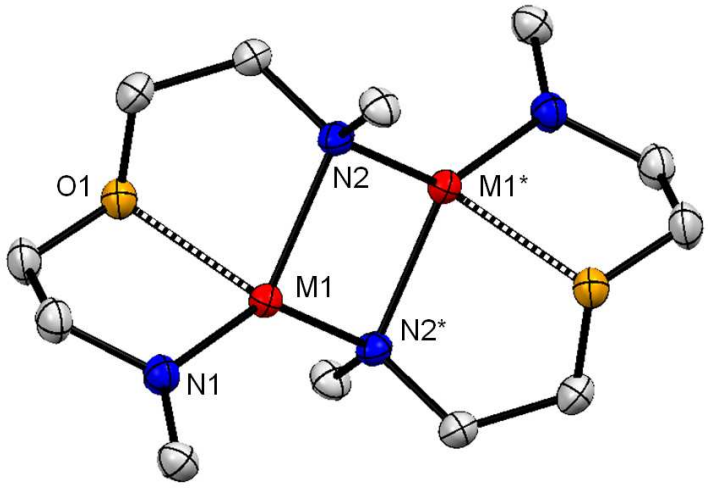

Figure 5.6. Molecular structure of **21** and **22** (iPr group simplified for clarity).

Single crystals suitable for X-ray diffraction were obtained by slow evaporation of a brown hexanes solution of **21** and a dark green hexanes solution of **22**. The X-ray structure is shown in Figure 5.6 with selected interatomic distances and bond angles in Table 5.2.

The structure of **21** and **22** reveals similar dinuclear M(II) diamidoether complexes to **19** and **20** with both bridging and terminal amido groups. The M(II) centres both also have a distorted four-coordinate geometry in which the distance between the Fe atoms is 2.8014(3) and Co atoms is 2.5428(4) Å. Each metal centre could be considered to have a distorted trigonal-monopyramidal geometry (Figure 5.4), with the bonded ether ligand in the apical position (Fe1-O1: 2.1902(8) Å , Co1-O1: 2.180(7) Å). The Co−N and Fe−N distances for the terminal and bridging amido groups are similar to **19** and **20** (Table 5.1 and Table 5.2).

Table 5.2. Selected interatomic distances (Å) and bond angles (°) for {Fe[^{iPr}NO′N]}$_2$ (**21**) and {Co[^{iPr}NO′N]}$_2$ (**22**)

M	**Fe (21)**	**Co (22)**
M1–M1*	2.8014(3)	2.5428(4)
M1–N1	1.9405(10)	1.858(9)
M1–N2	2.1366(10)	1.998(7)
M1–N2*	2.0241(9)	2.019(8)
M1–O1	2.1902(8)	2.180(7)
N1–C1	1.4537(16)	1.450(13)
N1–C4	1.4536(15)	1.487(12)
C4–C5	1.5165(18)	1.465(14)
C6–C7	1.5165(17)	1.585(14)
C2–N2	1.4802(14)	1.483(11)
N2–C7	1.4791(15)	1.529(11)
O1–C5	1.4474(15)	1.477(11)
O1–C6	1.4473(15)	1.456(11)
N2–Co1–N3	95.40(4)	101.2(4)
Co1–N2–Co2	84.60(4)	79.3(3)
N1–Co1–N2	126.69(4)	128.2(3)
N1–Co1–O1	82.13(4)	83.5(3)
O1–Co1–N2	80.80(3)	83.3(3)
O1–Co1–N3	121.87(4)	103.3(3)
C5–O1–C6	82.13(4)	117.9(7)

Symmetry operation *: -x, -y, -z

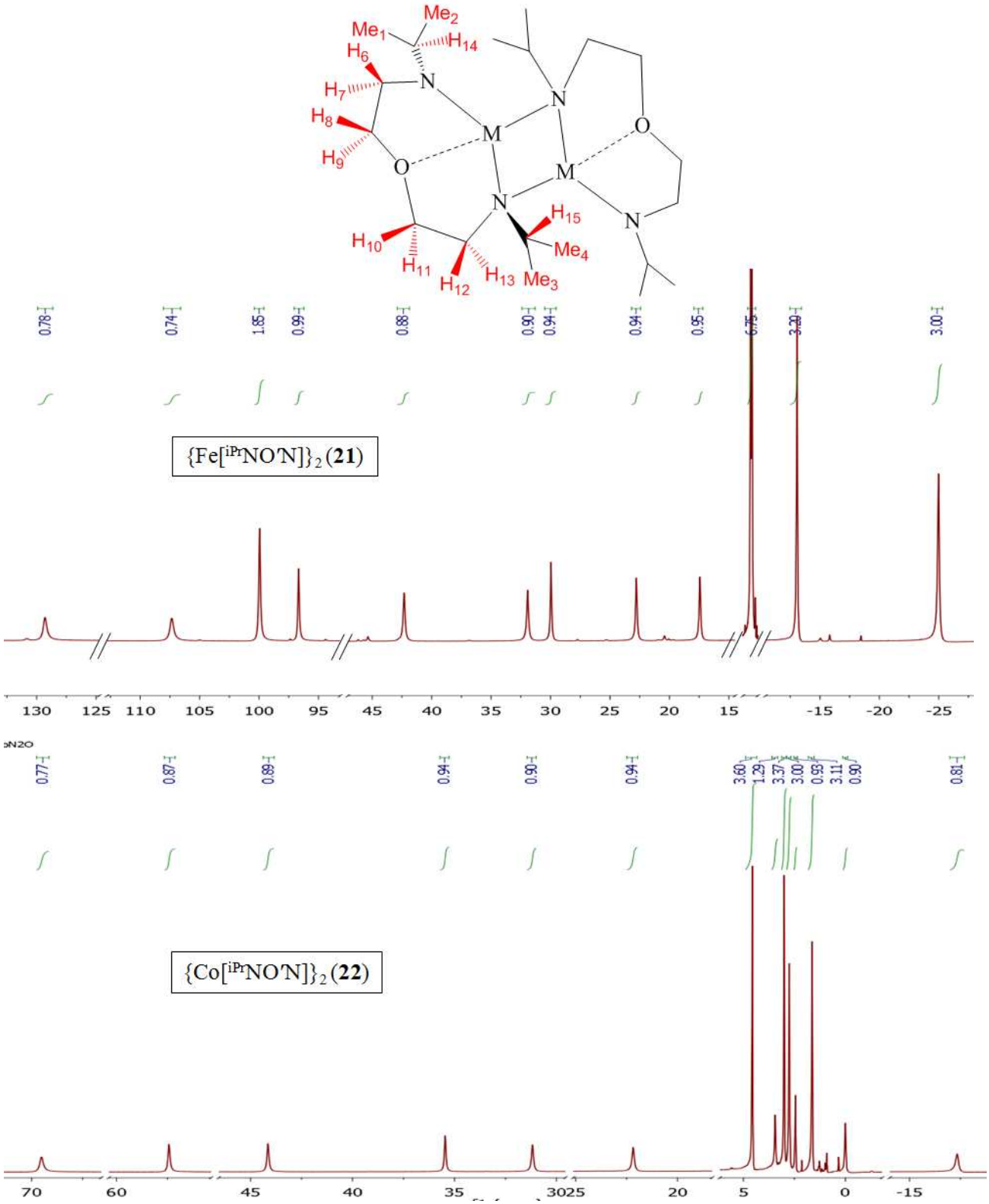

Figure 5.7. ^{1}H NMR spectra of **21** and **22** in benzene-d_6

The ^{1}H NMR spectrum of **21** showed paramagnetically shifted peaks in the range of -30 to +130 ppm, very similar to that of **19**. In total, 13 peaks were observed in the ^{1}H NMR spectrum of **21** (Figure 5.7), consistent with it keeping its solid state structure in solution. Four peaks correspond to four isopropyl methyl groups (the two peaks at 1.5 are two singlets) and eight peaks assignable to ten protons in the ligand backbone and isopropyl-*CH* protons; the backbone peaks are all different due to the non-planar, bridging amido N2 group. The ^{1}H NMR spectrum of **22** is also very similar to that of **20**, showing a similar pattern; (four methyl peaks and ten single proton peaks) consistent with the dinuclear structure being retained in solution for **22** as well.

Comparing ^{1}H NMR spectra of **19**-**22**, it is clear that both Fe(II) **19** and **21** complexes have very similar patterns and peak spreads (-26−130 ppm); This makes it easier to identify the peak at 28.82 ppm in the ^{1}H NMR spectrum of **19** as corresponding to the amine-CH_3, since it is absent in **21**. This confirms that the spin-state and geometries of the metal centres in both **19** and **21** are very similar since similar shifts and broadening are observed. As well, the Co(II) complexes **20** and **22** both have the same pattern and chemical shift range (-20−72 ppm), thereby allowing in this case the assignment of the amine-CH_3 peak at 8.02 ppm in **20** (it is absent in **22**). Comparing Fe(II) **19** and **21** to Co(II) **20** and **22** also indicates that the shifts and peak broadening are more substantial in the case of the Fe(II) complexes.

5.2.3. Solution magnetic properties and metal-metal overlap

The magnetic moments of **19**-**22** were measured in solution by Evans method[162] at room temperature (Table 5.3). Since based on the ^{1}H NMR data the solid state dimer structure remains intact in solution, and the M1-M1* distances are comparable to the Fe (1.43 Å)[309] and Co (1.23 Å) covalent radius,[172] magnetic coupling between the metals, mediated either by direct M-M overlap or the bridging amido groups can be expected.

Table 5.3. M−M and M−O(N) distances and solution magnetic moments of **19**-**22**.

	M1−M1* (Å)	**M1−O1(N3)**	μ_{eff} (μ_B)
(**19**) {Fe[^{iPr}NN′N]}$_2$	2.7428(6)	2.2125(17)	4.2
(**21**) {Fe[^{iPr}NO′N]}$_2$	2.8014(3)	2.1902(8)	4.0
{Fe[^{tBu}NON]}$_2$	2.700(3)	2.408(3)	3.37
(**20**) {Co[^{iPr}NN′N]}$_2$	2.5644(16)	2.196(5)	2.1
(**22**) {Co[^{iPr}NO′N]}$_2$	2.5428(4)	2.180(7)	2.2
{Co[^{tBu}NON]}$_2$	2.5682(13)	2.448(4)	1.84

The μ_{eff} of 4.2 and 4.0 μ_B for {Fe[^{iPr}NN′N]}$_2$ and {Fe[^{iPr}NO′N]}$_2$ are lower than the $\mu_{S.O}$ value of 4.9 μ_B for a d^6 high-spin iron(II) centre, indicating that indeed there is likely some antiferromagnetic coupling between iron centres in the dimer; this can be attributed to the amido bridges or metal-metal orbital overlap or a combination of both. However, the room temperature effective magnetic moments of iron(II)-containing **19** and **21** are higher than the reported μ_{eff} of 3.37 μ_B for the similar {Fe[^{tBu}NON]}$_2$ system; this could be as a result of the slightly longer Fe−Fe distances of 2.7428(6) and 2.8014(3) Å in {Fe[^{iPr}NN′N]}$_2$ and {Fe[^{iPr}NO′N]}$_2$ compared to the 2.700(3) Å in {Fe[^{tBu}NON]}$_2$, which can lead to a weaker iron-iron orbital overlap within the dimer in **19** and **21**. The other possibility that can make the iron-iron interaction weaker could be due to the more efficient binding of the iron to the nitrogen or oxygen donor in the ligand backbone. The neutral donor Fe−N istances of 2.2125(17) Å in **19** and the Fe−O distance of 2.1902(8) Å in **21** are considerably shorter than that of 2.408(3) Å in {Fe[^{tBu}NON]}$_2$, and perhaps this stronger interaction of the metal centre to the neutral atom donor in the ligand backbone can weaken the iron-iron overlap, thereby leading to less coupling. The μ_{eff} of 2.1 and 2.2 μ_B for {Co[^{iPr}NN′N]}$_2$ and {Co[^{iPr}NO′N]}$_2$ are also lower than the 3.87 μ_B expected for a high-spin, spin-only d^7 cobalt(II) centre, which indicates that there is some magnetic coupling within the dimer. These values are also higher than the reported μ_{eff} of 1.84 μ_B for the similar {Co[^{tBu}NON]}$_2$ system. Unlike the iron systems, the Co−Co interaction of 2.5644(16) and 2.5428(4) Å in {Co[^{iPr}NN′N]}$_2$ and {Co[^{iPr}NO′N]}$_2$ are close to that of 2.5682(13) Å in {Co[^{tBu}NON]}$_2$.[136] However, the neutral donor distance of Co−N (2.196(5) Å) in **20** and Co−O (2.180(7) Å) in **22** are considerably

shorter than that of the Co-O distance (2.448(4) Å) in {Co[^{tBu}NON]}$_2$, providing a stronger interaction of the metal centre to the neutral atom donor in the ligand backbone similar to the iron analogues **20** and **22**. The percent of the metal-metal orbital overlap, as mentioned in Chapter 2, can be measured and predicted more accurately based on MO (molecular orbital) diagram calculations, which is beyond the scope of this thesis but could be a worthwhile endeavour to help understand the nature of the system.

5.2.4. Synthesis and characterization of MCl$_2$[H$_2$^{iPr}NN'N] (M= Fe, Co)

The 1:1 reaction of [^{iPr}NN′N]Li$_2$ with FeCl$_3$ in Et$_2$O was targeted in order to synthesize iron(III) complexes analogous to the previously reported {FeCl[^{tBu}NON]}$_2$.[55]

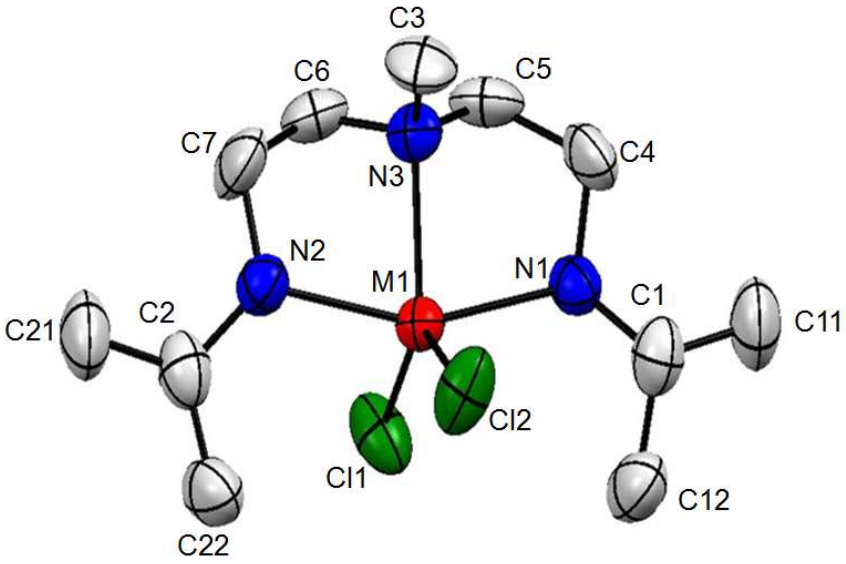

Figure 5.8. Molecular structure of **23** (M= Fe) and **24** (M= Co) (iPr groups simplified for clarity).

Upon addition of Li$_2$[^{iPr}NN′N] to FeCl$_3$ the colour changed from light brown to dark purple, as expected for the iron(III) species, however the colour changed from purple to brown gradually and after about an hour it was totally brown. Yellow crystals of the final product were obtained through slow evaporation of a THF solution and were identified as the iron(II)-containing FeCl$_2$[H$_2$^{iPr}NN′N] (**23**) (Figure 5.8). Hence, the result was unexpected and totally different than the reaction of the ligand with AlCl$_3$ (which gave AlCl[^{iPr}NN′N]).[306]

Attempts to access the iron(III) target indirectly also were tried, by the oxidation of {Fe[^{iPr}NN′N]} (**19**) with XeF_2. The XeF_2 was added to a solution of **19**, (prepared *in situ*, LiCl still is present) in THF. The brown THF solution initially turned to purple however it changed back to brown soon after, resulting in the same iron(II) product **23**, identified by X-ray crystallography. The X-ray structure of **23** showed a mononuclear iron centre with a five coordinate, trigonal-bipyramidal geometry (Figure 5.9).

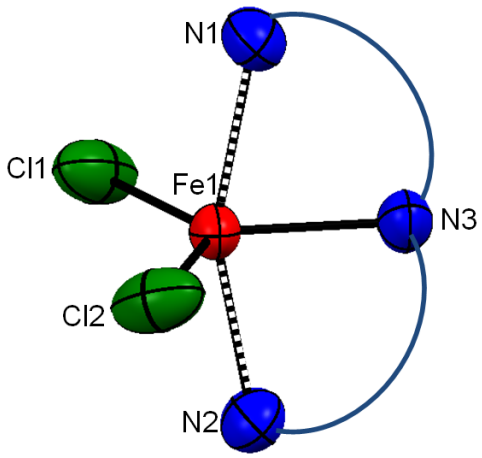

Figure 5.9. Trigonal-bipyramidal geometry around the iron centre in **23**

The iron centre is bonded to the amine nitrogens (see next section) in [H_2^{iPr}NN′N], which is chelated to $FeCl_2$, with Fe−N_{amine}= 2.285(3) Å and the amine in the ligand backbone as (Me)N−Fe: 2.139(5) Å, and is also to two terminal chlorides. The Fe1−N1 distance of 2.285(3) Å is much longer compared to the terminal Fe−N distances of 1.9284(17) Å in diamido iron(II) {Fe[^{iPr}NN′N]}$_2$ (**19**) and indeed are much longer than in any other Fe(II) amido complexes in this thesis. [140, 192] Thus, assuming that the diamido ligand was protonated to a neutral diamine, the iron centres oxidation state would be appear to be iron(II) and not iron(III). If the ligand were still assumed to be a diamide (despite the extremely long Fe-N distance), then the iron in $FeCl_2$[^{iPr}NN′N] would have to be a high-valent, reactive Fe(IV) species, which is known to polymerize THF.[37] Since **23** is stable in THF with no polymerization activity, this is also evidence to suggest that the ligand is a diamine rather than a diamide. The reaction of XeF_2 with *in situ* generated

{Co[^{iPr}NN′N]}$_2$ (**20**) in THF also resulted in the formation of $CoCl_2$[H_2^{iPr}NN′N] (**24**). Crystals of **24** were also obtained by the slow evaporation of the THF solution.

Table 5.4. Selected interatomic distances (Å) and bond angles (°) for $FeCl_2$[H_2^{iPr}NN′N] (**23**) and $CoCl_2$[H_2^{iPr}NN′N] (**24**)

M	**Fe (23)**	**Co (24)**
M1–Cl1	2.3157(2)	2.2940(13)
Fe1–N1	2.285(3)	2.249(4)
Fe1–N3	2.139(5)	2.090(6)
N1–C1	1.476(7)	1.473(7)
N1–C4	1.475(4)	1.485(7)
C4–C5	1.561(1)	1.561(13)
C1–C11	1.521(7)	1.539(9)
C1–C12	1.521(9)	1.545(7)
Cl1–M1–Cl1*	128.80(7)	126.67(9)
N1–M1–Cl1	93.0(1)	92.13(11)
N1–Co1–Cl1*	96.1(1)	96.28(12)
N1*–M1–N3	79.4(2)	80.60(11)
N3–M1–Cl1	115.6(2	116.66(5)
C4–N1–C1	113.2(5)	112.4(5)
C4–N1–Co1	107.2(5)	107.3(5)
M1–N1–C1	121.5(3)	120.5(3)

Symmetry operation *: -x, y, -z+1/2

The X-ray structure showed it to be isostructural with the iron analogue **23**, namely a five coordinate cobalt(II) centre with a similar trigonal-bipyramidal geometry. A similar Co(II) complex, $CoCl_2$[H_2^{Ar}NN′N] (Ar= 2,6-Me_2Ph)[310] has been reported, prepared by the direct reaction of [H_2^{Ar}NN′N] with high-spin $CoCl_2$ in n-butanol at 90 ^oC in

high yield, however they reported that the same reaction with $FeCl_2$ did not work. The Co−Cl bond distance of 2.2940(13) Å in **24** (Table 5.4) is in between those of 2.2472(16) and 2.3136(15) in $CoCl_2[H_2^{Ar}NN'N]$, and the terminal Co−N1 bond distance of 2.249(4) Å in **24** is slightly shorter than the 2.274(4) and 2.289(4) Å in $CoCl_2[H_2^{Ar}NN'N]$. The central amine Co−N3 bond distance of 2.090(6) Å in **24** is very close to the 2.088(3) Å in $CoCl_2[H_2^{Ar}NN'N]$.[310]

5.2.5. Synthesis and characterization of {$FeCl_2[H_2^{iPr}NO'N]$}

An attempt to make an iron(III) complex via the reaction of $Li_2[^{iPr}NO'N]$ with $FeCl_3$ in Et_2O solution also led to the formation of a similar mononuclear five-coordinate iron(II)/diamine species $FeCl_2[H_2^{iPr}NO'N]$ (**25**) (Figure 5.10).

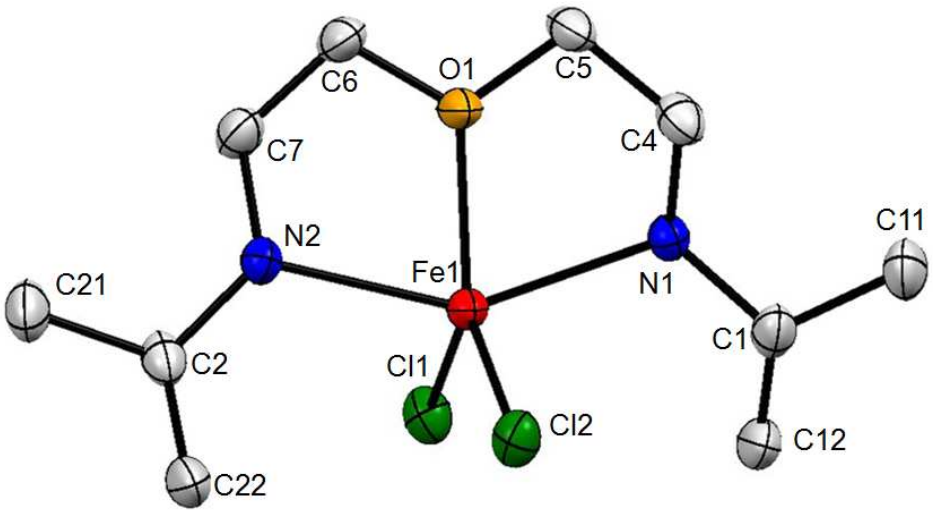

Figure 5.10. Molecular structure of **25** (iPr group simplified for clarity).

Light brown single crystals were obtained by slow evaporation of a THF solution. The diamine is chelated to the $FeCl_2$ moiety and the iron centre also is bonded to the ether in the ligand backbone with a Fe−O distance of 2.07614(17) Å (Table 5.5).

Table 5.5. Selected interatomic distances (Å) and bond angles (°) for $FeCl_2[H_2{}^{iPr}NON]$ (**25**).

Fe1–Cl1	2.31340(12)	N1*–Fe1–N1	148.752(3)
Fe1–N1	2.29266(12)	Cl1–Fe1–Cl1*	116.199(5)
Fe1–O1	2.07614(17)	N1–Fe1–Cl1	95.950(5)
N1–C1	1.49777(8)	N1–Fe1–Cl1*	100.427(5)
N1–C4	1.48737(9)	N1–Fe1–O1	74.376(6)
C4–C5	1.51547(8)	O1–Fe1–Cl1	121.900(5)
C1–C11	1.54319(9)	O1–Fe1–Cl1*	121.900(5)
C1–C12	1.52633(9)	C4–N1–C1	112.299(7)
		C4–N1–Fe1	104.419(7)
		Fe1–N1–C1	117.680(4)

Symmetry operation *: -x, y, -z+1/2

5.2.6. Amine vs. amido or imine.

As shown in Table 5.6 the M-amide bond in iron(II) **19** and **21** are slightly longer than the corresponding cobalt analogues **20** and **22**, as expected due to the smaller size of cobalt *vs* iron. The M-amide bond in iron(II) (**19** and **21**) and cobalt(II) (**20** and **22**) are very similar to those of known $\{M[^{tBu}NON\}_2$ (M= Fe, Co). However the central donor (ether) amine-metal bonds are considerably shorter in **19**-**22** compared to $\{M[^{tBu}NON\}_2$ systems. One explanation for this big difference might come from this fact that the diamido carbon-backbone ligands with 5 atoms in their backbone are more flexible compared to the diamido-siloxyl ether (NON) ligand with 3 atoms in the ligand backbone, hence allowing a closer interaction of the central donor atoms to the metal centre.

Table 5.6. Comparison of the M−N bond distances in **19**-**25** and {M[^{tBu}NON]$_2$ (M=Fe, Co)

	M1−N1	**M1−N2**	**M1−N2***	**M-N3(O1)**
{Fe[^{tBu}NON]}$_2$	1.934(3)	2.157(3)	2.058(3)	2.512(2)
{Fe[^{iPr}NN′N]}$_2$ (**19**)	1.9284(17)	2.1014(16)	2.0485(16)	2.2125(17)
{Fe[^{iPr}NO′N]}$_2$ (**21**)	1.9405(10)	2.1366(10)	2.0241(9)	2.1902(8)
{Co[^{tBu}NON]}$_2$	1.906(3)	2.0514(4)	2.029(3)	2.448(4)
{Co[^{iPr}NN′N]}$_2$ (**20**)	1.883(5)	2.015(4)	1.999(4)	2.196(5)
{Co[^{iPr}NO′N]}$_2$ (**22**)	1.858(9)	1.998(7)	2.019(8)	2.180(7)
FeCl$_2$[H$_2$^{iPr}NN′N] (**23**)	2.285(3)	2.285(3)	_	2.139(5)
CoCl$_2$[H$_2$^{iPr}NN′N] (**24**)	2.249(4)	2.249(4)	_	2.090(6)
FeCl$_2$[H$_2$^{iPr}NO′N] (**25**)	2.29266(12)	2.29266(12)	_	2.07614(17)

On the other hand the terminal M−N (M= Fe, Co) present in **23**-**25** are considerably longer than known high-spin M-amide bonds[135-136, 140, 192] and much longer than the corresponding diamido-cobalt(II) and iron(II) bonds in **19**-**22**; they are even considerably longer than the M-N3(amine) bond in their ligand backbone (**23** and **24**) as well, as shown in Table 5.6. As mentioned above, if the ligand present in complexes **23**-**25** is considered to be a diamide then the metal would be a high-valent Fe(IV) and Co(IV); this is not compatible with their stability in THF solution. The colour change from brown to deep purple upon formation of iron complexes **23** and **25** is indicative of the formation of an iron(III) species (this is the colour of {FeCl[NON]}$_2$),[37, 55, 137] but further intra-molecular redox chemistry can lead to the reduction of iron(III) to iron(II), although the nature of this reactivity remains unclear. Furthermore, comparing all of the bond lengths in the ligand backbone and the isopropyl substituent group on the nitrogen in **23**-**25** to the corresponding metal(II) dimers **19-22** show they are very similar; hence the ligand has not been otherwise oxidized (e.g. to imines). The source of the amine hydrogen in **23**-**25** is unknown. In theory, it could come from a solvent C−H activation or the reduction of half of the ligands to diimines, but further research is needed to examine this question.

There is more evidence to support the assignment that both [^{iPr}NN′N] and [^{iPr}NO′N] chelates in **23**-**25** are protonated ligands. In the X-ray structures of **23**-**25**, electron density around the terminal nitrogen atoms that correspond to the amine hydrogens could be located and identified, especially in the case of $FeCl_2[H_2{}^{iPr}NO'N]$ (**25**), for which its crystal data was collected at low temperature (-150 ℃), resulting in a very accurate structure (R=0.025), with small thermal ellipsoids. On its own, it is recognized that using X-ray crystallography, it is hard to clearly locate hydrogen atoms, (due to its low electron density) especially for those hydrogens around or close to heavy elements and thus although nitrogen is not considered to be heavy, due to its proximity to the iron centre, the presence and location of the amine-hydrogen atoms is not by itself definitive, however FT-IR measurement would be more accurate to distinguish between N-H and N=H which due to some difficulty I could not do this experiment.

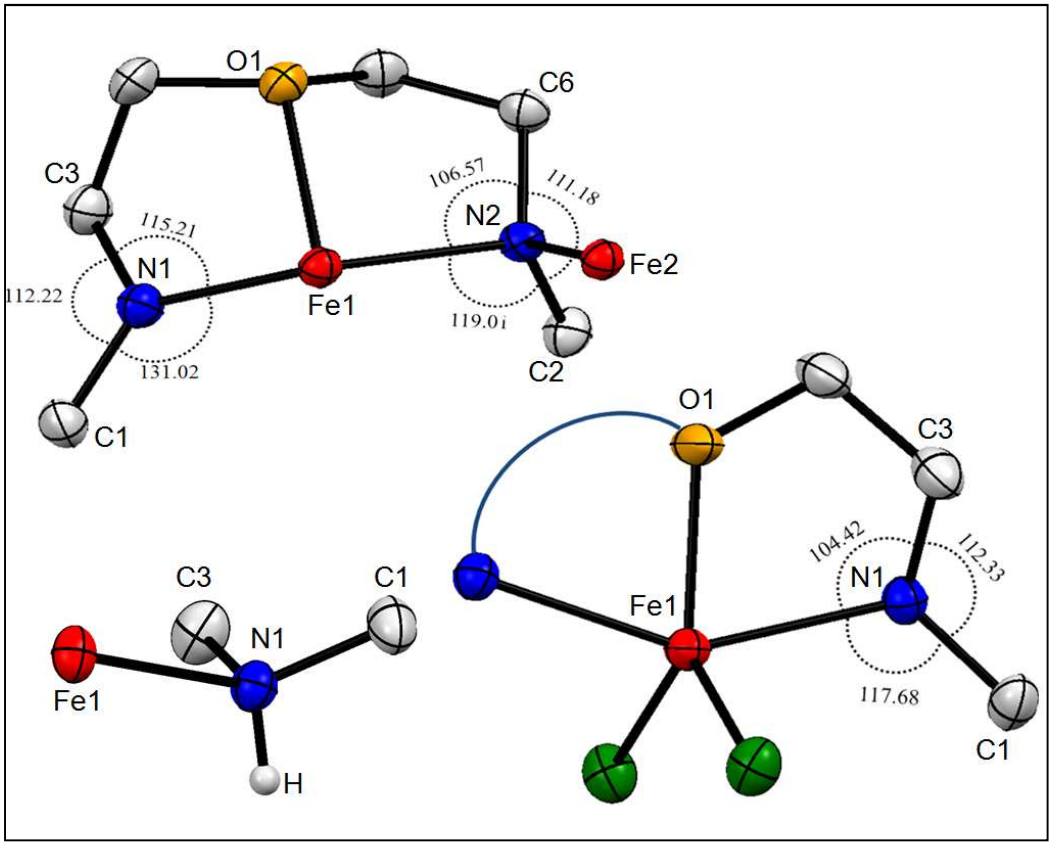

Figure 5.11. Bond angles around the amides in $\{Fe[^{iPr}NON]\}_2$ (**21**, top) and the amine in $FeCl_2[^{iPr}NO'N]$ (**25**, bottom)

More general support for the assignment of amines *vs* amide is the coordination geometry around the terminal nitrogens in **23**-**25** compared to those in **19**-**22**. There are two different geometries around amido nitrogens in $\{M[^{iPr}NN'N]\}_2$ and $\{M[^{iPr}NO'N]\}_2$ (**19**-**22**). For example the angles around nitrogen (N1) in the X-ray structure of $FeCl_2[^{iPr}NO'N]$ (**25**) compared to both geometries around amide (N1 and N2) in $\{Fe[^{iPr}NO'N]\}_2$ (**21**) are shown in Figure 5.11. The N1 atom in **21** is three-coordinate with a trigonal geometry while N2 has a four-coordinate, tetrahedral geometry (Figure 5.11). Looking into the angles around N showed the similarity of the N coordination in $\{FeCl_2[^{iPr}NN'N]\}$ and $\{FeCl_2[^{iPr}NO'N]\}$ systems to be very similar to the tetrahedral geometry around N2 of dinuclear analogous systems (N2 in **19**-**22**), not the trigonal amide (N1). (e.g., see Figure 5.11).

The structures of these diamine iron dichloride systems suggested the possibility of making them by a 1:1 addition of the diamine to $FeCl_2$. Hence, this direct synthetic route toward $FeCl_2[H_2{}^{iPr}NN'N]$ (**23**) was attempted by adding one equivalent of $[^{iPr}NN'N]H_2$ to a THF solution of $FeCl_2$ at room temperature. This was stirred for 2 days but there was no reaction (however it was reported that using $FeCl_2(THF)_{1.5}$ precursor let to the formation of **5**). The reaction was then heated up to 70 ℃ for 8 hours and still there was no reaction based on a ^1H NMR spectrum of the reaction mixture.

Based on these results it is obvious that even though the new carbon-backbone ligands were designed to stabilize high oxidation state metal centres, it appears that they were not suitable candidates since they could not even stabilize Fe(III) centres. However, the new synthesized $MCl_2[H_2{}^{iPr}NN'N]$ and $MCl_2[H_2{}^{iPr}NO'N]$ complexes **23**-**25** are potential platforms for further reactivity e.g. halide substitution.

5.3. Conclusion

The synthesis and characterization of a series of dimeric iron(II) and cobalt(II) complexes **19**-**22** of general formula $\{M[^{iPr}NN'N]\}_2$ and $\{M[^{iPr}NO'N]\}_2$ was achieved, and compared with previous similar $\{M[^{tBu}NON]\}_2$ complexes.

Unlike the formation of iron(III)-diamidoether complexes with $[^{tBu}NON]^{2-}$, attempts to prepare iron(III) and cobalt(III) compounds were not successful with the new

carbon-backbone ligands, indicating that the new ligands are not good candidates for stabilizing high-valent metal centres. However, new monomeric diamine iron(II) and cobalt(II) dichloride complexes **23**-**25** of the general formula {$MCl_2[H_2^{iPr}NN'N]$} and {$FeCl_2[H_2^{iPr}NO'N]$} were synthesized.

5.4. Future work

The dinuclear iron(II) and cobalt(II) complexes **19**-**22** have close metal-metal distances. The partial antiferromagnetic interaction observed is based on solution magnetic measurements, but in order to probe the extent of the metal-metal interaction vs. amido superexchange, the MO diagram of these systems should be calculated to obtain an accurate metal-metal orbital overlap percentage in these molecules. This will help to gain a better understanding of any metal-metal interaction and its relationship to the bond distance, geometry and also the impact of the metal-metal interaction strength to the amine or ether-binding from the ligand backbone.

The series of mononuclear $MCl_2[^{iPr}NN'N]$ and $MCl_2[^{iPr}NO'N]$ (M= Fe, Co) complexes were synthesized, however they were not fully characterized; especially their magnetic properties should be investigated. Also, these systems were synthesized both by starting with $FeCl_3$ or by oxidation of the corresponding $\{M[^{iPr}NN'N\}_2$ or $\{M[^{iPr}NO'N\}_2$. Attempts to prepare $FeCl_2[H_2^{iPr}NN'N]$ directly through $FeCl_2$ and free ligand were unsuccessful, however a higher reaction temperature or longer reflux time would be worth investigating. The $CoCl_2$ analogues should also be targeted in this fashion.

On the mechanistic side, further investigation is needed to find the source of the protons in the protonated ligands in **23**-**25**.

Due to the presence of the M-halide unit in **23**-**25**, there is an opportunity for further reactivity such as halide for alkyl substitution or dinitrogen activation in **23**-**25**. Althogh diamine metal halides are common in the literature, their water-free, organometallic and reduction chemistry is underdeveloped compared to diamido or diimine compounds and is worth pursuing.

5.5. Experimental section

General procedures and materials are as described in Chapter 2. The ligand $H_2[^{iPr}NN'N]$ and $H_2[^{iPr}NO'N]$ were prepared as reported in the literature.[306]

5.5.1. General Procedures and Materials

Synthesis of $Li_2[^{iPr}NN'N]$

To a THF solution (50 mL) of N-methyl-N,N-bis(diisopropyl)diethylenetriamine ($H_2[^{iPr}NN'N]$) (463 mg, 2.26 mmol), at -70 ℃, was added dropwise 2 equivalents (4.46 mmol) of ^{n}BuLi in hexanes (1.6 M). The solution was allowed to warm to room temperature and was stirred for 4 hours. The solution then was removed *in vacuo*, and washed with hexanes. The white precipitate of $Li_2[^{iPr}NN'N]$ was collected. Yield: 390 mg (83%).

Synthesis of $Li_2[^{iPr}NO'N]$

To a THF solution (50 mL) of $H_2[^{iPr}NO'N]$ (573 mg, 3.00 mmol), at -70 ℃, was added dropwise 2 equivalents (6.00 mmol) of ^{n}BuLi in hexanes (1.6 M). The solution was allowed to warm to room temperature and was stirred for 4 hours. The solution then was removed *in vacuo*, and washed with hexanes the white precipitate of $Li_2[^{iPr}NO'N]$ was collected. Yield: 485 mg (81%).

Synthesis of $\{Fe[^{iPr}NN'N]\}_2$ (19)

$Li_2[^{iPr}NN'N]$ (260 mg, 1.35 mmol) in 30 mL THF was added dropwise at -70 ^{o}C slowly to a solution of anhydrous $FeCl_2$ (172 mg, 1.35 mmol) in 50 mL THF while stirring. The resulting light brown mixture was stirred overnight, and then the THF was removed *in vacuo*. The product was extracted with hexanes and the resulting solution was filtered through Celite. Removal of the hexanes *in vacuo* resulted in a light brown product of $\{Fe[^{iPr}NN'N]\}_2$ (**19**). Crystals of **19** were obtained by slow evaporation of a hexanes solution. Yield: 220 mg (68%). Anal. Calcd. for $C_{11}H_{25}N_3Fe$: C: 51.77%; H: 9.87%; N: 16.46%. Found: C: 51.62%; H: 10.15%; N: 16.18%. ^{1}H NMR (Benzene-d_6): -12.8, -7.5, 4.2, 7.4 (each is a singlet, 3H, CH$(CH_3)_2$), 28.8 (s, 3H, amine-CH_3), 22.1, 28.3, 29.5,

45.2, 86.5, 94.0, 101.0, 106.9, 114.4 (each is a singlet, 1H). Evans method μ_{eff}: 4.2 μ_B at 300 K.

Synthesis of {Co[^{iPr}NN′N]}$_2$ (20)

Li_2[^{iPr}NN′N] (210 mg, 1.15 mmol) in 30 mL THF was added dropwise at -70 ^{o}C slowly to a solution of anhydrous $CoCl_2$ (150 mg, 1.15 mmol) in 50 mL THF while stirring. The resulting dark green mixture was stirred overnight, and then the THF was removed *in vacuo*. The product was extracted with hexanes and the resulting solution was filtered through Celite. Removal of the hexanes *in vacuo* resulted in green {Co[^{iPr}NN′N]}$_2$ (**20**). Crystals of **20** were obtained by slow evaporation of a hexanes solution. Yield: 170 mg (59%). Anal. Calcd. for $C_{11}H_{25}N_3Co$: C: 51.15%; H: 9.75%; N: 16.26%. Found: C: 50.97%; H: 9.82%; N: 16.66%. ^{1}H NMR (Benzene-d_6): 0.9, 2.5, 4.9, 6.2 (each is a singlet, 3H, CH*(CH$_3$)$_2$*), 8.0 (s, 3H, amine-*CH$_3$*), 3.7, 5.7, 9.8, 21.4, 38.5, 45.2, 65.4, 66.7,71.8 (each is a singlet, 1H). Evans method μ_{eff}: 2.1 μ_B at 300 K.

Synthesis of {Fe[^{iPr}NO′N]}$_2$ (21)

Li_2[^{iPr}NO′N] (190 mg, 0.97 mmol) in 30 mL THF was added dropwise at -70 ^{o}C slowly to a solution of anhydrous $FeCl_2$ (123 mg, 0.97 mmol) in 50 mL THF while stirring. The resulting light brown mixture was stirred overnight, and then the THF was removed *in vacuo*. The product was extracted with hexanes and the resulting solution was filtered through Celite. Removal of the hexanes *in vacuo* resulted in light brown {Fe[^{iPr}NON]}$_2$ (**21**). Crystals of **21** were obtained by slow evaporation of a hexanes solution. Yield: 150 mg (64%). Anal. Calcd. for $C_{10}H_{22}N_2FeO$: C: 49.60%; H: 9.15%; N: 11.56%. Found: C: 49.32%; H: 9.9%; N: 11.50%. ^{1}H NMR (Benzene-d_6): -25.1, -13.2 (each is a single, 3H, CH*(CH$_3$)$_2$*), 1.5 (two close singlets, 6H, CH*(CH$_3$)$_2$*), 17.3, 22.7, 29.9, 31.8, 42.2, 96.6, 99.9, 107.3, 129.2 (each is a singlet, 1H). Evans method μ_{eff}: 4.2 μ_B at 300 K.

Synthesis of {Co[^{iPr}NO′N]}$_2$ (22)

Li_2[^{iPr}NON] (215 mg, 1.15 mmol) in 30 mL THF was added dropwise at -70 ^{o}C slowly to a solution of anhydrous $CoCl_2$ (150 mg, 1.15 mmol) in 50 mL THF while stirring. The resulting dark green mixture was stirred overnight, and then the THF was removed *in vacuo*. The product was extracted with hexanes and the resulting solution was filtered

through Celite. Removal of the hexanes *in vacuo* resulted in dark green {Co[^{iPr}NO′N] }$_2$ (**22**). Crystals of **22** were obtained by slow evaporation of hexanes solution. Yield: 170 mg (61%). Anal. Calcd. for $C_{10}H_{22}N_2CoO$: C: 48.97%; H: 9.04%; N: 11.42%. Found: C: 48.98%; H: 8.98%; N: 11.50%. ^{1}H NMR (Benzene-d_6): 1.7, 2.8, 3.0, 4.6 (each is singlet, 3H, CH$(CH_3)_2$), -17.3, 0.0, 2.5, 3.5, 22.2, 31.2, 35.5, 44.2, 57.5, 69.6 (each is a singlet, 1H). Evans method μ_{eff}: 2.1 μ_B at 300 K.

Synthesis of $FeCl_2$[H_2^{iPr}NN′N] (23)

Li_2[^{iPr}NN′N] (235 mg, 1.23 mmol) in 20 mL THF was added dropwise at -70 ^{o}C slowly to a solution of anhydrous $FeCl_3$ (200 mg, 1.23 mmol) in 50 mL Et_2O while stirring. The colour changed to purple immediately but then started to change to brown after approximately 30 minutes at -70 ^{o}C. The resulting light brown mixture was stirred overnight, and then the THF/Et_2O was removed *in vacuo*. The product was extracted with THF and the resulting solution was filtered through Celite. Removal of the THF *in vacuo* resulted in dark yellow $FeCl_2$[H_2^{iPr}NN′N] (**23**). Crystals of **23** were obtained by slow evaporation of a THF solution. Attempts to obtain a pure product salt-free were not successful due to the insolubility of **23** in any solvent other than THF. Yield: 150 mg (43%). Anal. Calcd. for $C_{11}H_{27}N_3Cl_2Fe$: C: 40.26%; H: 8.29%; N: 12.80%. Found: C: 39.00%; H: 8.04%; N: 12.41%, (LiCl: 20%).

Reaction of {Fe[^{iPr}NN′N]}$_2$ (19) and XeF_2

In the first step, {Fe[^{iPr}NN′N]}$_2$ was prepared by the addition of Li_2[^{iPr}NN′N] (260 mg, 1.35 mmol) in 20 mL THF dropwise at -70 ^{o}C slowly to a solution of anhydrous $FeCl_2$ (172 mg, 1.35 mmol) in 40 mL THF while stirring. The resulting light brown mixture was stirred overnight. After 24 hours, XeF_2 (228 mg, 1.35 mmol) in 20 mL THF was added slowly at room temperature to the {Fe[^{iPr}NN′N]}$_2$ solution, after which the colour changed from brown to purple and soon back to brown. The resulting brown solution was stirred overnight, and then the THF was removed *in vacuo*. The product was extracted with THF and the resulting solution was filtered through Celite. Removal of the solvent *in vacuo* resulted in brown **23**, identified by X-ray crystallography.

Reaction of [^{iPr}NN′N]H_2 and $FeCl_2$

H_2[^{iPr}NN′N] (390 mg, 2.13 mmol) in 20 mL THF was added dropwise at room temperature slowly to a 50 mL THF solution of anhydrous $FeCl_2$ (270 mg, 2.13 mmol) while stirring. No colour change was observed upon or after addition of the diamine ligand. The solution was stirred for 4 hours, and then was heated up to 60 ℃ for 8 hours. The ^{1}H NMR spectrum only showed free ligand.

Synthesis of {$CoCl_2$[^{iPr}NN′N]} (24)

In the first step, {Co[^{iPr}NN′N]}$_2$ was prepared by addition of Li_2[^{iPr}NN′N] (237 mg, 1.24 mmol) in 15 mL THF dropwise at -70 ^{o}C slowly to a solution of anhydrous $CoCl_2$ (162 mg, 1.24 mmol) in 35 mL THF while stirring. The resulting green mixture was stirred overnight. After 24 hours, XeF_2 (209 mg, 1.24 mmol) in 20 mL THF was added slowly at room temperature to the {Co[^{iPr}NN′N]}$_2$ solution. The colour did not change considerably upon XeF_2 addition. The resulting green solution was stirred overnight, and then the THF was removed *in vacuo*. The product was extracted with THF and the resulting solution was filtered through Celite. Removal of the solvent *in vacuo*, resulted in green $CoCl_2$[H_2^{iPr}NN′N] (**24**). Crystals of **24** were obtained by slow evaporation of a THF solution. The attempt to get pure product salt free was not successful due to the insolubility of **24** in any solvent other than THF. Anal. Calcd. for $C_{11}H_{27}N_3Cl_2Co$: C: 38.89%; H: 8.22%; N: 12.69%, Found: C: 39.01%; H: 8.03%; N: 12.40%, (LiCl: 15%). ^{1}H NMR (THF-d_8):

Synthesis of $FeCl_2$[H_2^{iPr}NO′N] (25)

Li_2[^{iPr}NO′N] (231 mg, 1.23 mmol) in 20 mL THF was added dropwise at -70 ^{o}C slowly to a 50 mL Et_2O solution of anhydrous $FeCl_3$ (200 mg, 1.23 mmol) while stirring. The colour changed to purple immediately but then started to change to orange-brown after approximately 30 minutes at -70 ^{o}C. The resulting light brown mixture was stirred overnight, and then the solvent was removed *in vacuo*. The product was extracted in THF and the resulting solution was filtered through Celite. Removal of the THF *in vacuo* resulted in brown $FeCl_2$[H_2^{iPr}NO′N] (**25**). Crystals of **25** were obtained by slow evaporation of a THF solution. Attempts to obtain a pure salt-free product were not successful due to the insolubility of **25** in any solvent other than THF. Anal. Calcd. for

$C_{10}H_{24}N_2OCl_2Fe$: C: 37.51%; 7.60H: %; N: 8.81%. Found: C: 36.68%; H: 7.39%; N: 8.55%, (LiCl 18%).

5.5.2. X-ray Crystallography

Crystals of **19, 20** and **23** were sealed in glass capillaries at room temperature while crystals of **21**, **22, 24** and **25** were coated in Paratone-oil and mounted onto a MiTeGen Micro Mount at -150 ^{o}C. Crystal descriptions for each compound are as follows: **19** is a brown block having dimensions 0.30 × 0.25 × 0.40 mm^3; **20** is a green block having dimensions 0.40 × 0.35 × 0.25 mm^3; **21** is a brown cube having dimensions 0.40 × 0.35 × 0.45 mm^3; **22** is a green block having dimensions 0.42 × 0.37 × 0.25 mm^3, **23** is a yellow block having dimensions 0.35 × 0.25 × 0.25 mm^3; **24** is a brown cube having dimensions 0.30 × 0.30 × 0.40 mm^3 and **25** is dark yellow having dimensions 0.15 × 0.15 × 0.45 mm^3. The rest of the procedure is the same as was described in Chapter 2.

6. Conclusion

The main goal of this thesis was to investigate the coordination and organometallic chemistry of diamido-donor iron and cobalt complexes. As mentioned before, diamido-donor ligands have been synthesized, modified and investigated a lot with diamagnetic transition metals, and it is surprising to see how much less work has been done with paramagnetic transition metals such as iron and cobalt.

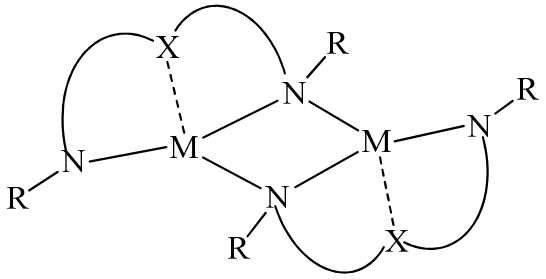

Figure 6.1. Diamido-donor M(II) dimer (X: O, NR', S; R= alkyl, aryl).

Most of the diamido donor complexes of iron(II) and cobalt(II) tend to dimerize[140] as shown in Figure 6.1; the dimer is usually stable in solution and as a result in most cases they do not show reactivity towards further substitution. For iron(II), they are easily oxidized to iron(III)[37, 40, 55, 137] complex which have limited useful reactivity; for example, in the case of alkylation attempts, reduction to iron(II) was observed.

One important goal that was achieved in this thesis was synthesizing new diamido donor iron(II) and cobalt(II) complexes by changing the stoichiometric addition of the ligand to the metal and formation of the new multinuclear diamido-ether/halide iron(II) (**1**, **3**) and cobalt(II) (**2**, **4**) complexes, as discussed in Chapter 2. Using a large metal : ligand ratio (i.e. not the usual 1 : 1) is an under-utilized technique which this

thesis shows can be used to access unusual clusters. The formation of these new complexes showed that it is possible to obtain amido/halide bridged complexes of transition metals with diamido-donor ligands, which opens the door to new reactivity studies. Complexes **1**-**4** have both amido and halide bridges; the halide bridge breaks up in solution. In addition, the metal centres in **1**-**4** showed low-coordinate metal centres (three-coordinate) that are much more uncommon and tend to be more reactive due to the metal centre unsaturation. Some preliminary reactivity studies of **1**-**4** were attempted, including examining redox reactivity of the metal centres. Reduction resulted in the formation of the known diamido dimer $\{M[^{tBu}NON]\}_2$ (and likely metal powder) and oxidation in the case of iron led to the formation of known Fe(III) complexes. Attempts to add extra neutral donors to the coordination sphere of the unsaturated metal centre also resulted in the formation of $\{M[^{tBu}NON]\}_2$ as well as the new carbene complex, $\{(NHC)FeCl_2\}_2$ (**5**) in the case of adding NHC. This illustrated a very unusual way to synthesize new carbenes that could not be obtained by more standard procedures. Even though some limited reactivity of these new systems has been explored, there is still much more to be investigated for these complexes.

The second achievement in this thesis was obtaining the new diamido ether organometallic iron(II) and cobalt(II) complexes by successful alkyl for halide substitution as shown in Chapter 3. The reactivity of amido iron(II) and cobalt(II) alkyl complexes are not well-known due to the limited number of these systems. Since the dinuclear cores of **1**-**4** contain two M-halide bonds, depending on the stoichiometry, full dialkylation to yield the dialkyl dinuclear iron(II) (**6**) and cobalt(II) (**7**) complexes, and mono-alkylation to form the monoalkyl/halide dinuclear iron(II) and cobalt(II) complexes **8**-**13**, with both Me- and Me_3SiCH_2- groups, was achieved. Magnetic measurements on the new systems showed them all to be high-spin, and since most of the known organometallic complexes of iron and cobalt are known to be low-spin, hence the chemistry and reactivity of the high-spin iron- and cobalt-carbon bond is mostly unknown and has to be investigated. A preliminary reactivity study of the metal centre in the dialkyl iron(II) and cobalt(II) complexes was conducted. Addition of ethylene to dialkyl **6** and **7** did not show the formation of any polymer and attempts to use $B(C_6F_5)_3$ as an activator did not help the activity but actually reacted with the metal centre and led to the formation of the aryl cobalt(II) (**14**) and iron(II) (**15**). The reaction of the dialkyl iron(II) (**6**) with CO resulted in

the formation of a trinuclear iron(II) complex which showed a variety of CO reactivity modes, including the rare insertion of CO into an Fe-N bond. These high-spin organometallic iron(II) and cobalt(II) complexes can form the basis of a much more substantial reactivity study. Comparing low-spin Fe-C bond distances with that of the high-spin iron and cobalt complexes reported here does not show any trend like what was observed for phosphines,[31] however with the observed rare reactivity of the dialkyl iron with CO, and $-C_6F_5$ substitution in the dialkyl iron and cobalt complexes, it can be suggested that the M-C bond in high-spin iron(II) and cobalt(II) complexes are weaker than low-spin complexes.

As high-valent iron and cobalt are known to be highly reactive and, in the case of iron, has biological importance too, one goal was to access high-valent iron and cobalt systems with the diamido-ether ligands since they were thought to be good candidates due to the π-donating ability of the amido group and the donor atom in the ligand backbone. However, attempts with different oxidizing agents such as a strongly oxidizing "Br^+" reagent did not led to the formation of stable iron(IV) or cobalt(III) complexes. It appears that the diamidoether ligand can not sufficiently stabilize iron(IV) or cobalt(III) metal centres.

In order to target diamido high-valent iron and cobalt complexes, a more flexible carbon-backbone diamido ligand was targeted. As shown in Chapter 5, two similar $[^{iPr}NN'N]^{2-}$ and $[^{iPr}NO'N]^{2-}$ ligands with iron(II) and cobalt(II) led to the formation of diamido iron(II) and cobalt(II) complexes, which formed dimers through amido bridges, however the oxidation of the metal centre in both cases resulted in the formation of diamine-dichloride iron(II) and cobalt(II) complexes. The result was very surprising since, with these ligands, even and iron(III) complex could not be isolated; this result was very different than the Si-based diamido donor ligands.

The works presented in this thesis raises big questions that requires more investigations. Even though some reactivity studies of the metal centre in the high-spin metal alkyl compounds have been attempted, there are many more reactivity types to be tried, and compared to low-spin systems. How much does a different spin state of the metal centre result in new reactivity, like what was observed for dialkyl iron (**6**) with CO and why? Is there any actual metal-metal interaction and if so how can it contribute to

the metal centre reactivity? In other words, does the presence of a metal-metal interaction impact the reactivity of these metal complexes and if so, how? More generally, do these bimetallic compounds act differently than analogous mononuclear compounds? These are all big questions that can easily form the basis of another Ph.D. thesis.

References

[1] J. P. Collman, R. G. Finke and J. R. Norton, *Principles and Applications of Organotransition Metal Chemistry*, University Science Books: Mill Valley, CA. Ch. 1., **1987**.

[2] R. H. Crabtree, *The Organometallic Chemistry of the Transition Metals* Wiley; 5 edition, **2009**.

[3] D. J. Cardin and K. R. Dixon, *Annual Reports on the Progress of Chemistry, Section A: Physical and Inorganic Chemistry* **1976**, *73*, 211-259.

[4] M. D. Johnson, *Accounts of Chemical Research* **1983**, *16*, 343-349.

[5] H. G. Richey, *Grignard reagents: new developments*, Wiley, Chichester, **2000**.

[6] J. D. Jones, R. Pearce and G. L. P. Randall, *Annual Reports Section "B" (Organic Chemistry)* **1973**, *70*, 243-267.

[7] R. Kempe, *Angewandte Chemie International Edition* **2000**, *39*, 468-493.

[8] M. F. Lappert, A. V. Protchenko, P. P. Power and A. L. Seeber, *Metal Amide Chemistry*, Wiley. U.K, **2009**.

[9] T. J. KEALY; P. L. PAUSON *Nature* **1951**, 168.

[10] A. J. Pearson, *Metallo Organic Chemistry*, John Wiley & Sons; 1 edition, **1985**.

[11] V. C. Gibson and S. K. Spitzmesser, *Chemical Reviews* **2002**, *103*, 283-316.

[12] S. Park, Y. Han, S. K. Kim, J. Lee, H. K. Kim and Y. Do, *Journal of Organometallic Chemistry* **2004**, *689*, 4263-4276.

[13] T. J. Donohoe, R. R. Harji, P. R. Moore and M. J. Waring, *Journal of the Chemical Society, Perkin Transactions 1* **1998**, 819-834.

[14] B. J. Thomas, S. K. Noh, G. K. Schulte, S. C. Sendlinger and K. H. Theopold, *Journal of the American Chemical Society* **1991**, *113*, 893-902.

[15] G. Bhandari, Y. Kim, J. M. McFarland, A. L. Rheingold and K. H. Theopold, *Organometallics* **1995**, *14*, 738-745.

[16] R. R. Schrock, *Accounts of Chemical Research* **2005**, *38*, 955-962.

[17] P. J. Toscano and L. G. Marzilli in *B12 and Related Organocobalt Chemistry: Formation and Cleavage of Cobalt Carbon Bonds*, *Vol.* John Wiley & Sons, Inc., **2007**, p. 105-204.

[18] M. P. Coogan, P. J. Dyson and M. Bochmann, *Organometallics* **2012**, *31*, 5671-5672.

[19] C. G. Hartinger, N. Metzler-Nolte and P. J. Dyson, *Organometallics* **2012**, *31*, 5677-5685.

[20] G. Gasser, I. Ott and N. Metzler-Nolte, *Journal of Medicinal Chemistry* **2010**, *54*, 3-25.

[21] A. F. A. Peacock and P. J. Sadler, *Chemistry – An Asian Journal* **2008**, *3*, 1890-1899.

[22] W. Wang, K. Wang, I. Span, J. Jauch, A. Bacher, M. Groll and E. Oldfield, *Journal of the American Chemical Society* **2012**, *134*, 11225-11234.

[23] R. Poli, *Chemical Reviews* **1996**, *96*, 2135-2204.

[24] G. J. P. Britovsek, V. C. Gibson and D. F. Wass, *Angewandte Chemie International Edition* **1999**, *38*, 428-447.

[25] W. Zhou, K. C. MacLeod, B. O. Patrick and K. M. Smith, *Organometallics* **2012**, *31*, 7324-7327.

[26] G. R. Knox, *Organometallic compounds of iron*, Chapman and Hall, the University of Michigan, **1985**.

[27] J. E. Baldwin and C.-S. Li, *Journal of the Chemical Society, Chemical Communications* **1987**, 166-168.

[28] B. P. Branchaud and Y. L. Choi, *The Journal of Organic Chemistry* **1988**, *53*, 4638-4641.

[29] V. F. Patel, G. Pattenden and D. M. Thompson, *Journal of the Chemical Society, Perkin Transactions 1* **1990**, 2729-2734.

[30] T. M. Brown, C. J. Cooksey, D. Crich, A. T. Dronsfield and R. Ellis, *Journal of the Chemical Society, Perkin Transactions 1* **1993**, 2131-2136.

[31] F.A. Cotton, G. Wilkinson, C. A. Murillo, M. Bochmann, *Advanced Inorganic Chemistry*, 6th Edn., Wiley, New York, **1999**.

[32] R. B. Bedford, M. Betham, D. W. Bruce, A. A. Danopoulos, R. M. Frost and M. Hird, *The Journal of Organic Chemistry* **2005**, *71*, 1104-1110.

[33] S. Kuppuswamy, M. W. Bezpalko, T. M. Powers, M. M. Turnbull, B. M. Foxman and C. M. Thomas, *Inorganic Chemistry* **2012**, *51*, 8225-8240.

[34] M. D. Fryzuk, D. B. Leznoff and S. J. Rettig, *Organometallics* **1997**, *16*, 5116-5119.

[35] G. Wilkinson , R.D. Gillard and J.A. Mc Cleverty *Comprehensive coordination chemistry* 1st. edn. , Pergammon Press , New York , **1987**.

[36] V. C. Gibson, S. K. Spitzmesser, A. J. P. White and D. J. Williams, *Dalton Transactions* **2003**, 2718-2727.

[37] A. K. Das, Z. Moatazedi, G. Mund, A. J. Bennet, R. J. Batchelor and D. B. Leznoff, *Inorganic Chemistry* **2006**, *46*, 366-368.

[38] L. H. Gade, *Chemical Communications* **2000**, 173-181.

[39] M. D. Fryzuk, D. B. Leznoff, R. C. Thompson and S. J. Rettig, *Journal of the American Chemical Society* **1998**, *120*, 10126-10135.

[40] M. D. Fryzuk, D. B. Leznoff, E. S. F. Ma, S. J. Rettig and V. G. Young, *Organometallics* **1998**, *17*, 2313-2323.

[41] W. A. Chomitz, S. F. Mickenberg and J. Arnold, *Inorganic Chemistry* **2007**, *47*, 373-380.

[42] W. A. Chomitz and J. Arnold, *Inorganic Chemistry* **2009**, *48*, 3274-3286.

[43] J. A. Hatnean, R. Raturi, J. Lefebvre, D. B. Leznoff, G. Lawes and S. A. Johnson, *Journal of the American Chemical Society* **2006**, *128*, 14992-14999.

[44] M. D. Fryzuk, B. A. MacKay and B. O. Patrick, *Journal of the American Chemical Society* **2003**, *125*, 3234-3235.

[45] S. Gambarotta and J. Scott, *Angewandte Chemie International Edition* **2004**, *43*, 5298-5308.

[46] G. Wilkinson, R. D. Gillard and J. A. McCleverty Pergamon *Comprehensive Organometallic Chemistry*, Oxford, **1987**.

[47] C. A. Tolman, *Chem. Soc. Rev.* **1972**, *1*, 337.

[48] P. J. Davidson, M. F. Lappert and R. Pearce, *Chemical Reviews* **1976**, *76*, 219-242.

[49] G. Yagupsky, W. Mowat, A. Shortland and G. Wilkinson, *Journal of the Chemical Society D: Chemical Communications* **1970**, 1369-1370.

[50] B. K. Bower and H. G. Tennent, *Journal of the American Chemical Society* **1972**, *94*, 2512-2514.

[51] P. J. Davidson, M. F. Lappert and R. Pearce, *Accounts of Chemical Research* **1974**, *7*, 209-217.

[52] G. K. Barker and M. F. Lappert, *Journal of Organometallic Chemistry* **1974**, *76*, 45-46.

[53] C. Ni, J. C. Fettinger, G. J. Long and P. P. Power, *Inorganic Chemistry* **2009**, *48*, 2443-2448.

[54] A. M. Bryan, W. A. Merrill, W. M. Reiff, J. C. Fettinger and P. P. Power, *Inorganic Chemistry* **2012**, *51*, 3366-3373.

[55] G. Mund, R. J. Batchelor, R. D. Sharma, C. H. W. Jones and D. B. Leznoff, *Journal of the Chemical Society, Dalton Transactions* **2002**, 136-137.

[56] F.-L. Yang, J. Tao, R.-B. Huang and L.-S. Zheng, *Inorganic Chemistry* **2010**, *50*, 911-917.

[57] J. Kuzelka, P. Legzdins, S. J. Rettig and K. M. Smith, *Organometallics* **1997**, *16*, 3569-3571.

[58] J. C. Doherty, K. H. D. Ballem, B. O. Patrick and K. M. Smith, *Organometallics* **2004**, *23*, 1487-1489.

[59] K. C. MacLeod, B. O. Patrick and K. M. Smith, *Organometallics* **2010**, *29*, 6639-6641.

[60] D. Sieb, R. W. Baker, H. Wadepohl and M. Enders, *Organometallics* **2012**, *31*, 7368-7374.

[61] S. Conde-Guadano, A. A. Danopoulos, R. Pattacini, M. Hanton and R. P. Tooze, *Organometallics* **2012**, *31*, 1643-1652.

[62] K. P. McGowan, K. A. Abboud and A. S. Veige, *Organometallics* **2011**, *30*, 4949-4957.

[63] Y. Champouret, K. C. MacLeod, K. M. Smith, B. O. Patrick and R. Poli, *Organometallics* **2010**, *29*, 3125-3132.

[64] Y. Champouret, K. C. MacLeod, U. Baisch, B. O. Patrick, K. M. Smith and R. Poli, *Organometallics* **2009**, *29*, 167-176.

[65] J. P. Krogman, B. M. Foxman and C. M. Thomas, *Journal of the American Chemical Society* **2011**, *133*, 14582-14585.

[66] S. C. Bart, A. C. Bowman, E. Lobkovsky and P. J. Chirik, *Journal of the American Chemical Society* **2007**, *129*, 7212-7213.

[67] M. Beller and C. Bolm, *Transition Metals for Organic Synthesis*, Wiley-VCH: Weinheim, **2004**.

[68] F. A. Cotton, G. Wilkinson, C. A. Murillo and M. Bochmann, *Advanced inorganic chemistry*, Wiley, New York, **1999**.

[69] R. A. Bartlett and P. P. Power, *Journal of the American Chemical Society* **1987**, *109*, 7563-7564.

[70] J. J. Ellison, K. Ruhlandt-Senge and P. P. Power, *Angewandte Chemie International Edition in English* **1994**, *33*, 1178-1180.

[71] M. M. Rodriguez, E. Bill, W. W. Brennessel and P. L. Holland, *Science* **2011**, *334*, 780-783.

[72] J. Vela, J. M. Smith, Y. Yu, N. A. Ketterer, C. J. Flaschenriem, R. J. Lachicotte and P. L. Holland, *Journal of the American Chemical Society* **2005**, *127*, 7857-7870.

[73] A. C. Bowman, S. C. Bart, F. W. Heinemann, K. Meyer and P. J. Chirik, *Inorganic Chemistry* **2009**, *48*, 5587-5589.

[74] C. Bolm, J. Legros, J. Le Paih and L. Zani, *Chemical Reviews* **2004**, *104*, 6217-6254.

[75] M. W. W. Adams and E. I. Stiefel, *Current Opinion in Chemical Biology* **2000**, *4*, 214-220.

[76] J. D. Jewson, L. M. Liable-Sands, G. P. A. Yap, A. L. Rheingold and K. H. Theopold, *Organometallics* **1998**, *18*, 300-305.

[77] D. C. Sauer, H. Wadepohl and L. H. Gade, *Inorganic Chemistry* **2012**.

[78] L. Xiang, J. Xiao and L. Deng, *Organometallics* **2011**, *30*, 2018-2025.

[79] R. S. Paley in *Iron: Organometallic Chemistry*, *Vol.* John Wiley & Sons, Ltd, **2011**.

[80] G. S. Girolami, C. G. Howard, G. Wilkinson, H. M. Dawes, M. Thornton-Pett, M. Motevalli and M. B. Hursthouse, *Journal of the Chemical Society, Dalton Transactions* **1985**, 921-929.

[81] N. Le Gall, D. Luart, J.-Y. Salaün, J. Talarmin, H. des Abbayes, L. Toupet, N. Menendez and F. Varret, *Organometallics* **2002**, *21*, 1775-1781.

[82] J. Vela, S. Vaddadi, T. R. Cundari, J. M. Smith, E. A. Gregory, R. J. Lachicotte, C. J. Flaschenriem and P. L. Holland, *Organometallics* **2004**, *23*, 5226-5239.

[83] S. Ostrovsky, Z. Tomkowicz and W. Haase, *Inorganic Chemistry* **2010**, *49*, 6942-6947.

[84] A. R. Hermes and G. S. Girolami, *Organometallics* **1988**, *7*, 394-401.

[85] M.-E. Moret and J. C. Peters, *Journal of the American Chemical Society* **2011**, *133*, 18118-18121.

[86] Z. Thammavongsy, T. Seda, L. N. Zakharov, W. Kaminsky and J. D. Gilbertson, *Inorganic Chemistry* **2012**, *51*, 9168-9170.

[87] N. Tewari, N. Maheshwari, R. Medhane, H. Nizar and M. Prasad, *Organic Process Research & Development* **2012**, *16*, 1566-1568.

[88] E. Nakamura and N. Yoshikai, *The Journal of Organic Chemistry* **2010**, *75*, 6061-6067.

[89] Z. Mo, Q. Zhang and L. Deng, *Organometallics* **2012**, *31*, 6518-6521.

[90] J. Norinder, A. Matsumoto, N. Yoshikai and E. Nakamura, *Journal of the American Chemical Society* **2008**, *130*, 5858-5859.

[91] A. M. Tondreau, C. Milsmann, A. D. Patrick, H. M. Hoyt, E. Lobkovsky, K. Wieghardt and P. J. Chirik, *Journal of the American Chemical Society* **2010**, *132*, 15046-15059.

[92] F. d. r. Hebrard and P. Kalck, *Chemical Reviews* **2009**, *109*, 4272-4282.

[93] R. R. Chowdhury, A. K. Crane, C. Fowler, P. Kwong and C. M. Kozak, *Chemical Communications* **2008**, 94-96.

[94] S. M. Massick, T. Büttner and P. C. Ford, *Inorganic Chemistry* **2002**, *42*, 575-580.

[95] S. A. Sulway, D. Collison, J. J. W. McDouall, F. Tuna and R. A. Layfield, *Inorganic Chemistry* **2011**, *50*, 2521-2526.

[96] D. C. Bradley and M. H. Chisholm, *Accounts of Chemical Research* **1976**, *9*, 273-280.

[97] D. C. Bradley, M. B. Hursthouse, R. J. Smallwood and A. J. Welch, *Journal of the Chemical Society, Chemical Communications* **1972**, 872-873.

[98] R. R. Schrock, R. Baumann, S. M. Reid, J. T. Goodman, R. Stumpf and W. M. Davis, *Organometallics* **1999**, *18*, 3649-3670.

[99] N. A. H. Male, M. Thornton-Pett and M. Bochmann, *Journal of the Chemical Society, Dalton Transactions* **1997**, 2487-2494.

[100] M. Aizenberg, L. Turculet, W. M. Davis, F. Schattenmann and R. R. Schrock, *Organometallics* **1998**, *17*, 4795-4812.

[101] R. Baumann, W. M. Davis and R. R. Schrock, *Journal of the American Chemical Society* **1997**, *119*, 3830-3831.

[102] A. R. Morgan, M. Kloskowski, F. Kalischewski, A. H. Phillips and J. L. Petersen, *Organometallics* **2005**, *24*, 5383-5392.

[103] H. Tsurugi, Y. Matsuo, T. Yamagata and K. Mashima, *Organometallics* **2004**, *23*, 2797-2805.

[104] A. D. Horton, J. de With, A. J. van der Linden and H. van de Weg, *Organometallics* **1996**, *15*, 2672-2674.

[105] P. Mehrkhodavandi, P. J. Bonitatebus and R. R. Schrock, *Journal of the American Chemical Society* **2000**, *122*, 7841-7842.

[106] C. E. Laplaza, M. J. A. Johnson, J. C. Peters, A. L. Odom, E. Kim, C. C. Cummins, G. N. George and I. J. Pickering, *Journal of the American Chemical Society* **1996**, *118*, 8623-8638.

[107] A. R. Fout, F. Basuli, H. Fan, J. Tomaszewski, J. C. Huffman, M.-H. Baik and D. J. Mindiola, *Angewandte Chemie International Edition* **2006**, *45*, 3291-3295.

[108] M. D. Fryzuk, T. S. Haddad and S. J. Rettig, *Journal of the American Chemical Society* **1990**, *112*, 8185-8186.

[109] A. A. Danopoulos, P. Braunstein, M. Wesolek, K. Y. Monakhov, P. Rabu and V. Robert, *Organometallics* **2012**, *31*, 4102-4105.

[110] P. P. Power, *Comments on Inorganic Chemistry* **1989**, *8*, 177-202.

[111] P. P. Power, *Chemical Reviews* **2012**, *112*, 3482-3507.

[112] J. KIRN and D. C. REES*, *Nature* **1992**, 553-560.

[113] H. Chen, R. A. Bartlett, H. V. R. Dias, M. M. Olmstead and P. P. Power, *Journal of the American Chemical Society* **1989**, *111*, 4338-4345.

[114] W. Alexander Merrill, T. A. Stich, M. Brynda, G. J. Yeagle, J. C. Fettinger, R. D. Hont, W. M. Reiff, C. E. Schulz, R. D. Britt and P. P. Power, *Journal of the American Chemical Society* **2009**, *131*, 12693-12702.

[115] H. Bürger and U. Wannagat, *Monatshefte für Chemie und verwandte Teile anderer Wissenschaften* **1963**, *94*, 1007-1012.

[116] H. Bürger and U. Wannagat, *Monatsh. Chem* **1964**, *95*, 1098.

[117] D. C. Bradley and K. J. Fisher, *J. Am. Chem. Soc* **1971**, *93*.

[118] R. A. Andersen, K. Faegri, J. C. Green, A. Haaland, M. F. Lappert, W. P. Leung and K. Rypdal, *Inorganic Chemistry* **1988**, *27*, 1782-1786.

[119] J. J. Curley, T. R. Cook, S. Y. Reece, P. Müller and C. C. Cummins, *Journal of the American Chemical Society* **2008**, *130*, 9394-9405.

[120] Z. Mo, D. Chen, X. Leng and L. Deng, *Organometallics* **2012**, *31*, 7040-7043.

[121] J. M. Smith, R. J. Lachicotte, K. A. Pittard, T. R. Cundari, G. Lukat-Rodgers, K. R. Rodgers and P. L. Holland, *Journal of the American Chemical Society* **2001**, *123*, 9222-9223.

[122] T. R. Dugan, J. M. Goldberg, W. W. Brennessel and P. L. Holland, *Organometallics* **2012**, *31*, 1349-1360.

[123] A. Panda, M. Stender, R. J. Wright, M. M. Olmstead, P. Klavins and P. P. Power, *Inorganic Chemistry* **2002**, *41*, 3909-3916.

[124] L. H. Gade, *Journal of Organometallic Chemistry* **2002**, *661*, 85-94.

[125] J. B. Love, H. C. S. Clark, F. G. N. Cloke, J. C. Green and P. B. Hitchcock, *Journal of the American Chemical Society* **1999**, *121*, 6843-6849.

[126] A. Athimoolam, S. Gambarotta and I. Korobkov, *Organometallics* **2005**, *24*, 1996-1999.

[127] M. V. Jiménez, E. Sola, F. J. Lahoz and L. A. Oro, *Organometallics* **2005**, *24*, 2722-2729.

[128] S. Daniele, P. B. Hitchcock and M. F. Lappert, *Chemical Communications* **1999**, 1909-1910.

[129] J. D. Scollard, D. H. McConville, J. J. Vittal and N. C. Payne, *Journal of Molecular Catalysis A: Chemical* **1998**, *128*, 201-214.

[130] C. S. Slone, D. A. Weinberger and C. A. Mirkin in *The Transition Metal Coordination Chemistry of Hemilabile Ligands*, *Vol.* John Wiley & Sons, Inc., **2007**, pp. 233-350.

[131] F. G. N. Cloke, P. B. Hitchcock and J. B. Love, *Journal of the Chemical Society, Dalton Transactions* **1995**, 25-30.

[132] F. Guérin, D. H. McConville and N. C. Payne, *Organometallics* **1996**, *15*, 5085-5089.

[133] L.-C. Liang, R. R. Schrock, W. M. Davis and D. H. McConville, *Journal of the American Chemical Society* **1999**, *121*, 5797-5798.

[134] D. D. Graf, R. R. Schrock, W. M. Davis and R. Stumpf, *Organometallics* **1999**, *18*, 843-852.

[135] G. Mund, A. J. Gabert, R. J. Batchelor, J. F. Britten and D. B. Leznoff, *Chemical Communications* **2002**, 2990-2991.

[136] D. B. Leznoff, G. Mund, K. C. Jantunen, P. H. Bhatia, A. J. Gabert and R. J. Batchelor, *J. Nucl. Sci. Technol.* **2002**, 406.

[137] G. Mund, D. Vidovic, R. J. Batchelor, J. F. Britten, R. D. Sharma, C. H. W. Jones and D. B. Leznoff, *Chemistry – A European Journal* **2003**, *9*, 4757-4763.

[138] F. Haftbaradaran, A. M. Kuchison, M. J. Katz, G. Schatte and D. B. Leznoff, *Inorganic Chemistry* **2008**, *47*, 812-822.

[139] E. A. MacLachlan, F. M. Hess, B. O. Patrick and M. D. Fryzuk, *Journal of the American Chemical Society* **2007**, *129*, 10895-10905.

[140] A. J. S. Elias, Hans Goerg; Noltemeyer, Mathias; Roesky, Herbert W., *European Journal of Solid State and Inorganic Chemistry* **1992**, *29*, 23.

[141] R. Baumann, R. Stumpf, W. M. Davis, L.-C. Liang and R. R. Schrock, *Journal of the American Chemical Society* **1999**, *121*, 7822-7836.

[142] J. T. Goodman and R. R. Schrock, *Organometallics* **2001**, *20*, 5205-5211.

[143] L.-C. Liang, R. R. Schrock and W. M. Davis, *Organometallics* **2000**, *19*, 2526-2531.

[144] P. Mehrkhodavandi and R. R. Schrock, *Journal of the American Chemical Society* **2001**, *123*, 10746-10747.

[145] F. Haftbaradaran, G. Mund, R. J. Batchelor, J. F. Britten and D. B. Leznoff, *Dalton Transactions* **2005**, 2343-2345.

[146] E. A. V. Ebsworth, D. W. H. Rankin and S. Cradock, *Structural Methods in Inorganic Chemistry*, Blackwell; 2 edition **1991**.

[147] G. N. Lamar, W. D. Horrocks and R. H. Holm, *NMR of Paramagnetic Molecules*, Academic Press: New York, **1973**.

[148] R. S. Drago, *Physical methods for chemists*, Saunders College Pub., **1992**, p.

[149] G. N. LaMar, W. D. Horrocks and R. H. Holm, *Nuclear Magnetic Resonance of Paramagnetic Molecules: Principles and Applications*, New York, Academic Press, **1973**.

[150] S. K. Sur, *Journal of Magnetic Resonance (1969)* **1989**, *82*, 169-173.

[151] M. D. Fryzuk, *Coordination Chemistry Reviews* **1989**, *95*, 1.

[152] M. D. Roundhill, *Chemical Reviews* **1992**, *92*, 1.

[153] M. D. Fryzuk, S. A. Johnson and S. J. Rettig, *Journal of the American Chemical Society* **1998**, *120*, 11024-11025.

[154] R. R. Schrock, F. Schattenmann, M. Aizenberg and W. M. Davis, *Chemical Communications* **1998**, 199-200.

[155] A. J. Elias, H. W. Roesky, W. T. Robinson and G. M. Sheldrick, *Journal of the Chemical Society, Dalton Transactions* **1993**, 495-500.

[156] H. Ikeda, T. Monoi, Y. Nakayama and H. Yasuda, *Journal of Organometallic Chemistry* **2002**, *642*, 156-162.

[157] M. B. Hursthouse and P. F. Rodesiler, *Journal of the Chemical Society, Dalton Transactions* **1972**, 2100-2102.

[158] W. A. Chomitz and J. Arnold, *Journal of the Chemical Society , Dalton Transactions* **2009**, 1714-1720.

[159] W. A. Chomitz and J. Arnold, *Chemical Communications* **2007**, 4797-4799.

[160] I. Silaghi-Dumitrescu, T. E. Bitterwolf and R. B. King, *Journal of the American Chemical Society* **2006**, *128*, 5342-5343.

[161] M.-H. Baik, T. Ziegler and C. K. Schauer, *Journal of the American Chemical Society* **2000**, *122*, 9143-9154.

[162] D. F. Evans, *Journal of the Chemical Society (Resumed)* **1959**, 2003-2005.

[163] H. Vahrenkamp, *Angewandte Chemie International Edition* **1978**, *17*, 379.

[164] S. Petrie and R. Stranger, *Inorganic Chemistry* **2002**, *42*, 4417.

[165] C. D. Delfs and R. Stranger, *Inorganic Chemistry* **2000**, *39*, 491.

[166] P. Belanzoni, N. Re, M. Rosi, A. Sgamellotti, E. J. Baerends and C. Floriani, *Inorganic Chemistry* **1996**, *35*, 7776-7785.

[167] Z. Zhang, Q.-s. Li, Y. Xie, R. B. King and H. F. Schaefer, *Inorganic Chemistry* **2009**, *48*, 5973-5982.

[168] R. L. Carlin, *Magnetochemistry; Springer-Verlag: Heidelberg*, **1986**.

[169] O. Kahn, *Molecular Magnetism*, John Wiley & Sons Canada, **1993**.

[170] V. Brito, H. FrBhlich and B. Z. Miiller, *Chem. Commun* **1979**, *19*, 28-29.

[171] B. D. Murray and P. P. Power, *Inorganic Chemistry* **1984**, *23*, 4584-4588.

[172] L. Pauling, *Proceedings of the National Academy of Sciences of the United States of America* **1976**, *73*, 4290-4293.

[173] C. M. Zall, D. Zherebetskyy, A. L. Dzubak, E. Bill, L. Gagliardi and C. C. Lu, *Inorganic Chemistry* **2011**, *51*, 728-736.

[174] S. Petrie and R. Stranger, *Inorganic Chemistry* **2004**, *43*, 2597-2610.

[175] F. A. Cotton and X. Feng, *Journal of the American Chemical Society* **1998**, *120*, 3387-3397.

[176] B. T. Sterenberg, R. W. Hilts, G. Moro, R. McDonald and M. Cowie, *Journal of the American Chemical Society* **1995**, *117*, 245-258.

[177] D. Ristic-Petrovic, D. J. Anderson, J. R. Torkelson, M. J. Ferguson, R. McDonald and M. Cowie, *Organometallics* **2005**, *24*, 3711-3724.

[178] J. R. Torkelson, R. McDonald and M. Cowie, *Journal of the American Chemical Society* **1998**, *120*, 4047-4048.

[179] F. A. Cotton and X. Feng, *Journal of the American Chemical Society* **1997**, *119*, 7514-7520.

[180] M. Di Vaira, S. Midollini and L. Sacconi, *Inorganic Chemistry* **1981**, *20*, 3430-3435.

[181] H. Jacobsen, A. Correa, A. Poater, C. Costabile and L. Cavallo, *Coordination Chemistry Reviews* **2009**, *253*, 687-703.

[182] V. Lavallo and R. H. Grubbs*, *Science* **2012**, *326*.

[183] J. A. Przyojski, H. D. Arman and Z. J. Tonzetich, *Organometallics* **2012**, *31*, 3264-3271.

[184] A. A. Danopoulos, P. Braunstein, N. Stylianides and M. Wesolek, *Organometallics* **2011**, *30*, 6514-6517.

[185] C. Fliedel, A. Maisse-François and S. Bellemin-Laponnaz, *Inorganica Chimica Acta* **2007**, *360*, 143-148.

[186] R. A. Layfield, J. J. W. McDouall, M. Scheer, C. Schwarzmaier and F. Tuna, *Chemical Communications* **2011**, *47*, 10623-10625.

[187] J. Louie and R. H. Grubbs, *Chemical Communications* **2000**, 1479.

[188] P. W. Betteridge, J. R. Carruthers, R. I. Cooper, K. Prout and D. J. Watkin, *Journal of Applied Crystallography* **2003**, *36*, 1487.

[189] S. Parsons, *ROTAX. Version 26th*, R. Cooper (Oxford, England) and L. Farrugia (Glasgow, Scotland), November. University of Edinburgh, **2001**.

[190] D. J. Watkin, C. K. Prout and L. J. Pearce, *CAMERON*, Oxford, U.K, Chemical Crystallography Laboratory, University of Oxford, **1996**.

[191] P. L. Holland, T. R. Cundari, L. L. Perez, N. A. Eckert and R. J. Lachicotte, *Journal of the American Chemical Society* **2002**, *124*, 14416-14424.

[192] Z. Moatazedi, M. J. Katz and D. B. Leznoff, *Dalton Transactions* **2010**, *39*, 9889-9896.

[193] M. Akita, *Journal of Organometallic Chemistry* **2004**, *689*, 4540-4551.

[194] J. Volbeda, A. Meetsma and M. W. Bouwkamp, *Organometallics* **2008**, *28*, 209-215.

[195] W.-P. Leung, H. Kay Lee, L.-H. Weng, Z.-Y. Zhou and T. C. W. Mak, *Journal of the Chemical Society, Dalton Transactions* **1997**, 779-784.

[196] E. K. Byrne, D. S. Richeson and K. H. Theopold, *Journal of the Chemical Society, Chemical Communications* **1986**, 1491-1492.

[197] A. S. Batsanov, B. M. Bridgewater, J. A. K. Howard, A. K. Hughes and C. Wilson, *Journal of Organometallic Chemistry* **1999**, *590*, 169-179.

[198] J. K. Stille, C. Smith, O. P. Anderson and M. M. Miller, *Organometallics* **1989**, *8*, 1040-1047.

[199] K. H. Pannell, J. Cervantes, L. Parkanyi and F. Cervantes-Lee, *Organometallics* **1990**, *9*, 859-863.

[200] T. Mizuta, T. Yamasaki, H. Nakazawa and K. Miyoshi, *Organometallics* **1996**, *15*, 1093-1100.

[201] M. Okazaki, K. A. Jung, K. Satoh, H. Okada, J. Naito, T. Akagi, H. Tobita and H. Ogino, *Journal of the American Chemical Society* **2004**, *126*, 5060-5061.

[202] J. M. Smith, R. J. Lachicotte and P. L. Holland, *Organometallics* **2002**, *21*, 4808-4814.

[203] M. W. Bouwkamp, S. C. Bart, E. J. Hawrelak, R. J. Trovitch, E. Lobkovsky and P. J. Chirik, *Chemical Communications* **2005**, 3406-3408.

[204] J. D. Scollard, D. H. McConville and S. J. Rettig, *Organometallics* **1997**, *16*, 1810-1812.

[205] S. C. Bart, E. J. Hawrelak, A. K. Schmisseur, E. Lobkovsky and P. J. Chirik, *Organometallics* **2003**, *23*, 237-246.

[206] S. S. Rozenel, W. A. Chomitz and J. Arnold, *Organometallics* **2009**, *28*, 6243-6253.

[207] M. D. Fryzuk, D. B. Leznoff, S. J. Rettig, V. G. Young and J. Daniel B. Leznoff Steven J. Rettig Victor G. Young, *Journal of the Chemical Society, Dalton Transactions* **1999**, 147-154.

[208] J. B. Willems, H. W. Rohm, C. Geers and M. Köckerling, *Inorganic Chemistry* **2007**, *46*, 6197-6203.

[209] T. Hughbanks, *Journal of Alloys and Compounds* **1995**, *229*, 40-53.

[210] J. D. Harris and T. Hughbanks, *Journal of the American Chemical Society* **1997**, *119*, 9449-9459.

[211] D. Sun and T. Hughbanks, *Inorganic Chemistry* **2000**, *39*, 1964-1968.

[212] A. Klose, E. Solari, C. Floriani, A. Chiesi-Villa, C. Rizzoli and N. Re, *Journal of the American Chemical Society* **1994**, *116*, 9123-9135.

[213] F. Albert Cotton, L. M. Daniels, L. R. Falvello and C. A. Murillo, *Inorganica Chimica Acta* **1994**, *219*, 7-10.

[214] L. J. Radonovich, K. J. Klabunde, C. B. Behrens, D. P. McCollor and B. B. Anderson, *Inorganic Chemistry* **1980**, *19*, 1221-1226.

[215] S. L. Gipson, L. A. Bryson and K. K. Klausmeyer, *Inorganica Chimica Acta* **2002**, *340*, 221-224.

[216] R. Chukwu, A. D. Hunter, B. D. Santarsiero, S. G. Bott, J. L. Atwood and J. Chassaignac, *Organometallics* **1992**, *11*, 589-597.

[217] M. Ganesan and F. P. Gabbaï, *Organometallics* **2004**, *23*, 4608-4613.

[218] L. Postigo, J. Sanchez-Nieves, P. Royo and M. E. G. Mosquera, *Dalton Transactions* **2009**, *0*, 3756-3765.

[219] M. J. Nelsen and G. S. Girolami, *Journal of Organometallic Chemistry* **1999**, *585*, 275-284.

[220] S. Garratt, A. Guerrero, D. L. Hughes and M. Bochmann, *Angewandte Chemie International Edition* **2004**, *43*, 2166-2169.

[221] E. Y.-X. Chen and T. J. Marks, *Chemical Reviews* **2000**, *100*, 1391-1434.

[222] A. G. Massey and A. J. Park, *Journal of Organometallic Chemistry* **1964**, *2*, 245-250.

[223] M. W. Bouwkamp, E. Lobkovsky and P. J. Chirik, *Journal of the American Chemical Society* **2005**, *127*, 9660-9661.

[224] T. Wondimagegn, Z. Xu, K. Vanka and T. Ziegler, *Organometallics* **2004**, *23*, 3847-3852.

[225] T. J. Woodman, M. Thornton-Pett and M. Bochmann, *Chemical Communications* **2001**, 329-330.

[226] D. D. Wick and W. D. Jones, *Organometallics* **1999**, *18*, 495-505.

[227] W. Kläui and H. Werner, *Angewandte Chemie International Edition in English* **1976**, *15*, 172-173.

[228] M. A. Walters and J. C. Dewan, *Inorganic Chemistry* **1986**, *25*, 4889-4893.

[229] U. Berger and J. Strähle, *Zeitschrift für anorganische und allgemeine Chemie* **1984**, *516*, 19-29.

[230] W.-F. Liaw, C.-H. Chen, C.-M. Lee, G.-Y. Lin, C.-Y. Ching, G.-H. Lee and S.-M. Peng, *Journal of the Chemical Society, Dalton Transactions* **1998**, *0*, 353-358.

[231] N. El Murr, A. Chaloyard and W. Klaeui, *Inorganic Chemistry* **1979**, *18*, 2629-2631.

[232] M. K. Kolel-Veetil, M. A. Khan and K. M. Nicholas, *Organometallics* **2000**, *19*, 3754-3756.

[233] Y. Liu, D. Zhang, S. Bi and C. Liu, *Organometallics* **2011**, *31*, 365-371.

[234] M. Rahim, C. H. Bushweller and K. J. Ahmed, *Organometallics* **1994**, *13*, 4952-4958.

[235] P. J. Fagan, J. M. Manriquez, S. H. Vollmer, C. S. Day, V. W. Day and T. J. Marks, *Journal of the American Chemical Society* **1981**, *103*, 2206-2220.

[236] F. L. Joslin, M. P. Johnson, J. T. Mague and D. M. Roundhill, *Organometallics* **1991**, *10*, 2781-2794.

[237] S. Anderson, T. E. Berridge, A. F. Hill, Y. T. Ng, A. J. P. White and D. J. Williams, *Organometallics* **2004**, *23*, 2686-2693.

[238] S. Anderson, D. J. Cook and A. F. Hill, *Organometallics* **1997**, *16*, 5595-5597.

[239] L.-C. Liang, Y.-T. Hung, Y.-L. Huang, P.-S. Chien, P.-Y. Lee and W.-C. Chen, *Organometallics* **2011**, *31*, 700-708.

[240] T.-F. Wang, C.-C. Hwu, C.-W. Tsai and Y.-S. Wen, *Organometallics* **1998**, *17*, 131-138.

[241] J. T. Chen, W. H. Tzeng, F. Y. Tsai, M. C. Cheng and Y. Wang, *Organometallics* **1991**, *10*, 3954-3955.

[242] J. N. Coalter, J. C. Huffman and K. G. Caulton, *Organometallics* **2000**, *19*, 3569-3578.

[243] A. Müller, U. Seyer and W. Eltzner, *Inorganica Chimica Acta* **1979**, *32*, L65-L66.

[244] I. G. Denisov, T. M. Makris, S. G. Sligar and I. Schlichting, *Chemical Reviews* **2005**, *105*, 2253-2278.

[245] B. Meunier, S. P. de Visser and S. Shaik, *Chemical Reviews* **2004**, *104*, 3947-3980.

[246] M. M. Abu-Omar, A. Loaiza and N. Hontzeas, *Chemical Reviews* **2005**, *105*, 2227-2252.

[247] M. Costas, M. P. Mehn, M. P. Jensen and L. Que, *Chemical Reviews* **2004**, *104*, 939-986.

[248] X. Shan and L. Que Jr, *Journal of Inorganic Biochemistry* **2006**, *100*, 421-433.

[249] S. V. Kryatov, E. V. Rybak-Akimova and S. Schindler, *Chemical Reviews* **2005**, *105*, 2175-2226.

[250] J. M. Bollinger Jr and C. Krebs, *Journal of Inorganic Biochemistry* **2006**, *100*, 586-605.

[251] D. P. Galonic, E. W. Barr, C. T. Walsh, J. M. Bollinger and C. Krebs, *Nature Chemical Biology* **2007**, *3*, 113-116.

[252] W. Nam, *Accounts of Chemical Research* **2007**, *40*, 522-531.

[253] J.-U. Rohde, J.-H. In, M. H. Lim, W. W. Brennessel, M. R. Bukowski, A. Stubna, E. Münck, W. Nam and L. Que, *Science* **2003**, *299*, 1037-1039.

[254] J. Kaizer, E. J. Klinker, N. Y. Oh, J.-U. Rohde, W. J. Song, A. Stubna, J. Kim, E. Münck, W. Nam and L. Que, *Journal of the American Chemical Society* **2003**, *126*, 472-473.

[255] C. V. Sastri, M. Sook Seo, M. Joo Park, K. Mook Kim and W. Nam, *Chemical Communications* **2005**, 1405-1407.

[256] K. M. Kadish, E. Van Caemelbecke, F. D'Souza, C. J. Medforth, K. M. Smith, A. Tabard and R. Guilard, *Organometallics* **1993**, *12*, 2411-2413.

[257] S. O. Kim, C. V. Sastri, M. S. Seo, J. Kim and W. Nam, *Journal of the American Chemical Society* **2005**, *127*, 4178-4179.

[258] C. V. Sastri, M. J. Park, T. Ohta, T. A. Jackson, A. Stubna, M. S. Seo, J. Lee, J. Kim, T. Kitagawa, E. Münck, L. Que and W. Nam, *Journal of the American Chemical Society* **2005**, *127*, 12494-12495.

[259] M. Martinho, F. Banse, J.-F. Bartoli, T. A. Mattioli, P. Battioni, O. Horner, S. Bourcier and J.-J. Girerd, *Inorganic Chemistry* **2005**, *44*, 9592-9596.

[260] E. J. Klinker, J. Kaizer, W. W. Brennessel, N. L. Woodrum, C. J. Cramer and L. Que, *Angewandte Chemie International Edition* **2005**, *44*, 3690-3694.

[261] C. V. Sastri, K. Oh, Y. J. Lee, M. S. Seo, W. Shin and W. Nam, *Angewandte Chemie International Edition* **2006**, *45*, 3992-3995.

[262] Y. Suh, M. S. Seo, K. M. Kim, Y. S. Kim, H. G. Jang, T. Tosha, T. Kitagawa, J. Kim and W. Nam, *Journal of Inorganic Biochemistry* **2006**, *100*, 627-633.

[263] K. Nehru, M. S. Seo, J. Kim and W. Nam, *Inorganic Chemistry* **2006**, *46*, 293-298.

[264] V. Balland, M.-F. Charlot, F. Banse, J.-J. Girerd, Tony A. Mattioli, E. Bill, J.-F. Bartoli, P. Battioni and D. Mansuy, *European Journal of Inorganic Chemistry* **2004**, *2004*, 301-308.

[265] D. T. Shay, G. P. A. Yap, L. N. Zakharov, A. L. Rheingold and K. H. Theopold, *Angewandte Chemie International Edition* **2005**, *44*, 1508-1510.

[266] X. Hu and K. Meyer, *Journal of the American Chemical Society* **2004**, *126*, 16322-16323.

[267] E. R. King, G. T. Sazama and T. A. Betley, *Journal of the American Chemical Society* **2012**, *134*, 17858-17861.

[268] R. E. Cowley, R. P. Bontchev, J. Sorrell, O. Sarracino, Y. Feng, H. Wang and J. M. Smith, *Journal of the American Chemical Society* **2007**, *129*, 2424-2425.

[269] M. Ingleson, H. Fan, M. Pink, J. Tomaszewski and K. G. Caulton, *Journal of the American Chemical Society* **2006**, *128*, 1804-1805.

[270] M. M. Maltempo, T. H. Moss and M. A. Cusanovich, *Biochim Biophys Acta* **1974**, *342*, 290-305.

[271] P. Legzdins, W. S. McNeil, K. M. Smith and R. Poli, *Organometallics* **1998**, *17*, 615-622.

[272] R. B. King, *Inorganic Chemistry* **1967**, *6*, 30-34.

[273] D. Seddon, W. G. Kita, J. Bray, J. A. McCleverty, S. P. Anand and R. B. King in *Dicarbonyl-η-Cyclopentadienylnitrosyl-Molybdenum and bis(Dihalo-η-Cyclopentadienylnitrosyl-Molybdenum) Derivatives*, *Vol.* John Wiley & Sons, Inc., **2007**, p. 24-29.

[274] W. Zhou, L. Tang, B. O. Patrick and K. M. Smith, *Organometallics* **2011**, *30*, 603-610.

[275] K. C. MacLeod, J. L. Conway, L. Tang, J. J. Smith, L. D. Corcoran, K. H. D. Ballem, B. O. Patrick and K. M. Smith, *Organometallics* **2009**, *28*, 6798-6806.

[276] K. M. Smith, *Organometallics* **2005**, *24*, 778-784.

[277] J. L. Durham, J. N. Tirado, S. A. Knott, M. K. Oh, R. McDonald and L. F. Szczepura, *Inorganic Chemistry* **2012**, *51*, 7825-7836.

[278] P. D. Metelski, V. A. Adamian and J. H. Espenson, *Inorganic Chemistry* **2000**, *39*, 2434-2439.

[279] M. Periasamy, A. Mukkanti and D. S. Raj, *Organometallics* **2004**, *23*, 6323-6326.

[280] A. Vigalok, *Organometallics* **2011**, *30*, 4802-4810.

[281] H.-J. Frohn and V. V. Bardin, *Organometallics* **2001**, *20*, 4750-4762.

[282] H. K. Nagra, R. J. Batchelor, A. J. Bennet, F. W. B. Einstein, E. C. Lathioor, R. K. Pomeroy and W. Wang, *Journal of the American Chemical Society* **1996**, *118*, 1207-1208.

[283] R. S. Brown, R. W. Nagorski, A. J. Bennet, R. E. D. McClung, G. H. M. Aarts, M. Klobukowski, R. McDonald and B. D. Santarsiero, *Journal of the American Chemical Society* **1994**, *116*, 2448-2456.

[284] H. Slebocka-Tilk, R. G. Ball and R. S. Brown, *Journal of the American Chemical Society* **1985**, *107*, 4504-4508.

[285] A. A. Neverov and R. S. Brown, *Canadian Journal of Chemistry* **1994**, *72*, 2540-2543.

[286] A. J. Bennet, R. S. Brown, R. E. D. McClung, M. Klobukowski, G. H. M. Aarts, B. D. Santarsiero, G. Bellucci and R. Bianchini, *Journal of the American Chemical Society* **1991**, *113*, 8532-8534.

[287] I. Krossing and I. Raabe, *Angewandte Chemie International Edition* **2004**, *43*, 2066-2090.

[288] H. Salem, L. J. W. Shimon, G. Leitus, L. Weiner and D. Milstein, *Organometallics* **2008**, *27*, 2293-2299.

[289] S. H. Strauss, *Chemical Reviews* **1993**, *93*, 927-942.

[290] W. V. Konze, B. L. Scott and G. J. Kubas, *Chemical Communications* **1999**, *0*, 1807-1808.

[291] L. Jia, X. Yang, C. L. Stern and T. J. Marks, *Organometallics* **1997**, *16*, 842-857.

[292] L. Jia, X. Yang, A. Ishihara and T. J. Marks, *Organometallics* **1995**, *14*, 3135-3137.

[293] K. Seppelt, *Angewandte Chemie International Edition in English* **1993**, *32*, 1025-1027.

[294] S. A. Cummings, M. Iimura, C. J. Harlan, R. J. Kwaan, I. V. Trieu, J. R. Norton, B. M. Bridgewater, F. Jäkle, A. Sundararaman and M. Tilset, *Organometallics* **2006**, *25*, 1565-1568.

[295] D. H. Hill, M. A. Parvez and A. Sen, *Journal of the American Chemical Society* **1994**, *116*, 2889-2901.

[296] S. Chang, J. Yoon and M. Brookhart, *Journal of the American Chemical Society* **1994**, *116*, 1869-1879.

[297] D. Lexa, J. M. Saveant, B. Su Khac and D. L. Wang, *Journal of the American Chemical Society* **1988**, *110*, 7617-7625.

[298] C. Gueutin, D. Lexa, J. M. Saveant and D. L. Wang, *Organometallics* **1989**, *8*, 1607-1613.

[299] A. Bondi, *The Journal of Physical Chemistry* **1964**, *68*, 441-451.

[300] S. L. Stokes, W. M. Davis, A. L. Odom and C. C. Cummins, *Organometallics* **1996**, *15*, 4521-4530.

[301] S. Pohl, U. Bierbach and W. Saak, *Angewandte Chemie* **1989**, *101*, 796-797.

[302] P. Hamon, L. Toupet, J. R. Hamon and C. Lapinte, *Organometallics* **1992**, *11*, 1429-1431.

[303] K. C. Jantunen, F. Haftbaradaran, M. J. Katz, R. J. Batchelor, G. Schatte and D. B. Leznoff, *Dalton Transactions* **2005**, *0*, 3083-3091.

[304] C. E. Hayes and D. B. Leznoff, *Organometallics* **2010**, *29*, 767-774.

[305] R. R. Schrock, A. L. Casado, J. T. Goodman, L.-C. Liang, P. J. Bonitatebus and W. M. Davis, *Organometallics* **2000**, *19*, 5325-5341.

[306] N. Emig, H. Nguyen, H. Krautscheid, R. Réau, J.-B. Cazaux and G. Bertrand, *Organometallics* **1998**, *17*, 3599-3608.

[307] H. C. S. Clark, F. G. N. Cloke, P. B. Hitchcock, J. B. Love and A. P. Wainwright, *Journal of Organometallic Chemistry* **1995**, *501*, 333-340.

[308] J. Xiao and L. Deng, *Organometallics* **2011**, *31*, 428-434.

[309] D. Luart, M. Sellin, P. Laurent, J.-Y. Salauen, R. Pichon, L. Toupet and H. Des Abbayes, *Organometallics* **1995**, *14*, 4989-4991.

[310] C. J. Davies, S. J. Hilton, G. A. Solan, W. Stannard and J. Fawcett, *Polyhedron* **2005**, *24*, 2017-2026.

Appendices

Appendix A. Crystallographic data

A.1. Crystallographic data for 1-4

	1	2	3	4
Empirical Formula	$C_{24}H_{60}Br_4Fe_4N_4O_2Si_4$	$C_{24}H_{60}Br_4Co_4N_4O_2Si_4$	$C_{12}H_{30}Cl_2Fe_2N_2O_1Si_2$	$C_{40}H_{92}Cl_6Co_4Li_2N_4O_6Si_4$
Formula weight	1092.12	1104.46	457.15	1299.86
Crystal system	Monoclinic	Monoclinic	Triclinic	Triclinic
Space group	$P2_1/n$	$P2_1/n$	P -1	P -1
a (Å)	9.9613(16)	9.9296(2)	8.678(4)	11.0506(19)
b (Å)	14.460(2)	14.2666(3)	10.910(5)	12.391(2)
c (Å)	15.729(2)	15.5281(3)	12.131(5)	13.330(2)
α (°)	90	90	73.617(5)	89.942(2)
β (°)	104.525(2)	104.2860(10)	89.898(6)	88.776(2)
γ (°)	90	90	68.368(6)	64.740(2)
V ($Å^3$)	2193.2(6)	2131.71(8)	1017.4(8)	1650.3(5)
Z	2	2	2	1
T (K)	293	149(2)	150(2)	293
ρ_{calcd} ($g.cm^{-3}$)	1.654	1.721	1.492	1.309
μ (mm^{-1})	5.075	5.417	1.805	1.342
Unique Reflections collected	25725	88444	4630	19235
Observed reflections	5236	10515	4630	7580
R [$I_o \geq 3\sigma(I_o)$]	0.0255	0.0211	0.0694	0.0503
R_w [$I_o \geq 3\sigma(I_o)$]	0.0247	0.0213	0.0776	0.0587
Goodness of fit	2.6652	0.7141	1.3226	2.6647

A.2. Crystallographic data for 5

Empirical Formula	$C_{42}H_{48}Cl_4Fe_2N_4$
Formula weight	862.37
Crystal system	'Monoclinic'
Space group	$P2_1/n$
a (Å)	11.399(2)
b (Å)	18.051(3)
c (Å)	11.370(2)
α (°)	90
β (°)	115.4950(10)
γ (°)	90
V ($Å^3$)	2111.9(6)
Z	2
T (K)	293
ρ_{calcd} ($g.cm^{-3}$)	1.356
μ (mm^{-1})	0.974
Unique Reflections collected	25030
Observed reflections	5077
R [$I_o \geq 3\sigma(I_o)$]	0.0343
R_w [$I_o \geq 3\sigma(I_o)$]	0.0356
Goodness of fit	1.0495

A.3. Crystallographic data for 6-7

	6	**7**
Empirical Formula	$C_{20}H_{52}Fe_2N_2OSi_4$	$C_{20}H_{52}Co_2N_2OSi_4$
Formula weight	560.68	566.86
Crystal system	'Monoclinic'	Triclinic
Space group	$P2_1/c$	P -1
a (Å)	9.8765(12)	10.85(3)
b (Å)	21.792(3)	11.62(3)
c (Å)	15.3340(19)	14.67(7)
α (°)	90	100.32(4)
β (°)	108.0260(10)	103.76(4)
γ (°)	90	113.45(3)
V ($Å^3$)	3138.4(7)	1568(10)
Z	4	2
T (K)	293	293
ρ_{calcd} ($g.cm^{-3}$)	1.187	1.2
μ (mm^{-1})	1.09	1.223
Unique Reflections collected	37159	14320
Observed reflections	7502	7317
R [$I_o \geq 3\sigma(I_o)$]	0.022	0.0602
R_w [$I_o \geq 3\sigma(I_o)$]	0.0362	0.0535
Goodness of fit	1.3722	1.3142

A.4. Crystallographic data for 8-11

	8	**9**	**10**	**11**
Empirical Formula	$C_{16}H_{41}ClFe_2N_2OSi_3$	$C_{16}H_{41}ClCo_2N_2OSi_3$	$C_{16}H_{41}BrFe_2N_2OSi_3$	$C_{16}H_{41}BrCo_2N_2OSi_3$
Formula weight	508.92	515.09	553.37	559.54
Crystal system	'Monoclinic'	'Monoclinic'	'Triclinic'	'Triclinic'
Space group	$P2_1/c$	$P2_1/c$	P -1	P 1
a (Å)	34.266(3)	15.300(2)	8.6236(8)	10.1151(9)
b (Å)	10.7540(9)	10.4403(17)	10.8572(10)	10.9494(9)
c (Å)	15.4569(13)	16.293(3)	14.8851(14)	13.1148(11)
α (°)	90	90	85.4050(10)	83.3390(10)
β (°)	113.8740(10)	95.902(2)	73.5130(10)	79.0720(10)
γ (°)	90	90	78.0840(10)	71.7840(10)
V ($Å^3$)	5208.4(8)	2588.8(7)	1307.2(2)	1352.2(2)
Z	8	4	2	2
T (K)	293	293	150	150
ρ_{calcd} ($g.cm^{-3}$)	1.298	1.321	1.406	1.374
μ (mm^{-1})	1.362	1.531	2.783	2.844
Unique Reflections collected	30975	30577	15365	15695
Observed reflections	6262	6205	6059	6194
R [$I_o \geq 3\sigma(I_o)$]	0.031	0.0741	0.0214	0.0261
R_w [$I_o \geq 3\sigma(I_o)$]	0.0327	0.0677	0.0231	0.0279
Goodness of fit	1.1504	0.9564	1.0931	1.1025

A.5. Crystallographic data for 12-13

	12	**13**
Empirical Formula	$C_{13}H_{33}BrFe_2N_2OSi_2$	$C_{13}H_{33}ClCo_2N_2OSi_2$
Formula weight	481.19	442.91
Crystal system	'Monoclinic'	'Monoclinic'
Space group	$P2_1/n$	$P2_1/n$
a (Å)	9.9814(6)	10.0976(15)
b (Å)	14.5943(8)	14.306(2)
c (Å)	15.7273(9)	15.404(2)
α (°)	90	90
β (°)	104.1440(10)	103.144(2)
γ (°)	90	90
V ($Å^3$)	2221.6(2)	2166.8(6)
Z	4	4
T (K)	293	150
ρ_{calcd} ($g.cm^{-3}$)	1.439	1.358
μ (mm^{-1})	3.212	1.765
Unique Reflections collected	26027	25500
Observed reflections	5302	5185
R [$I_o \geq 3\sigma(I_o)$]	0.0585	0.0316
R_w [$I_o \geq 3\sigma(I_o)$]	0.0574	0.0286
Goodness of fit	0.9894	1.1035

A.6. Crystallographic data for 14-15

	14	**15**
Empirical Formula	$C_{24}H_{30}Co_2F_{10}N_2OSi_2$	$C_{18}H_{30}ClF_5Fe_2N_2OSi_2$
Formula weight	726.53	588.76
Crystal system	'Triclinic'	'Monoclinic'
Space group	P -1	$P2_1/c$
a (Å)	9.6344(15)	10.0302(12)
b (Å)	11.7218(19)	27.482(3)
c (Å)	14.912(2)	10.5323(12)
α (°)	85.727(2)	90
β (°)	75.814(2)	96.4120(10)
γ (°)	67.788(2)	90
V ($Å^3$)	1511.3(4)	2885.0(6)
Z	2	4
T (K)	150	293
ρ_{calcd} ($g.cm^{-3}$)	1.597	1.355
μ (mm^{-1})	1.26	1.225
Unique Reflections collected	18037	34089
Observed reflections	7057	6979
R [$I_o \geq 3\sigma(I_o)$]	0.0294	0.08
R_w [$I_o \geq 3\sigma(I_o)$]	0.0301	0.0768
Goodness of fit	1.1303	1.0057

A.7. Crystallographic data for 16

Empirical Formula	$C_{24}H_{41}Fe_{1.5}N_2O_6Si_3$
Formula weight	621.63
Crystal system	'Monoclinic'
Space group	$P2_1/n$
a (Å)	22.512(2)
b (Å)	13.8849(14)
c (Å)	22.720(4)
α (°)	90
β (°)	110.8700(10)
γ (°)	90
V (Å^3)	6635.7(14)
Z	8
T (K)	150
ρ_{calcd} (g.cm^{-3})	1.244
μ (mm^{-1})	0.808
Unique Reflections collected	39347
Observed reflections	7876
R [$I_o \geq 3\sigma(I_o)$]	0.0321
R_w [$I_o \geq 3\sigma(I_o)$]	0.0339
Goodness of fit	1.0636

A.8. Crystallographic data for 17

Empirical Formula	$C_{22}H_{34}BrFeN_2OSi_2$
Formula weight	534.45
Crystal system	'Monoclinic'
Space group	$P2_1/n$
a (Å)	15.990(7)
b (Å)	12.009(2)
c (Å)	15.105(5)
α (°)	90
β (°)	117.06(3)
γ (°)	90
V ($Å^3$)	2583.0(16)
Z	4
T (K)	293
ρ_{calcd} ($g.cm^{-3}$)	1.374
μ (mm^{-1})	2.239
Unique Reflections collected	3822
Observed reflections	3614
R [$I_o \geq 3\sigma(I_o)$]	0.0482
R_w [$I_o \geq 3\sigma(I_o)$]	0.0431
Goodness of fit	1.5026

A.9. Crystallographic data for 18

Empirical Formula	$C_{30}H_{76}Cl_2Fe_2N_4O_2P_2Si_4$
Formula weight	881.85
Crystal system	'Monoclinic'
Space group	$P2_1/c$
a (Å)	13.1494(5)
b (Å)	8.5175(3)
c (Å)	22.2569(9)
α (°)	90
β (°)	101.16
γ (°)	90
V ($Å^3$)	2445.63(16)
Z	2
T (K)	150
ρ_{calcd} ($g.cm^{-3}$)	1.197
μ (mm^{-1})	0.894
Unique Reflections collected	28760
Observed reflections	5820
R [$I_o \geq 3\sigma(I_o)$]	0.0258
R_w [$I_o \geq 3\sigma(I_o)$]	0.0268
Goodness of fit	1.0595

A.10. Crystallographic data for 19-22

	19	20	21	22
Empirical Formula	$C_{11}H_{25}FeN_3$	$C_{9.43}H_{21.43}Co_{0.86}N_{2.57}$	$C_{10}H_{22}FeN_2O$	$C_{10}H_{21}CoN_2O$
Formula weight	255.19	221.38	242.14	244.22
Crystal system	'Monoclinic'	'Monoclinic'	'Monoclinic'	'Triclinic'
Space group	$P2_1/c$	$P2_1/c$	$P2_1/c$	P 1
a (Å)	8.7585(14)	8.6916(15)	9.0688(5)	8.5688(5)
b (Å)	14.596(2)	17.344(3)	10.7499(6)	8.8033(5)
c (Å)	11.2495(18)	27.579(5)	12.8612(8)	9.3338(5)
α (°)	90	90	90	65.3970(10)
β (°)	97.603(2)	93.670(2)	100.0290(10)	77.5070(10)
γ (°)	90	90	90	82.9790(10)
V ($Å^3$)	1425.5(4)	4149.0(12)	1234.66(12)	624.59(6)
Z	4	14	4	2
T (K)	293	293	150	150
ρ_{calcd} ($g.cm^{-3}$)	1.189	1.24	1.303	1.298
μ (mm^{-1})	1.036	1.218	1.196	1.348
Unique Reflections collected	16766	48980	14516	7390
Observed reflections	3411	9936	2957	5498
R [$I_o \geq 3\sigma(I_o)$]	0.025	0.045	0.0194	0.025
R_w [$I_o \geq 3\sigma(I_o)$]	0.027	0.0407	0.0216	0.0283
Goodness of fit	1.1019	1.1378	1.0729	0.1519

A.11. Crystallographic data for 23-25

	23	**24**	**25**
Empirical Formula	$C_{11}H_{27}Cl_2FeN_3$	$C_{11}H_{27}Cl_2CoN_3$	$C_{10}H_{24}Cl_2FeN_2O$
Formula weight	328.11	331.19	315.07
Crystal system	'Monoclinic'	'Monoclinic'	'Monoclinic'
Space group	$P2_1/c$	C2/c	C2/c
a (Å)	20.682(8)	20.534(3)	19.5577(16)
b (Å)	7.619(3)	7.6321(9)	7.4115(6)
c (Å)	12.663(5)	12.5481(15)	11.5235(10)
α (°)	90	90	90
β (°)	125.743(4)	125.6720(10)	117.0000(10)
γ (°)	90	90	90
V ($Å^3$)	1619.5(10)	1597.5(3)	1488.3(2)
Z	4	4	4
T (K)	293	150	150
ρ_{calcd} ($g.cm^{-3}$)	1.346	1.377	1.406
μ (mm^{-1})	1.247	1.394	1.357
Unique Reflections collected	9573	19015	8732
Observed reflections	1946	1916	1780
R [$I_o \geq 3\sigma(I_o)$]	0.0637	0.0331	0.0263
R_w [$I_o \geq 3\sigma(I_o)$]	0.0642	0.0287	0.0266
Goodness of fit	1.1254	1.1183	1.1044

Appendix B. Fractional atomic coordinates and isotropic thermal parameters

B.1. Fractional atomic coordinates and Uiso for $\{Fe_2Br_2[^{tBu}NON]\}_2$ (**1**)

Atom	x	y	z	U(iso)
Fe1	0.53519(4)	0.60328(2)	0.44150(2)	0.0342
Fe2	0.67970(4)	0.75159(3)	0.42147(3)	0.04
Br1	0.34045(3)	0.48839(2)	0.421218(19)	0.0461
Br2	0.81645(4)	0.88091(3)	0.41766(3)	0.0858
Si1	0.37106(8)	0.76729(5)	0.36547(5)	0.041
Si2	0.52856(8)	0.64546(5)	0.25846(5)	0.0386
N1	0.5019(2)	0.74197(14)	0.46100(13)	0.0339
N2	0.6591(2)	0.62937(14)	0.35640(13)	0.033
O1	0.40359(17)	0.68531(12)	0.30021(11)	0.0379
C1	0.1917(3)	0.7493(2)	0.3742(2)	0.0673
C2	0.3869(3)	0.88286(19)	0.3161(2)	0.0661
C3	0.4631(3)	0.5383(2)	0.19911(19)	0.0576
C4	0.5673(3)	0.7335(2)	0.1816(2)	0.0666
C11	0.5040(3)	0.78225(19)	0.54964(19)	0.0464
C21	0.6518(3)	0.7789(2)	0.60743(19)	0.0652
C111	0.4123(3)	0.7251(2)	0.5934(2)	0.0645
C112	0.7939(3)	0.57943(19)	0.35937(19)	0.0438
C113	0.4537(4)	0.8826(2)	0.5408(2)	0.0782
C211	0.7727(3)	0.47545(19)	0.3601(2)	0.0604
C212	0.8475(3)	0.6062(2)	0.2791(2)	0.0661
C213	0.9020(3)	0.6083(2)	0.4426(2)	0.056
H11	0.1297	0.7489	0.3172	0.094(2)
H12	0.1862	0.69	0.4045	0.094(2)
H13	0.1659	0.7974	0.4085	0.094(2)
H21	0.4797	0.8908	0.3118	0.070(2)
H22	0.3646	0.93	0.3523	0.070(2)
H23	0.3256	0.8865	0.2592	0.070(2)
H31	0.3912	0.5587	0.1487	0.075(2)
H32	0.424	0.4989	0.2354	0.075(2)
H33	0.5366	0.51	0.1792	0.075(2)
H41	0.4828	0.7511	0.1415	0.090(2)
H42	0.6279	0.7047	0.1504	0.090(2)
H43	0.6102	0.7842	0.2132	0.090(2)

H211	0.653	0.8064	0.6636	0.094(2)
H212	0.6846	0.7161	0.6174	0.095(2)
H213	0.7148	0.8156	0.5808	0.095(2)
H1111	0.4148	0.752	0.6496	0.085(2)
H1112	0.3174	0.7242	0.5586	0.085(2)
H1113	0.4464	0.6625	0.6	0.085(2)
H1131	0.5113	0.9166	0.5109	0.109(2)
H1132	0.4651	0.9075	0.5991	0.110(2)
H1133	0.3555	0.8868	0.5101	0.109(2)
H2111	0.7355	0.4614	0.4112	0.082(2)
H2112	0.8579	0.4448	0.3668	0.082(2)
H2113	0.7055	0.4564	0.3069	0.082(2)
H2121	0.8551	0.6719	0.2762	0.091(2)
H2122	0.9358	0.5783	0.2818	0.091(2)
H2123	0.7799	0.5866	0.2251	0.090(2)
H2131	0.9141	0.6752	0.4443	0.075(2)
H2132	0.9897	0.5767	0.4451	0.075(2)
H2133	0.8683	0.591	0.4907	0.075(2)

B.2. Fractional atomic coordinates and Uiso for $\{Co_2Br_2[^{tBu}NON]\}_2$ (**2**)

Atom	x	y	z	U(iso)
Co1	0.53398(2)	0.896771(14)	0.443228(13)	0.0147
Co2	0.67614(2)	0.749726(15)	0.423176(14)	0.0188
Br1	0.343733(15)	1.010829(11)	0.420044(10)	0.0197
Br2	0.80170(2)	0.615982(14)	0.411360(16)	0.0418
Si1	0.52767(4)	0.85582(3)	0.26005(3)	0.0179
Si2	0.36982(4)	0.73333(3)	0.37046(3)	0.0186
N1	0.65815(12)	0.87090(9)	0.35919(8)	0.0161
N2	0.50334(12)	0.75915(9)	0.46507(8)	0.0162
O1	0.40251(10)	0.81541(7)	0.30326(7)	0.018
C1	0.46453(17)	0.96452(13)	0.19972(11)	0.0269
C2	0.56702(19)	0.76610(14)	0.18299(12)	0.0337
C3	0.19122(16)	0.75198(14)	0.38286(13)	0.0321
C4	0.38425(19)	0.61653(12)	0.32066(13)	0.0313
C11	0.79425(15)	0.91947(11)	0.36393(11)	0.02
C21	0.51055(17)	0.71987(11)	0.55584(10)	0.0219
C111	0.85129(17)	0.89039(14)	0.28459(12)	0.0308
C112	0.89833(15)	0.88884(12)	0.44941(11)	0.0244
C113	0.77691(17)	1.02535(12)	0.36414(12)	0.0265

C211	0.4642(2)	0.61755(12)	0.54901(13)	0.0341
C212	0.41852(19)	0.77749(13)	0.60142(12)	0.0294
C213	0.66021(18)	0.72457(13)	0.61104(11)	0.0295
H11	0.433	1.007	0.2378	0.0359(11)
H12	0.5356	0.992	0.1778	0.0360(11)
H13	0.3879	0.9483	0.152	0.0363(11)
H21	0.4819	0.7423	0.1467	0.0482(11)
H22	0.6182	0.7147	0.2147	0.0494(11)
H23	0.6208	0.7927	0.1471	0.0479(11)
H31	0.1816	0.8152	0.4063	0.0453(11)
H32	0.1682	0.7057	0.4232	0.0452(11)
H33	0.1259	0.7456	0.3258	0.0455(11)
H41	0.3272	0.614	0.2602	0.0412(11)
H42	0.4769	0.6027	0.3194	0.0414(11)
H43	0.3559	0.5671	0.3546	0.0425(11)
H1111	0.8598	0.8229	0.2815	0.0444(11)
H1112	0.788	0.9128	0.2298	0.0434(11)
H1113	0.9428	0.9182	0.2902	0.0430(11)
H1121	0.9843	0.9217	0.4554	0.0312(11)
H1122	0.9123	0.8193	0.4493	0.0306(11)
H1123	0.8642	0.9054	0.5005	0.0300(11)
H1131	0.8653	1.056	0.3674	0.0351(11)
H1132	0.7404	1.0456	0.4145	0.0352(11)
H1133	0.7121	1.0452	0.3099	0.0361(11)
H2111	0.5191	0.5845	0.5179	0.0486(11)
H2112	0.477	0.5922	0.6059	0.0473(11)
H2113	0.3683	0.6113	0.517	0.0467(11)
H2121	0.4518	0.8402	0.608	0.0408(11)
H2122	0.425	0.751	0.6589	0.0417(11)
H2123	0.3239	0.776	0.5692	0.0422(11)
H2131	0.6648	0.7018	0.6695	0.0383(11)
H2132	0.7186	0.6866	0.5835	0.0391(11)
H2133	0.6934	0.7891	0.615	0.0388(11)

B.3. Fractional atomic coordinates and Uiso for $\{Fe_2Cl_2[^{tBu}NON]\}_n$ (**3**)

Atom	x	y	z	U(iso)
Fe1	0.0650(2)	0.48596(17)	0.14278(14)	0.0192
Fe2	0.0588(2)	0.49838(17)	0.35834(14)	0.0185
Cl1	0.1882(4)	0.4750(3)	-0.0331(2)	0.0278

Cl2	-0.1828(3)	0.5134(3)	0.4603(2)	0.0259
Si1	0.3759(4)	0.2973(3)	0.2999(3)	0.0218
Si2	0.2737(4)	0.6259(3)	0.2120(3)	0.0214
O1	0.3661(9)	0.4572(7)	0.2482(8)	0.0278
N1	0.1596(10)	0.3288(8)	0.2962(8)	0.0174
N2	0.0602(10)	0.6450(8)	0.2082(8)	0.0156
C1	0.4998(15)	0.2167(13)	0.4440(11)	0.0323
C2	0.4925(16)	0.2014(13)	0.2039(11)	0.0365
C3	0.3499(16)	0.6860(13)	0.3208(11)	0.036
C4	0.3396(15)	0.6987(12)	0.0705(10)	0.0302
C11	0.1035(14)	0.2093(11)	0.3401(10)	0.0233
C21	-0.0765(13)	0.7871(11)	0.1619(10)	0.0227
C111	0.2059(15)	0.0863(12)	0.3011(10)	0.0294
C112	-0.0796(14)	0.2529(11)	0.2949(10)	0.0291
C113	0.1192(15)	0.1620(13)	0.4747(9)	0.0287
C211	-0.0983(15)	0.8358(12)	0.0278(10)	0.0303
C212	-0.2416(14)	0.7820(12)	0.2026(11)	0.0338
C213	-0.0409(15)	0.8923(11)	0.2055(10)	0.0276
H11	0.4498	0.2695	0.4972	0.039(6)
H12	0.6133	0.2126	0.4404	0.038(6)
H13	0.5043	0.1238	0.4781	0.038(6)
H21	0.5278	0.1001	0.2418	0.041(6)
H22	0.5931	0.2184	0.1882	0.041(6)
H23	0.427	0.2237	0.1324	0.041(6)
H31	0.2965	0.6716	0.3902	0.044(6)
H32	0.4701	0.6363	0.3415	0.044(6)
H33	0.3286	0.7838	0.29	0.044(6)
H41	0.2935	0.7974	0.0453	0.041(6)
H42	0.3017	0.6693	0.0099	0.041(6)
H43	0.4585	0.6676	0.0726	0.041(6)
H1111	0.1692	0.0116	0.3288	0.034(6)
H1112	0.2019	0.1114	0.2186	0.034(6)
H1113	0.3248	0.0524	0.3333	0.034(6)
H1121	-0.1176	0.1795	0.3252	0.031(6)
H1122	-0.0945	0.2785	0.2108	0.031(6)
H1123	-0.1504	0.3324	0.3162	0.031(6)
H1131	0.0815	0.0881	0.5025	0.032(6)
H1132	0.2346	0.1337	0.505	0.032(6)
H1133	0.0509	0.2411	0.5009	0.032(6)
H2111	-0.1233	0.7698	-0.001	0.027(6)
H2112	-0.1855	0.9244	-0.0025	0.027(6)

H2113	0.0057	0.8401	-0.0007	0.027(6)
H2121	-0.3318	0.8689	0.1697	0.034(6)
H2122	-0.236	0.7585	0.287	0.034(6)
H2123	-0.2651	0.711	0.1811	0.034(6)
H2131	-0.0299	0.8655	0.2895	0.031(6)
H2132	0.0624	0.8996	0.1811	0.031(6)
H2133	-0.129	0.9824	0.1771	0.031(6)

B.4. Fractional atomic coordinates and Uiso for $\{Co_2Cl_2[^{tBu}NON](LiCl)\cdot 2THF\}_2$ (**4**)

Atom	x	y	z	U(iso)
Co1	0.59814(8)	0.38873(7)	0.41937(6)	0.0504
Co2	0.71131(9)	0.28108(8)	0.24761(7)	0.065
Cl1	0.43991(16)	0.59164(13)	0.40862(12)	0.0643
Cl2	0.8541(2)	0.12033(18)	0.15347(15)	0.099
Cl3	0.6280(3)	0.41007(18)	0.11479(15)	0.1144
Si1	0.65474(18)	0.13107(16)	0.40803(16)	0.0672
Si2	0.88635(17)	0.21493(16)	0.43123(14)	0.0611
N1	0.5682(5)	0.2613(4)	0.3397(4)	0.0602
N2	0.7878(4)	0.3424(4)	0.3634(3)	0.0522
O1	0.7920(4)	0.1441(4)	0.4347(3)	0.0745
O3	0.9098(8)	0.2765(9)	-0.0511(7)	0.185(3)
O41	0.6745(15)	0.1895(14)	-0.0695(11)	0.130(2)
O42	0.7070(14)	0.1999(13)	-0.0945(10)	0.130(2)
C1	0.5769(7)	0.1200(6)	0.5307(5)	0.0937
C2	0.7033(7)	-0.0125(5)	0.3412(6)	0.096
C3	1.0494(6)	0.1138(6)	0.3730(6)	0.0885
C4	0.9178(7)	0.2392(6)	0.5636(5)	0.0903
C11	0.4377(7)	0.2801(7)	0.2920(7)	0.0913
C21	0.8409(6)	0.4340(5)	0.3413(5)	0.0792
C31	0.934(2)	0.279(3)	-0.1563(10)	0.235(3)
C32	1.050(2)	0.298(3)	-0.1682(16)	0.235(3)
C33	1.1213(16)	0.265(3)	-0.071(2)	0.235(3)
C34	1.0386(18)	0.234(3)	-0.0064(16)	0.235(3)
C35	1.0309(19)	0.1850(16)	-0.089(3)	0.235(3)
C36	1.1246(15)	0.235(2)	-0.103(2)	0.235(3)
C37	1.060(2)	0.356(2)	-0.055(2)	0.235(3)
C38	0.921(2)	0.3869(12)	-0.064(2)	0.235(3)
C41	0.5390(17)	0.2502(13)	-0.0967(17)	0.130(2)
C42	0.4923(14)	0.1653(17)	-0.1226(17)	0.130(2)

C43	0.6044(19)	0.0506(13)	-0.1202(17)	0.130(2)
C44	0.7123(17)	0.0657(14)	-0.0796(17)	0.130(2)
C45	0.5887(18)	0.2631(12)	-0.1464(14)	0.130(2)
C46	0.5381(15)	0.1819(15)	-0.1797(14)	0.130(2)
C47	0.6542(18)	0.0662(12)	-0.1804(15)	0.130(2)
C48	0.7606(14)	0.0876(14)	-0.1423(15)	0.130(2)
C111	0.3553(7)	0.4089(7)	0.2676(7)	0.1341
C112	0.4653(9)	0.2088(8)	0.1936(8)	0.1535
C113	0.3557(8)	0.2336(8)	0.3573(9)	0.1573
C211	0.7380(9)	0.5523(6)	0.3085(8)	0.07
C212	0.9412(9)	0.3803(8)	0.2444(7)	0.0884
C213	0.9296(11)	0.4447(10)	0.4210(7)	0.0913
C214	0.9860(9)	0.3914(13)	0.3195(15)	0.089
C215	0.8119(18)	0.5139(13)	0.4434(9)	0.0784
C216	0.7562(16)	0.5271(12)	0.2651(11)	0.0799
Li1	0.7692(15)	0.2498(15)	0.0162(9)	0.1187
H11	0.5504	0.1934	0.5675	0.105(5)
H12	0.6413	0.0557	0.5681	0.105(5)
H13	0.4998	0.1049	0.52	0.105(5)
H21	0.7427	-0.0086	0.2772	0.109(5)
H22	0.7671	-0.0761	0.3796	0.109(5)
H23	0.6256	-0.0269	0.3315	0.109(5)
H31	1.1107	0.1495	0.3769	0.128(5)
H32	1.0359	0.1	0.3041	0.128(5)
H33	1.0837	0.0396	0.4085	0.128(5)
H41	0.9428	0.1654	0.5989	0.131(5)
H42	0.8375	0.2987	0.5938	0.131(5)
H43	0.9884	0.2645	0.5658	0.131(5)
H311	0.8862	0.364	-0.15	0.55(4)
H312	0.8927	0.2502	-0.2057	0.55(4)
H321	1.0608	0.3653	-0.196	0.55(4)
H322	1.081	0.234	-0.2164	0.55(4)
H331	1.1289	0.3314	-0.0396	0.55(4)
H332	1.209	0.2036	-0.0861	0.55(4)
H341	1.0433	0.2528	0.0627	0.55(4)
H342	1.0716	0.1486	-0.0141	0.55(4)
H351	0.9977	0.2148	-0.1539	0.55(4)
H352	1.0504	0.1018	-0.0854	0.55(4)
H361	1.1685	0.2405	-0.1639	0.55(4)
H362	1.1859	0.1705	-0.0632	0.55(4)
H371	1.0872	0.4113	-0.0872	0.55(4)

H372	1.0926	0.3425	0.0126	0.55(4)
H381	0.8843	0.4337	-0.1228	0.55(4)
H382	0.8812	0.4339	-0.0052	0.55(4)
H411	0.5388	0.2967	-0.1544	0.44(4)
H412	0.4814	0.3017	-0.0451	0.44(4)
H421	0.4522	0.1816	-0.1874	0.44(4)
H422	0.4284	0.1636	-0.0735	0.44(4)
H431	0.6325	0.027	-0.1885	0.44(4)
H432	0.5836	-0.0089	-0.088	0.44(4)
H441	0.7944	0.0325	-0.1184	0.44(4)
H442	0.7256	0.0272	-0.0156	0.44(4)
H451	0.6087	0.3017	-0.2026	0.44(4)
H452	0.524	0.3221	-0.1027	0.44(4)
H461	0.5009	0.2029	-0.2452	0.44(4)
H462	0.4709	0.1805	-0.1335	0.44(4)
H471	0.6748	0.038	-0.2484	0.44(4)
H472	0.6358	0.0097	-0.1411	0.44(4)
H481	0.822	0.0863	-0.1949	0.44(4)
H482	0.8066	0.0259	-0.095	0.44(4)
H1111	0.3331	0.4558	0.3283	0.144(5)
H1112	0.4068	0.4353	0.2234	0.144(5)
H1113	0.2746	0.4183	0.2355	0.144(5)
H1121	0.5159	0.2368	0.15	0.164(5)
H1122	0.5169	0.1255	0.2067	0.164(5)
H1123	0.3836	0.2199	0.162	0.164(5)
H1131	0.3344	0.2768	0.4198	0.173(5)
H1132	0.4078	0.1503	0.3697	0.173(5)
H1133	0.2745	0.2446	0.325	0.173(5)
H2111	0.6866	0.5403	0.2561	0.086(5)
H2112	0.7799	0.6013	0.2843	0.086(5)
H2113	0.68	0.591	0.3648	0.086(5)
H2121	0.8924	0.3714	0.1887	0.105(5)
H2122	0.9798	0.4342	0.2268	0.105(5)
H2123	1.011	0.304	0.2608	0.105(5)
H2131	0.8755	0.4758	0.4806	0.105(5)
H2132	0.9683	0.4975	0.4004	0.105(5)
H2133	0.9995	0.3673	0.4345	0.105(5)
H2141	1.0358	0.3907	0.3778	0.105(5)
H2142	1.0002	0.4402	0.2688	0.105(5)
H2143	1.0154	0.3115	0.2942	0.105(5)
H2151	0.8629	0.4629	0.496	0.090(5)

H2152	0.8406	0.5761	0.4325	0.090(5)
H2153	0.7186	0.5486	0.4622	0.090(5)
H2161	0.7643	0.4879	0.2015	0.092(5)
H2162	0.7862	0.5889	0.2579	0.092(5)
H2163	0.6642	0.5614	0.2876	0.092(5)

B.5. Fractional atomic coordinates and Uiso for {[NHC]$FeCl_2$}$_2$ (**5**)

Atom	x	y	z	U(iso)
Fe1	0.49641(2)	0.516174(13)	0.35575(2)	0.0235
Cl1	0.49205(5)	0.42914(2)	0.21385(5)	0.0341
Cl2	0.33263(4)	0.50151(3)	0.43034(4)	0.03
N1	0.60556(14)	0.67201(8)	0.33663(15)	0.0235
N2	0.39892(14)	0.67168(8)	0.23255(14)	0.0235
C1	0.50075(15)	0.62649(9)	0.30229(16)	0.0209
C2	0.56903(18)	0.74350(10)	0.29078(19)	0.0288
C3	0.43923(19)	0.74319(10)	0.2250(2)	0.0303
C11	0.74033(16)	0.65017(9)	0.40537(18)	0.0238
C12	0.17492(18)	0.66498(10)	0.20814(19)	0.0291
C13	0.04528(19)	0.64648(12)	0.1294(2)	0.036
C14	0.72184(19)	0.58682(11)	0.19859(19)	0.0308
C15	0.80944(18)	0.67234(10)	0.53512(19)	0.0285
C16	1.00333(18)	0.61772(11)	0.5332(2)	0.0305
C17	0.23244(19)	0.61464(10)	0.03937(19)	0.03
C18	0.00724(19)	0.61323(12)	0.0083(2)	0.0374
C19	0.93057(18)	0.59559(10)	0.40446(19)	0.0293
C20	0.3332(2)	0.59811(12)	-0.0099(2)	0.0379
C21	0.1020(2)	0.59717(12)	-0.0345(2)	0.0365
C22	0.26599(17)	0.64819(9)	0.16014(18)	0.0252
C23	0.2141(2)	0.70168(12)	0.3382(2)	0.0381
C24	0.7423(2)	0.71129(13)	0.6062(2)	0.0413
C25	-0.1341(2)	0.59501(15)	-0.0755(3)	0.0511
C26	1.1464(2)	0.60081(13)	0.6022(2)	0.0409
C28	0.79813(17)	0.61151(9)	0.33780(18)	0.0249
C29	0.94086(19)	0.65550(11)	0.59666(19)	0.0312
H71	0.3856	0.7837	0.1823	0.0362
H81	0.6256	0.7839	0.3046	0.0352
H131	-0.0193	0.6566	0.1593	0.0432
H141	0.7798	0.5744	0.1598	0.0482
H142	0.6642	0.6252	0.1451	0.048

H143	0.6705	0.5428	0.1922	0.0482
H191	0.9716	0.5697	0.3612	0.0354
H201	0.2919	0.5851	-0.1011	0.0569
H202	0.3868	0.5567	0.0353	0.0571
H203	0.3886	0.6407	-0.0021	0.057
H211	0.0763	0.5748	-0.1168	0.0401
H221	0.9906	0.6693	0.685	0.0379
H231	0.2487	0.7504	0.3384	0.059
H232	0.1442	0.7048	0.3608	0.059
H233	0.2839	0.6724	0.4053	0.0588
H241	0.6958	0.7539	0.5592	0.0619
H242	0.8019	0.725	0.6917	0.062
H243	0.6791	0.6769	0.6128	0.0619
H251	-0.1901	0.633	-0.0671	0.0674
H252	-0.1513	0.5913	-0.1658	0.0673
H253	-0.1582	0.5489	-0.0489	0.0674
H261	1.1819	0.5951	0.5399	0.0582
H262	1.1904	0.6409	0.6597	0.0582
H263	1.1611	0.5561	0.652	0.0585

B.6. Fractional atomic coordinates and Uiso for {$Fe_2(TMS)_2[^{tBu}NON]$} (**6**)

Atom	x	y	z	U(iso)
Fe1	0.74152(2)	0.728297(9)	0.402471(13)	0.0196
Fe2	0.85771(2)	0.645400(10)	0.322225(14)	0.0215
Si1	0.95255(4)	0.63859(2)	0.52712(3)	0.0252
Si2	0.65020(4)	0.597149(19)	0.41416(3)	0.0257
Si3	1.00576(5)	0.54906(2)	0.20819(3)	0.0273
Si4	0.57782(5)	0.867567(19)	0.37344(3)	0.0275
N1	0.94596(12)	0.69318(5)	0.44157(8)	0.0202
N2	0.65456(12)	0.65057(5)	0.32964(8)	0.0207
O1	0.82110(11)	0.59235(5)	0.47256(7)	0.0284
C1	1.06309(16)	0.73925(7)	0.44944(11)	0.0268
C2	0.53138(16)	0.66083(7)	0.24398(10)	0.0264
C3	0.93320(18)	0.62622(8)	0.21692(11)	0.0306
C4	0.66121(17)	0.80249(7)	0.44863(10)	0.0285
C10	1.19330(19)	0.70812(9)	0.43480(14)	0.045
C11	1.1073(2)	0.77057(9)	0.54289(13)	0.0429
C12	1.00885(19)	0.78766(9)	0.37543(13)	0.042
C13	1.11446(18)	0.59014(8)	0.56332(12)	0.038

C14	0.9173(2)	0.67011(9)	0.63093(12)	0.0439
C15	0.55111(18)	0.62228(9)	0.49351(12)	0.0389
C16	0.58962(18)	0.51864(8)	0.37362(14)	0.0425
C18	0.39489(17)	0.67050(8)	0.26918(11)	0.0328
C19	0.56201(18)	0.71779(8)	0.19504(11)	0.0329
C20	0.51412(19)	0.60608(9)	0.17849(12)	0.0427
C23	1.0919(2)	0.54687(9)	0.11486(13)	0.0442
C24	1.14280(18)	0.52671(8)	0.31859(12)	0.0379
C25	0.8622(2)	0.48978(9)	0.18227(14)	0.0464
C28	0.6755(2)	0.88834(8)	0.29045(13)	0.043
C29	0.3895(2)	0.84936(9)	0.30560(15)	0.0507
C30	0.5744(3)	0.93858(9)	0.44068(14)	0.0535
H101	1.1681	0.6869	0.3747	0.0733
H102	1.2657	0.7383	0.4376	0.0715
H103	1.2324	0.6782	0.4828	0.0729
H111	1.1499	0.7409	0.5929	0.0649
H112	1.0253	0.7904	0.5537	0.0646
H113	1.1763	0.8017	0.5431	0.0644
H121	1.0837	0.8166	0.3757	0.0633
H122	0.9314	0.8106	0.3855	0.0636
H123	0.9771	0.7683	0.3157	0.0637
H131	1.0988	0.5565	0.5998	0.0562
H132	1.1941	0.6137	0.5994	0.0555
H133	1.1349	0.5738	0.5115	0.055
H141	0.8926	0.6377	0.6641	0.0696
H142	1.0015	0.6893	0.6691	0.0708
H143	0.8418	0.6996	0.6149	0.0698
H151	0.57	0.6643	0.5118	0.0633
H152	0.4498	0.618	0.466	0.0633
H153	0.5796	0.5981	0.5478	0.0628
H161	0.4881	0.5182	0.3421	0.0641
H162	0.6386	0.5038	0.3331	0.0635
H163	0.6103	0.4913	0.4267	0.064
H181	0.3694	0.6338	0.2964	0.0499
H182	0.3168	0.6797	0.214	0.0497
H183	0.4063	0.7038	0.3133	0.0491
H191	0.6488	0.7125	0.1779	0.0483
H192	0.572	0.7542	0.2337	0.0479
H193	0.4852	0.7255	0.1402	0.0486
H201	0.4389	0.6149	0.1223	0.0606
H202	0.6018	0.5997	0.1633	0.06

H203	0.4889	0.5688	0.2053	0.0613
H211	1.0072	0.6553	0.2191	0.0402
H212	0.857	0.6332	0.1611	0.0402
H231	1.1703	0.5753	0.1282	0.0723
H232	1.1246	0.5067	0.1082	0.0723
H233	1.0225	0.5587	0.057	0.0716
H241	1.1915	0.49	0.3113	0.0572
H242	1.2129	0.5585	0.3404	0.0571
H243	1.0976	0.5192	0.3656	0.0572
H251	0.9031	0.45	0.1816	0.0704
H252	0.7921	0.4969	0.1243	0.0706
H253	0.8151	0.4897	0.2273	0.07
H261	0.7377	0.8193	0.4973	0.0376
H262	0.5907	0.7871	0.4742	0.0376
H281	0.6275	0.9223	0.2532	0.0715
H282	0.7697	0.9006	0.3237	0.071
H283	0.6804	0.8542	0.2508	0.0711
H291	0.3375	0.8376	0.3464	0.0728
H292	0.3452	0.8847	0.2734	0.0721
H293	0.3856	0.8159	0.2607	0.0735
H301	0.6693	0.9496	0.4768	0.0844
H302	0.5317	0.9725	0.4014	0.0838
H303	0.5196	0.9311	0.4811	0.0837

B.7. Fractional atomic coordinates and Uiso for $\{Co_2(TMS)_2[^{tBu}NON]\}$ (**7**)

Atom	x	y	z	U(iso)
Co1	0.38992(13)	0.16003(12)	0.71652(9)	0.0466
Co2	0.51257(12)	0.41138(12)	0.79918(9)	0.0449
Si1	0.6506(3)	0.3253(3)	0.6830(2)	0.067
Si2	0.3660(3)	0.3304(3)	0.5932(2)	0.0621
Si4	0.7251(3)	0.7387(3)	0.8938(2)	0.0624
Si30	0.2071(7)	-0.1649(6)	0.6913(4)	0.0525
Si31	0.2372(10)	-0.1718(9)	0.6876(7)	0.0525
N1	0.5953(7)	0.2884(6)	0.7794(6)	0.0481
N2	0.3235(7)	0.2930(6)	0.6937(5)	0.0419
O1	0.5371(6)	0.3756(6)	0.6346(4)	0.0581
C1	0.6297(12)	0.1839(10)	0.5902(9)	0.1091
C2	0.8296(10)	0.4623(10)	0.7150(9)	0.0957
C3	0.3431(11)	0.4682(10)	0.5619(8)	0.0953
C4	0.2807(11)	0.1879(11)	0.4798(7)	0.1012
C11	0.6747(11)	0.2628(10)	0.8641(9)	0.0711

C21	0.1890(10)	0.2717(10)	0.7106(8)	0.0585
C31	0.2919(9)	-0.0293(7)	0.6458(6)	0.071
C32	0.1157(10)	-0.3245(8)	0.5907(6)	0.1016
C33	0.0667(15)	-0.1515(12)	0.7318(12)	0.0785
C34	0.3230(17)	-0.1780(12)	0.7923(8)	0.0918
C35	0.159(2)	-0.1558(14)	0.7821(9)	0.0771
C36	0.3915(14)	-0.1923(14)	0.7488(13)	0.0708
C41	0.5777(9)	0.5879(8)	0.8883(7)	0.0581
C42	0.9002(9)	0.7459(10)	0.9514(7)	0.0857
C43	0.7090(11)	0.7530(11)	0.7688(7)	0.0951
C44	0.7281(11)	0.8894(9)	0.9679(8)	0.0912
C111	0.7227(13)	0.1617(12)	0.8305(10)	0.1236
C112	0.8007(11)	0.3880(11)	0.9358(8)	0.113
C113	0.5776(11)	0.2087(10)	0.9200(7)	0.0856
C211	0.1893(10)	0.2236(11)	0.7987(8)	0.0869
C212	0.0610(9)	0.1675(11)	0.6242(8)	0.0919
C213	0.1750(11)	0.3965(11)	0.7310(9)	0.1064
H11	0.6493	0.2103	0.5347	0.134(12)
H12	0.5337	0.1148	0.5693	0.134(12)
H13	0.6953	0.1535	0.6187	0.134(12)
H21	0.8529	0.4692	0.6565	0.119(12)
H22	0.8327	0.5432	0.7474	0.119(12)
H23	0.8976	0.4458	0.7583	0.119(12)
H31	0.3785	0.4848	0.5092	0.115(12)
H32	0.2435	0.446	0.5417	0.116(12)
H33	0.3958	0.545	0.6189	0.115(12)
H41	0.3146	0.2155	0.429	0.119(12)
H42	0.1789	0.1547	0.4592	0.119(12)
H43	0.3052	0.1205	0.4934	0.119(12)
H311	0.3629	-0.0461	0.6261	0.091(17)
H312	0.2185	-0.0399	0.5886	0.091(17)
H313	0.3542	-0.0405	0.6122	0.091(17)
H314	0.2056	-0.0424	0.5986	0.091(17)
H321	0.0441	-0.3236	0.5383	0.142(12)
H322	0.0717	-0.3949	0.6163	0.142(12)
H323	0.1851	-0.3375	0.566	0.142(12)
H324	0.0339	-0.318	0.5544	0.142(12)
H325	0.0853	-0.3959	0.618	0.142(12)
H326	0.165	-0.3404	0.5474	0.142(12)
H331	0.1066	-0.1016	0.8015	0.126(12)
H332	-0.0075	-0.239	0.7211	0.126(12)

H333	0.0269	-0.1067	0.6936	0.126(12)
H341	0.3183	-0.1363	0.8535	0.140(12)
H342	0.2952	-0.2696	0.7858	0.140(12)
H343	0.4191	-0.1343	0.7918	0.140(12)
H351	0.0769	-0.1452	0.752	0.126(12)
H352	0.129	-0.2334	0.8028	0.126(12)
H353	0.224	-0.0801	0.8383	0.126(12)
H361	0.3582	-0.2794	0.7555	0.128(12)
H362	0.455	-0.1807	0.7115	0.128(12)
H363	0.4411	-0.1273	0.8131	0.128(12)
H411	0.6014	0.5804	0.9536	0.077(17)
H412	0.4959	0.6038	0.8746	0.077(17)
H421	0.9744	0.8258	0.951	0.152(12)
H422	0.912	0.7447	1.0182	0.152(12)
H423	0.9048	0.6712	0.9148	0.152(12)
H431	0.7854	0.8352	0.7736	0.165(12)
H432	0.6189	0.7509	0.7394	0.165(12)
H433	0.7149	0.6813	0.7295	0.165(12)
H441	0.7362	0.886	1.0338	0.130(12)
H442	0.8081	0.9668	0.9697	0.130(12)
H443	0.6411	0.8925	0.938	0.130(12)
H1111	0.7674	0.1413	0.8857	0.139(10)
H1112	0.7892	0.1978	0.7979	0.139(10)
H1113	0.6404	0.0837	0.7852	0.139(10)
H1121	0.8534	0.3695	0.9887	0.129(10)
H1122	0.7666	0.4465	0.9621	0.129(10)
H1123	0.8615	0.4281	0.9007	0.129(10)
H1131	0.5496	0.2734	0.9446	0.090(10)
H1132	0.6258	0.1891	0.9743	0.090(10)
H1133	0.4946	0.1297	0.8763	0.090(10)
H2111	0.2659	0.2914	0.8559	0.095(10)
H2112	0.0998	0.2015	0.8092	0.095(10)
H2113	0.2036	0.1465	0.787	0.095(10)
H2121	0.0703	0.088	0.6109	0.103(10)
H2122	-0.0253	0.1502	0.6385	0.103(10)
H2123	0.058	0.1988	0.5679	0.103(10)
H2131	0.2608	0.4658	0.7812	0.119(10)
H2132	0.0949	0.3839	0.7523	0.119(10)
H2133	0.1612	0.4199	0.671	0.119(10)

B.8. Fractional atomic coordinates and Uiso for $\{Fe_2Cl(TMS)[^{tBu}NON]\}_2$ (**8**)

Atom	x	y	z	U(iso)
Fe1	0.697845(10)	0.75775(3)	0.49469(2)	0.0162
Fe2	0.630456(11)	0.71879(3)	0.54206(2)	0.0181
Cl1	0.734841(18)	0.82581(6)	0.40041(4)	0.0245
Si1	0.63865(2)	0.96458(6)	0.45443(5)	0.0197
Si2	0.61492(2)	0.71820(6)	0.33644(5)	0.0194
Si3	0.53779(2)	0.73156(7)	0.58879(5)	0.0283
N8	0.64678(6)	0.63833(16)	0.44022(13)	0.0166
N9	0.66748(6)	0.87371(17)	0.55449(13)	0.0173
O1	0.63119(5)	0.86243(14)	0.36924(11)	0.0203
C3	0.58648(8)	0.6559(2)	0.58921(18)	0.0261
C10	0.65211(7)	0.4987(2)	0.44546(17)	0.0219
C11	0.66920(9)	1.0958(2)	0.43468(19)	0.0301
C12	0.73118(8)	0.9893(3)	0.66608(18)	0.0323
C13	0.68389(9)	0.4598(2)	0.40351(19)	0.0298
C14	0.66990(8)	0.4586(2)	0.54908(19)	0.0301
C16	0.62538(8)	0.6830(2)	0.23018(17)	0.0281
C17	0.60940(9)	0.4346(2)	0.3918(2)	0.0351
C18	0.68907(8)	0.9263(2)	0.65296(17)	0.0229
C19	0.55662(8)	0.7099(3)	0.30452(18)	0.0316
C20	0.58602(9)	1.0227(3)	0.44496(19)	0.0337
C21	0.66004(9)	1.0202(3)	0.67207(19)	0.035
C22	0.50763(10)	0.6199(3)	0.6324(2)	0.0527
C23	0.49908(9)	0.7799(3)	0.4689(2)	0.0439
C24	0.69878(9)	0.8201(3)	0.72435(18)	0.0327
C25	0.55119(10)	0.8703(3)	0.6683(2)	0.0573
H111	0.6527	1.1307	0.3737	0.0499
H112	0.6737	1.1585	0.4814	0.05
H113	0.6963	1.0678	0.4372	0.0502
H121	0.75	0.929	0.6561	0.0491
H122	0.7259	1.0572	0.6205	0.0488
H123	0.745	1.0223	0.7292	0.0488
H131	0.7118	0.4974	0.4396	0.0497
H132	0.6871	0.3708	0.4055	0.0498
H133	0.6735	0.4869	0.3389	0.0494
H141	0.6969	0.4983	0.5847	0.0466
H142	0.674	0.3708	0.5521	0.0469
H143	0.6503	0.4787	0.5766	0.0465
H151	0.6037	0.6345	0.6548	0.0431
H153	0.5747	0.5834	0.5484	0.0437

H161	0.616	0.6002	0.2071	0.045
H162	0.6549	0.6888	0.2435	0.0447
H163	0.6099	0.7413	0.1797	0.045
H171	0.613	0.3462	0.4	0.0535
H172	0.5984	0.4535	0.3248	0.0534
H173	0.5888	0.4616	0.4152	0.0537
H191	0.545	0.6322	0.2737	0.0484
H192	0.5499	0.7177	0.3586	0.0482
H193	0.5424	0.7767	0.2612	0.0481
H201	0.5681	1.0381	0.3804	0.0521
H202	0.5896	1.0988	0.4792	0.0524
H203	0.5719	0.9633	0.4691	0.0522
H211	0.6326	0.9822	0.66	0.0539
H212	0.6556	1.0913	0.6296	0.0535
H213	0.6726	1.0481	0.7364	0.0535
H221	0.483	0.6593	0.6343	0.0827
H222	0.5257	0.591	0.6951	0.0835
H223	0.4987	0.5472	0.5904	0.0833
H231	0.4902	0.7081	0.428	0.0663
H232	0.5115	0.8412	0.4409	0.0661
H233	0.4741	0.8163	0.4739	0.0658
H241	0.6722	0.7831	0.7192	0.049
H242	0.7157	0.757	0.7118	0.0492
H243	0.7141	0.8507	0.7874	0.0486
H251	0.5264	0.9005	0.676	0.0868
H252	0.5616	0.9386	0.6419	0.0874
H253	0.5729	0.8504	0.7296	0.087

B.9. Fractional atomic coordinates and Uiso for $\{Co_2Cl(TMS)[^{tBu}NON]\}_2$ (**9**)

Atom	x	y	z	U(iso)
Co1	0.89911(9)	0.55223(13)	0.45201(8)	0.0426
Co2	0.76674(7)	0.58844(10)	0.32850(6)	0.0199
Cl1	0.97385(12)	0.55767(18)	0.58768(11)	0.026
Si1	0.72404(14)	0.5281(2)	0.49920(13)	0.0257
Si2	0.80668(14)	0.79025(19)	0.45808(12)	0.0201
Si3	0.58463(15)	0.5454(2)	0.18377(14)	0.0307
N1	0.7811(4)	0.4611(5)	0.4225(3)	0.0181
N2	0.8602(4)	0.7100(5)	0.3839(3)	0.0164
O1	0.7775(3)	0.6661(5)	0.5116(3)	0.0226
C10	0.9164(5)	0.7754(7)	0.3252(4)	0.0229
C11	0.9280(5)	0.6831(8)	0.2536(4)	0.0272

C12	0.8139(6)	0.3136(8)	0.3126(5)	0.0329
C13	0.7756(5)	0.3238(7)	0.3948(5)	0.028
C14	0.8789(6)	0.8929(7)	0.5300(5)	0.0287
C15	0.6778(5)	0.6377(8)	0.2363(5)	0.0324
C16	0.7353(7)	0.4456(9)	0.6001(5)	0.0429
C17	1.0063(5)	0.8064(8)	0.3678(5)	0.0324
C18	0.7076(6)	0.8822(8)	0.4198(5)	0.0326
C19	0.8726(6)	0.8969(8)	0.2897(5)	0.0372
C20	0.6800(6)	0.2790(8)	0.3844(6)	0.0393
C21	0.4956(6)	0.5128(10)	0.2513(7)	0.0474
C22	0.8289(6)	0.2368(8)	0.4568(6)	0.0361
C23	0.6065(5)	0.5611(9)	0.4680(6)	0.0397
C24	0.5319(6)	0.6385(9)	0.0931(6)	0.043
C25	0.6217(7)	0.3909(10)	0.1412(6)	0.0566
H111	0.9528	0.6045	0.2749	0.0441
H112	0.9661	0.7203	0.2169	0.044
H113	0.8708	0.6659	0.2241	0.0441
H121	0.8746	0.3324	0.317	0.05
H122	0.7833	0.3708	0.2721	0.0501
H123	0.8056	0.2263	0.2898	0.05
H141	0.9306	0.8457	0.5486	0.0437
H142	0.8492	0.9147	0.5771	0.044
H143	0.8953	0.9691	0.5041	0.044
H151	0.711	0.6621	0.1922	0.038
H152	0.6501	0.713	0.2553	0.038
H161	0.7038	0.3659	0.5949	0.0681
H162	0.7951	0.431	0.617	0.0679
H163	0.7091	0.4987	0.6397	0.068
H171	1.0368	0.7291	0.3843	0.047
H172	1.0016	0.8598	0.4147	0.047
H173	1.0395	0.8515	0.3295	0.047
H181	0.6858	0.9248	0.4663	0.051
H182	0.7239	0.9452	0.3815	0.0509
H183	0.6644	0.8265	0.3941	0.0511
H191	0.8163	0.8746	0.2595	0.057
H192	0.8612	0.9541	0.3336	0.0569
H193	0.9084	0.9386	0.254	0.057
H201	0.677	0.1913	0.3658	0.0599
H202	0.6552	0.2834	0.4374	0.0599
H203	0.6454	0.3317	0.3454	0.0602
H211	0.5181	0.4754	0.3019	0.071

H212	0.4655	0.593	0.2624	0.071
H213	0.4515	0.4569	0.2233	0.071
H221	0.8193	0.1502	0.4416	0.058
H222	0.8897	0.2583	0.4608	0.058
H223	0.8079	0.2503	0.5112	0.0579
H231	0.5739	0.485	0.4592	0.063
H232	0.6002	0.6107	0.4169	0.063
H233	0.5822	0.6125	0.5089	0.0629
H241	0.5102	0.7194	0.111	0.0621
H242	0.5753	0.6567	0.0547	0.0621
H243	0.4848	0.5916	0.0645	0.0621
H251	0.5748	0.3498	0.1084	0.079
H252	0.6684	0.4071	0.1048	0.079
H253	0.6451	0.3345	0.1839	0.0789

B.10. Fractional atomic coordinates and Uiso for $\{Fe_2Br(TMS)[^{tBu}NON]\}_2$ (**10**)

Atom	x	y	z	U(iso)
Fe1	0.54544(3)	0.93424(2)	0.110696(15)	0.02
Fe2	0.48198(3)	0.82095(2)	0.281079(15)	0.0197
Br1	0.70361(2)	1.021404(18)	-0.042867(12)	0.0282
Si1	0.82310(6)	0.74893(4)	0.14962(3)	0.0226
Si2	0.70512(6)	1.01256(4)	0.24042(3)	0.0215
Si3	0.25691(6)	0.66325(5)	0.46370(3)	0.0268
N1	0.61763(17)	0.75053(12)	0.15187(9)	0.0201
N2	0.50271(17)	1.00480(12)	0.24093(9)	0.0197
O1	0.81162(15)	0.89890(11)	0.16766(8)	0.0248
C3	0.4333(2)	0.74276(18)	0.41239(12)	0.0283
C11	0.7529(2)	0.97733(19)	0.35490(13)	0.0323
C12	0.7756(3)	1.15896(18)	0.18801(13)	0.0324
C13	0.5646(2)	0.64240(16)	0.11955(12)	0.0259
C14	0.0647(3)	0.7554(2)	0.43879(16)	0.0414
C15	0.8979(2)	0.65113(19)	0.24294(14)	0.035
C16	0.3569(2)	1.10491(16)	0.28548(12)	0.0253
C17	0.3403(3)	1.21793(18)	0.21816(14)	0.0353
C18	0.9784(2)	0.70998(19)	0.03548(14)	0.0359
C19	0.3745(3)	1.14837(19)	0.37705(13)	0.0357
C20	0.2947(3)	0.5009(2)	0.41762(17)	0.048
C21	0.6068(3)	0.64612(19)	0.01246(13)	0.0363
C22	0.2012(2)	1.04946(19)	0.30803(14)	0.0339
C23	0.6491(3)	0.51617(17)	0.15341(15)	0.0358
C24	0.2100(3)	0.6464(2)	0.59467(15)	0.0436

C25	0.3782(2)	0.65464(18)	0.15953(13)	0.031
H111	0.8696	0.961	0.3436	0.0501
H112	0.7074	1.0483	0.3939	0.0506
H113	0.7104	0.9068	0.3849	0.0497
H121	0.8904	1.1489	0.1818	0.0504
H122	0.7191	1.2284	0.2286	0.0499
H123	0.7541	1.1764	0.1278	0.0495
H143	-0.0232	0.7093	0.4642	0.0629
H142	0.0374	0.8366	0.4671	0.0629
H141	0.0809	0.7662	0.3714	0.0625
H151	0.9991	0.6705	0.2446	0.0532
H152	0.8226	0.6649	0.3028	0.0531
H153	0.9157	0.5637	0.2296	0.0539
H171	0.2511	1.2826	0.2485	0.054
H172	0.441	1.2511	0.2003	0.0533
H173	0.3177	1.1931	0.1625	0.0537
H183	1.0791	0.7292	0.0381	0.0549
H182	0.943	0.7583	-0.0139	0.055
H181	0.9942	0.6226	0.0233	0.0556
H191	0.2778	1.2074	0.4054	0.0548
H192	0.4696	1.1889	0.363	0.0542
H193	0.389	1.077	0.4194	0.0545
H203	0.1986	0.4661	0.4456	0.073
H202	0.3871	0.4502	0.4349	0.0738
H201	0.3152	0.503	0.3512	0.073
H211	0.5759	0.5762	-0.008	0.0555
H212	0.7236	0.6407	-0.0142	0.0554
H213	0.5481	0.7221	-0.0102	0.0561
H221	0.1082	1.1127	0.3324	0.052
H222	0.2046	0.9808	0.3534	0.0519
H223	0.1887	1.0211	0.2511	0.0518
H233	0.6102	0.4487	0.1351	0.0544
H232	0.769	0.5031	0.1277	0.0544
H231	0.6251	0.5146	0.2205	0.0541
H241	0.1152	0.6081	0.6171	0.0672
H242	0.1884	0.7276	0.6211	0.0673
H243	0.3025	0.5939	0.6114	0.0672
H251	0.3412	0.5868	0.139	0.0467
H252	0.3217	0.7339	0.1386	0.0469
H253	0.35	0.6516	0.2272	0.0467
H31	0.4213	0.8091	0.4539	0.0346

H32	0.5297	0.682	0.4145	0.0346

B.11. Fractional atomic coordinates and Uiso for $\{Co_2Br(TMS)[^{tBu}NON]\}_2$ (**11**)

Atom	x	y	z	U(iso)
Co3	0.2172(3)	0.8902(2)	0.8342(2)	0.0365
Co2	-0.2153(3)	1.1328(3)	1.2045(2)	0.0411
Co1	0.0070(3)	0.9958(2)	1.0806(2)	0.0353
Co6	0.4397(3)	0.7539(2)	0.7100(2)	0.0359
Br1	0.2458(2)	0.8496(2)	1.0234(2)	0.0552
Br2	-0.0209(3)	1.0367(2)	0.8892(2)	0.0558
Si1	-0.0608(5)	0.8651(5)	1.2791(4)	0.0472
Si2	0.0731(6)	1.0895(5)	1.2556(4)	0.0608
Si3	-0.5155(6)	1.3751(5)	1.2857(5)	0.0603
Si7	0.2902(5)	1.0245(4)	0.6398(4)	0.0423
Si9	0.7386(6)	0.5110(5)	0.6289(4)	0.0604
Si11	0.1523(5)	0.8048(4)	0.6538(4)	0.042
N1	-0.1516(11)	0.9440(9)	1.1735(8)	0.0319
N2	-0.0199(13)	1.1606(10)	1.1561(10)	0.0438
N14	0.2491(13)	0.7353(11)	0.7567(9)	0.0402
N15	0.3762(9)	0.9425(10)	0.7374(8)	0.0402
O1	0.0562(12)	0.9436(11)	1.2709(9)	0.0511
O13	0.1698(12)	0.9495(9)	0.6505(9)	0.0467
C3	-0.3822(11)	1.2167(13)	1.3092(11)	0.0465
C18	-0.6785(18)	1.389(2)	1.3911(19)	0.0886
C19	-0.2611(13)	0.8959(12)	1.1381(10)	0.0473
C21	0.248(2)	0.5978(17)	0.8195(17)	0.0749
C22	0.6082(16)	0.6647(14)	0.6119(12)	0.0639
C25	0.227(2)	0.725(2)	0.5283(16)	0.1058
C26	0.3940(18)	1.0122(16)	0.5074(11)	0.0702
C27	-0.1682(15)	0.8906(14)	1.4126(9)	0.0712
C28	0.5774(18)	1.0355(18)	0.6837(16)	0.081
C29	-0.3526(19)	1.0174(18)	1.0795(13)	0.0561
C30	0.0007(17)	1.1535(16)	1.3880(10)	0.0641
C31	0.036(2)	0.6993(17)	1.2584(18)	0.0741
C32	-0.563(2)	1.401(2)	1.163(2)	0.1082
C33	0.4171(14)	1.0973(13)	0.8514(12)	0.0635
C34	-0.1830(18)	0.7928(16)	1.0638(15)	0.077
C35	0.4839(11)	0.9837(13)	0.7775(10)	0.0531
C36	0.5757(19)	0.881(2)	0.8324(16)	0.0698
C37	0.365(3)	0.5503(18)	0.8621(17)	0.0729
C38	0.2485(19)	0.5098(12)	0.7301(14)	0.0837

C39	-0.3540(16)	0.8528(13)	1.2270(17)	0.0672
C40	0.191(2)	1.2031(15)	0.6519(16)	0.0673
C41	0.2632(16)	1.0572(17)	1.2324(11)	0.0703
C42	-0.017(2)	1.2783(16)	1.1068(16)	0.0536
C43	-0.0412(12)	0.8112(19)	0.6914(15)	0.0901
C44	-0.157(2)	1.3336(15)	1.0446(16)	0.0815
C47	-0.023(2)	1.3824(17)	1.1704(16)	0.1053
C48	0.894(2)	0.497(2)	0.533(2)	0.1027
C49	0.103(2)	0.6201(17)	0.8914(17)	0.0834
C50	0.106(2)	1.2646(17)	1.0155(17)	0.0942
C51	0.663(2)	0.3821(18)	0.6141(16)	0.1021
C52	-0.456(2)	1.5213(19)	1.292(2)	0.1153
C54	0.801(2)	0.502(2)	0.7635(16)	0.0818
H31	-0.3509	1.2175	1.3781	0.0729
H32	-0.4402	1.1502	1.3299	0.0729
H282	0.6753	1.0345	0.6967	0.1181
H281	0.5424	1.1061	0.6443	0.118
H283	0.6229	0.9602	0.6248	0.1181
H301	0.0288	1.0975	1.4384	0.1178
H302	0.0117	1.2358	1.3872	0.118
H303	-0.1101	1.1739	1.3966	0.1178
H313	0.0941	0.6597	1.3176	0.1087
H312	-0.0233	0.6429	1.2632	0.1089
H311	0.1035	0.6822	1.1972	0.1087
H333	0.501	1.114	0.8804	0.0781
H331	0.3609	1.076	0.9079	0.0782
H332	0.3801	1.1742	0.8125	0.078
H343	-0.228	0.748	1.0417	0.1111
H341	-0.0957	0.7261	1.0962	0.1109
H342	-0.1219	0.8277	1.0004	0.1112
H371	0.3528	0.4642	0.9021	0.09
H372	0.364	0.5988	0.9227	0.0902
H373	0.4525	0.5284	0.823	0.0903
H382	0.2781	0.4222	0.7621	0.127
H381	0.3381	0.5098	0.6731	0.1271
H383	0.174	0.5303	0.6992	0.1271
H391	-0.4001	0.8035	1.2003	0.0979
H392	-0.4047	0.916	1.266	0.0982
H393	-0.2849	0.7841	1.2703	0.098
H411	0.3054	0.9986	1.2792	0.0858
H412	0.2808	1.1413	1.2372	0.0861

H413	0.298	1.0362	1.1617	0.0858
H441	-0.1743	1.4073	1.002	0.14
H442	-0.2475	1.3501	1.1056	0.1402
H443	-0.1696	1.2616	1.0123	0.14
H473	-0.0037	1.4621	1.1378	0.148
H472	-0.0948	1.3987	1.2257	0.1481
H471	0.0705	1.3415	1.206	0.148
H483	0.9607	0.4148	0.5295	0.1137
H481	0.9254	0.5628	0.512	0.114
H482	0.8553	0.4894	0.4545	0.1139
H542	0.8858	0.4003	0.751	0.1139
H541	0.8554	0.5479	0.7579	0.1139
H543	0.7423	0.4817	0.8089	0.114
H221	0.6518	0.7301	0.5932	0.0626
H222	0.5614	0.6584	0.5555	0.0626
H511	0.7426	0.3029	0.6217	0.1342
H512	0.5909	0.3859	0.6637	0.1342
H513	0.6487	0.392	0.5455	0.1342
H361	0.6143	0.8106	0.7826	0.0589
H362	0.6497	0.9014	0.8487	0.0589
H363	0.5217	0.8497	0.8892	0.0589
H491	0.013	0.6619	0.8633	0.115
H492	0.0881	0.6774	0.9516	0.115
H493	0.0867	0.5417	0.9294	0.115
H251	0.3153	0.7206	0.5033	0.0878
H252	0.166	0.778	0.4731	0.0878
H253	0.2068	0.6435	0.5316	0.0878
H431	-0.0845	0.8506	0.75	0.1334
H432	-0.091	0.8618	0.6319	0.1334
H433	-0.0502	0.7272	0.6904	0.1334
H261	0.4414	0.9191	0.5058	0.0648
H262	0.4536	1.0569	0.5057	0.0648
H263	0.3288	1.0365	0.464	0.0648
H401	0.1355	1.213	0.7173	0.099
H402	0.2562	1.2491	0.6404	0.099
H403	0.1314	1.2287	0.5988	0.099
H271	-0.2264	0.9763	1.4332	0.0871
H272	-0.117	0.8566	1.4755	0.0871
H273	-0.2444	0.8405	1.4346	0.0871
H291	-0.2981	1.0568	1.0137	0.0883
H292	-0.4095	1.0933	1.113	0.0883

H293	-0.4221	0.9975	1.0397	0.0883
H501	0.0991	1.2082	0.9737	0.0955
H502	0.1043	1.346	0.9853	0.0955
H503	0.186	1.2304	1.0516	0.0955
H521	-0.3563	1.515	1.2412	0.1003
H522	-0.4255	1.531	1.3569	0.1003
H523	-0.5097	1.6034	1.2695	0.1003
H181	-0.7594	1.4673	1.37	0.0906
H182	-0.676	1.3761	1.4511	0.0906
H183	-0.7275	1.3194	1.3684	0.0906
H321	-0.5936	1.3138	1.1411	0.1128
H322	-0.6276	1.4625	1.1333	0.1128
H323	-0.4753	1.3767	1.0966	0.1128

B.12. Fractional atomic coordinates and Uiso for $\{Fe_2Br(Me)[^{tBu}NON]\}_2$ (**12**)

Atom	x	y	z	U(iso)
Fe2	0.68763(8)	0.74697(5)	0.41679(5)	0.0397
Fe1	0.53840(10)	0.89777(6)	0.44152(6)	0.0539
Br1	0.33894(6)	1.01202(4)	0.42004(4)	0.0468
Si2	0.53368(15)	0.85788(10)	0.25894(9)	0.0357
Si1	0.37844(14)	0.73555(10)	0.36542(10)	0.0377
N1	0.5081(4)	0.7593(3)	0.4598(3)	0.0322
N2	0.6625(4)	0.8732(3)	0.3552(3)	0.0321
O1	0.4083(3)	0.8193(2)	0.3013(2)	0.0369
C9	0.1980(6)	0.7508(5)	0.3747(5)	0.0641
C10	0.7762(7)	1.0261(4)	0.3583(5)	0.0592
C11	0.4672(7)	0.9643(5)	0.1987(4)	0.0569
C12	0.4175(9)	0.7723(5)	0.5936(5)	0.065
C13	0.5691(7)	0.7714(5)	0.1798(4)	0.0632
C14	0.3920(8)	0.6233(5)	0.3132(5)	0.0674
C15	0.6591(8)	0.7206(5)	0.6039(4)	0.0636
C16	0.7973(5)	0.9225(4)	0.3578(4)	0.0413
C4	0.8123(8)	0.6362(6)	0.4112(6)	0.0756
C18	0.8526(7)	0.8966(6)	0.2777(5)	0.0655
C19	0.5110(6)	0.7164(4)	0.5478(4)	0.0447
C20	0.4646(11)	0.6184(5)	0.5373(6)	0.0819
C21	0.9048(6)	0.8943(4)	0.4403(5)	0.0529
H91	0.1341	0.7363	0.3216	0.092
H93	0.1839	0.8131	0.3902	0.092
H92	0.181	0.7122	0.421	0.092
H101	0.8611	1.0586	0.364	0.087

H103	0.739	1.043	0.4081	0.0869
H102	0.7112	1.0461	0.3062	0.0869
H111	0.3801	0.953	0.1572	0.083
H112	0.531	0.9874	0.1671	0.083
H113	0.4525	1.0107	0.2385	0.083
H122	0.4241	0.747	0.6518	0.101
H121	0.4428	0.8356	0.6002	0.1011
H123	0.3219	0.7669	0.5608	0.101
H132	0.4857	0.7514	0.1414	0.096
H131	0.6289	0.7966	0.1461	0.096
H133	0.6153	0.7183	0.2113	0.0959
H141	0.3341	0.623	0.2547	0.098
H143	0.4865	0.6131	0.308	0.0979
H142	0.3661	0.574	0.3455	0.0979
H151	0.664	0.6903	0.6586	0.0899
H153	0.6901	0.7828	0.6159	0.0899
H152	0.7225	0.6904	0.5751	0.0899
H181	0.9396	0.9266	0.2805	0.1
H182	0.7877	0.9135	0.2247	0.0999
H183	0.8669	0.8307	0.2773	0.1
H202	0.4648	0.5937	0.5948	0.1201
H201	0.529	0.5814	0.5138	0.12
H203	0.3745	0.6141	0.4994	0.1199
H212	0.9919	0.9242	0.4414	0.078
H211	0.8751	0.9134	0.4907	0.0778
H213	0.9177	0.8301	0.4411	0.078
H41	0.8883	0.6537	0.3878	0.0861
H42	0.8478	0.611	0.4683	0.0861
H43	0.7612	0.5893	0.3744	0.0861

B.13. Fractional atomic coordinates and Uiso for $\{Co_2Cl(Me)[^{tBu}NON]\}_2$ (**13**)

Atom	x	y	z	U(iso)
Co1	0.03348(4)	0.90122(3)	0.44445(3)	0.0331
Co2	0.17499(4)	0.75133(3)	0.41830(3)	0.0414
Cl1	-0.14127(8)	1.01172(5)	0.42502(5)	0.0443
Si1	0.02901(9)	0.86364(6)	0.26016(5)	0.0397
Si2	-0.12685(9)	0.73991(6)	0.37100(6)	0.0427
N1	0.1550(2)	0.87724(16)	0.35794(15)	0.0344
N2	0.0039(2)	0.76340(16)	0.46408(16)	0.0361
O1	-0.09500(19)	0.82141(15)	0.30291(13)	0.0414
C1	0.2904(3)	0.9254(2)	0.3642(2)	0.0438

C2	0.2743(4)	1.0307(2)	0.3668(3)	0.0584
C11	0.3492(4)	0.8988(3)	0.2843(3)	0.068
C12	0.3890(3)	0.8933(3)	0.4493(2)	0.0557
C13	0.0147(4)	0.7220(2)	0.5552(2)	0.0493
C3	0.2795(4)	0.6386(3)	0.3989(3)	0.077
C21	-0.0285(5)	0.6194(2)	0.5481(3)	0.0762
C22	0.1622(4)	0.7275(3)	0.6065(2)	0.0673
C23	-0.0737(4)	0.7763(3)	0.6051(3)	0.0665
C111	-0.0343(4)	0.9730(3)	0.2014(2)	0.0593
C122	0.0674(4)	0.7768(3)	0.1794(3)	0.0702
C211	-0.1179(4)	0.6234(2)	0.3184(3)	0.0696
C222	-0.3013(3)	0.7601(3)	0.3861(3)	0.0714
H21	0.3585	1.0609	0.3684	0.074(2)
H23	0.2452	1.0494	0.419	0.074(2)
H22	0.2106	1.0532	0.3161	0.074(2)
H111	0.4356	0.9278	0.2896	0.093(2)
H113	0.2885	0.9188	0.2294	0.092(2)
H112	0.359	0.8318	0.284	0.092(2)
H121	0.4761	0.9215	0.4545	0.066(2)
H122	0.3535	0.9101	0.4994	0.066(2)
H123	0.3973	0.826	0.4473	0.066(2)
H212	-0.0146	0.5926	0.6061	0.099(2)
H211	-0.1225	0.6144	0.5198	0.099(2)
H213	0.0232	0.5855	0.5134	0.099(2)
H222	0.1694	0.7031	0.6649	0.082(2)
H221	0.1912	0.7914	0.6102	0.082(2)
H223	0.2173	0.6917	0.5761	0.082(2)
H231	-0.0663	0.7497	0.6632	0.088(2)
H233	-0.0445	0.8403	0.6114	0.088(2)
H232	-0.1673	0.7743	0.573	0.088(2)
H1111	-0.1136	0.9578	0.1577	0.072(2)
H1113	-0.0558	1.0169	0.2422	0.072(2)
H1112	0.0319	0.9967	0.1729	0.073(2)
H1221	-0.0155	0.7575	0.141	0.092(2)
H1222	0.1233	0.8066	0.1447	0.092(2)
H1223	0.1129	0.723	0.2097	0.092(2)
H2112	-0.1762	0.6226	0.2606	0.086(2)
H2111	-0.1455	0.5763	0.3543	0.085(2)
H2113	-0.027	0.6105	0.3133	0.085(2)
H2222	-0.3647	0.7568	0.33	0.092(2)
H2221	-0.3059	0.82	0.4114	0.092(2)

H2223	-0.3234	0.7142	0.4248	0.093(2)
H201	0.2663	0.5908	0.4392	0.0916
H202	0.3729	0.6536	0.4092	0.0916
H203	0.2477	0.6173	0.3395	0.0916

B.14. Fractional atomic coordinates and Uiso for {$Fe_2(C_6F_5)_2[^{tBu}NON]$} (**14**)

Atom	x	y	z	U(iso)
Co2	0.79865(3)	0.83419(3)	0.23024(2)	0.0243
Co1	1.04709(3)	0.65392(3)	0.23116(2)	0.0228
F1	0.71268(16)	0.96931(13)	0.05197(10)	0.04
F2	1.25020(16)	0.52713(13)	0.04860(10)	0.037
F3	1.53494(17)	0.35350(13)	-0.00056(10)	0.0412
F4	1.69631(16)	0.24891(13)	0.12977(12)	0.0466
F5	0.4546(2)	1.14077(15)	0.01899(13)	0.0553
F6	1.28196(18)	0.48841(16)	0.36094(10)	0.0478
F7	1.56733(19)	0.31621(16)	0.31028(12)	0.0554
F8	0.4737(2)	0.99462(18)	0.37042(13)	0.0688
F9	0.20405(19)	1.24006(15)	0.16013(17)	0.0714
F10	0.2165(2)	1.16695(19)	0.33568(17)	0.0836
Si2	0.96679(9)	0.82787(7)	0.37344(5)	0.0374
Si1	0.80883(8)	0.63350(6)	0.37275(5)	0.0319
N2	0.9955(2)	0.83094(16)	0.25235(13)	0.0254
N1	0.8342(2)	0.65724(16)	0.25248(13)	0.0248
O1	0.9195(2)	0.70427(17)	0.39202(11)	0.0394
C1	0.8061(5)	0.9648(3)	0.4322(2)	0.0696
C11	0.8943(3)	0.4709(3)	0.4051(2)	0.0452
C12	1.1395(5)	0.7950(3)	0.4191(2)	0.063
C18	1.4719(3)	0.3880(2)	0.08867(16)	0.0294
C3	1.2531(2)	0.51629(19)	0.20680(16)	0.0256
C4	0.6059(3)	0.9725(2)	0.21295(18)	0.0322
C21	1.3258(3)	0.47624(19)	0.11670(16)	0.0266
C22	1.5536(3)	0.3346(2)	0.15461(18)	0.0326
C23	1.3400(3)	0.4578(2)	0.27014(16)	0.0322
C24	1.0775(3)	0.8994(2)	0.18467(18)	0.0329
C25	0.7883(3)	0.5994(2)	0.18385(17)	0.0306
C26	0.5920(3)	1.0151(2)	0.12567(19)	0.0339
C27	0.8322(4)	0.6518(3)	0.08922(19)	0.0439
C29	1.0759(3)	0.8674(3)	0.08750(18)	0.0435
C30	0.4751(3)	1.0280(2)	0.2812(2)	0.0444
C31	0.3401(3)	1.1171(3)	0.2656(3)	0.0531
C32	0.8736(3)	0.4599(2)	0.1787(2)	0.0427

C33	1.2462(3)	0.8581(3)	0.1902(2)	0.0413
C34	1.4874(3)	0.3685(2)	0.24610(18)	0.035
C35	0.9962(3)	1.0378(2)	0.2033(3)	0.0552
C36	0.3339(3)	1.1539(2)	0.1769(3)	0.0478
C37	0.4600(3)	1.1035(2)	0.1059(2)	0.0399
C38	0.6101(4)	0.7064(3)	0.4434(2)	0.0593
C39	0.6152(3)	0.6300(3)	0.2111(3)	0.0546
H12	0.787	0.953	0.497	0.0959
H11	0.8314	1.0362	0.4187	0.0961
H13	0.7124	0.9786	0.4114	0.0967
H111	0.8997	0.4686	0.469	0.0696
H113	0.9939	0.4303	0.3674	0.0703
H112	0.8295	0.4291	0.3987	0.0699
H122	1.1165	0.7767	0.4837	0.1078
H121	1.1664	0.8665	0.4127	0.1077
H123	1.2246	0.7272	0.3873	0.1076
H271	0.804	0.6161	0.044	0.0702
H273	0.9428	0.6338	0.0713	0.0711
H272	0.7766	0.7412	0.0906	0.0714
H292	1.1259	0.911	0.0415	0.0696
H291	1.1299	0.7782	0.0744	0.07
H293	0.9711	0.8913	0.0816	0.0699
H322	0.8484	0.4247	0.1319	0.0663
H323	0.9813	0.4415	0.1645	0.0667
H321	0.8442	0.4247	0.2393	0.0669
H333	1.2982	0.898	0.1436	0.0643
H331	1.2478	0.8817	0.2522	0.0644
H332	1.2946	0.769	0.182	0.0646
H351	1.0459	1.0821	0.1579	0.082
H353	0.9984	1.0586	0.2656	0.0818
H352	0.8905	1.0638	0.2002	0.0819
H382	0.6108	0.7039	0.5076	0.0775
H381	0.5625	0.7892	0.4263	0.0772
H383	0.5486	0.6618	0.4342	0.0775
H392	0.5846	0.5972	0.1648	0.0845
H393	0.562	0.7177	0.2166	0.0846
H391	0.5877	0.594	0.2708	0.0849

B.15. Fractional atomic coordinates and Uiso for $\{Fe_2Cl(C_6F_5)[^{tBu}NON]\}_2$ (**15**)

Atom	x	y	z	U(iso)
Fe1	0.55219(6)	0.55887(2)	0.96937(6)	0.0254

Fe2	0.70358(6)	0.63924(2)	1.00228(6)	0.0282
Cl3	0.36705(12)	0.50781(4)	0.89688(12)	0.0379
F7	0.9632(4)	0.64455(12)	1.2085(4)	0.0543
F8	0.7400(4)	0.75045(13)	0.8998(4)	0.059
F10	1.1208(5)	0.80305(17)	1.1568(5)	0.0848
F11	1.1392(4)	0.71521(17)	1.2791(5)	0.0758
F13	0.9186(4)	0.81983(12)	0.9689(5)	0.0704
Si4	0.40186(13)	0.65036(5)	0.94320(17)	0.044
Si5	0.57676(18)	0.61204(6)	0.73506(13)	0.0496
N6	0.5207(4)	0.62437(12)	1.0583(4)	0.0286
N12	0.6906(4)	0.58940(14)	0.8603(4)	0.0331
O9	0.4462(4)	0.62374(15)	0.8138(4)	0.0506
C14	0.8407(5)	0.69463(17)	1.0489(5)	0.0361
C15	0.2248(5)	0.6334(2)	0.9574(8)	0.0568
C16	0.9107(5)	0.56340(19)	0.9640(6)	0.0458
C17	0.8217(5)	0.56554(19)	0.8400(6)	0.0442
C18	0.9292(6)	0.7764(2)	1.0274(7)	0.0522
C19	0.8380(5)	0.73965(19)	0.9935(6)	0.0425
C20	0.5121(5)	0.62801(19)	1.1998(5)	0.04
C21	1.0404(6)	0.7236(2)	1.1841(6)	0.0533
C22	0.9470(5)	0.68801(19)	1.1462(6)	0.0421
C23	0.6480(6)	0.6154(2)	1.2723(5)	0.0464
C24	1.0301(6)	0.7686(2)	1.1225(7)	0.0552
C25	0.4072(6)	0.5917(3)	1.2379(5)	0.0545
C26	0.6267(8)	0.6692(3)	0.6575(6)	0.0697
C27	0.4122(7)	0.7178(2)	0.9255(10)	0.0791
C28	0.7981(7)	0.5132(2)	0.7902(8)	0.064
C30	0.8935(7)	0.5944(3)	0.7444(7)	0.0679
C31	0.4742(7)	0.6795(3)	1.2376(9)	0.0738
C32	0.5224(10)	0.5667(3)	0.6105(6)	0.0822
H151	0.2181	0.5989	0.9647	0.0695
H152	0.191	0.6495	1.0216	0.0695
H153	0.1709	0.6417	0.8748	0.0695
H161	0.9292	0.5953	0.998	0.0643
H162	0.9956	0.5481	0.9546	0.0643
H163	0.8693	0.545	1.0269	0.0643
H231	0.7195	0.6261	1.3308	0.0533
H232	0.6077	0.5872	1.3048	0.0533
H233	0.6795	0.6073	1.1928	0.0533
H251	0.4315	0.5599	1.2167	0.052
H252	0.4046	0.5935	1.3293	0.052

H253	0.3218	0.5998	1.1969	0.052
H261	0.6525	0.6931	0.722	0.061
H262	0.5533	0.6815	0.6021	0.061
H263	0.7002	0.663	0.6108	0.061
H271	0.5033	0.7258	0.913	0.0682
H272	0.3798	0.7334	0.9874	0.0682
H273	0.3598	0.7256	0.8406	0.0682
H281	0.7402	0.5146	0.7089	0.0628
H282	0.8784	0.4977	0.7752	0.0628
H283	0.7521	0.4947	0.8475	0.0628
H301	0.9107	0.6264	0.7757	0.0655
H302	0.9758	0.5791	0.7309	0.0655
H303	0.8374	0.5959	0.6651	0.0655
H311	0.5408	0.703	1.2121	0.0656
H312	0.4727	0.683	1.3265	0.0656
H313	0.3899	0.6892	1.1941	0.0656
H321	0.5009	0.5373	0.651	0.0721
H322	0.4529	0.5784	0.5556	0.0721
H323	0.5999	0.5599	0.5644	0.0721

B.16. Fractional atomic coordinates and Uiso for ([CO^{NON}OC]Fe(CO)$_2$(COCH$_2$SiMe$_3$))$_2$Fe} (**16**)

Atom	x	y	z	U(iso)
Fe1	0.5	0.5	0.5	0.0195
Fe2	0.343982(12)	0.565149(19)	0.386754(12)	0.022
Si1	0.27303(3)	0.37767(5)	0.32686(3)	0.0366
Si2	0.24130(3)	0.48559(5)	0.43428(3)	0.0386
Si3	0.45625(3)	0.83515(4)	0.43657(3)	0.0344
O1	0.44581(6)	0.42217(9)	0.41754(6)	0.0253
O2	0.41769(6)	0.52875(10)	0.51786(6)	0.0254
O3	0.47396(6)	0.61711(9)	0.43971(6)	0.0263
O4	0.28277(9)	0.74698(13)	0.39908(10)	0.057
O5	0.33205(9)	0.59309(14)	0.25466(7)	0.0501
O6	0.26643(6)	0.46373(11)	0.37506(7)	0.033
N1	0.35423(8)	0.37620(11)	0.33958(7)	0.0263
N2	0.31162(8)	0.51699(12)	0.49589(7)	0.0276
C1	0.39012(8)	0.44221(13)	0.38513(8)	0.0223
C2	0	0.1027(4)	0.25	0.0803
C2	0.36345(9)	0.53325(13)	0.47746(8)	0.0232
C3	0	0.3837(5)	0.25	0.108

C3	0.42079(9)	0.64185(13)	0.40460(8)	0.0225
C4	0.30446(10)	0.67403(16)	0.39406(10)	0.0346
C5	0	0.5633(5)	0.25	0.1111
C5	0.33410(9)	0.58148(15)	0.30530(9)	0.0317
C6	0	0.2836(5)	0.25	0.1602
C8	-0.0277(3)	0.2068(6)	0.2287(3)	0.0674
C10	-0.0322(4)	0.4628(6)	0.2220(4)	0.0836
C10	0.38743(11)	0.29802(15)	0.31641(9)	0.0348
C11	0.34062(13)	0.25730(18)	0.25455(11)	0.0461
C13	0.44243(12)	0.34181(19)	0.30090(12)	0.0454
C20	0.32163(11)	0.51278(18)	0.56542(10)	0.038
C21	0.35796(13)	0.6024(2)	0.59874(12)	0.0544
C31	0.41055(15)	0.21734(18)	0.36477(12)	0.0531
C32	0.43046(13)	0.8173(2)	0.50512(12)	0.0522
C33	0.42823(19)	0.95499(19)	0.39995(16)	0.0794
C34	0.54402(12)	0.8273(2)	0.46103(12)	0.0533
C41	0.24859(18)	0.2596(2)	0.35011(17)	0.0733
C42	0.21940(12)	0.4127(3)	0.24674(12)	0.0606
C43	0.20292(16)	0.3754(3)	0.45004(15)	0.0765
C66	0.25716(13)	0.5147(2)	0.57393(13)	0.056
C77	0.35658(14)	0.4203(2)	0.59438(12)	0.0542
C88	0.41961(10)	0.74044(14)	0.37434(9)	0.0287
C99	0.18007(13)	0.5818(3)	0.40874(15)	0.0729
H11	0.2229	0.3661	0.217	0.0844
H12	0.2314	0.4758	0.236	0.0842
H13	0.1767	0.416	0.2455	0.0846
H91	0.3759	0.7595	0.348	0.0343
H92	0.4463	0.7359	0.3482	0.0349
H111	0.4518	0.8633	0.5376	0.0812
H112	0.4425	0.7528	0.5224	0.0814
H113	0.3859	0.8246	0.4928	0.0809
H121	0.5565	0.8374	0.426	0.0783
H122	0.5633	0.8751	0.4926	0.078
H123	0.5585	0.7635	0.4789	0.0786
H131	0.4368	0.9617	0.3613	0.1024
H132	0.451	1.0045	0.4283	0.102
H133	0.3833	0.963	0.3907	0.1023
H181	0.3987	0.4207	0.5922	0.0828
H182	0.3612	0.4171	0.6379	0.0826
H183	0.3337	0.3634	0.5721	0.0832
H191	0.2342	0.4561	0.5586	0.0917

H192	0.2633	0.5229	0.6173	0.0916
H193	0.2314	0.5698	0.55	0.092
H211	0.3611	0.6029	0.642	0.0857
H212	0.3358	0.6613	0.5782	0.0861
H213	0.4001	0.6027	0.5973	0.0855
H221	0.1733	0.3507	0.4111	0.1208
H222	0.2359	0.3263	0.4696	0.121
H223	0.1816	0.3907	0.4781	0.1209
H231	0.16	0.5806	0.3644	0.1064
H232	0.1989	0.6455	0.4224	0.1065
H233	0.1485	0.5701	0.4279	0.1063
H291	0.3256	0.3071	0.2235	0.0667
H292	0.3621	0.2086	0.2385	0.0669
H293	0.3038	0.2282	0.2602	0.0668
H301	0.4774	0.3599	0.3382	0.0716
H302	0.4571	0.2937	0.2781	0.0721
H303	0.4275	0.3981	0.2729	0.0721
H311	0.4402	0.2424	0.4033	0.0777
H312	0.4305	0.1686	0.3484	0.0781
H313	0.3741	0.1886	0.3722	0.0781
H331	0.2734	0.246	0.3946	0.1181
H332	0.2046	0.2643	0.3436	0.1176
H333	0.2553	0.2095	0.3239	0.118

B.17. Fractional atomic coordinates and Uiso for {FeBr[^{Me_3Ph}NON]}$_2$ (**17**)

tom	x	y	z	U(iso)
Fe1	0.61153(10)	-0.47520(12)	0.55580(11)	0.0388
Br1	0.49322(8)	-0.43105(10)	0.38437(8)	0.0452
Si2	0.5629(2)	-0.2333(3)	0.5922(3)	0.0528
Si10	0.6472(5)	-0.6950(7)	0.4618(6)	0.035(3)
Si11	0.6496(6)	-0.7129(7)	0.4932(7)	0.046(3)
O1	0.5375(4)	-0.7041(5)	0.4436(5)	0.0426
N1	0.6909(5)	-0.5804(6)	0.5427(5)	0.0365
N2	0.6461(5)	-0.3388(6)	0.6241(6)	0.0374
C1	0.6447(16)	-0.691(2)	0.3407(16)	0.068(4)
C2	0.7113(16)	-0.821(2)	0.5252(17)	0.068(4)
C3	0.5554(8)	-0.1464(10)	0.4865(9)	0.083(4)
C4	0.5870(8)	-0.1409(10)	0.6983(8)	0.082(4)
C5	0.7897(7)	-0.5554(8)	0.5896(7)	0.041(3)
C6	0.8454(7)	-0.5819(9)	0.6895(8)	0.045(3)
C7	0.9391(7)	-0.5522(9)	0.7332(8)	0.056(3)

C8	0.9799(8)	-0.4997(10)	0.6823(9)	0.060(3)
C9	0.9254(8)	-0.4759(9)	0.5858(9)	0.060(3)
C10	0.8297(7)	-0.5018(9)	0.5362(8)	0.051(3)
C11	0.7370(7)	-0.3257(9)	0.7065(8)	0.044(3)
C12	0.7570(7)	-0.3644(9)	0.8030(8)	0.047(3)
C13	0.8477(8)	-0.3532(9)	0.8785(9)	0.061(4)
C14	0.9191(8)	-0.3082(10)	0.8647(9)	0.056(3)
C15	0.9012(8)	-0.2730(9)	0.7736(8)	0.057(3)
C16	0.8099(7)	-0.2783(9)	0.6916(8)	0.045(3)
C17	0.8059(8)	-0.6382(10)	0.7512(8)	0.0692
C18	1.0822(7)	-0.4663(11)	0.7325(10)	0.1145
C19	0.7729(8)	-0.4649(10)	0.4310(8)	0.0747
C20	0.6816(8)	-0.4101(10)	0.8243(7)	0.0736
C21	1.0185(7)	-0.3019(11)	0.9493(9)	0.1006
C22	0.7938(7)	-0.2333(10)	0.5922(8)	0.0671
C23	0.6814(16)	-0.738(2)	0.3859(17)	0.068(4)
C24	0.6926(17)	-0.831(2)	0.5721(17)	0.068(4)
H11	0.613	-0.6259	0.3042	0.077(8)
H12	0.7089	-0.6899	0.3524	0.077(8)
H13	0.6143	-0.7564	0.303	0.077(8)
H21	0.7099	-0.8237	0.588	0.077(8)
H22	0.7753	-0.8187	0.5361	0.077(8)
H23	0.6807	-0.8852	0.4866	0.077(8)
H31	0.6063	-0.0935	0.5108	0.113(8)
H32	0.5601	-0.1935	0.4376	0.113(8)
H33	0.4963	-0.1077	0.4575	0.113(8)
H41	0.651	-0.1159	0.7253	0.123(8)
H42	0.5774	-0.1817	0.7478	0.123(8)
H43	0.545	-0.0783	0.6753	0.123(8)
H71	0.9754	-0.5692	0.8003	0.065(8)
H91	0.9516	-0.44	0.5498	0.067(8)
H131	0.8601	-0.3767	0.9421	0.067(8)
H151	0.9503	-0.2445	0.7635	0.063(8)
H171	0.8403	-0.6142	0.819	0.110(8)
H172	0.8117	-0.7177	0.7476	0.110(8)
H173	0.741	-0.6188	0.7267	0.110(8)
H181	1.0936	-0.4132	0.6913	0.138(8)
H182	1.1212	-0.5308	0.7427	0.138(8)
H183	1.0961	-0.4328	0.7955	0.138(8)
H191	0.8071	-0.4098	0.4147	0.112(8)
H192	0.7593	-0.5276	0.387	0.112(8)

H193	0.7154	-0.4335	0.4249	0.112(8)
H201	0.6925	-0.3879	0.8896	0.118(8)
H202	0.6822	-0.4899	0.8211	0.118(8)
H203	0.6219	-0.3819	0.7764	0.118(8)
H211	1.0609	-0.2752	0.9252	0.122(8)
H212	1.0376	-0.3746	0.9775	0.122(8)
H213	1.0185	-0.2519	0.9987	0.122(8)
H221	0.852	-0.2294	0.5887	0.096(8)
H222	0.7509	-0.2806	0.5401	0.096(8)
H223	0.7675	-0.1598	0.5849	0.096(8)
H231	0.6603	-0.6773	0.3395	0.077(8)
H232	0.7483	-0.7459	0.4123	0.077(8)
H233	0.6513	-0.8056	0.3525	0.077(8)
H241	0.6782	-0.8191	0.6267	0.077(8)
H242	0.7593	-0.8376	0.5969	0.077(8)
H243	0.6623	-0.8972	0.5372	0.077(8)

B.18. Fractional atomic coordinates and Uiso for $\{FeCl[^{tBu}NON]\}_2(\mu\text{-}Me_2PCH_2CH_2PMe_2)$ (**18**)

Atom	x	y	z	U(iso)
Fe1	0.806572(15)	0.64756(2)	0.392571(9)	0.0335
Cl1	0.89272(4)	0.43048(6)	0.43038(2)	0.0616
Si2	0.62799(3)	0.86200(6)	0.40337(2)	0.0456
Si1	0.67987(4)	0.78422(6)	0.27657(2)	0.0458
P1	0.94789(3)	0.84856(5)	0.415659(17)	0.0383
N1	0.77494(10)	0.64878(15)	0.30406(5)	0.0413
N2	0.70889(9)	0.71912(15)	0.44120(6)	0.0391
O1	0.66820(9)	0.88104(13)	0.33848(5)	0.0481
C9	0.69714(13)	0.6492(2)	0.50115(7)	0.0475
C10	0.96117(12)	0.93295(19)	0.49236(7)	0.042
C11	0.92792(15)	1.0155(2)	0.36415(8)	0.0562
C12	0.80103(15)	0.6466(2)	0.54591(8)	0.0556
C13	1.07779(14)	0.7805(2)	0.41265(9)	0.0571
C14	0.81523(16)	0.5319(2)	0.26455(8)	0.0563
C15	0.7670(2)	0.3726(2)	0.27133(11)	0.0807
C16	0.6442(2)	1.0623(3)	0.43835(11)	0.0772
C17	0.7128(2)	0.9362(3)	0.22301(9)	0.0728
C18	0.93312(18)	0.5211(3)	0.28279(10)	0.0771
C19	0.55189(18)	0.6960(3)	0.24166(12)	0.086
C20	0.48696(16)	0.8117(3)	0.38661(12)	0.0817
C21	0.62173(18)	0.7420(3)	0.53211(10)	0.0791

C22	0.7900(2)	0.5799(3)	0.19641(9)	0.0917
C23	0.65578(18)	0.4812(3)	0.48994(10)	0.0755
H101	0.9833	0.8479	0.5218	0.0526
H102	0.8927	0.9731	0.4971	0.0527
H112	0.9257	0.9809	0.3228	0.084
H113	0.9842	1.0889	0.3742	0.0836
H111	0.865	1.0675	0.3659	0.0844
H123	0.7924	0.5897	0.5836	0.0829
H121	0.8191	0.7535	0.5566	0.0828
H122	0.8536	0.5943	0.5284	0.0826
H131	1.0804	0.737	0.373	0.0881
H132	1.1283	0.8634	0.4206	0.088
H133	1.0963	0.7018	0.4419	0.0881
H152	0.7966	0.2979	0.2468	0.1188
H153	0.7819	0.3362	0.3129	0.119
H151	0.6934	0.378	0.2562	0.1188
H163	0.6047	1.1371	0.4132	0.1181
H161	0.7155	1.0949	0.4478	0.1187
H162	0.6204	1.0622	0.4768	0.1186
H171	0.6753	1.0289	0.225	0.1096
H172	0.7876	0.9647	0.2321	0.1095
H173	0.697	0.9001	0.1811	0.1094
H183	0.9575	0.443	0.2574	0.117
H181	0.9656	0.6211	0.2766	0.1172
H182	0.9559	0.4888	0.3249	0.1165
H191	0.4991	0.7781	0.2342	0.1198
H193	0.5363	0.6171	0.2702	0.1196
H192	0.5592	0.6496	0.2046	0.1189
H202	0.4515	0.8688	0.3516	0.1201
H201	0.4537	0.8353	0.421	0.1206
H203	0.4781	0.7025	0.3781	0.1198
H213	0.6173	0.6936	0.5704	0.1235
H211	0.649	0.8491	0.5398	0.124
H212	0.5536	0.7452	0.5067	0.1233
H221	0.8153	0.4975	0.1726	0.1346
H223	0.8257	0.6799	0.1911	0.1352
H222	0.7164	0.5901	0.183	0.1344
H232	0.6461	0.4319	0.5284	0.1148
H231	0.7028	0.4173	0.474	0.1142
H233	0.5885	0.4825	0.4623	0.1148

B.19. Fractional atomic coordinates and Uiso for $\{Fe[^{iPr}NN'N]\}_2$ (**19**)

Atom	x	y	z	U(iso)
Fe1	0.56505(2)	0.537565(15)	0.606543(19)	0.0381
N1	0.64722(18)	0.61619(11)	0.73728(13)	0.055
N2	0.34828(15)	0.55495(9)	0.50412(12)	0.041
N3	0.42093(18)	0.48131(10)	0.73645(13)	0.0509
C1	0.7897(2)	0.66893(14)	0.7560(2)	0.0672
C2	0.3162(2)	0.64316(12)	0.44096(16)	0.0494
C3	0.4786(3)	0.40363(17)	0.81419(19)	0.0763
C4	0.22127(19)	0.52761(13)	0.57092(17)	0.0526
C5	0.2735(2)	0.45694(14)	0.66613(18)	0.0588
C6	0.4135(3)	0.56504(15)	0.81022(18)	0.0639
C7	0.5727(3)	0.60570(16)	0.84354(18)	0.0703
C14	0.8373(3)	0.6959(2)	0.6368(3)	0.0936
C15	0.9204(3)	0.6194(2)	0.8323(3)	0.1156
C21	0.3073(3)	0.72470(13)	0.5250(2)	0.0675
C22	0.1760(3)	0.64087(16)	0.3447(2)	0.0772
H51	0.4117	0.6531	0.3985	0.0624
H61	0.1769	0.5837	0.6119	0.0668
H62	0.1309	0.5023	0.5146	0.0664
H71	0.3641	0.551	0.8816	0.0803
H72	0.3436	0.6096	0.7594	0.0805
H81	0.1903	0.4503	0.7208	0.074
H82	0.2856	0.3961	0.6275	0.0747
H91	0.2132	0.7226	0.5643	0.1037
H92	0.3027	0.7791	0.4777	0.1037
H93	0.3978	0.7274	0.5848	0.1038
H101	0.771	0.7269	0.7991	0.0805
H111	0.4795	0.3498	0.7619	0.116
H112	0.5837	0.4199	0.8522	0.1163
H113	0.4078	0.3947	0.873	0.1161
H121	0.5609	0.6667	0.8813	0.087
H122	0.6362	0.5667	0.905	0.0869
H131	0.1826	0.5904	0.2891	0.1117
H132	0.1693	0.6988	0.2997	0.1122
H133	0.0805	0.6327	0.3815	0.1122
H141	0.7555	0.7287	0.5883	0.1399
H142	0.9283	0.7363	0.6495	0.1397
H143	0.8643	0.6401	0.5943	0.1403
H151	0.8891	0.6009	0.9086	0.1636
H152	1.011	0.657	0.8471	0.1641

H153	0.946	0.5644	0.7917	0.1639

B.20. Fractional atomic coordinates and Uiso for $\{Co[^{iPr}NN'N]\}_2$ (**20**)

Atom	x	y	z	U(iso)
Co1	0.47669(6)	0.42252(3)	0.35103(2)	0.0417
Co2	0.37865(6)	0.56005(3)	0.33489(2)	0.0426
Co3	-0.06087(6)	0.97142(3)	0.46041(2)	0.0435
N1	0.5508(4)	0.3263(2)	0.37327(14)	0.0559
N2	0.2781(4)	0.4730(2)	0.36904(12)	0.0468
N3	0.3262(4)	0.3541(2)	0.30100(13)	0.049
N4	0.5765(4)	0.51029(19)	0.31655(13)	0.0441
N11	0.1383(4)	1.0298(2)	0.47284(12)	0.0481
N12	0.3057(4)	0.6570(2)	0.31244(14)	0.053
N23	0.5294(4)	0.6290(2)	0.38627(14)	0.0545
N24	-0.1520(4)	0.9476(2)	0.39840(13)	0.059
N32	0.0881(4)	0.8718(2)	0.44835(15)	0.0625
C1	0.6803(6)	0.3052(3)	0.4067(2)	0.0704
C2	0.2509(5)	0.4868(3)	0.42074(18)	0.0626
C4	0.4723(6)	0.2599(3)	0.3516(2)	0.0651
C5	0.3129(6)	0.2845(3)	0.3312(2)	0.0734
C6	0.1837(6)	0.3991(3)	0.2957(2)	0.0729
C7	0.1431(5)	0.4354(3)	0.34308(18)	0.0572
C8	0.4947(10)	0.6473(5)	0.4357(3)	0.1264
C9	0.2290(7)	0.4125(4)	0.4500(2)	0.0916
C12	0.1197(6)	0.5436(4)	0.4272(2)	0.0894
C13	0.3824(6)	0.7225(3)	0.3356(2)	0.0654
C14	0.7302(6)	0.4412(3)	0.2564(2)	0.0731
C18	0.0540(9)	0.7945(4)	0.4608(3)	0.1194
C21	0.6711(7)	0.5836(4)	0.3902(3)	0.0997
C22	0.0858(8)	0.8796(4)	0.3941(2)	0.1036
C23	0.5364(10)	0.6974(4)	0.3589(3)	0.1297
C24	0.2714(5)	0.9801(3)	0.46467(19)	0.0651
C26	0.2366(6)	0.8971(4)	0.4715(2)	0.0866
C3	0.3699(7)	0.3304(4)	0.2527(2)	0.0855
C29	0.6018(5)	0.4988(3)	0.26476(16)	0.0511
C30	0.6252(6)	0.5745(3)	0.2372(2)	0.0749
C31	0.7098(5)	0.5468(3)	0.34303(18)	0.0558
C33	0.1521(6)	1.1073(3)	0.45028(19)	0.0643
C37	-0.4252(6)	0.9244(3)	0.3726(2)	0.0728
C42	0.2869(7)	1.1536(4)	0.4726(3)	0.0949
C43	-0.2882(5)	0.9778(3)	0.37231(16)	0.0556

C45	0.1544(7)	1.1048(4)	0.3948(2)	0.0905
C46	-0.0794(7)	0.8851(4)	0.3731(2)	0.0842
C47	-0.3304(7)	1.0554(3)	0.3928(2)	0.0839
C48	0.7260(8)	0.3728(4)	0.4385(2)	0.0996
C49	0.0532(9)	0.7150(5)	0.2895(4)	0.1513
C53	0.1478(8)	0.6065(4)	0.2431(2)	0.0969
C54	0.8182(7)	0.2765(4)	0.3810(3)	0.0983
C55	0.1946(6)	0.6759(3)	0.2730(2)	0.0674
H11	0.3465	0.5111	0.436	0.077(2)
H21	0.3242	0.742	0.3617	0.084(2)
H22	0.3928	0.7642	0.3109	0.084(2)
H31	0.1122	0.5561	0.462	0.125(2)
H32	0.1376	0.592	0.4106	0.125(2)
H33	0.0235	0.5222	0.4151	0.125(2)
H41	0.7573	0.6179	0.4026	0.108(2)
H42	0.6592	0.5426	0.4164	0.108(2)
H51	0.1459	0.9264	0.3849	0.115(2)
H52	0.1414	0.8344	0.3799	0.115(2)
H61	0.5888	0.739	0.3767	0.134(2)
H62	0.6122	0.6853	0.3301	0.134(2)
H71	0.3592	0.997	0.4863	0.078(2)
H72	0.2996	0.9887	0.4304	0.078(2)
H81	0.3975	0.6765	0.4347	0.170(2)
H82	0.576	0.6814	0.4496	0.170(2)
H83	0.4889	0.6024	0.4551	0.170(2)
H91	0.2356	0.4212	0.4834	0.133(2)
H92	0.3055	0.3735	0.4418	0.133(2)
H93	0.1278	0.3902	0.4399	0.133(2)
H141	0.7273	0.4267	0.2231	0.104(2)
H142	0.8274	0.4652	0.2658	0.104(2)
H143	0.7185	0.3956	0.2763	0.104(2)
H161	0.1946	0.4399	0.2707	0.094(2)
H162	0.0987	0.3644	0.2835	0.094(2)
H171	0.0609	0.4732	0.3374	0.074(2)
H172	0.1036	0.3936	0.3641	0.074(2)
H181	-0.0468	0.7798	0.445	0.158(2)
H182	0.0518	0.7886	0.4952	0.158(2)
H183	0.1312	0.7597	0.4488	0.158(2)
H201	0.6452	0.2627	0.4286	0.082(2)
H261	0.2376	0.8854	0.5066	0.098(2)
H262	0.321	0.8655	0.4584	0.098(2)

H271	0.464	0.2188	0.3763	0.077(2)
H272	0.531	0.2391	0.325	0.077(2)
H281	0.2946	0.293	0.2383	0.128(2)
H282	0.368	0.3749	0.2305	0.128(2)
H283	0.4708	0.3072	0.254	0.128(2)
H291	0.5053	0.4751	0.2498	0.063(2)
H301	0.6192	0.5651	0.2024	0.113(2)
H302	0.7267	0.5952	0.2462	0.113(2)
H303	0.5495	0.612	0.2441	0.113(2)
H311	0.7478	0.5885	0.3226	0.067(2)
H312	0.7906	0.5088	0.349	0.067(2)
H331	0.0566	1.1366	0.457	0.081(2)
H371	-0.5161	0.947	0.3558	0.107(2)
H372	-0.4492	0.9138	0.406	0.107(2)
H373	-0.4034	0.8757	0.357	0.107(2)
H411	0.2477	0.2955	0.3581	0.092(2)
H412	0.2651	0.2417	0.3111	0.092(2)
H421	0.2843	1.2054	0.4607	0.134(2)
H422	0.2829	1.1555	0.5082	0.134(2)
H423	0.3841	1.1295	0.4655	0.134(2)
H431	-0.2648	0.9853	0.3375	0.068(2)
H451	0.136	1.1554	0.3808	0.132(2)
H452	0.2526	1.0857	0.3854	0.132(2)
H453	0.0739	1.0702	0.3809	0.132(2)
H461	-0.0854	0.8942	0.3379	0.101(2)
H462	-0.1336	0.8346	0.3787	0.101(2)
H471	-0.2459	1.0908	0.3918	0.121(2)
H472	-0.3607	1.0503	0.426	0.121(2)
H473	-0.4189	1.0777	0.3736	0.121(2)
H481	0.8075	0.3579	0.4631	0.141(2)
H482	0.6378	0.39	0.457	0.141(2)
H483	0.7617	0.4147	0.4203	0.141(2)
H491	-0.0229	0.7228	0.2616	0.184(2)
H492	0.0796	0.765	0.3029	0.184(2)
H493	0.0069	0.6834	0.3133	0.184(2)
H531	0.2362	0.5775	0.2337	0.136(2)
H532	0.0849	0.573	0.2623	0.136(2)
H533	0.086	0.6206	0.2136	0.136(2)
H541	0.9046	0.2667	0.4038	0.136(2)
H542	0.8475	0.3154	0.3578	0.136(2)
H543	0.792	0.2296	0.3629	0.136(2)

H551	0.2459	0.7123	0.2493	0.090(2)

B.21. Fractional atomic coordinates and Uiso for {Fe[^{iPr}NO′N]}$_2$ (**21**)

Atom	x	y	z	U(iso)
Fe1	0.398853(13)	0.414782(11)	0.444499(9)	0.018
O2	0.27635(7)	0.51995(6)	0.31097(5)	0.0237
N3	0.37444(8)	0.58731(6)	0.52223(6)	0.0193
N4	0.24270(8)	0.29345(7)	0.39825(6)	0.0231
C5	0.19671(10)	0.61730(9)	0.35458(7)	0.0269
C6	0.18050(12)	0.43096(9)	0.24721(7)	0.0288
C7	0.12110(10)	0.33683(9)	0.31744(7)	0.0268
C8	0.28980(10)	0.58966(8)	0.61073(7)	0.0238
C9	0.31265(10)	0.67718(8)	0.43915(7)	0.0236
C10	0.34481(12)	0.12710(10)	0.51857(9)	0.0342
C11	0.20728(10)	0.17654(8)	0.44498(7)	0.0264
C12	0.07513(12)	0.18560(11)	0.50436(9)	0.0373
C13	0.32629(13)	0.47595(10)	0.68059(8)	0.0353
C14	0.32029(12)	0.70724(10)	0.67777(8)	0.034
H51	0.1563	0.6754	0.2981	0.032
H52	0.1113	0.5822	0.3863	0.0315
H61	0.0988	0.4751	0.201	0.0347
H62	0.247	0.3897	0.2034	0.0348
H71	0.0358	0.3745	0.3483	0.0317
H72	0.0763	0.2674	0.2735	0.0326
H81	0.1819	0.5876	0.5812	0.0295
H91	0.2668	0.7503	0.4691	0.0287
H92	0.3935	0.7093	0.4048	0.029
H101	0.3259	0.0453	0.5432	0.0513
H102	0.3717	0.1814	0.5803	0.0497
H103	0.4287	0.1215	0.4838	0.0493
H111	0.1795	0.1137	0.3896	0.032
H122	0.0587	0.1059	0.5374	0.057
H123	0.0955	0.2493	0.5594	0.0578
H121	-0.0154	0.206	0.4559	0.057
H131	0.2694	0.4788	0.738	0.0541
H133	0.4331	0.4739	0.711	0.0551
H132	0.3	0.4002	0.6409	0.0547
H142	0.257	0.7089	0.7318	0.0519
H141	0.4225	0.7079	0.7123	0.0511
H143	0.3008	0.7828	0.6354	0.052

B.22. Fractional atomic coordinates and Uiso for $\{Co[^{iPr}NO'N]\}_2$ (**22**)

Atom	x	y	z	U(iso)
Co1	0.0006(2)	0.1150(3)	0.4715(2)	0.032
Co2	0.0957(2)	-0.1634(3)	0.6689(2)	0.0318
N3	0.2125(9)	-0.0054(10)	0.4620(10)	0.0315
O4	-0.0222(8)	-0.3176(9)	0.5969(8)	0.0412
C5	0.1113(11)	-0.5153(12)	0.8025(12)	0.0394
O6	0.1261(8)	0.2686(9)	0.5390(8)	0.0341
N7	-0.1193(9)	-0.0404(10)	0.6823(10)	0.0351
N8	0.1603(9)	-0.3758(10)	0.8192(10)	0.0385
N9	-0.0617(9)	0.3171(10)	0.3246(10)	0.0401
C10	-0.1751(9)	0.0271(10)	0.8078(10)	0.0338
C11	-0.1715(10)	-0.2359(12)	0.5648(9)	0.0388
C12	-0.1744(12)	0.3528(13)	0.2206(12)	0.0515
C13	-0.2333(11)	-0.1357(12)	0.6713(13)	0.0435
C14	-0.3099(13)	0.1541(16)	0.7761(16)	0.0562
C15	0.1386(11)	0.4310(11)	0.3991(9)	0.0427
C16	-0.2012(14)	-0.1062(14)	0.9686(13)	0.0733
C17	0.2547(11)	-0.0769(11)	0.3399(11)	0.0509
C18	0.2730(9)	0.1689(12)	0.5805(12)	0.0492
C19	-0.0490(11)	-0.4651(12)	0.7401(11)	0.0459
C20	0.2774(11)	-0.4240(12)	0.9265(11)	0.0375
C21	0.2869(13)	-0.2633(12)	0.9645(13)	0.0679
C22	0.3450(11)	0.0913(13)	0.4681(14)	0.0415
C23	0.2998(12)	0.0599(13)	0.1611(12)	0.0618
C24	-0.3387(12)	0.4345(17)	0.2924(16)	0.0736
C25	0.4086(14)	-0.1968(17)	0.3717(16)	0.0723
C26	-0.2163(11)	0.2090(13)	0.2005(14)	0.0605
C27	-0.0168(13)	0.4627(14)	0.3455(13)	0.0525
C28	0.4309(14)	-0.4848(16)	0.8723(16)	0.0641
H51	0.0855	-0.6114	0.9114	0.0529
H52	0.1909	-0.5548	0.7303	0.0532
H111	-0.2487	-0.3225	0.5828	0.0406
H112	-0.1506	-0.1663	0.4475	0.0414
H121	-0.1354	0.4412	0.1192	0.0371
H131	-0.2953	-0.2073	0.7751	0.0451
H132	-0.3217	-0.05	0.6106	0.0447
H142	-0.319	0.1958	0.8626	0.077
H143	-0.4003	0.1102	0.7812	0.0781
H141	-0.2726	0.2465	0.6772	0.0767

H151	0.1547	0.5211	0.4408	0.0426
H152	0.2273	0.4319	0.3137	0.0434
H162	-0.1937	-0.0621	1.0463	0.0816
H163	-0.09	-0.1789	0.9699	0.0814
H161	-0.2807	-0.1763	0.9927	0.0816
H171	0.162	-0.1425	0.3377	0.0694
H182	0.3507	0.2342	0.5899	0.0754
H181	0.2471	0.0748	0.6876	0.0758
H192	-0.1393	-0.4384	0.8282	0.0641
H191	-0.0913	-0.5513	0.7226	0.0646
H201	0.2252	-0.5217	1.042	0.0641
H211	0.3782	-0.289	1.0445	0.1449
H213	0.1685	-0.2238	1.0274	0.1448
H212	0.3301	-0.1552	0.8296	0.1447
H222	0.4378	0.0339	0.4861	0.0701
H221	0.365	0.1929	0.3527	0.0706
H231	0.3153	0.0152	0.0766	0.0927
H233	0.4279	0.0881	0.1447	0.0926
H232	0.2482	0.1573	0.1383	0.0924
H242	-0.4129	0.4564	0.2253	0.1263
H241	-0.3148	0.5207	0.3137	0.1256
H243	-0.3837	0.3395	0.402	0.1263
H253	0.4396	-0.2606	0.3102	0.1012
H251	0.408	-0.267	0.4845	0.1009
H252	0.5118	-0.123	0.3446	0.1017
H261	-0.2807	0.2292	0.1302	0.0625
H262	-0.1641	0.114	0.2407	0.063
H272	-0.1064	0.4865	0.4341	0.0631
H271	-0.0196	0.5673	0.2498	0.0629
H282	0.5087	-0.5096	0.9495	0.0757
H281	0.4291	-0.5969	0.8615	0.0748
H283	0.4839	-0.4055	0.7677	0.0757

B.23. Fractional atomic coordinates and Uiso for $FeCl_2[^{iPr}NN'N]$ (**23**)

Atom	x	y	z	U(iso)
Fe1	0.5	0.51098(12)	0.25	0.0286
Cl1	0.42965(8)	0.6424(2)	0.31903(12)	0.0488
N1	0.6080(2)	0.4556(5)	0.4577(4)	0.0371
N3	0.5	0.2303(7)	0.25	0.0343
C1	0.6781(3)	0.5697(8)	0.5234(5)	0.0459
C3	0.5279(8)	0.1457(14)	0.1820(11)	0.0488

C4	0.6277(4)	0.2679(7)	0.4646(6)	0.0617
C5	0.5654(12)	0.1844(11)	0.3534(14)	0.4924
C11	0.7430(3)	0.5231(9)	0.6643(5)	0.058
C12	0.6510(4)	0.7579(8)	0.5152(5)	0.058
H111	0.7605	0.4045	0.67	0.0706
H112	0.7872	0.5993	0.6997	0.0706
H113	0.7223	0.5315	0.7148	0.0706
H121	0.6105	0.7902	0.4275	0.0684
H122	0.6945	0.8376	0.5499	0.0684
H123	0.6296	0.7698	0.565	0.0684
H11	0.7007	0.5634	0.475	0.0561
H12	0.5883	0.4653	0.5102	0.0446
H31	0.4872	0.1567	0.0893	0.0683
H32	0.5749	0.1964	0.2032	0.0683
H33	0.5352	0.0232	0.2023	0.0683
H41	0.6757	0.2562	0.4693	0.0735
H42	0.6378	0.2158	0.5423	0.0735
H51	0.5912	0.1205	0.3251	0.5486
H52	0.5479	0.1025	0.3915	0.5486

B.24. Fractional atomic coordinates and Uiso for $CoCl_2[^{iPr}NN'N]$ (**24**)

Atom	x	y	z	U(iso)
Co1	0.5	0.99499(7)	0.25	0.0249
Cl1	0.43057(4)	0.86016(10)	0.31856(6)	0.0424
N1	0.60691(12)	1.0431(3)	0.4568(2)	0.0329
N3	0.5	1.2689(4)	0.25	0.0316
C1	0.67640(16)	0.9257(4)	0.5209(3)	0.0415
C3	0.4708(3)	1.3523(7)	0.3179(5)	0.038
C4	0.6280(2)	1.2295(4)	0.4655(3)	0.0564
C5	0.5388(3)	1.3268(7)	0.3847(5)	0.0361
C6	0.5914(3)	1.3066(7)	0.3274(5)	0.0354
C11	0.74184(16)	0.9727(5)	0.6636(3)	0.0528
C12	0.64868(18)	0.7390(4)	0.5130(3)	0.049
H41	0.5866	1.0329	0.5091	0.0393
H51	0.6992	0.932	0.4725	0.0504
H61	0.6858	1.2403	0.5194	0.0684
H62	0.6089	1.2946	0.5073	0.0684
H63	0.6549	1.2522	0.4259	0.0684
H64	0.6626	1.2684	0.556	0.0684
H71	0.6079	0.7072	0.4245	0.06
H72	0.6924	0.6588	0.5476	0.06

H73	0.6273	0.7276	0.5633	0.06
H81	0.7601	1.09	0.6697	0.0641
H82	0.7864	0.8951	0.6992	0.0641
H83	0.7213	0.9639	0.7148	0.0641
H91	0.4151	1.3311	0.2729	0.0496
H92	0.48	1.4755	0.3228	0.0496
H93	0.4987	1.3068	0.405	0.0496
H101	0.603	1.4292	0.3323	0.045
H102	0.6147	1.2494	0.288	0.045
H111	0.5425	1.4501	0.3926	0.0443
H112	0.5085	1.2864	0.4178	0.0443

B.25. Fractional atomic coordinates and Uiso for $FeCl_2[^{iPr}NO'N]$ (**25**)

Atom	x	y	z	U(iso)
Fe1	0.5	0.5684	0.75	0.0234
Cl1	0.5738	0.7334	0.678	0.03
N1	0.4004	0.4851	0.5548	0.0234
O1	0.5	0.2883	0.75	0.0339
C1	0.3372	0.6189	0.4873	0.0309
C4	0.372	0.313	0.5836	0.0317
C5	0.439	0.1849	0.6505	0.0322
C11	0.27	0.5424	0.3635	0.0389
C12	0.3712	0.7835	0.4528	0.0436
H1	0.4206	0.4546	0.4997	0.05
H2	0.4573	0.1379	0.5867	0.05
H3	0.2884	0.4921	0.3031	0.05
H4	0.3495	0.3421	0.6428	0.05
H5	0.3373	0.2504	0.5069	0.05
H6	0.3231	0.655	0.5572	0.05
H7	0.4291	0.0783	0.6939	0.05
H8	0.3323	0.8687	0.4181	0.05
H9	0.2425	0.4404	0.3836	0.05
H10	0.3884	0.7475	0.3886	0.05
H11	0.4111	0.8308	0.5267	0.05
H12	0.2355	0.6375	0.3233	0.05